CELLULAR REPROGRAMMING STRATEGIES FOR DEGENERATIVE DISORDERS INVOLVING THE RETINAL PIGMENT EPITHELIUM

CRISTIANA FERREIRA PIRES

Tese para obtenção do grau de Doutor em Ciências da Vida
na Especialidade em Biomedicina
na Faculdade de Ciências Médicas

Junho de 2014

CELLULAR REPROGRAMMING STRATEGIES FOR DEGENERATIVE DISORDERS INVOLVING THE RETINAL PIGMENT EPITHELIUM

Cristiana Ferreira Pires

Orientador: Miguel C. Seabra, Professor Doutor

Co-orientador: António Jacinto, Professor Doutor

Tese para obtenção do grau de Doutor em Ciências da Vida
na Especialidade em Biomedicina

Junho de 2014

This work was performed by Cristiana Ferreira Pires in CEDOC – CHRONIC DISEASES RESEARCH CENTER, Molecular Mechanisms of Disease group, NOVA Medical School – Faculdade de Ciências Médicas da Universidade Nova de Lisboa, under the supervision of Miguel C. Seabra, MD PhD, and António Jacinto, PhD.

Financial support for this project was attained from the Portuguese Foundation for Science and Technology (FCT) in the form of a PhD fellowship addressed to the author (SFRH / BD / 33541 / 2008) and attributed in the context of the GABBA Program - Graduate Program in Areas of Basic and Applied Biology from Universidade do Porto. Additional financial support was obtained from the Choroideremia Research Foundation (CRF) in the form of a research grant addressed to Miguel C. Seabra.

Acknowledgements

"Passou a nuvem; o sol volta.

A alegria girassolou."

Fernando Pessoa

The happy feeling of fulfillment is only complete once the joy is shared with everyone that helped and supported me along this path.

My first acknowledgement goes to Miguel Seabra, my PhD supervisor, for accepting me as a PhD student and enthusiastically drawing the first sketch of this project with me over lunch. Even when physically absent, his ideas and tremendous support had a major influence in this thesis. Miguel gave me the freedom to explore on my own, whilst still being present. I am deeply grateful for his mentoring and for teaching me how to stay focused and motivated, throughout the numerous scientific adversities.

I would also like to acknowledge the GABBA Phd Program for my PhD fellowship and, more importantly, for the opportunity to learn how to think as a scientist.

I owe my sincere gratitude to my PhD co-supervisor António Jacinto, for harbouring me as his student and for his support and always helpful opinions.

I was also luckily assigned to two "informal" supervisors. José Ramalho received me in his lab and taught me all the basic notions on cell and molecular biology techniques. I always tried to be an eager student of his lessons, including the hard work rhythm. I hope he agrees with me that even our vivid and loud discussions had positive outcomes. Duarte Barral was also a helpful support, allowing me to perform some experiments in his lab and to attend lab meetings and lab retreats. I am very thankful for his readiness to help me when I needed.

I would like to express my genuine gratitude to the CRF team, Sara Maia, Martim Portal and Catarina Sequeira. I believe that a good team always facilitates the attainment of the assigned objectives and I was lucky enough to have you working on my side. Thank you for your partnership, encouragement and friendship.

I owe my sincere gratitude to Dr. Tanya Tolmachova for welcoming me at Imperial College London and for the possibility to use the animal models.

I would like to thank Doutor Domingos Henrique and Doutora Elsa Abranches for the helpful discussions and suggestions.

I would also like to acknowledge Doutora Jacinta Serpa and Professora Doutora Ana Félix for their helpful collaboration with the teratomas' formation and analysis.

In addition, past and present members from the lab always supported me and enriched my work with their questions and helpful suggestions. Thank you to Magui and our cigarrette/fresh air-breaks! Thank you to Zézé Sandoval, Pedro Olho Azul, "Lau-Lau" Portelinha, Cristina Casalou, Cecília ("dos cílios"), Mary, Xiquilim, Elsa Seixas, Lucio "bacaninho" and Abulinho. I am particularly grateful for the friendship we have built over the years. A thankful word goes to Augusta, Firmina and Teresa Salreta, and also to Isabel, Isabelinha, Ana Sofia, Clara and Teresa Barona for all the joyful lunches and coffees at FCM.

A very special thank you goes to my PhD "sisterhood", Carolina "Carolzinha" and Inês "Agnes". I was told, even before we met, that Carolzinha and I would get along! And we did! Oh yes we did. By the contrary, Agnes knew first that we were meant to be friends. And we did! Oh yes we did! Carolzinha and Agnes, we are a great team together. I am very proud of both of you and now it is my turn to finish this. We made it together (Carrapito power!!!), but the PhD is just a small piece of it…Thank you for smiling with me!

Thank you to Carlos, the honorary member of our "sisterhood"! You have been more than just Inês' husband. Thank you for your friendship and support in so many occasions! The fox was right…"cativar é criar laços".

To Alex, thank you for being my scientific mentor and my friend throughout these years. Thank you for teaching me that accepting our limitations is the first step to overcome them.

Thank you to my special GABBA friends. Di, Bi and Marghi, thank you for falling in the dance floor with me! And for always helping me to rise again and to keep on dancing! And smiling! And thank you to Bernie and Rosinha, for being my family in London (KT rules!).

Aproveito também para manifestar a minha sentida gratidão a todos os meus amigos de Aveiro, Palhaça e Família Académia alargada, aos "meus" profissionais de saúde, aos amigos-família e a toda a minha família, por sempre me perguntarem como estavam os meus bichos, células e ratinhos. Apesar da maioria nem perceber o que realmente andei a fazer estes anos todos, o vosso apoio e amizade foi muito importante. Um obrigada especial para todos os meus "Priminhos" por brincarem comigo, numa óptima terapêutica para esquecer as desventuras do trabalho. E um bem-haja ao "refúgio familiar" de Oeiras, por todos os inspiradores almoços e jantares, pré ou pós-laboratório.

À minha irmã Diana, minha companheira de sempre! Talvez já não do banco de trás do carro, mas certamente da Vida. Ao meu cunhado Francisco, pelas longas conversas telefónicas e em viagens de carro na A1. Às minhas sobrinhas Carolina e Benedita, simplesmente por existirem e me encherem o coração de Amor. Obrigada.

E por fim, aos meus Pais, a quem dedico esta tese. Por me terem mostrado os princípios que devem reger a vida e o trabalho ("rigor e disciplina"). Por me darem força e motivação para atingir os meus objectivos. Por fazerem sempre tudo, com o propósito último de nos sentirmos felizes e amadas! Bem-haja pelo porto de abrigo que tão bem sabem criar e manter.

Here it is.

A tese "girassolou".

Abstract

Cellular reprogramming is an emerging research field in which a somatic cell is reprogrammed into a different cell type by forcing the expression of lineage-specific transcription factors (TFs). Cellular identities can be manipulated using experimental techniques with the attainment of pluripotency properties and the generation of induced Pluripotent Stem (iPS) cells, or the direct conversion of one somatic cell into another somatic cell type. These pioneering discoveries offer new unprecedented opportunities for the establishment of novel cell-based therapies and disease models, as well as serving as valuable tools for the study of molecular mechanisms governing cell fate establishment and developmental processes.

Several retinal degenerative disorders, inherited and acquired, lead to visual impairment due to an underlying dysfunction of the support cells of the retina, the retinal pigment epithelium (RPE). Choroideremia (CHM), an X-linked monogenic disease caused by a loss of function mutation in a key regulator of intracellular trafficking, is characterized by a progressive degeneration of the RPE and other components of the retina, such as the photoreceptors and the choroid. Evidence suggest that RPE plays an important role in CHM pathogenesis, thus implying that regenerative approaches aiming at rescuing RPE function may be of great benefit for CHM patients. Additionally, lack of appropriate *in vitro* models has contributed to the still poorly-characterized molecular events in the base of CHM degenerative process. Therefore, the main focus of this work was to explore the potential applications of cellular reprogramming technology in the context of RPE-related retinal degenerations.

The generation of mouse iPS cells was established and optimized using an inducible lentiviral system to force the expression of the classic set of TFs, namely Oct4, Sox2, Klf4 and c-Myc. Wild-type cells, as well as cells derived from a conditional knockout (KO) mouse model of Chm, were successfully converted into a pluripotent state, that displayed morphology, molecular and functional equivalence to Embryonic Stem (ES) cells. Generated iPS cells were then subjected to differentiation protocols towards the attainment of a RPE cell fate, with promising results highlighting the possibility of generating a valuable Chm-RPE *in vitro* model. In alternative, direct lineage conversion of fibroblasts into RPE-like cells was also tackled. A TF-mediated approach was implemented after the generation of a panoply of molecular tools needed for such studies. After transduction with pools of 10 or less TFs, selected for their key role on RPE developmental process and specification, fibroblasts acquired a pigmented morphology and expression of some RPE-specific markers. Additionally, promoter

regions of RPE-specific genes were activated indicating that the transcriptional identity of the cells was being altered into the pursued cell fate.

In conclusion, highly significant progress was made towards the implementation of already established cellular reprogramming technologies, as well as the designing of new innovative ones. Reprogramming into pluripotency and lineage conversion methodologies were applied to ultimately generate RPE cells. These studies open new avenues for the establishment of cell replacement therapies and, more straightforwardly, raise the possibility of modelling retinal degenerations with underlying RPE defects in a petri dish, particularly CHM.

Resumo

A reprogramação celular permite que uma célula somática seja reprogramada para outra célula diferente através da expressão forçada de factores de transcrição (FTs) específicos de determinada linhagem celular, e constitui uma área de investigação emergente nos últimos anos. As células somáticas podem ser experimentalmente manipuladas de modo a obter células estaminais pluripotentes induzidas (CEPi), ou convertidas directamente noutro tipo de célula somática. Estas descobertas inovadoras oferecem oportunidades promissoras para o desenvolvimento de novas terapias de substituição celular e modelos de doença, funcionando também como ferramentas valiosas para o estudo dos mecanismos moleculares que estabelecem a identidade celular e regulam os processos de desenvolvimento.

Existem várias doenças degenerativas hereditárias e adquiridas da retina que causam deficiência visual devido a uma disfunção no tecido de suporte da retina, o epitélio pigmentar da retina (EPR). Uma destas doenças é a Coroideremia (CHM), uma doença hereditária monogénica ligada ao cromossoma X causada por mutações que implicam a perda de função duma proteína com funções importantes na regulação do tráfico intracelular. A CHM é caracterizada pela degenerescência progressiva do EPR, assim como dos foto-receptores e da coróide. Resultados experimentais sugerem que o EPR desempenha um papel importante na patogénese da CHM, o que parece indicar uma possível vantagem terapêutica na substituição do EPR nos doentes com CHM. Por outro lado, existe uma lacuna em termos de modelos *in vitro* de EPR para estudar a CHM, o que pode explicar o ainda desconhecimento dos mecanismos moleculares que explicam a patogénese desta doença. Assim, este trabalho focou-se principalmente na exploração das potencialidades das técnicas de reprogramação celular no contexto das doenças de degenerescência da retina, em particular no caso da CHM.

Células de murganho de estirpe selvagem, bem como células derivadas de um ratinho modelo de knockout condicional de Chm, foram convertidos com sucesso em CEPi recorrendo a um sistema lentiviral induzido que permite a expressão forçada dos 4 factores clássicos de reprogramação, a saber Oct4, Sox2, Klf4 e c-Myc. Estas células mostraram ter equivalência morfológica, molecular e funcional a células estaminais embrionárias (CES). As CEPi obtidas foram seguidamente submetidas a protocolos de diferenciação com o objectivo final de obter células do EPR. Os resultados promissores obtidos revelam a possibilidade de gerar um valioso modelo de EPR-CHM para estudos *in vitro*. Em alternativa, a conversão directa de linhagens partindo de fibroblastos para obter células do EPR foi também abordada. Uma vasta gama de ferramentas moleculares foi gerada de modo a implementar uma estratégia mediada por FTs-chave,

seleccionados devido ao seu papel fundamental no desenvolvimento embrionário e especificação do EPR. Conjuntos de 10 ou menos FTs foram usados para transduzir fibroblastos, que adquiriram morfologia pigmentada e expressão de alguns marcadores específicos do EPR. Adicionalmente, observou-se a activação de regiões promotoras de genes específicos de EPR, indicando que a identidade transcricional das células foi alterada no sentido pretendido.

Em conclusão, avanços significativos foram atingidos no sentido da implementação de tecnologias de reprogramação celular já estabelecidas, bem como na concepção de novas estratégias inovadoras. Metodologias de reprogramação, quer para pluripotência, quer via conversão directa, foram aplicadas com o objectivo final de gerar células do EPR. O trabalho aqui descrito abre novos caminhos para o estabelecimento de terapias de substituição celular e, de uma maneira mais directa, levanta a possibilidade de modelar doenças degenerativas da retina com disfunção do EPR numa placa de petri, em particular no caso da CHM.

Publications

Papers in International Scientific Periodicals with Referees

Carolina Thieleke-Matos, Mafalda Lopes da Silva, Laura Cabrita-Santos, **Cristiana F. Pires**, José S. Ramalho, Ognian Ikonomov, Assia Shisheva, Miguel C. Seabra, and Duarte C. Barral. "Host PI(3,5)P2 activity is required for Plasmodium berghei growth during liver stage infection". Traffic. 2014; 15(10):1066-82. DOI: 10.1111/tra.12190.

Cristiana F. Pires *et al.*, Modelling Choroideremia using induced Pluripotent Stem cell technology. (Manuscript in preparation)

Cristiana F. Pires *et al.*, Direct conversion of fibroblastos into RPE-like cells. (Manuscript in preparation)

Inês P. Rodrigues, Sara Maia, **Cristiana F. Pires**, Martim D. Portal, Carolina Thieleke-Matos, Olaf Strauss, Miguel C. Seabra & Jose S. Ramalho. New roles of Rab GTPases on RPE: targeting VEGF secretion. (Manuscript in preparation)

Papers in Conference Proceedings

Cristiana F. Pires, Martim D. Portal, Sara Maia, Inês P. Rodrigues, Carolina Thieleke-Matos, Tanya Tolmachova, José S. Ramalho, António Jacinto, Miguel C. Seabra. Generation of induced Pluripotent Stem cells from a model of retinal degeneration. 2013. Pigment Cell Melanoma Res. 26, 5, E16-E17. DOI: 10.1111/pcmr.12152.

Sara Maia*, **Cristiana F. Pires***, Martim D. Portal, Margarida S. Silva, Inês P. Rodrigues, Catarina Sequeira, Teresa M. Barona, José S. Ramalho, Miguel C. Seabra. Towards the direct conversion of fibroblasts into RPE by defined factors. 2013. Pigment Cell Melanoma Res. 26, 5, E17. (**These authors contributed equally to this work)*

Martim D. Portal*, **Cristiana F. Pires***, Sara Maia, Inês P. Rodrigues, Margarida S. Silva, José S. Ramalho, Miguel C. Seabra. Molecular tools for direct differentiation of retinal pigment epithelium. Pigment Cell Melanoma Res. 2013. 26, 5, E18. (**These authors contributed equally to this work)*

Inês P. Rodrigues, Sara Maia, **Cristiana F. Pires**, Martim D. Portal, Carolina Thieleke-Matos, Olaf Strauss, Miguel C. Seabra, José S. Ramalho. VEGF secretion by retinal pigment epithelium is regulated by Rab GTPases. Pigment Cell Melanoma Res. 2013. 26, 5, E17.

Cristiana F. Pires, Inês P. Rodrigues, Sara Maia, Martim D. Portal, José S. Ramalho, Miguel C. Seabra. Optimization of a Retinal Pigment Epithelium differentiation protocol driven by ectopic expression of eye transcription factors. Pigment Cell Melanoma Res. 2012. 25; 659.

Oral Communications by Invitation

Inês P. Rodrigues, Sara Maia, **Cristiana F. Pires**, Martim D. Portal, Carolina Thieleke-Matos, Olaf Strauss, Henrique Girão, Miguel C. Seabra, José S. Ramalho. Rab GTPases as regulators of VEGF secretion by retinal pigment epithelium. 7th Meeting on Cell Signaling – SINAL 2013. Aveiro, Portugal. 2013.

Cristiana F. Pires, Martim D. Portal, Sara Maia, Inês P. Rodrigues, Carolina Thieleke-Matos, Tanya Tolmachova, José S. Ramalho, António Jacinto, Miguel C. Seabra. Generation of induced Pluripotent Stem cells from a model of retinal degeneration. 18th ESPCR Meeting. Lisboa, Portugal. 2013.

Inês P. Rodrigues, Sara Maia, **Cristiana F. Pires**, Martim D. Portal, Carolina Thieleke-Matos, Olaf Strauss, Miguel C. Seabra, José S. Ramalho. VEGF secretion by retinal pigment epithelium is regulated by Rab GTPases. 18th ESPCR Meeting. Lisboa, Portugal. 2013.

Cristiana F. Pires, Inês P. Rodrigues, Sara Maia, Martim D. Portal, José S. Ramalho, Miguel C. Seabra. Optimization of a Retinal Pigment Epithelium differentiation protocol driven by ectopic expression of eye transcription factors. 17th ESPCR Meeting. Genève, Switzerland. 2012.

Inês P. Rodrigues, **Cristiana F. Pires**, Miguel C. Seabra & José S. Ramalho. Uncovering the VEGF Secretory Pathway in Retinal Pigment Epithelium: the Rab proteins' role. Pan-American Research Day 2012. Fort Lauderdale, USA. 2012.

Posters in Conferences

Inês P. Rodrigues, Sara Maia, **Cristiana F. Pires**, Martim D. Portal, Carolina Thieleke-Matos, Olaf Strauss, Henrique Girão, Miguel C. Seabra, José S. Ramalho. Rab GTPases as regulators of VEGF secretion by retinal pigment epithelium. V Annual Meeting of IBILI. Coimbra, Portugal. 2013.

Inês P. Rodrigues, Sara Maia, **Cristiana F. Pires**, Martim D. Portal, Carolina Thieleke-Matos, Olaf Strauss, Miguel C. Seabra, José S. Ramalho. New roles of Rab GTPases on eye diseases: targeting VEGF secretion. The EMBO Meeting 2013. Amsterdam, Netherlands. 2013.

Carolina Thieleke-Matos, Mafalda Lopes da Silva, Laura Cabrita-Santos, **Cristiana F. Pires**, José S. Ramalho, Ognian Ikonomov, Assia Shisheva, Miguel C. Seabra, and Duarte C. Barral. "Host PI(3,5)P2 activity is required for Plasmodium berghei growth during liver stage infection". The EMBO Meeting 2013. Amsterdam, Netherlands. 2013.

Cristiana F. Pires, Martim D. Portal, Sara Maia, Inês P. Rodrigues, Carolina Thieleke-Matos, Tanya Tolmachova, José S. Ramalho, António Jacinto, Miguel C. Seabra. Generation of induced Pluripotent Stem cells from a model of retinal degeneration. 18th ESPCR Meeting. Lisboa, Portugal. 2013.

Sara Maia*, **Cristiana F. Pires***, Martim D. Portal, Margarida S. Silva, Inês P. Rodrigues, Catarina Sequeira, Teresa M. Barona, José S. Ramalho, Miguel C. Seabra. Towards the direct conversion of fibroblasts into RPE by defined factors. 18th ESPCR Meeting. Lisboa, Portugal. 2013. (**These authors contributed equally to this work)*

Martim D. Portal*, **Cristiana F. Pires***, Sara Maia, Inês P. Rodrigues, Margarida S. Silva, José S. Ramalho, Miguel C. Seabra. Molecular tools for direct differentiation of retinal pigment epithelium. 18th ESPCR Meeting. Lisboa, Portugal. 2013. (**These authors contributed equally to this work)*

Inês P. Rodrigues, Sara Maia, **Cristiana F. Pires**, Martim D. Portal, Carolina Thieleke-Matos, Olaf Strauss, Miguel C. Seabra, José S. Ramalho. VEGF secretion by retinal pigment epithelium is regulated by Rab GTPases. 18th ESPCR Meeting. Lisboa, Portugal. 2013.

Inês P. Rodrigues, Sara Maia, **Cristiana F. Pires**, Martim D. Portal, Carolina Thieleke-Matos, Olaf Strauss, Miguel C. Seabra, José S. Ramalho. A novel in vitro model to study hypoxia-induced effects in retinal pigment epithelium. Molecular Biology in Portugal and EMBL (and EMBL Alumni). Lisbon, Portugal. 2013.

Inês P. Rodrigues, Sara Maia, **Cristiana F. Pires**, Martim D. Portal, Carolina Thieleke-Matos, Olaf Strauss, Miguel C. Seabra, José S. Ramalho. A novel in vitro model to study hypoxia-induced effects in retinal pigment epithelium. EMBO Young Scientists' Forum. Lisbon, Portugal. 2013.

Cristiana F. Pires, Sara Maia, Martim D. Portal, Inês P. Rodrigues, Tanya Tolmachova, José S. Ramalho, António Jacinto, Miguel C. Seabra. Towards the generation of induced Pluripotent Stem cells from a model of retinal degeneration: following reprogramming events. 8th International Meeting of the Portuguese Society for Stem Cells and Cell Therapies. Faro, Portugal. 2013.

Cristiana F. Pires, Inês P. Rodrigues, Sara Maia, Martim D. Portal, José S. Ramalho, Miguel C. Seabra. Optimization of a Retinal Pigment Epithelium differentiation protocol driven by ectopic expression of eye transcription factors. 17th ESPCR Meeting. Genève, Switzerland. 2012.

Inês P. Rodrigues, **Cristiana F. Pires**, Miguel C. Seabra & José S. Ramalho. Uncovering the VEGF Secretory Pathway in Retinal Pigment Epithelium: the Rab proteins' role. ARVO 2012 Annual Meeting. Fort Lauderdale, USA. 2012.

Pires, Cristiana F., Ramalho, José S., Seabra, Miguel C. Induced pluripotent stem cell-based therapy for Choroideremia. Cell Symposia: Stem Cell Programming and Reprogramming. Lisboa, Portugal. 2011.

Inês P. Rodrigues, José S. Ramalho, Marta S. Pedro, **Cristiana F. Pires**, Margarida S. Silva, Miguel C. Seabra. Tools for studying Rab proteins' function in secretory pathways in RPE. 1st International Symposium on "Protein Trafficking in Health and Disease". Hamburg, Germany. 2010.

Contents

List of figures

List of tables

Abbreviations

2i	Dual inhibitors (1 µM of MEK inhibitor PD 0325901 and 3 µM of GSK3 inhibitor CHIR99021)
3D	Three-dimensional
a.u.	Arbitrary units
ABC	ATP binding cassette
AMD	Age-related Macular Degeneration
ANOVA	Analysis of variance
AP	Alkaline phosphatase
BMP	Bone morphogenetic protein
cDNA	Complementary DNA
CMZ	Ciliary marginal zone
DAPI	4',6-diamidino-2-phenylindole
DMEM	Dulbecco's Modified Eagle Medium
DMEM/F12	DMEM and Ham's F12 nutrient mixture 1:1
DNA	Deoxyribonucleic acid
DOX	Doxycyclin
DR	Diabetic Retinopathy
E13.5	Embryonic day 13.5
EB	Embryoid body
EF	Eye field
EFTF	Eye field transcription factor
EMT	Epithelial-to-mesenchymal
EpiS cell	Epiblast stem cell
ERK	Extracellular signal regulated kinases 1 and 2
ES cell	Embryonic stem cell
FBS	Fetal Bovine Serum
FGF	Fibroblast growth factor
GFP	Green fluorescent protein
GGTase II	Rab geranylgeranyl transferase
GMP	Good Manufacturing Practice
HLA	Human leucocyte antigen
ICM	Inner cell mass
IF	Immunofluorescence
IGF-1	Insulin-like growth factor-1
iPS cell	induced Pluripotent Stem cell
JAK/STAT	Janus kinase/signal transducers and activators of transcription
KO	knockout
LCA	Leber Congenital Amaurosis
LIF	Leukaemia Inhibitory Factor
M2rtTA	Reverse tetracycline-controllable transactivator
MAPK or MEK	Mitogen-activated protein kinase
MEF	Mouse embryonic fibroblast
Melan Ink4a	Bl6 (Black6) Ink4a -/- Melanocytes
MET	Mesenchymal-to-epithelial
MFI	Median Fluorescent Intensity

miRNA	microRNA
MOI	Multiplicity of infection
MTT	3-[4,5-dimethylthiazol-2-yl]-2,5 diphenyl tetrazolium bromide
NOD.Scid	Non-obese diabetic/ severe combined immunodeficiency
NPC	Neural progenitor cell
NR	Neuroretina
OC	Optic cup
OS	Outer-segment
OSKM	OCT4, SOX2, KLF4, c-MYC
OV	Optic vesicle
PBS	Phosphate buffered saline
PCR	Polymerase Chain Reaction
PEDF	Pigment epithelium-derived factor
PFA	Paraformaldehyde
PI3K	Phosphatidylinositol 3' –kinase
PR	Photoreceptors
Rab GDI	Rab GDP-dissociation inhibitor
RCS	Royal College of Surgeons
REP1	Rab Escort Protein 1
RGC	Retinal ganglion cells
RNA	Ribonucleic acid
ROS	Reactive oxygen species
RPE	Retinal pigment epithelium
RPE	Retinitis Pigmentosa
RT	Room temperature
RT-qPCR	Reverse Transcriptase - quantitative PCR
SCNT	Somatic-cell nuclear transfer
SFEBq	Serum-free floating cultures of EB-like aggregates with quick reaggregation
Smad	Small Body Size / Mothers Against Decapentaplegic
SSEA-1	Stage-specific embryonic antigen-1
TetO	Tetracycline operator minimal promoter
TF	Transcription factor
TGF	Transforming growth factor
UD	Undifferentiated
VEGF	Vascular endothelial growth factor
WT	Wild-type

All the work presented in this thesis was performed by Cristiana Ferreira Pires. Doutora Inês P. Rodrigues helped throughout. From 2012, Doutora Sara Maia, Martim Portal and Catarina Sequeira collaborated in the experiments. Molecular cloning was performed under the guidance of Doutor José Ramalho and with the help of Margarida Silva. Confocal images were acquired with the help of Doutora Carolina Matos. Teratoma formation assay was performed in collaboration with Doutora Jacinta Serpa, who generated the animal models, and Professora Doutora Ana Félix, who performed the histopathological analysis (CEDOC - Morphological Patterns of Disease and Tumor Microenvironment group).

Chapter 1 Introduction

Chapter 1 : Introduction

Cellular Reprogramming

Reprogramming concepts

Multicellular organisms are composed of an assortment of differentiated cells responsible for different functions and whose stability is essential for the growth, survival and perpetuation of the whole organism. During development, uncommitted stem cells differentiate into various tissue-specific cell types, in a process established and maintained by a complex interplay of endogenous and exogenous factors. For a long time, lineage commitment and differentiation was believed to be unidirectional and irreversible, as Conrad Waddington represented in his model in 1957 (Figure 1.1). In this classic view of cell fate hierarchy, the undifferentiated cell resides above the different committed and differentiated states. Furthermore, it was long thought that along with the differentiation process, there was a concomitant loss of chromosomes or permanent inactivation of genes that were no longer needed.

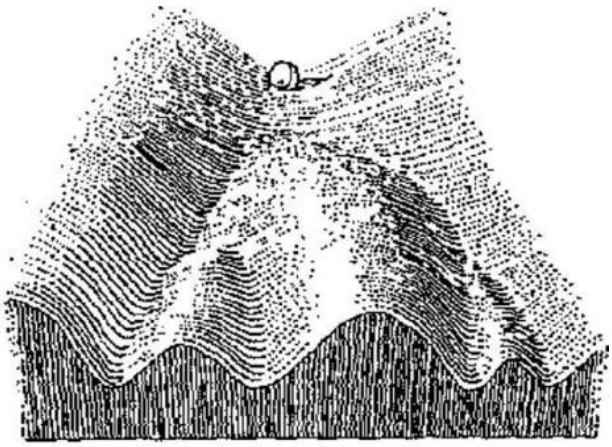

Figure 1.1: Waddington's "epigenetic landscape" model.

In this model, a cell moving towards terminal differentiation is represented as a marble rolling down the landscape that segregates into different grooves on the slope, thereby determining its final and definitive fate. Adapted from (Waddington, 1957).

For instance, in a mammalian organism, the unicellular totipotent zygote lies in the beginning of the developmental process given its ability to give rise to all cells of an organism, including embryonic and extra-embryonic tissues (such as the placenta). At the blastocyst stage of the early embryo, the cells from the inner mass are pluripotent: they are able to generate all the cells of the embryo, and so they form each of the three

germ layers – endoderm, mesoderm and ectoderm. As differentiation follows, cells become progressively more committed to their cell fate and more restricted in terms of developmental potency. Cells that are committed to each of the germ layers specialize to give rise to the tissues of the adult body, which still contains multipotent and unipotent cells. The former retain the ability to differentiate into multiple cell types within the same lineage (such as hematopoietic stem cells and neural stem cells), whilst the later only have the capacity to differentiate into one type of cell as spermatogonial stem cells (Jaenisch and Young, 2008).

Contrarily to this unidirectional developmental process, studies suggesting cellular plasticity in the animal kingdom go back to 1895 when Wolff reported that, after surgical removal of lens from the adult eye of newts, a structurally and functionally complete lens regenerated from the dorsal, pigmented epithelial cells (Wolff, 1895). This example constituted the first experimental evidence of *in vivo* adult cellular reprogramming (or transdifferentiation). Cellular reprogramming (or nuclear reprogramming) refers to the concept of "rewiring the epigenetic and transcriptional network of one cell state to that of a different cell type" (Hanna et al., 2008). Three different experimental approaches have definitively confirmed that, although the differentiated state of a cell is generally stable, cellular identity is dynamically controlled and subjected to perturbations in the stoichiometry of the transcriptional and epigenetic regulators present in the cell in any given time. Nuclear transfer, cell fusion and transcription factor (TF)-transduction have provided means to induce *in vitro* reprogramming of defined and specialized cells either into a different somatic cell type (lineage conversion) or into an embryonic pluripotent state (Figure 1.2) (Yamanaka and Blau, 2010). On 2012, the Nobel Prize in Physiology or Medicine was jointly attributed to John B. Gurdon and Shinya Yamanaka "for the discovery that mature cells can be reprogrammed to become pluripotent".

1. Nuclear transfer

Gurdon efficiently transferred nuclei from highly specialized tadpole intestinal cells into irradiated oocytes, obtaining normal adult frogs. Despite it was a low frequency event, Gurdon interpreted his results as evidence supporting that the process of cell specialization did not require irreversible nuclear changes with permanent gene loss or silencing (Gurdon, 1962). Contrarily, when a nucleus from a differentiated somatic cell is transplanted into an enucleated oocyte, cellular reprogramming is initiated, giving rise to the generation of an entire adult organism, genetically identical to the original somatic cell, thus a clone. This process of

somatic-cell nuclear transfer (SCNT), or cloning, provided definite evidence that cell specialization involves changes in gene expression rather than gene content. Thus, it is a reversible process, once genes that are required to create an entire organism are still present in the nucleus of the specialized cell (despite silenced) and are activated after exposure to the existing reprogramming factors of the oocyte.

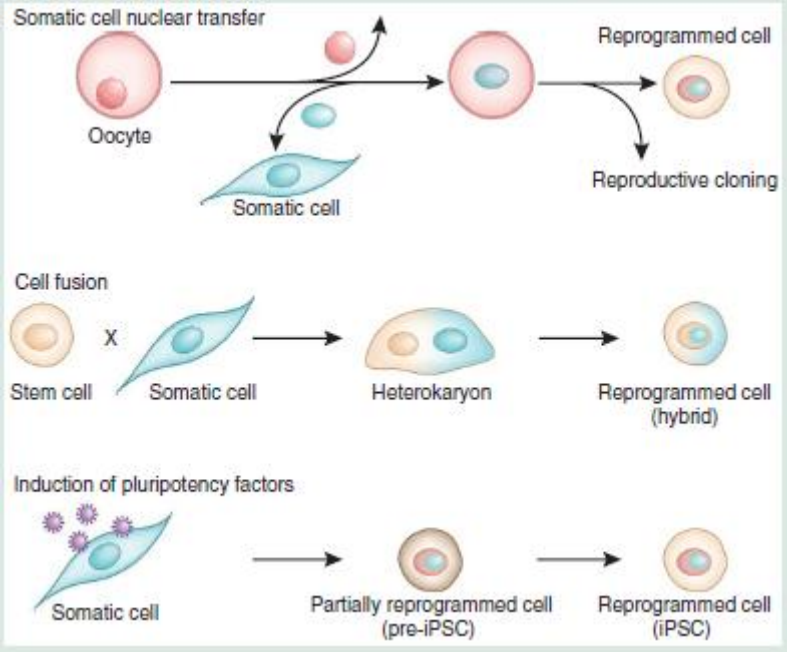

Figure 1.2: Experimental approaches for cellular reprogramming to pluripotency.

In the first approach (top schematic), the nucleus of a somatic cell (diploid) is transplanted into an enucleated oocyte. The somatic cell nucleus now integrated in the environment of the occyte is reprogrammed into a pluripotent state. From this oocyte, a blastocyst is generated and, if development is allowed to occur until completion, an entire cloned organism is generated (reproductive cloning). By cell fusion (middle schematic), two distinct cell types are combined to form a single entity. The resultant fused cell can become a heterokaryon where the nuclei from the original cells are maintained and the genotype of one cell influences the other. Alternatively, if the fused cells proliferate, on cell division the nuclei fuse given rise to hybrids. The third approach (bottom panel), transduction of somatic cells with pluripotency TFs, can be used to generate induced Pluripotent Stem cells (iPSC), once a partially reprogrammed state is overcame. Adapted from (Cantone and Fisher, 2013).

The first successfully cloned mammal was Dolly the sheep by Wilmut and colleagues, mice followed as a wide range of different species. Relevantly, the hypothesis that the reprogramming was only due to contaminating cells was put to rest when a mouse clone was produced from the nuclei of B cells in which the immunoglobulin had been rearranged (Hochedlinger and Jaenisch, 2002; Wakayama et al., 1998; Wilmut et al., 1997). Instrumental contributes to allow

reprogramming of somatic cell into pluripotency was the derivation and stable maintenance of pluripotent cell lines *in vitro*, specifically the derivation of embryonic stem (ES) cells from the blastocyst inner cell mass (Evans and Kaufman, 1981). The efficiency of generating cloned mice is usually low (1-2%), but increases substantially (20%) when the cell source for nuclei is nuclear-transfer-derived ES cells suggesting that the process of nuclear reprogramming is enhanced by a passage through an ES cell state (Hochedlinger and Jaenisch, 2002). Additionally, developmental defects in cloned animals are common and believed to stem from incomplete erasure of "epigenetic memory", meaning that epigenetic factors, such as regulators of DNA methylation, histone modifications and replacements and ATP-dependent chromatin remodelers, have not been completely reprogrammed into a pluripotent state (Simonsson and Gurdon, 2004). Recently, optimized nuclear transfer approach, designed to circumvent early embryonic arrest on prior attempts, allowed the derivation of human nuclear-transfer-derived ES cells (Tachibana et al., 2013).

2. Cell fusion

Cell fusion involves fusing two or more cell types to form a single entity, which can result in heterokaryons (that do not proliferate and thus contain more than one nucleus) or in hybrids (that proliferate, with fusion of the nuclei of the original cell occurring due to cell division). In the 1960s, the existence of trans-acting repressors acting on DNA to regulate gene expression was uncovered by cell fusion experiments of a fibroblast with a melanocyte given rise to a hybrid with no melanin synthesis (Davidson et al., 1966). Moreover, in 1983, heterokaryons of mouse muscle cells and human amniotic cells have been shown to express human muscle proteins (such as human myosin light chains 1 and 2) indicating that previously silenced genes were activated (Blau et al., 1983). Equivalent experiments for other cell types were rapidly performed, with the relative ratio of the nuclei, or the gene dosage, of the two cell types dictating the outcome of the reprogramming, and therefore confirming that the differentiated state was continuously controlled by the balance of regulators present at any given time (Yamanaka and Blau, 2010).

Fusion experiments involving pluripotent cells were also performed and Tada and colleagues showed that thymocytes could acquire a pluripotent state after fusion with ES cells, with activation of a GFP reporter transgene driven by the promoter of

mouse *Oct4* (Tada et al., 2001). Fusion-based nuclear reprogramming was also shown to be strongly enhanced (up to 200-fold) after overexpression of the pluripotency TF *Nanog* (Silva et al., 2006). Moreover, experiments with heterokaryons are well suited for elucidating the molecular mechanisms required for the initiation of reprogramming into a pluripotent state, given their rapid rate of reprogramming. Loss-of-function and gain-of-function approaches have allowed to uncover essential molecular players, namely Oct4 and enzymes responsible for DNA demethylation (Bhutani et al., 2010; Pereira et al., 2008).

3. Trancription factor transduction

In the previously described molecularly undefined reprogramming methods, a milieu of components or elements (e.g., transcription factors, histone-modifying and chromatin-remodelling enzymes, and DNA demethylases) that are largely unknown contribute to achieve cellular reprogramming. Conversely, direct reprogramming methods use defined genetic or nongenetic elements to induce rewiring of the cell state (Hanna et al., 2008). Overexpression of a single tissue-specific TF in somatic cells was surprisingly able to activate genes typical of other somatic cell types and alter the cell fate. First report was by Gehring and co-workers using *Drosophila melanogaster* in 1987, followed by another work showing that ectopic expression of *eyeless* (*Pax6* in mice), a master regulator of eye morphogenesis, lead to induction of ectopic eye structures on the wings, the legs and the antennae (Halder et al., 1995; Schneuwly et al., 1987). Davis and colleagues have demonstrated reprogramming of mouse fibroblasts into myoblast-like cells upon ectopic expression of the MyoD transcription factor (Davis et al., 1987). More recent work has shown that overexpression of a myeloid transcription factor CCAAT/ enhancer-binding protein α (C/EBPα) promotes conversion of lineage-committed B and T cells into macrophage-like cells (Xie et al., 2004).

More surprisingly, Takahashi and Yamanaka reported in 2006 that forced expression of a combination of only 4 TF-encoding genes could generate ES cell-like pluripotent cells from mouse fibroblasts (Takahashi and Yamanaka, 2006). The authors first selected 24 genes expressed by ES cells as candidates for factors that would induce pluripotency in somatic cells. Retroviral-mediated transduction of mouse fibroblasts with the 24 genes followed by drug selection for reactivation of the *Fbx15* gene was used to test their ability to induce pluripotency. *Fbx15* gene is specific of ES cells and a reporter system containing *Fbx15* promoter driving

expression of neomycin resistance cassette was used. Drug-resistant clones were isolated and demonstrated morphology, proliferation and gene expression similar to ES cells. To confirm pluripotency, cells were injected into immunodeficient mice, forming teratomas, tumours including all three germ layers, endoderm, mesoderm and ectoderm. To further determine which of the 24 candidates were critical for the reprogramming process, the effect of withdrawal of individual factors from the pool of transduced candidate genes on the formation of drug-resistant colonies was assessed. Four TFs were identified as being essential for the reprogramming of fibroblasts into pluripotent cells, Oct4, Sox2, Klf4 and c-Myc, and resulting cells were named **induced Pluripotent Stem cells (iPS cells).** After Yamanaka's seminal discovery, a panoply of subsequent works followed, demonstrating optimized ways of generating iPS cells or providing mechanistic insights of the reprogramming process. Importantly, human iPS cells were generated and proof-of-principle experiments demonstrated its therapeutic potential, as such cells can be used as a cell source for tissue repair or replacement while avoiding ethical and immunological concerns associated with the use of ES cells (Takahashi et al., 2007a; Yu et al., 2007). Besides patient-specific, disease-specific pluripotent cell lines derived from human patients with specific diseases were obtained, constituting invaluable tools and an unlimited source for biological material that can be used to study these complex diseases in the Petri dish (Park et al., 2008; Raya et al., 2009).

Furthermore, the unexpected finding that somatic cells can revert all the way back to the embryonic state by a handful of transcription factors soon inspired the discovery of TF-mediated conversion of pancreatic exocrine cells to β cells and fibroblasts into other cell lineages, namely neurons, hepatocytes, and cardiomyocytes (Huang et al., 2011; Ieda et al., 2010; Vierbuchen et al., 2010; Zhou et al., 2008). Both TF-mediated approaches to directly reprogram somatic cells into pluripotency or into another cell type, and their applications, will be extensively discussed in subsequent sections.

All the three mentioned approaches to cellular reprogramming display common features, such that in each case if the balance of regulators is tilted to favour pluripotency (or other somatic cell fate), the epigenome is altered and the expression of pluripotency/cell-specific factors that otherwise would be silenced in a stably differentiated cells. In order to maintain the new phenotypic identity of the reprogrammed cell, there must be activation of feedback and auto-regulatory mechanisms to attain critical threshold levels of endogenous cell-specific transcriptional regulators. Nevertheless, when comparing the 3 approaches, there are differences in terms of technical feasibility, time required for reprogramming, efficiency of the process, cell yield and probably also in the underlying molecular mechanism. In terms of cell yield, TF-transduction provides the abundant and easily reproducible across the world generation of iPS cells, which concurs to their advantageous prospective use in therapeutic settings, as well as usefulness for disease-modelling and drug testing (Hanna et al., 2008; Yamanaka and Blau, 2010). Additionally, the advent of these technological breakthroughs has put to argue the paradigm of unidirectional development. A non-hierarchical “epigenetic disc” model to explain interconversion of somatic and pluripotent cell fates has been recently proposed as an alternative to Waddington’s classical view (Ladewig et al., 2013).

Somatic to pluripotent TF-mediated reprogramming

Pluripotent stem cell lines can be obtained through the reprogramming of somatic cells, by ectopic expression of defined factors known to be important for the maintenance pluripotent stem cells identity. Generated iPS cell lines are characterized and compared with their biological counterparts (ES cells) in order to assess reprogramming efficiency and fidelity. Moreover, several studies of the molecular basis, both genetic or epigenetic, of these natural and induced pluripotent states, as well as investigations into how pluripotency is maintained and the mechanisms of lineage commitment have provided insights for improving the understanding of mammalian embryogenesis and cellular differentiation, but also for developing successful stem cell-based therapies for regenerative medicine.

Pluripotency regulation: transcriptional network and signalling pathways

Pluripotent stem cells have two remarkable properties: immortality, or the faculty of indefinite self-renewal, and pluripotency, the ability to give rise to all the tissues of

the adult body. ES cells were first isolated from the inner cell mass (ICM) of pre-implantation mouse blastocyst embryos at embryonic day 3.5 (E3.5). Mouse ES cells are rapidly proliferating cells that form tight, dome-shaped colonies (Evans and Kaufman, 1981). To maintain their self-renewal capacity in an undifferentiated state, they require the growth factors leukaemia inhibitory factor (LIF) and bone morphogenetic protein 4 (BMP4) in mouse embryonic fibroblast (MEF)- and serum-free conditions, respectively (Figure 1.3) (Williams et al., 1988a; Ying et al., 2003). The pluripotent cells in the pre-implantation embryo are considered naïve because they have unbiased developmental potential and can give rise to germline-competent chimeras when reintroduced into a blastocyst. Contrarily, another stem cell population derived from post-implantation embryo, epiblast stem (EpiS) cells, exhibits a "primed" state of pluripotency (Nichols and Smith, 2009; Tesar et al., 2007). Human ES cells are derived from human blastocysts but, in contrast to murine ES cells, form flat 2D colonies dependent on basic fibroblast growth factor (bFGF) and activin/transforming grothw factor-β (TGFβ) signalling (Figure 1.3) (Thomson et al., 1998). Human ES cells share several molecular features with naïve mouse ES cells but they also share a variety of epigenetic properties with primed murine EpiS cells, displaying a "primed" pluripotency. Very recently however, derivation conditions for the establishment of human naïve pluripotent cells was also reported (Gafni et al., 2013).

There is a **core regulatory circuitry** composed of a set of TF that functions to maintain the pluripotent state in pluripotent stem cells, natural or induced and in humans and mice. OCT4 (also known as POU5F1), NANOG and SOX2 function together to positively regulate their own promoters, forming an interconnected autoregulatory loop. Additionally, they co-occupy promoter regions of genes that are involved in pluripotency maintenance (keeping them in an active state) and early lineage differentiation (repressing them) (Figure 1.3) (Masui et al., 2007; Silva and Smith, 2008; Young, 2011).

POU family TF Oct4 was found to be required for the formation of the naïve epiblast, from which pluripotent cells emerge during pre-implantation. In Oct4-null embryos, the inner cell mass lacks pluripotent characteristics. In addition, Oct4 is also critical for maintaining mouse ES cells since abrogation of Oct4 expression leads to their differentiation along the trophoblast lineage (Nichols et al., 1998; Niwa et al., 2000).

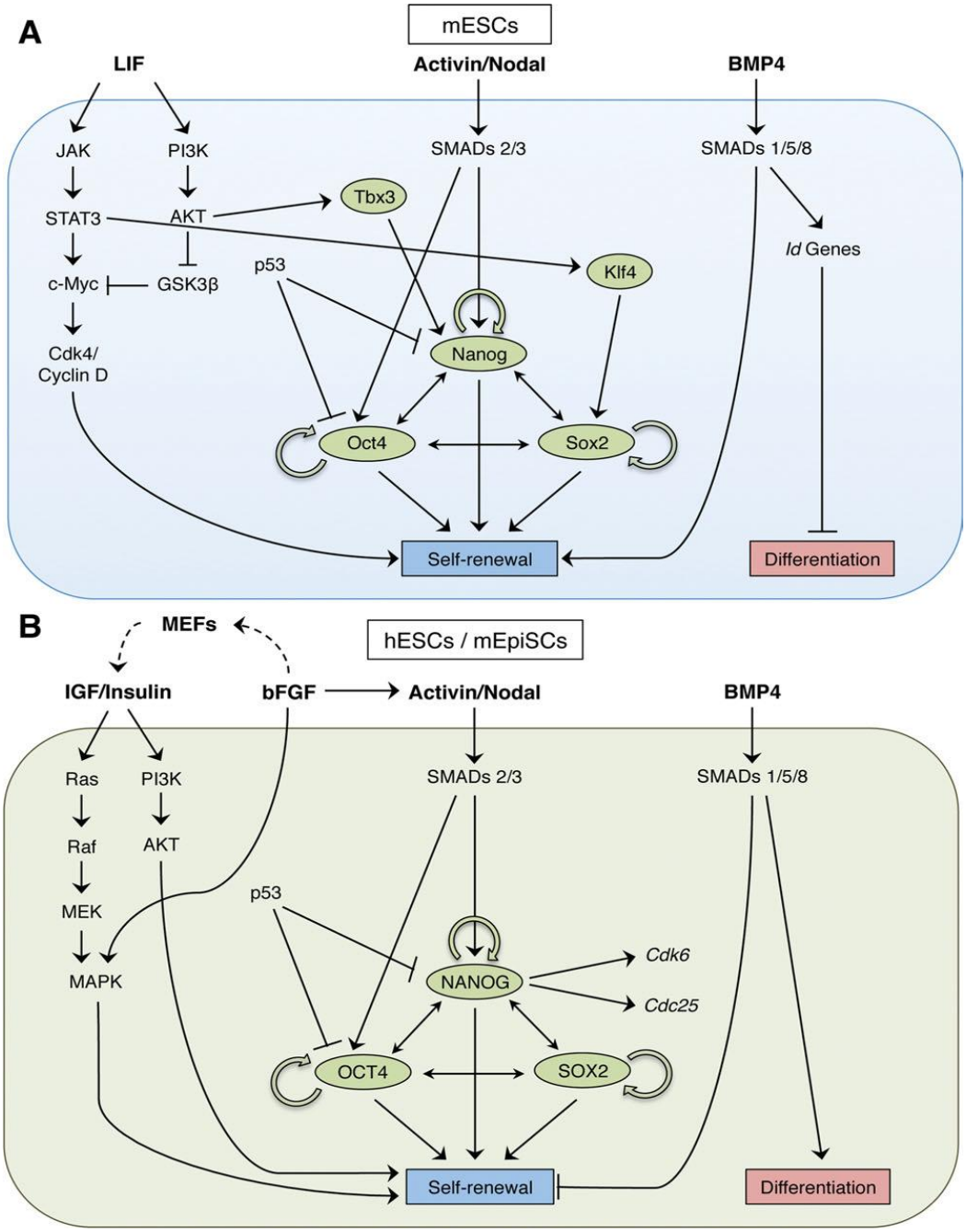

Figure 1.3: Pluripotency maintenance circuitry in mouse and human ES cells.

In both cell types, Nanog, Oct4, and Sox2 form a positive autoregulatory loop that regulates self-renewal and pluripotency. (A) Mouse ES cells require LIF and BMP4 for maintenance. LIF promotes self-renewal by activating the Janus kinase/signal transducers and activators of transcription (JAK/STAT3) and phosphatidylinositol 3' –kinase (PI3K)/AKT signalling pathways. There's an upregulation of *Klf4* and *Tbx3*, which then activate *Sox2* and *Nanog*, respectively. BMP4 upregulates transcription of inhibitor of differentiation (*Id*) genes through activation of SMAD (Small Body Size / Mothers Against Decapentaplegic) proteins 1, 5, and 8. (B) Human ES cells and mouse EpiS cells require *insulin*-like growth factor IGF/insulin and bFGF for maintenance. bFGF activates the mitogen-activated protein kinase (MAPK) as well as the Activin/Nodal signalling pathways, and IGF activates the Ras and PI3K pathways. MEFs are also stimulated by bFGF in culture to secrete IGF (dashed arrows). SMADs 2 and 3 propagate Activin/Nodal signalling as well as directly bind and upregulate *NANOG*. Adapted from (Saunders et al., 2013 and references herein).

Sox2, a SRY-related TF containing the high-mobility group-box DNA-binding domain, has also been shown to possess a loss-of-function phenotype similar to that of Oct4 in both embryos and ES cells. Ectopic expression of wild-type levels of Oct4 can rescue the Sox2-null phenotype in ES cells, which, in addition to the similarity of phenotypes, suggests a synergistic action of the two TFs in regulating the expression of themselves and other ES cells-specific genes (Avilion et al., 2003; Masui et al., 2007).

Nanog is a homeodomain protein that was discovered in a screen for self-renewal factors that could sustain mouse ES cells in the absence of LIF signalling. Nanog is critical for mammalian development and is required for specification of the ICM in the pre-implantation embryo. Although ES cells can be propagated in the absence of Nanog, it promotes a stable undifferentiated ES cell state. Overexpression of Nanog leads to enhanced self-renewal of ES cells, illustrating a positive effect on the pluripotent network (Chambers et al., 2007; Saunders et al., 2013).

The interconnected regulatory loop of Oct4, Sox2 and Nanog promotes a bistable state for ES cells: residence in a positive-feedback-controlled gene expression program when the factors are expressed at appropriate levels, *versus* entrance into a differentiation program when any one of the master transcription factors is no longer functionally available. The core TFs collaboratively activate a substantial fraction of the actively transcribed protein-coding and microRNAs (miRNAs) genes in ES cells. A large proportion of these actively transcribed genes are bound and regulated by both the core transcription factors and also c-Myc, which plays important roles in ES cells proliferation and self-renewal. While Oct4, Sox2, and Nanog core regulators are involved in RNA polymerase II recruitment, c-Myc is believed to stimulate the transcriptional pause release of RNA polymerase II. Consequently, Oct4/Sox2/Nanog apparently play dominant roles in selecting the set of ES cell genes that will be actively transcribed and recruiting RNA polymerase II to these genes, while c-Myc regulates the efficiency with which these selected genes are fully transcribed (Rahl et al., 2010; Young, 2011).

Simultaneously, the core regulators repress the expression of a wide spectrum of cell-lineage-specific regulatory genes, through a process mediated by SetDB1 and Polycomb group (PcG) chromatin regulators. Once their repressive signal is lost, a rapid induction of expression occurs indicating that these genes are poised for activation. Interestingly, the chromatin conformation associated with many of these key developmental genes is composed of ‘bivalent domains’ consisting of both inhibitory histone H3 lysine 27 methylation marks and activating histone H3 lysine

4 methylation marks. These bivalent domains are lost in differentiated cells. Thus, the core regulatory circuitry, and additional collaborative regulators of gene expression, are responsible for maintaining ES cells in a stable pluripotent state whilst remaining poised to differentiation (Bernstein et al., 2006).

In addition to Oct4, Sox2, Nanog, and c-Myc, the transcription factors Tcf3, Smad1, Stat3, Esrrb, Sall4, Tbx3, Zfx, Ronin, Klf2, Klf4, Klf5, and PRDM14 have been shown to play important roles in control of ES cell state. Transcriptional regulation of pluripotency state is also dependent on cofactors, protein complexes that contribute to activation (coactivators) and repression (corepressors) of expression but do not have DNA-binding properties of their own. Chromatin regulators, such as cohesin/condensin protein complexes, histone-modifying enzymes, ATP-dependent chromatin-remodeling complexes and DNA methyltransferases, also play a role in maintaining the ES cell viability and stability. A variety of non-coding RNA species have also been implicated in control of ES cell state, including miRNAs, which can regulate the stability and translatability of mRNAs, and longer non-coding RNAs, which have been implicated in recruitment of chromatin regulators (Yeo and Ng, 2013; Young, 2011).

As mentioned earlier, **signal transduction pathways** are involved in cells' response to their surrounding cellular and biochemical environment. For ES cells, maintenance of the pluripotent state is dependent on the absence or inhibition of signals that stimulate differentiation. Traditionally, mouse ES cells were cultured and kept pluripotent on a layer of mitotically inactivated feeder cells in serum-supplemented media. The combinatorial use of LIF and BMP4 allowed the establishment of a defined feeder- and serum-free culture sufficient to derive and maintain germ-line transmittable mouse ES cells. LIF and BMP4 induce phosphorylation and activation of their downstream TFs Stat3 and Smad1, respectively, which in turn co-bind at Oct4, Sox2 and Nanog regions and thus sustain the core ES cell transcriptional network (Niwa et al., 1998; Pera and Tam, 2010; Ying et al., 2003).

FGF - MEK (mitogen activated protein kinase) - ERK (extracellular signal regulated kinases 1 and 2) signalling has a pro-differentiation effect. Explicitly, stimulation of mouse ES cells by Fgf4, working through the Mek/Erk signalling pathway, is known to induce mouse ES cells to exit self-renewal and initiate differentiation (Kunath et al., 2007). Additionally, mouse ES cells are also responsive to Wnt/β-catenin signalling, which contributes to maintenance of pluripotency. Active canonical Wnt-signalling leads to stabilization of β-catenin which in turn antagonizes the activity of

Tcf3, the most abundantly expressed member of TCF/LEF family of TFs in mouse ES cells. This nuclear effector of Wnt/β-catenin signalling, Tcf3, is bound to the same regulatory regions as Oct4 and Nanog, and has been known to negatively balance their effects in the maintenance of the pluripotent state (Wray et al., 2011). Recently, β-catenin was also shown to contribute to pluripotency acting through an Oct4 complex, on a transcriptional-independent manner (Faunes et al., 2013).

Hallmarks of naïve pluripotency include driving Oct4 transcription by its distal enhancer, retaining a pre-inactivation X chromosome state, and global reduction in DNA methylation and in H3K27me3 repressive chromatin mark deposition on developmental regulatory gene promoters. In recent years a combination of small-molecule inhibitors has been identified that greatly facilitates murine ES cells derivation and maintenance in a naïve pluripotent state. This so-called **2i inhibitor cocktail** consists of a MEK/ERK inhibitor (PD0325901) and a GSK3 inhibitor (CHIR99021). 2i culture conditions promotes the achievement of a “ground state” pluripotency by blocking the pro-differentiation effect of the FGF–MEK–ERK signalling pathway and simultaneously inhibiting glycogen synthase kinase GSK3b, thereby promoting the self-renewal positive effect of Wnt/β-catenin signalling. Moreover, factors associated with lineage-specification are repressed under 2i culture conditions, at an epigenetic level. A more homogeneous expression of key pluripotency regulators is also induced in 2i culture conditions. Particularly, biallelic expression of the key pluripotency regulator Nanog is achieved (whilst in serum conditions Nanog is only expressed by one allele), which has been shown to be important for the survival of the peri-implantation inner cell mass (Marks et al., 2012; Miyanari and Torres-Padilla, 2012; Silva et al., 2008; Ying et al., 2008).

Mechanistic insights into the reprogramming process

The precise molecular mechanisms that underlie the reprogramming of differentiated cells to iPS cells remain largely unknown. However, systematic studies addressing this issue have been demonstrating that the cells transit through distinct intermediate states, which can be simplified in two major phases, one transgene dependent followed by a transgene independent phase (Figure 1.4).

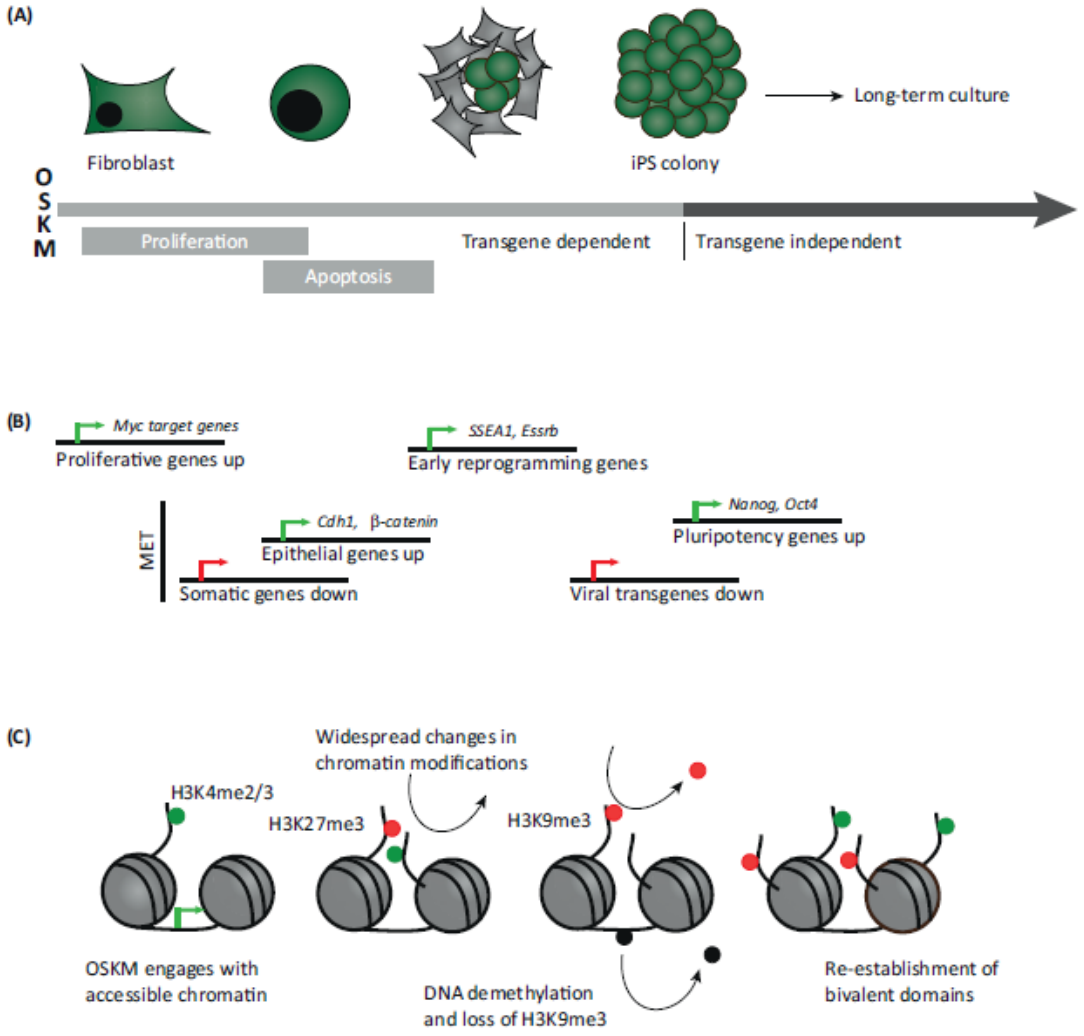

Figure 1.4: Selected molecular events occurring during reprogramming.

(A) The reprogramming process involves intermediate cell states, defining two general phases. In the first, removal of exogenous factors results in reversion into the differentiated state. During this transgene-dependent phase, a set of morphological alterations is observed, with early reprogramming cells rapidly dividing and beginning to form clusters. Following this expansion, apoptosis is observed and eventually cells will form tight colonies of fully-reprogrammed cells. At this point, a transgene-independent state is achieved with the withdrawn of reprogramming factors no longer preventing the final transition to pluripotency. (B) Concomitantly, alterations in gene expression are observed along the process. First, there is an upregulation of proliferative genes followed by a mesenchymal-to-epithelial (MET) transition seen at an intermediate state. Silencing of the somatic program occurs, whilst the permanent reactivation of the core pluripotency network is observed later on the process. (C) Reprogramming factors (OSKM) initially bind to accessible chromatin locations, as defined by the epigenetic status of the somatic cell. A general loss of repressive histone and DNA modifications is observed. DNA demethylation is a crucial barrier for reprogramming and, once overcome, fully reprogrammed cells are obtained. X- chromosome reactivation and telomere elongation are also observed. Adapted from (Federation et al., 2013).

Reprogramming process is initiated by the forced expression of traditional OSKM factors. However, in the nucleus, the majority of DNA is packed into nucleosomes, occluded by higher order chromatin structure and repressors. Cell proliferation may facilitate reprogramming by allowing TF access to otherwise occluded cis-regulatory regions through nucleosome displacement during DNA replication. In the absence of cell division, several models have been proposed to account for the access of transcription factors to their relevant binding sites, including the 'pioneer' TF model. Contrarily to other factors, pioneer factors can access their target sites in repressed regions of the genome, through inducing local chromatin opening, nucleosome repositioning, and recruitment of chromatin modifiers and co-regulators. OCT4, SOX2 and KLF4 might act as pioneer factors, facilitated by C-MYC proliferative action. This initiation is then followed by feed-forward induction of additional TFs to execute the reprogramming process (Soufi et al., 2012; Taberlay et al., 2011; Vierbuchen and Wernig, 2012).

In the early stages of reprogramming, gene expression is stochastic with resulting differential expression of genes involved in cell-division cycle, DNA replication and a process called the mesenchymal-to-epithelial (MET) transition, which also occurs during normal development (Li et al., 2010a). In parallel, some cells show reduction in the expression of genes associated with cell–cell interaction and cell adhesion, and of markers that are typical of the initial differentiated-cell population. MET is one of the earliest observable events occurring during fibroblast reprogramming, with elongated cells become rounded and aggregated in small clusters. This transition correlates with alkaline phosphatase (AP) positivity and stage-specific embryonic antigen-1 (SSEA-1) upregulation. There is also an up-regulation of epithelial junction components and involvement of the TGFβ signalling pathway. In terms of epigenetic modification, histone modifications and structural changes that are associated with a more open chromatin conformation are also observed during the early phase of reprogramming (Buganim et al., 2012; Polo et al., 2012).

A progressive increase in the expression of early - albeit not definitive - markers of pluripotency is observed. At this point, reprogramming-refractory and reprogramming-competent cells coexist, expressing different levels of the reprogramming factors and giving rise to heterogeneous cell populations. A second "wave" of molecular events follows, with cells hierarchically increasing the expression of genes that are involved in the establishment and maintenance of pluripotency. DNA demethylation has been proposed to be a crucial barrier for reprogramming, occurring in the late stage of reprogramming and contributing to

locking the defined pluripotent state (Buganim et al., 2012; Cantone and Fisher, 2013; Polo et al., 2012).

Oct4 has an established importance in the reprogramming process since it can be used alone to obtain iPS cells. Mechanistically, experimental evidence suggests that Oct4 participates in the induction of the MET and in the derepression of somatic cell chromatin. In addition, Oct4 in cooperation with Sox2 was proposed to prevent the acquisition of alternative cell states during reprogramming. Furthermore, Oct4 dose and cellular localisation were proposed as important parameters of successful reprogramming: an ES cell level of Oct4 must be attained at the late stages of reprogramming for cells to enter the pluripotent cell state (reviewed by (Radzisheuskaya and Silva, 2013).

Technological overview of reprogramming into pluripotency

At first, Yamanaka reported the generation of iPS cells through forced expression of a set of core pluripotency-related TF (OCT4, SOX2, KLF4 and c-MYC – or abbreviated as OSKM) in fibroblasts (Takahashi and Yamanaka, 2006). After TF transduction, tightly compacted colonies appeared on the culture dish, which resembled ES cells morphologically, molecularly and phenotypically (Okita et al., 2007). Several protocols for iPS cells generation have been developed in the following years. They use, for example, different mouse and human donor populations or vary the number, identity and delivery mode of the reprogramming factors (Aasen et al., 2008; Aoi et al., 2008; Carey et al., 2009; Kim et al., 2009; Nakagawa et al., 2008; Okita et al., 2008; Takahashi et al., 2007a). The multitude of the different approaches undertaken over the past few years will not be exhaustively mentioned here, but was recently reviewed by (Bayart and Cohen-Haguenauer, 2013; González et al., 2011).

Direct reprogramming into pluripotency is conceptually and technically simple. Nonetheless it is still an extremely slow and inefficient process influenced by several variables that affect its efficiency, reproducibility and the quality of the resulting iPS cells. Several parameters must be considered prior to the generation of iPS cells, namely the cell type to be reprogrammed, the reprogramming factors to be used and their delivery method (Figure 1.5).

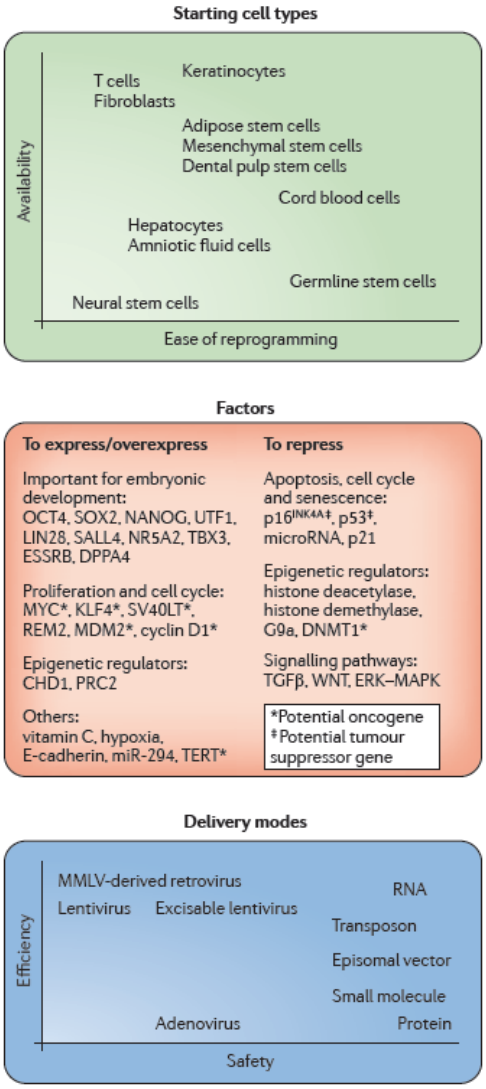

Figure 1.5: Parameters to consider before each reprogramming experiment.

Any reprogramming experiment is determined by a number of preliminary choices regarding the donor cell type to reprogram, the factors to use and the mode of their delivery. The choice of the initial cell type depends not only on its availability but also the ease of reproducing the reprogramming process. The TFs important for embryonic development must be overexpressed, alone or in conjunction with other positive or negative regulators of cell cycle, epigenetic markers or signalling pathways. Forced expression of the reprogramming factors can be achieved through several available delivery modes with variable efficiency and safety. CHD1, chromodomain-helicase-DNA-binding protein 1; DNMT1, DNA methyltransferase 1; DPPA4, developmental pluripotency associated 4; E-cadherin, epithelial cadherin; ERK, extracellular signal-regulated kinase; MAPK, mitogen-activated protein kinase; MMLV, Moloney murine leukaemia virus; PRC2, Polycomb repressive complex 2; SV40LT, SV40 large T antigen; TERT, telomerase reverse transcriptase; TGFβ, transforming growth factor-β. Adapted from (González et al., 2011).

Different efficiencies and kinetics have been observed depending on the **starting cell**. The reprogramming process requires the delivery of certain factors into a specific cell and their adequate expression for a proper period of time, usually smaller for mouse than for human cells. Fibroblasts are still the most widely used

cells, however reprogramming efficiency may be higher in different cellular populations, such as keratinocytes (with the further advantage of their ease to obtain from human donors) (Aasen et al., 2008). Moreover, in some certain populations, the reprogramming efficiency is higher or the requirement for factors is smaller given the high levels of endogenous expression of reprogramming TFs. For instance, neural progenitor cells, which express SOX2 endogenously, are reprogrammed in the absence of exogenous SOX2 or with OCT4 alone (Kim et al., 2009). The differentiation status of the donor cell has also shown to influence both the efficiency of the process and the quality of the generated cells.

The **factors** that induce reprogramming are genes that are normally expressed early during development and are involved in the maintenance of the pluripotency of cells from the inner cell mass of the pre-implantation embryo. Core regulatory TFs Oct4, Sox2 and Nanog are usually included in reprogramming cocktails, such as OSKM and also early-described alternative cocktail of Oct4, Sox2, Nanog and Lin28 (Yu et al., 2007). Other TFs expressed by ES cells, such as SALL4 and UTF1, have been shown to positively affect reprogramming efficiency or kinetics. Influence of cell-cycle regulators on reprogramming has also been highlighted once some factors such as MYC and KLF4, which directly or indirectly affect cell proliferation, have been shown to increase reprogramming efficiency. Contrarily, some factors inhibit reprogramming barriers, such as senescence and apoptosis, and allow an increase in both the speed and efficiency of reprogramming (for instance inhibition of p53) (González et al., 2011; Kawamura et al., 2009).

Besides improvements in the cocktail of TFs, modulation of the reprogramming process has also been achieved by small-molecule compounds, which specifically target kinase signalling pathways or epigenetic regulators. MEK and GSK3 inhibitors used in 2i culture conditions, when in combination with LIF, stabilize iPS cells while inhibiting growth of non-pluripotent cells, and promote the conversion of pre-iPS cells into “ground-state” pluripotency. TGFβ inhibitors (such as ALK4, 5 and 7) have also been used. In conjunction with OSK cocktail, these inhibitors were responsible for the activation of Nanog in partially reprogrammed cells to facilitate transition to fully-reprogrammed iPS cells. Moreover, they also inhibit pro-EMT signals (Maherali and Hochedlinger, 2009; Silva et al., 2008). Targeting the epigenome has also been shown to benefit the reprogramming process and small molecules that function as DNA methylation inhibitors (azacytidine), histone deacetylase inhibitors (valproic acid) and lysine methyltransferase inhibitors have been used to achieve it (Federation et al., 2013). These small molecules have

exclusively been used in combination with the exogenous TFs, until very recently. Hou and colleagues reported the generation of pluripotent stem cells from mouse somatic cells at a frequency up to 0.2% using a combination of seven small-molecule compounds, bypassing the need of TFs (Hou et al., 2013).

Additionally, while most factors used as reprogramming transgenes can be replaced by other means, Oct4 has remained essential until very recently. Shu and colleagues and Montserrat and co-workers reported that mouse and human cells could be reprogrammed into iPS cells using nuclear factors that control lineage specification and are not considered to be core factors of pluripotent stem cells. A ‘‘seesaw’’ model was proposed placing in the centre of the reprogramming process the balance between counteracting differentiation cues. Accordingly, lineage specifiers facilitate reprogramming when they are balanced with other mutually exclusive lineage specifier: Gata3, as well as other mesendodermal specifiers, can replace Oct4, presumably by counteracting the upregulation of ectodermal genes induced by Sox2; Gmnn, an ectodermal specifier, can replace Sox2 in reprogramming, as it attenuates the elevation of mesendodermal genes induced by Oct4. With simultaneous replacement of Oct4 and Sox2 by the mesendodermal and ectodermal specificiers, respectively, the opposing differentiation potentials are balanced and pluripotency state is achieved (Montserrat et al., 2013; Shu et al., 2013).

Finally, **reprogramming methods** can be divided in two classes: integrative and non-integrative. The former involves the integration of the exogenous factors in the host genome whilst the latter is characterized by the absence of genome alterations on the initial cells. Additionally, delivery methods can also be classified in viral and non-viral vectors. Included on the integrative category, retroviral and lentiviral vectors have been used since the early experiments and still provide the higher efficiency of reprogramming. Comparing with retroviral-based strategies, lentiviral vectors have the advantage of transducing both dividing and non-dividing cells. Additionally, the use of inducible promoters has allowed expression of the reprogramming factors in a controllable manner. However, concerns have been raised given the probability of random transgene integration in the genome which could affect the expression of nearby tumour-suppressor genes or oncogenes. Even if properly silenced after the reprogramming process, viral transgenes can eventually be reactivated during differentiation or during the life of iPS cell-derived cells on transplanted animals, leading to tumours. Potential of damage was diminished with polycistronic vectors that allow the expression of several cDNAs

from the same promoter (Carey et al., 2009; Maherali and Hochedlinger, 2008). Integration-free viral methods have also been tried, using adenoviral vectors; however the efficiency of iPS cell generation using this system in the mouse ranges between 0.0001% and 0.0018%, which is approximately three orders of magnitude lower than that for retroviruses (Stadtfeld et al., 2008). Viral methods used for reprogramming into pluripotency are summarized in Table 1.1.

Table 1.1: Viral delivery methods of reprogramming factors.

The main viral delivery methods are summarized, with their advantages and caveats shown below. For each of the methods, details for the design of the vector is shown at the top, followed by the status of the cell after initial delivery of the vector, then the status of the vector in reprogrammed cells (iPS cells). Finally, the status of the transgenes after the differentiation of the pluripotent cell is also highlighted. DOX, doxycyclin; MLV, Moloney murine leukaemia virus. Adapted from (González et al., 2011) and references herein.

Viral delivery methods

	MMLV-derived retrovirus	Lentivirus			Adenovirus
		Constitutive lentivirus	DOX-inducible lentivirus	Excisable lentivirus	
	Multiple single gene or single polycistronic vector.				
Factor delivery	Infects dividing cells. Efficient infection and genome integration.	Infects dividing and non-dividing cells. Efficient infection and genome integration.			Infects dividing and non-dividing cells. Not very efficient infection but no genome integration.
Cell after initial factor delivery	Vector integrated/ active.	Vector integrated/ active.	Vector integrated/ active (+DOX).	Vector integrated/ active.	In theory, vector not integrated.
Reprogammed cell (iPS cell)	Vector integrated, silenced.	Vector integrated, may or may not be silenced.	Vector integrated, silenced when DOX is removed.	Vector integrated, deleted in presence of Cre.	In theory, vectors not integrated; lost by dilution.
Differentiated cell	Transgenes reactivated?	Transgenes active or reactivated?	In theory, transgenes off.	Transgenes deleted.	In theory, no transgenes.
Advantages	Very efficient and stable.			Transgene-free; little scar on the genome.	Transgene-free and vector-free; no genomic integration.
Disadvantages	Many viral integrations (fewer with polycistronic system); transgenes present in the genome.	Genome integration; residual transgenes' expression.	Viral integrations (fewer with polycistronic system); transgenes present in the genome but silent in the absence of DOX.	Possible long terminal repeat integration close to oncogene.	Slow and inefficient.

Alternates to viral delivery systems, non-viral approaches have been attempted based on standard DNA transfection using liposomes or electroporation. A polycistronic plasmid, in which the OSKM transgene is flanked by *lox*P sites, and thus can be deleted by transient expression of Cre recombinase was developed (Kaji et al., 2009). PiggyBac transposon system was also tested, which includes a donor plasmid containing the transposon (containing the sequence of interest flanked by the 5′ and 3′ terminal repeats required for transposition), co-transfected with a helper plasmid expressing the transposase. PBs are, in theory, precisely deleted without modifying the sequence of the integration site upon remobilization by the transposase, contrarily to Cre-excisable linear transgenes which leave a genomic scar (Kaji et al., 2009; Woltjen et al., 2009). Non-integrative approaches were also established, taking advantage of non-replicating or replicating episomal vectors, the latter being maintained through cell division and possibly being removed by culturing the cells in the absence of drug selection (Yu et al., 2009). Alternatively, minicircle vectors allow the expression of the reprogramming factors as non-integrating, non-replicating episomes, but with higher transfection efficiency and longer ectopic expression of the transgene (Jia et al., 2010). In order to completely eliminate plasmid or viral vectors, reprogramming of somatic cells into pluripotency was also achieved by delivery of synthetic modified mRNAs or recombinant proteins. In the first case, the efficiency reached was much higher than that achieved with other non-integrative systems, with 2% of neonatal fibroblasts being converted into iPS cells in just 17 days (Warren et al., 2010). Protein-based strategies, although very promising, are difficult to use routinely due to the difficulties in purifying the recombinant protein. Moreover, this approach show extremely slow kinetics and poor efficiency (Zhou et al., 2009). Non-viral approaches of reprogramming to pluripotency are summarized in Table 1.2.

.

Table 1.2: Non-viral delivery methods of reprogramming factors.

The main non-viral delivery methods are summarized, with their advantages and caveats shown below. DNA-based delivery methods include those that do or do not involve integration into the genome. For each of the methods, the status of the cell after initial delivery of the vector is shown, followed by the status of the vector in reprogrammed cells (iPS cells) and finally the status of the cells after differentiation — in each case the cells should be transgene-free. PB, piggyBac; oriP/EBNA1, oriP/Epstein–Barr nuclear antigen-1-based episomal vector. Adapted from (González et al., 2011) and references herein.

Non-viral delivery methods

	DNA-based				Others	
	Integrative		Non-integrative		RNA	Proteins
	PB transposon + Helper plasmid (PB transposase).	Linear DNA fragment (flanked by *lox*P sites).	Episomal non-replicative vectors or minicircle.	Replicative episomal vectors + oriP/EBNA1.	Modified RNAs.	Proteins.
Factor delivery	Liposome or electroporation.					
Cell after initial factor delivery	Vector integrated.		In theory, vector not integrated.		No possibility of integration.	
Reprogammed cell (iPS cell)	Integrated vector deleted (PB transposase).	Vector integrated, deleted in presence of Cre.	In theory, vectors not integrated; lost by dilution.	In theory vectors not integrated; 2/3 maintain vectors, 1/3 lose vectors.	No possibility of integration.	
Differentiated cell	Transgene-free.					
Advantages	Transgene-free and vector-free; average efficiency.		Transgene-free and vector-free; no genomic integration.		Transgene-free and vector-free; no genomic integration; no need to screen numerous colonies (all integration-free); as efficient as retrovirus.	Transgene-free and vector-free; no genomic integration; no need to screen numerous colonies (all integration-free).
Disadvantages	Genomic integration; negative selection strongly advised.		Slow and inefficient; need to check numerous lines to find integration-free ones; labour-intensive.		Multiple transfections required.	Slow and inefficient.

Regardless of the initial cell type, reprogramming factors and delivery mode implemented, obtained iPS cell lines must be thoroughly characterized and an array of criteria must be attained to confirm the fidelity and efficiency of the reprogramming process. Fully reprogrammed iPS cells must demonstrate morphological, molecular and functional equivalence with their biological counterparts, ES cells. Morphologically, iPS cells must appear identical to ES cells and display unlimited self-renewal. At a molecular level, genuine iPS cells must be independent of transgene expression and thus lack expression of the delivered factors. Additionally, gene expression profiles of iPS cells must be indistinguishable of ES cells, particularly in terms of endogenous expression of key pluripotency factors and ES cell-specific surface antigens. Finally, iPS cells must demonstrate their functional pluripotency attribute, explicitly the ability to differentiate into lineages from all three embryonic germ layers (Bayart and Cohen-Haguenauer, 2013; Maherali and Hochedlinger, 2008).

Somatic to somatic TF-mediated reprogramming

Early experiments from Davis and colleagues describing the conversion of fibroblasts into myoblasts through ectopic expression of MyoD TF provided proof-of-principle of cellular plasticity, further demonstrating that a somatic cell could be converted into a different somatic cell type without reversion to pluripotency (Davis et al., 1987). Subsequently, several studies exploiting this direct lineage conversion approach (or transdifferentiation) mediated by overexpression of TFs were performed. Cells from mesodermal, ectodermal and endodermal lineages were successfully converted into distinct somatic cell types of related lineages **within the same germ layer**, with particular attention being dedicated to clinically relevant cell types (Figure 1.6).

Besides myoblast cells, other cellular conversions within the mesodermal lineages were attained. The existing knowledge of the TFs' instructive roles in lineage specification in the haematopoietic system facilitated the conversion of certain haematopoietic lineages into different yet related ones. Conversion of fully committed B cell and T cell progenitors into functional macrophages was achieved through the ectopic expression of the basic Leu zipper transcription factor C/EBPα, the activity of which is required for the formation of granulocyte and macrophage precursors (Xie et al., 2004). A stable macrophage phenotype could be observed as soon as 48 hours after induction. Further work demonstrated that the combination of C/EBPα and another TF important for early lineage decisions of haematopoietic progenitors towards a granulocyte and monocyte fate (PU.1) was sufficient to induce macrophage-like cells from fibroblasts, with the resulting cells

exhibiting upregulation of lineage-specific genes and phagocytic functionality *in vitro* (Feng et al., 2008).

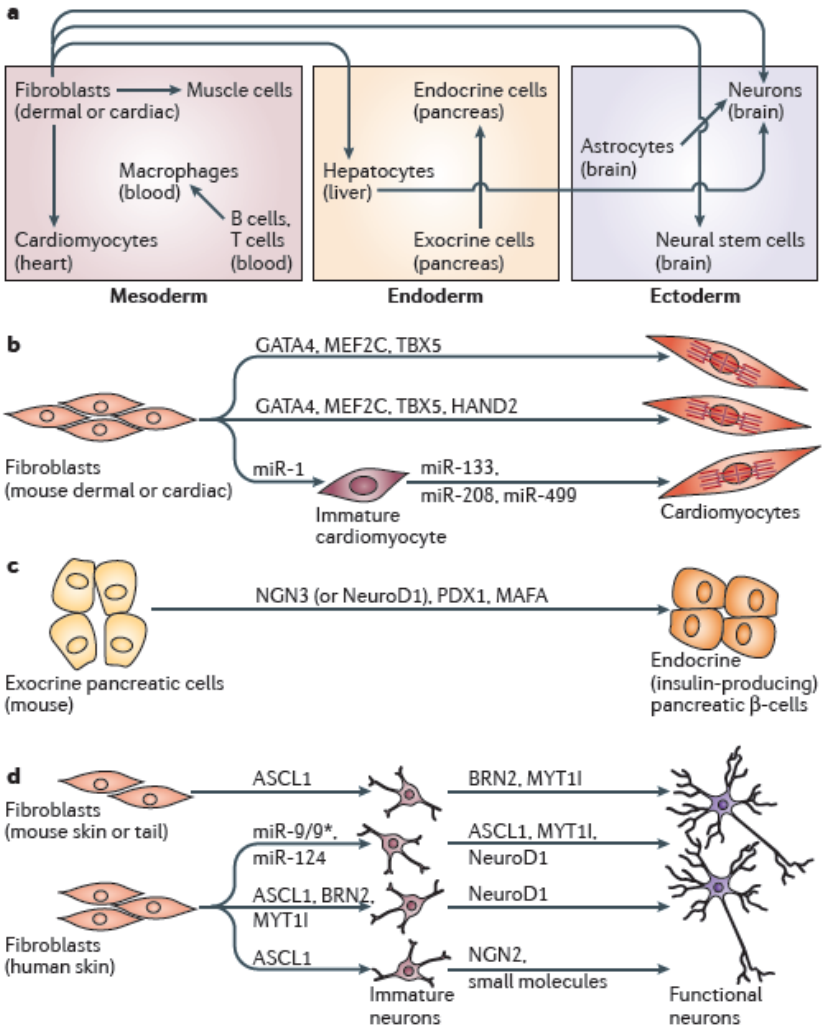

Figure 1.6: Direct lineage conversion of somatic cells.

a) The schematic illustrates successful intra- and trans-germ layer conversion approaches. b) Transdifferentiation within the mesoderm. Different combinations of TFs or miRNAs have the potential to convert fibroblasts into immature or fully mature cardiomyocytes. c) Transdifferentiation within the endoderm. A combination of 3 TFs can convert exocrine pancreatic cells into endocrine insulin-producing pancreatic β-cells. d) Transdifferentiation across different germ layers from the mesoderm to the ectoderm. Induced neurons can be generated by different sets of TFs or miRNAs. Additional factors or small molecules increase the maturity of the generated neurons. Adapted from (Ladewig et al., 2013).

The limited regenerative capacity of cardiac muscle inspired the search for alternative cell sources for replacement therapies. Mouse cardiac and dermal fibroblasts have been converted to cardiomyocyte-like cells. Candidate factors were selected from a suite of genes expressed in cardiomyocytes and associated with clear developmental cardiac

defects in mutants. A initial pool of 14 factors was further refined into 3 TFs GATA4, MEF2C and TBX5 capable of inducing the expression of cardiac markers in fibroblasts without transitioning through a cardiac-progenitor state (Ieda et al., 2010). The conversion occurred very rapidly, with the first induced cells appearing 3 days after transduction. Induced cardiomyocytes expressed cardiac-specific markers, had a global gene expression profile similar to cardiomyocytes, and contracted spontaneously, after a further maturation step. Additionally, fibroblasts transplanted into mouse hearts one day after transduction of the 3 factors also differentiated into cardiomyocyte-like cells *in situ*. Using the same cocktail of TF, it was also possible to directly convert *in vivo* resident cardiac fibroblasts into functional cardiomyocytes, with resulting decreased infarct size and attenuated cardiac dysfunction (Qian et al., 2012). Alternatively, cardiomyocytes could also be obtained from *in vitro* and *in vivo* transdifferentiation of fibroblasts when adding a fourth TF to the cocktail, HAND2 (Song et al., 2012). Importantly, beside TFs, miRNAs known to be involved in cardiac development were shown to mediate conversion of fibroblasts into cardiomyocytes both *in vitro* and *in vivo* (Figure 1.6b) (Jayawardena et al., 2012).

Cell fate conversion within the endoderm was achieved by overexpression of 3 TFs in pancreatic exocrine cells, which was sufficient to induce transdifferentiation into functionally insulin-producing β-cells. NGN3 (or NeuroD1), PDX1 and MAFA correspond to TFs known to be expressed in mature β-cells and their precursors, and to originate disturbed β-cell development when mutated (Zhou et al., 2008) (Figure 1.6c).

It was assumed for long time that lineage reprogramming was only possible between closely related cell types, which likely share some epigenetic features as a result of their recent descent from a common progenitor cell. Inspired for increased knowledge in cellular reprogramming mechanisms and the generation of iPS cells, several teams began to assess combinations of lineage-specific TFs for their capacity to directly convert somatic cells into developmentally unrelated cell fates, and so **across germ layers**.

Pioneering experiments by Wernig and colleagues demonstrated the direct conversion of fibroblasts into induced neurons (iN) (Figure 1.6d). A combination of only 3 factors, Ascl1, Brn2 and Myt1l was enough to rapidly and efficiently convert mouse embryonic and postnatal fibroblasts into functional neurons *in vitro*. The resulting iN cells expressed multiple neuron-specific proteins, generated action potentials and formed functional synapses (Vierbuchen et al., 2010). The generation of iNs from human fibroblasts was also achieved, with the conversion being facilitated by the addition of the NeuroD1 TF to the reprogramming cocktail (Pang et al., 2011). Subsequently, refinement of the initial iN

cocktail was attempted in order to enhance the conversion efficiency and to achieve direct conversion into disease-relevant specific neuronal types. Dopaminergic neurons and spinal cord motor neurons were obtained by combining overexpression of generic neurogenic factors with TF that instruct distinct regional subtypes (Caiazzo et al., 2011; Son et al., 2011). Similarly to cardiac muscle cells, miRNAs were also found to be potent tools for neuronal conversion (Yoo et al., 2011). In an attempt to exploit this approach for studying neurodegenerative disease in human neurons, fibroblasts of a patient with Alzheimer's disease were subjected to a TF cocktail. Obtained iN cells were characterized, displaying features associated with Alzheimer's disease, such as the accumulation of the beta amyloid peptides, highlighting the potential use of this system in disease modelling studies (Qiang et al., 2011).

Conversion of mesodermal into ectodermal lineage was also demonstrated. Hnf4α, Foxa1, Foxa2 and Foxa3 TFs were found to drive the direct conversion of mouse embryonic and dermal fibroblasts of mesodermal origin towards the hepatocyte lineage, which develops from the endoderm. Obtained cells showed typical epithelial morphology, expressed hepatic genes and acquired hepatocyte functions (Huang et al., 2011).

Contrarily to pluripotency-inducing reprogramming, all the above mentioned direct lineage conversion protocols do not involve transition through a de-differentiated state. Consequently, transdifferentiation depends on the ability of ectopic TFs to overwhelm pre-existent genetic and epigenetic marks and force the establishment of the target cell identity gene network. Therefore high expression of the reprogramming factors is essential in direct lineage conversion protocols. The direct change in identity-specific genetic networks correlates with rapid kinetics of reprogramming, with specific phenotypic changes being observed as early as a few hours or days after overexpression, contrary to days or weeks in the case of iPS cells. Additionally, direct conversion can proceed in the absence of cell proliferation, generating post-mitotic cells and not progenitor cells, contrarily to iPS cell generation which occurs by step-wise proliferation and de-differentiation (Figure 1.7A and C) (Sancho-Martinez et al., 2012).

Alternatively, several groups have recently reported another approach to cellular conversion exploiting the Yamanaka factors. Transient expression of these factors is thought to lead to an "open" epigenetic state, in the form of multipotent, partially reprogrammed intermediates. These partially reprogrammed intermediates can be differentiated into specific cell types by modulating extracellular developmental cues and without reversion into pluripotency, unless left in medium amenable to pluripotent cell derivation (Figure 1.7B).

Lineage conversion by plastic induction was first used to generate functional cardiomyocytes by Efe and colleagues. After an initial 4 days-period of transgenic expression of OSKM, MEFs could be directly reprogrammed to spontaneously contracting patches of differentiated cardiomyocytes over a period of 11-12 days, once cultured in media containing developmental cues specifically promoting cardiogenesis. The authors further demonstrated that a pluripotent intermediate was not involved in this lineage conversion (Efe et al., 2011).

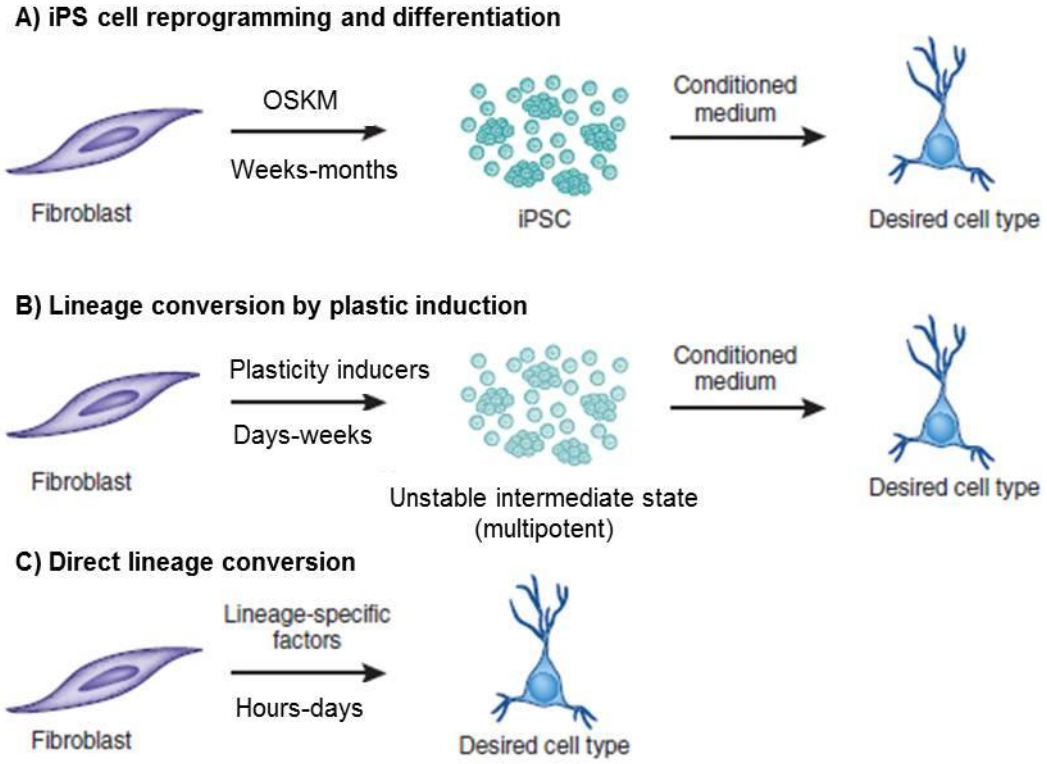

Figure 1.7: Cellular reprogramming strategies allowing the generation of specific cell types.

A) Reprogramming to pluripotency gives rise to iPS cells (iPSC) with unlimited self-renewal capacity (albeit with low efficiencies). The generated iPS cells can be further differentiated into every major cell lineage comprising an adult individual. B) Lineage conversion by induction of cellular plasticity relies on the use of iPS cells reprogramming factors during an initial 'epigenetic activation phase'. Unstable intermediate states can be further differentiated into specific lineages when the appropriate developmental cues are provided by chemically defined differentiation media. Plastic induction is generally accompanied by cell proliferation and allows for the generation of multipotent progenitor cells. C) Direct lineage conversion originates specific cell types as defined by the TF cocktail employed for reprogramming. Generally it implies the generation of post-mitotic cells with limited differentiation and expansion potential. Adapted from (Lujan and Wernig, 2013).

Also exploiting an early “epigenetic activation phase”, the same group demonstrated the conversion of mouse fibroblasts into distantly related ectodermal neural progenitor cells (NPCs). Transient induction of the 4 reprogramming factors (OSKM) followed by induction with defined media gave rise to neural rosettes expressing typical neuronal and NPC markers. An intermediate pluripotent state was not involved in the process and generated NPCs could be expandable *in vitro*, retaining the ability to give rise to multiple neuronal subtypes and glial cells (Kim et al., 2011). Other combinations of pluripotency-related TFs, including Sox2 alone, or in conjunction with neuronal lineage-related TFs were also attempted with the successful generation of intermediate progenitor states bearing multilineage potential (Han et al., 2012; Lujan et al., 2012; Ring et al., 2012; Thier et al., 2012).

Indirect lineage conversion has also permitted the conversion of human fibroblasts into mesodermal progenitor cells. First, an 8 day-period of plastic induction through exogenous expression of OSKM mediated by retroviral or non-integrative delivery methods generated CD34+ angioblast-like cells with bipotent differentiation potential. These progenitor cells could generate endothelial and smooth muscle lineages by treatment with mesodermal induction medium for another 8 days. Differentiated endothelial cells exhibited neo-angiogenesis and anastomosis *in vivo* (Kurian et al., 2013).

In conclusion, two different reprogramming approaches complementary to iPS cell generation (followed by differentiation) have been described to promote somatic to somatic cell conversion. First, a direct lineage conversion without going through undifferentiated states allows identity switch of cell type A into cell type B in the absence of proliferation. Secondly, indirect conversion through a de-differentiation process leads to the generation of intermediate proliferative states with multilineage differentiation capacity. This plastic state can be subsequently committed into a differentiation state by exposure to developmental cues (extracellular signals or late-identity specification TFs) (Ladewig et al., 2013; Sancho-Martinez et al., 2012).

Applications

The discovery that differentiated cells can be reprogrammed to pluripotency or other cell fates by treatment with defined factors opened up unprecedented opportunities for biomedical sciences. Although the details and mechanisms underlying the reprogramming events are still being elucidated, the resulting cells are very promising for regenerative medicine applications and other emerging purposes, such as disease

modelling, drug screening and toxicology studies. Additionally, the ability to induce cell fate conversion is also attractive for basic research fields, such as development, cancer, epigenetics and ageing (Figure 1.8).

Cell transplantation therapy

Since human ES cells' isolation, great expectations were put on these cells to provided treatment to incurable disorders, such as Parkinson's disease or heart failure (Thomson et al., 1998). However, prospective use of human ES cells also raised ethical concerns about the usage of human embryos, and medical concerns about the possibility of immunological rejection.

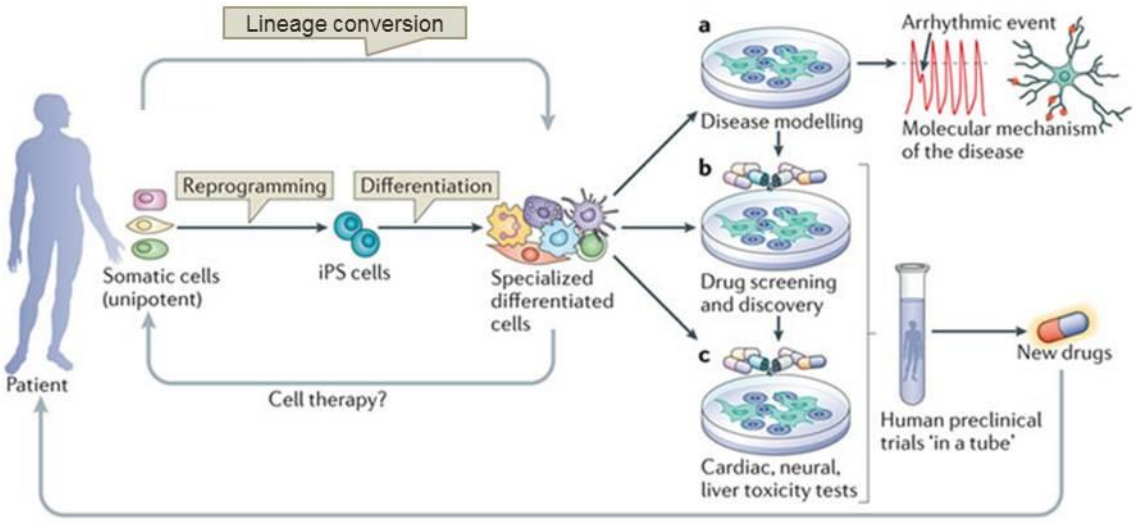

Figure 1.8: Major applications of differentiated cells obtained by reprogramming strategies.

Adult somatic cells (unipotent) from human patients can be subjected to reprogramming protocols. Generated iPS cells can be differentiated *in vitro* into the desired specialized cells. Alternatively, lineage conversion strategies can be applied with the direct conversion of the original somatic cell into another somatic cell fate. Either way, specialized differentiated cells obtained by reprogramming strategies can be used for cell replacement therapies. More straightforwardly, obtained cells can be used for disease modelling to understand the molecular mechanisms underlying disease phenotypes, for example the molecular causes for arrhythmia in cardiomyocytes (a). Another potencial application is in drug screening and discovery, to determine the effects of candidate drugs and new compounds and identify target pathways (b). Human cells derived from reprogramming technologies are also valuable in cardiac, neural and liver toxicity tests to assess cellular toxic responses (c). Drug screening and toxicity tests together represent human preclinical trials "in a tube" which strongly contribute to the early stages of the drug discovery process. Adapted from (Bellin et al., 2012).

Cellular reprogramming into pluripotency with the generation of human iPS cells potentially overcame these drawbacks. Proof-of-concept that iPS cells could be valuable therapeutic tools was first demonstrated in 2007 for a mouse model of sickle-cell anemia. A genetic defect in the β-globin gene is responsible for this disorder and mutated iPS cells were corrected for the single gene defect through homologous recombination. It was shown that mice could be rescued after transplantation with hematopoietic progenitors obtained *in vitro* from autologous corrected iPS cells (Hanna et al., 2007). iPS cell-based autologous transplantation methods have the advantage of minimizing the risk of immunological rejection, when compared to the current allografts from other donors. However, there are reasons to question this assumption of an immune-privilege, including recent studies that have tested iPS cells immunogenicity in various ways with conflicting results. This immunogenicity might result from the immaturity of cells differentiated from iPS cells, the genetic and epigenetic changes that arise from reprogramming or adaptation to culture conditions, the usage of xenogeneic or non-physiological culture reagents, and the gene correction strategies applied to restore proper expression of missing or dysfunctional proteins (Scheiner et al., 2014). Moreover, realistically, an individualized patient-specific iPS cell-based therapy implies high medical costs and an experimental timeframe that might be incompatible with the disease progression. Thus, at present, a collection of human iPS cell stocks from various HLA (human leucocyte antigen)-homozygous donors might be the most promising approach and guidelines for the collection of such cells are being discussed by the scientific community (Turner et al., 2013).

Nevertheless, for either an autologous or allogeneic transplantation, and besides immunogenicity issues, significant roadblocks to translating iPS cells to the bedside still remain. Tumorigenicity is one of such concerns. The current gold standard test of pluripotency for human iPS cells is the teratoma formation, which is inherently a tumorigenesis assay. Any residual undifferentiated cells present in differentiated cell cultures used for transplantation can cause a teratoma, and should be removed before use. Hence, effective methods for the removal of undifferentiated cell contamination as well as more efficient differentiation protocols must be developed. Additionally, much research has focused on removing or replacing the potent oncogene c-Myc in the reprogramming cocktail, as well as in developing non-integrative reprogramming techniques to minimize the risk of insertional mutagenesis and reactivation of transgenes after differentiation. Many of these technological issues have been resolved by recent technological

innovations in an effort to, in the near future, generate clinical-grade iPS cells under Good Manufacturing Practice (GMP) compliance (Barrilleaux and Knoepfler, 2011; Takahashi and Yamanaka, 2013).

Another concern with human iPS cell-based regenerative medicine is associated with the genetic and epigenetic alterations that have been described. Genomic changes, such as copy number variations, point mutations and karyotype alterations, are acquired by iPS cells as they proliferate and differentiate. Strategies to minimize genomic damage based on minimizing reprogramming- and propagation-induced oxidative stress are currently being developed, in order to avoid the overexpression of oncogenes and inactivation of tumour suppressors that might result from the DNA alterations. At the epigenetic level, reprogrammed cells can retain a memory of the starting tissue from which they were derived. Abnormalities in DNA methylation patterns and aberrant histone modifications can occur. Cells can also vary in X chromosome inactivation status (Barrilleaux and Knoepfler, 2011; Hong et al., 2013; Peterson and Loring, 2014).

Besides the described problems related to immune rejection, genetic instability, and tumorigenicity that must be solved, early stage preclinical studies have highlighted additional challenges that must be addressed before moving to clinical trials. These include rigorous quality control and efficient production of required cell populations, improvement of cell survival and engraftment, and development of technologies to monitor transplanted cell behaviour for extended periods of time. Regarding the key step of precisely correcting the gene defect in patient-specific iPS cells, a rapid and positive evolution of novel genome editing technologies was observed in recent years, with the development zinc finger nucleases, transcription activator-like effector nucleases and clustered regularly interspaced short palindromic repeat/CAS9 RNA-guided nucleases (Harding and Mirochnitchenko, 2014; Li et al., 2014).

Disease modelling

Animal models have contributed tremendously to a better understanding of disease mechanisms, but with some limitations due to species-specific differences and the non-accurate recapitulation of human disease in some cases. Moreover, the majority of drugs that are effective in mice have failed in human clinical trials. Thus, a novel and more human-relevant model is in order and human iPS cell-based disease models seem to be a good alternative to existing models, yet

complementary. These human *in vitro* models are not confounded by species-specific differences, allow cell-autonomous and non-cell-autonomous functions to be distinguished and also permit to study the effect of a genetic variant on the cellular phenotype. Furthermore, cultured cells can be produced and cultured relatively rapidly and in large quantities, which is compatible with the development of large-scale genetic and chemical screens for phenotypic modifiers (Merkle and Eggan, 2013).

Disease-specific iPS cells were generated for the first time in 2008 from patients with a variety of disease including Parkinson's disease, and a year later, iPS cells from a type 1 spinal muscle atrophy patient and his unaffected mother were generated and differentiated into neural tissue and motor neurons. As these differentiated cells displayed the genetic defect and the disease phenotype of selective motor neuron death, this report provided the proof-of principle of human iPS cell-based disease modelling (Ebert et al., 2009; Park et al., 2008). Following this first report, many disease-specific iPS cell lines have been established and used for *in vitro* disease modeling. In essence, it consists of differentiating control and disease-bearing human iPS cells into the target cell type affected in disease and comparing these target cells for disease-relevant phenotypes. The confluence of human iPS cell-based disease models with new gene-editing technologies, genome-wide association as well as DNA sequencing studies provide a promising workflow for interrogating the contribution of disease-associated candidate genetic variants to disease-relevant phenotypes in the attempt to illuminate the molecular basis of human disease (Bellin et al., 2012; Merkle and Eggan, 2013).

Drug screening and toxicological assessment

Our understanding of disease pathology in humans has been limited by a lack of appropriate models but also by insufficient research on drug–gene interactions. New technologies, such as *in vitro* differentiated human iPS cell-derived cells, have the power to transform the drug discovery process. Recent papers have shown that cell-autonomous disease phenotypes can be modelled *in vitro*. For example, the addition of propanolol and nadolol, two β-adrenergic blocking agents, attenuated catecholamine-induced tachyarrhythmia in cardiomyocytes. These cells were derived from human iPS cells from patients with Long QT syndromes that are caused by mutations in ion channel genes (Moretti et al., 2010). These results confirmed the efficacy of the β-blockade therapy that is already in clinical use for

the management of cardiac arrhythmia. Similar studies further suggested a paradigm in which biological and physiologically relevant assays in human cells can drive drug discovery to deliver potentially safer, more efficacious medicines as well as to iteratively relate patient information from the clinic back to the drug discovery laboratory (Bellin et al., 2012).

For the past 20 years, the drug discovery industry has relied heavily upon high-throughput screening to identify biologically active small drugs for further optimization into candidate drugs. Panels of patient-specific human iPS cells representing the spectrum of the disease and/or drug response can be generated and differentiated into relevant cell type(s) making it possible to investigate the genotype-phenotype-drug response relationship in a controlled and systematic manner. To date, some handful of drug efficacy screens evaluating from hundreds to thousands of small molecules in human iPSC-derived cells (neurons and hepatocytes) have already been reported (Engle and Vincent, 2014). Examples from neurons, hepatocytes, and cardiomyocytes have demonstrated physiologically relevant disease phenotypes as well as drug-induced toxicities, demonstrating their prospective use in safety assessment by toxicological studies (Kolaja, 2014). Although the current studies have been focused on the very early preclinical stages of drug discovery, as the technology progresses and the costs to generate patient cells and models decreases, it is likely that the technology will find additional applications at the clinical trial stage and in postmarketing surveillance (Engle and Puppala, 2013).

Applications in the basic sciences

The advent of reprogramming technologies has helped to elucidate, although not entirely yet, the relationship between epigenetic modification and cellular identity, as the identified roadblocks to reprogramming serve as barriers that ensure the stability of cellular identity (Vierbuchen and Wernig, 2012). Reprogramming techniques can also be used to dissect the role of transcriptional and epigenetic changes in cancer development, given the shared features of carcinogenesis with the reprogramming process such as MET and involvement of cancer-related proteins such as Myc and p53 (Bernhardt et al., 2012). Reprogramming somatic cells to iPS cells also allows obtaining ‘rejuvenated’ cells that can provide a tool for *in vitro* ageing studies. Additionally, as *in vitro* differentiation protocols usually mimic developmental processes, these techniques can also be used to increase

our knowledge in this field. Recent reports on three-dimensional complex tissues formed by differentiation of iPS cells have been highlighting self-organization of tissue development-based studies as an extremely valuable tool. Applications range from the next generation of organ transplantation to disease modelling (Sasai, 2013a; Takahashi and Yamanaka, 2013).

Retinal Pigment Epithelium

Vertebrate eye, retina and RPE

It is believed that around 500 million years ago, on the Cambrian period, lateral light-sensing organs with a non-imaging function evolved into a specialized structure which included all crucial features that characterize the modern vertebrate eye. As these visual systems emerged, several attributes as sight and rapid movement provided evolutionary advantages (Lamb et al., 2007). Image-forming eyes developed differently in the various phyla, however sharing some common underlying traits in terms of patterning and developmental pathways, namely between insects and mammals (Chow and Lang, 2001).

The mature eye is a very complex organ that develops through an extremely organized process during embryogenesis. It is responsible for the vision sensory capacity, with severe handicapping diseases occurring due to its loss of function. Three major tissues, the cornea, the lens and the retina, constitute the vertebrate eye (Figure 1.9) (Graw, 2003).

The eye works as an optical device that detects and perceives visual information, conducting it into the retina. Being a component of the central nervous system located peripherally, the retina is responsible for light sensing, imaging processing and information delivery into the brain through the optic nerve. Though a very thin tissue (around 200 μm in humans), the retina has a profoundly organized structure with several layers of cells: the complex neuronal circuitry named neuroretina (NR), and the underlying retinal pigment epithelium (RPE). Regarding the NR, five types of neurons compose it: photoreceptors (PRs), horizontal cells, amacrine cells, bipolar cells and retinal ganglion cells (RGCs) (Sung and Chuang, 2010).

PRs are light-sensitive neurons located in the outer part of the retina. They capture photons and generate electrophysiological signals, being divided in rods that respond to single photons, responsible for night vision, and cone PRs, specialized in sensing daytime high-intensity light, including colour vision. Both PRs types have an outer-segment (OS) constituted by membranous discs containing a visual pigment composed of a vitamin A-based chromophore (11-*cis*-retinal) and a seven-transmembrane-helix apoprotein, opsin. Phototransduction is initiated by photon absorption by opsin and associated isomerization of 11-*cis*-retinal into all-*trans*-retinal. A G protein-coupled signalling cascade of events is activated leading to alterations in membrane potential, with resultant modifications on the level of neurotransmitters' release on synaptic junctions (Yau and Hardie, 2009).

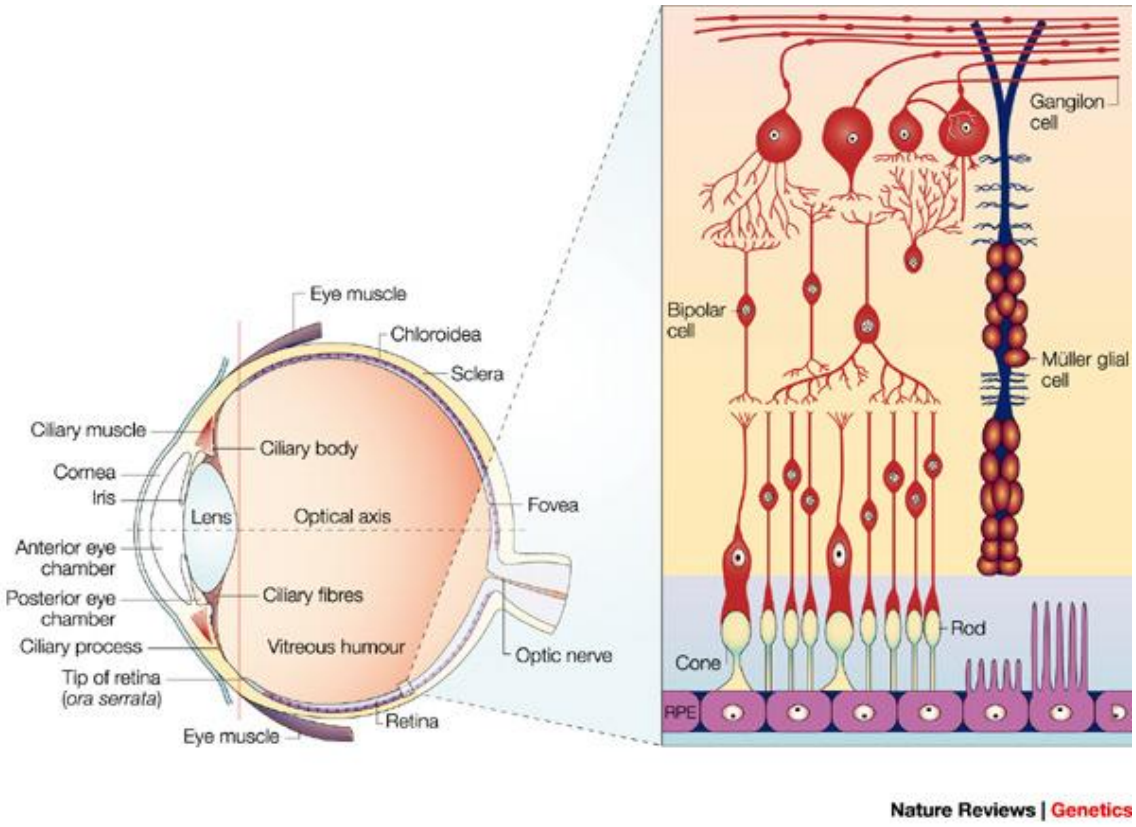

Figure 1.9: Structure of the adult human eye.

Schematic representation of a section of the human eye, depicting its composing tissues. The vertical red line separates the anterior segment from the posterior segment of the eye. Anteriorly, the eye is composed by the cornea, the iris, the lens and the ciliary body. Light enters the eye through the cornea, anterior chamber and lens, along the optical axis. Then it travels to the posterior segment, composed by the vitreous humour, the retina and the choroid. The retina has several components represented on the right close-up panel: ganglion cells, bipolar cells, Müller glial cells, photoreceptors (cones and rods) and retinal pigment epithelium (RPE). Amacrine and horizontal cells, though not represented, are also present. Adapted from (Graw, 2003).

PRs' electric response is transmitted first to a group of retinal interneurons called bipolar cells, and then to RGCs, which long axons form the optic nerve, leaving the eye and transmitting the information to the visual centres of the brain. Concomitantly, information relayed by the PRs can be altered by other types of interneurons, namely horizontal and amacrine cells. The different types of retinal neurons are distributed along 3 distinct layers of cell bodies: the outermost containing PRs cell bodies (outer nuclear layer), the inner nuclear layer where interneurons' cell bodies are located, and, on the inner part the ganglion cell layer with RGCs' nuclei. Additionally to neuronal cells, Müller cells are also present performing glial-supportive functions, such as maintenance of the homeostasis of the retina extracellular milieu, control of angiogenesis and release of neurotrophic

factors. Müller glia also play important roles in the response to retinal pathological conditions (Bringmann et al., 2006; Sung and Chuang, 2010).

At first sight, the organization of retina's cell layers might seem counterintuitive, since light must travel through a complex organization of non-light-sensing cells located on the inner side before reaching the outermost portion of the retina and being captured by photo-sensible OS. Contrarily, this spatial arrangement unveils the key supportive role of the RPE lying on the apical side of PRs in close relation to them.

The RPE is an epithelial monolayer of polarized pigmented cells, hexagonally-packed and tight junction-connected. It composes the outer blood-retina barrier, separating the outer retina from the choroidal capillary bed and regulating the movement of solutes between both, therefore maintaining a microenvironment adequate to proper function of neuronal layers of the NR (Rizzolo et al., 2011; Sparrrow et al., 2010). Apical microvilli of RPE cells surround the light-sensitive OS of PRs. On the basolateral side, RPE displays membrane infoldings and is in close contact with a specialized Bruch's membrane, which separates it from the underlying fenestrated endothelium of choroidal capillaries (Figure 1.10) (Strauss, 2005).

The Bruch's membrane is an approximately 2 µm-connective tissue constituted by five laminar layers including the basement membrane of the RPE and of the endothelium of choriocapillaries, 2 collagen-rich layers and an elastic sheet (Nakaizumi, 1964). Being an extracellular matrix, it is composed of collagens, elastin, laminin, fibronectin and proteoglycans containing heparin sulphates (Hewirr et al., 1989) Due to its strategic location, the Bruch's membrane is responsible for flow of nutrients, water, ions, oxygen, biomolecules and metabolic byproducts between the metabolically active RPE cells and the choriocapillaries (Booij et al., 2010; Sivaprasad et al., 2005). It has also been implicated in regulating RPE cell adhesion and attainment of proper epithelial polarization (Del Priore et al., 2002; Rizzolo, 1991). It has been described that aging and other pathological conditions contribute to an increased thickness of Bruch's membrane, due to the deposition of noncollagen proteins, lipid deposits, heparin sulfate, laminin, and fibronectin. These calcification and fragmentation processes affect Bruch's membrane permeability and the movement of nutritional factors from the choriocapillaries through the RPE layer into the outer retina (Ehrlich et al., 2008; Spraul et al., 1999).

The choroid is the vascular layer of the eye composed of single layer of fenestrated blood vessels (choriocapillaris) and large vessels such as feeding arterioles and draining venules. The choroidal vasculature lies posteriorly to the Bruch's membrane and its

composing endothelial cells are fenestrated mostly on the side facing the outer retina, being responsible for its metabolic and oxygen supply (Bhutto and Lutty, 2012).

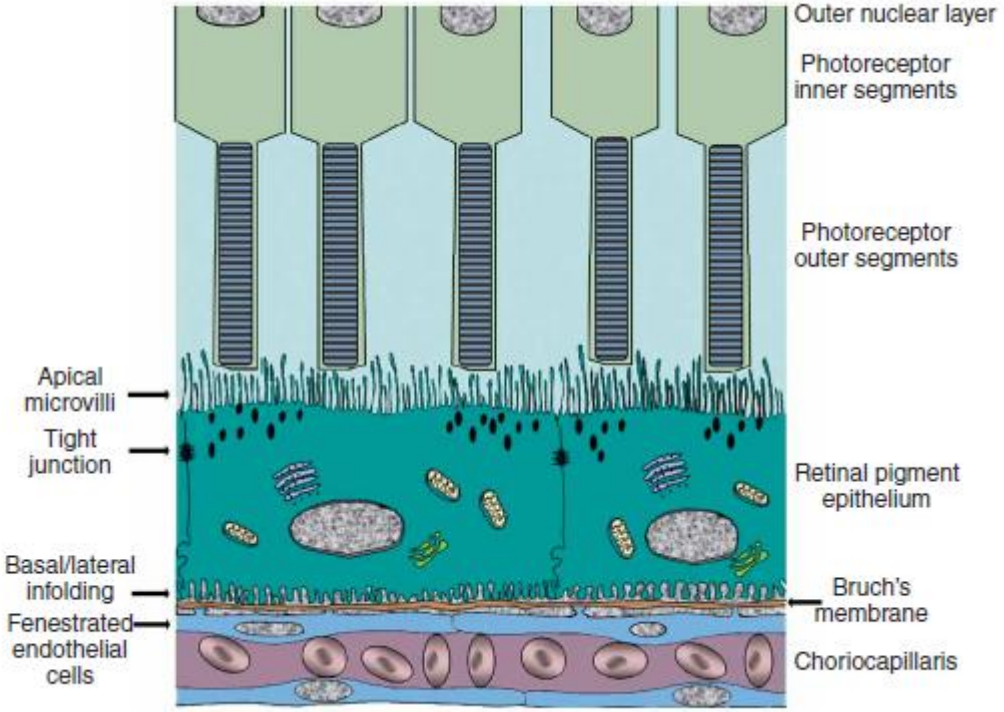

Figure 1.10: The Retinal Pigment Epithelium, located in the outer retina.

Schematic diagram of the RPE cell layer and its close relationship with the OS of the PRs apically, and with Bruch's membrane and choriocapillaries on the basal side. Pigmented granules and characteristic membrane specializations are also depicted: apical microvilli, tight junctions on the lateral sides and basolateral infoldings. Adapted from (Sonoda et al., 2009).

In addition to being a component of the outer blood-retina barrier regulating epithelial transport, the RPE also plays a crucial role in **light absorption**, spatial ion buffering, the visual cycle, phagocytosis of PRs' OS and secretion of growth factors and immunosuppressive factors. The functional integrity of the retina relies on the maintenance of these diverse RPE functions and any alteration affecting them will result in retinal degeneration with consequent loss of visual function (Sparrrow et al., 2010; Strauss, 2005).

In average, the human retina absorbs approximately 10^{12} to 10^{15} photons each day. Light enters the optical device and is focused by the lens in the retina, where photons are captured by PRs. Scattered or unabsorbed light is absorbed by the RPE cells lying just beneath the PR layer. PRs and RPE cells work in conjunction in order to maximize the

optical quality of visual imaging whilst keeping the risk of photodamage to its minimum. Exposure to bright light leads to two types of photodamage in cells: thermal damage and photochemical damage, which occurs as a result of energy transfer from photons to irradiated molecules leading to changes in electron orbitals or breakage of bonds (Hunter et al., 2012).

In addition to the high photo-oxidative environment caused by light exposure, RPE cells are also exposed to a high oxygen overflow given the high blood perfusion rates of choroidal capillaries (probably to avoid the light-induce thermal damage) (Parver, 1991). Moreover, photo-oxidative activity in the RPE is increased by the production of reactive oxygen species (ROS) during the phagocytosis of daily shed OS of PR cells (see more details later on). RPE cells have established three lines of defence against these sources of oxidative stress. First, cells contain pigmented light absorbers such as melanin, lipofuscin and retinoids. Secondly, antioxidants, either enzymatic (as catalase and superoxide dismutase) or non-enzymatic (such as carotenoids, ascorbate, glutathione, α-tocopherol, and melanin itself) are also accumulated by RPE cells and neutralize ROS before they can cause damage to cellular macromolecules. When such damage occurs, the third line of defence responds, and damage to lipids, proteins and DNA are recognized and repaired (Winkler et al., 1999).

Before reaching the RPE cells, environmental light passes through other eye layers with transmission and absorption capacities, such as cornea, lens and the PRs themselves. PRs contain carotenoids, mainly lutein and zeaxanthin, acting as a sink for blue incoming light, and as antioxidants due to quenching of ROS and free radicals (Beatty et al., 1999; Sliney, 2005). Then, on the RPE cells, light absorption is mainly mediated by melanin granules present in lysosome-related organelles named melanosomes. Here the melanin is mainly eumelanin, which is a heterogenous macromolecule derived from tyrosine or dopa (dihydroxyphenylalanine) with brown/black colour. Melanin synthesis and storage occurs in melanosomes. It is formed in a series of oxidation and tautomerization reactions catalyzed by several enzymes, being tyrosinase (monophenol monooxygenase) the rate-limiting one responsible for the first step (Murisier and Beermann, 2006). Besides light absorption, melanin also plays a role as anti-oxidant ROS and free radicals-scavenging properties, conferring some cytoprotection to apoptosis. Moreover it has been described its ability to bind to metals, such as zinc, and drugs (Burke et al., 2011; Schraermeyer and Heimann, 1999; Seagle et al., 2005).

Along with retinoids and melanin, another pigment involved in light absorption is auto-fluorescent lipofuscin. Lipofuscin granules are an agglomerate of modified lipids and bisretinoids that accumulate in the RPE's lysosomes during life as a by-product of the

visual cycle and phagocytosis of OS. Lipofuscin is highly susceptible to photochemical changes, acting as a photosensitizer and is known to reach a toxic concentration level in the elderly eye. Consequently, the oxidative-antioxidative equilibrium may be unbalanced with ageing and accounts for the onset of some pathological retinal conditions (Hunter et al., 2012; Winkler et al., 1999).

As abovementioned, RPE forms the outer blood-retinal barrier regulating the movement of solutes and molecules between the fenestrated choroidal capillaries and the PR layer of the outer retina. Tight junctions contribute to the barrier once they selectively limit diffusion through paracellular spaces between RPE cells (Rizzolo et al., 2011). **Epithelial transport** occurring through RPE cells is responsible for supplying nutrients from the blood to the PR. Glucose as an energy supply is transported by GLUT1 and GLUT3 transporters in a facilitated diffusion manner (Ban and Rizzolo, 2000). Transport of retinol to ensure the supply of retinal for the visual cycle also occurs. Also important for maintaining the visual function is the delivery of omega-3 fatty acids, used as building blocks of the phospholipids present in retinal neurons' membranes and PRs' disks (Bazan et al., 1992).

Transport also occurs in the opposite direction, from the PRs into the basolateral side or blood stream, mainly of water, ions and metabolic waste products (as lactic acid). Relevantly, the RPE regulates the passage of a variety of ions (like Cl^-, K^+, Na^+, HCO_3^-) which are important in the polarisation/hyperpolarization of cell membranes, in fluid transport and the regulation of pH. Ion pumps, such as the Na^+/K^+-ATPase present in the RPE's apical membrane, provide energy in the form of ATP for transepithelial transport. Consequently, electrochemical gradients are generated and drive other solutes vectorially through channels, cotransporters, and antiporters (Rizzolo et al., 2011; Strauss, 2005). Ca^{2+}-activated Cl^- channels, like Bestrophin-1, are also present in the RPE cells and are widely regarded as a marker of RPE maturation (Marmorstein et al., 2009).

RPE cells along with Müller glial cells are responsible for stabilizing ion homeostasis in the subretinal space. RPE cells accomplish this **spatial ion buffering** task through the mentioned ion epithelial transport regulation and also fast-adapting voltage-dependent ion channels. Light-dependent alterations on overall excitability of PRs and other retinal neurons occur at a very fast rate, requiring a fast compensating mechanism from RPE cells. Light-evoked responses of the RPE membrane potentials are secondary to rod PR activity, mediated by paracrine signals and can be monitored by electroretinogram techniques allowing the diagnose of alterations in RPE functions (Steinberg et al., 1983; Wu et al., 2004).

Phototransduction by the rods PRs begins with photons reaching rhodopsin, which is composed of the 7 transmembrane domain G-coupled receptor protein, opsin, and the chromophore 11-*cis*-retinal. Absorption of photonic energy occurs with conformational change of 11-*cis*-retinal into all-*trans*-retinal. PRs lack *cis*-*trans* isomerase function for retinal, thus 11-*cis*-retinal is recycled by a reisomerization pathway occurring in RPE cells and named as **visual cycle** (Figure 1.11). A similar pathway is present for cones, notwithstanding an alternative pathway for production of 11-*cis*-retinal occurring in Müller cells (Miyazono et al., 2008; Yau and Hardie, 2009).

An alternative pathway also occurs depending on the activity of retinal G protein-coupled receptor (RGR) of the RPE and Müller cells. RGR is an abundant opsin that after light induction generates 11-*cis*-retinal by stereospecific isomerization of its bound all-*trans*-retinal chromophore, an inverted reaction of the one occurring for rhodopsin. This pathway is important to maintain constant levels of 11-*cis*-retinal independently of changes in ambient light. Fine tuning of fast adapting demands for 11-*cis*-retinal in the sudden transitions from darkness to light is achieved by several retinal pools of retinal binding proteins: rod OS, IRBP in the subretinal space, CRALBP and RPE65 in the RPE cells (Chen et al., 2001; Strauss, 2005).

Another important interaction between RPE and PR crucial for the maintenance of the retina's structure and functionality is the cyclic **phagocytosis of PRs' OS** by RPE cells (Kevany and Palczewski, 2010). RPE cells extend their apical microvilli sheathing the OS, which are constantly subjected to photo-oxidative damage as already described. Thus, OS are constantly renewed and invariable length is kept due to daily shedding of degraded tips of OS in a circadian regulated process (LaVail, 1976). RPE cells efficiently phagocyte OS from subretinal space and recycle some of their components (Young and Bok, 1969). Several players have been identified in the regulation of the phagocytosis events by the RPE. Among others, type B scavenger receptor CD36 is required for OS internalization, αvβ5 integrin is essential for binding of OS and receptor tyrosine kinase c-mer (MertK) is necessary for activation of phagocytosis (D'Cruz et al., 2000; Feng et al., 2002; Finnemann and Silverstein, 2001; Finnemann et al., 1997).

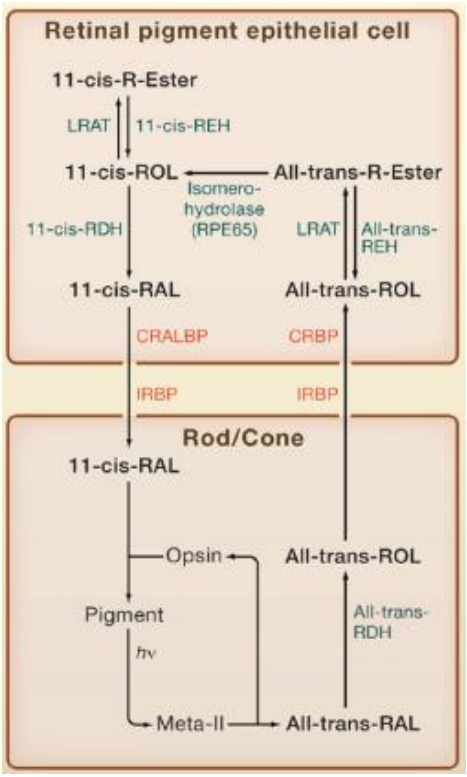

Figure 1.11: Visual cycle of retinal in RPE cells and PRs.

Phototransduction events begin with photons (hv) being absorbed by 11-*cis*-retinal (11-cis-RAL), the chromophore associated with PRs' opsin. Opsin is converted into its meta form for a period of time and all-*trans*-retinal (All-trans-RAL) is formed. After signal transduction has occurred, opsin releases All-trans-RAL and substitutes it for 11-cis-RAL in order to permit absorption of another photon. All-*trans*-retinol (All-trans-ROL), formed by reduction of all-trans-RAL catalyzed by a membrane bound retinol-dehydrogenase (RDH), is then delivered to the subretinal space where it is loaded to IRBP (interphotoreceptor retinoid-binding protein). This carrier protein transports it into the RPE cells, where it is first transferred to cellular retinol-binding protein (CRBP) and then delivered to an enzymatic complex responsible for the recycling of 11-cis-RAL. First, lecithin:retinol acyl transferase (LRAT) catalyzes esterification of retinol; RPE65 (RPE specific protein 65kDa) is responsible for re-isomerisation to 11-cis using the energy from ester-hydrolysis; finally 11-cis-RDH promotes oxidation of retinol into 11-cis-RAL. The reaction is accelerated by CRALBP (cellular retinaldehyde-binding protein) which is also part of the enzyme complex and to which 11-cis-RAL is immediately transferred. Finally, 11-cis-RAL is released to IRBP and transported back to photoreceptors. Adapted from (Yau and Hardie, 2009).

Being a polarized epithelial tissue, RPE cells display polarity traits in the cellular localization of some proteins (as apically localized Na^+/K^+-ATPase pump), but also in the **secretion** of various factors and signalling molecules. Secretion of numerous growth factors occurs in a polarized way allowing the RPE cell to communicate with adjacent tissues on either sides, as reviewed by (Kay et al., 2013): adenosine triphosphate (ATP), ciliary neurotrophic factor (CNTF), connective tissue growth factor (CTGF), fas-ligand (fas-L), fibroblast growth factors (FGF-1, FGF-2, and FGF-5), lens epithelium-derived

growth factor (LEDGF), insulin-like growth factor-1 (IGF-1), members of the interleukin family (such as IL-6 and IL-8), platelet-derived growth factor (PDGF), pigment epithelium-derived factor (PEDF), TGF-β, tissue inhibitor of matrix metalloprotease (TIMP) and vascular endothelial growth factor (VEGF), just to mention some. For example PDGF is secreted on the apical side and plays a role in retinal neurons' development and integrity due to its neurotrophic properties. It also maintains a non-angiogenic retinal environment (Barnstable and Tombran-Tink, 2004; Patricia Becerra et al., 2004). VEGF, on the other hand, is secreted basolaterally, mediating paracrine vascular survival signals for adjacent endothelia (Sonoda et al., 2010; Witmer, 2003). Secretory activity of RPE cells is triggered by an increase in intracellular Ca^{2+} content and voltage-dependent Ca^{2+} channels expressed by these cells act as its regulators (Wimmers et al., 2007).

Finally, RPE cells contribute to the **immune privilege** of the vertebrate eye. Firstly, through the presence of tight junctions in the polarized epithelium, a physical barrier is formed separating the inner space eye from the bloodstream. Secondly, RPE cells are able to communicate with the immune system either by secretion of immunomodulatory molecules (such as interleukins, PEDF, galectin-1) or by sensing immune signalling molecules due to their expression of toll-like receptors or tumor-necrosis α-receptor (Mochizuki et al., 2013; Strauss, 2005). The fact that RPE functions as an immune-privileged tissue is extremely relevant for the development of therapeutic strategies for several retinal disorders, mainly for gene therapy or cell-based therapy approaches (Wenkel and Streilein, 2000).

Eye development: the view from the RPE

Organogenesis of the eye is a highly organized multistep process taking place during embryogenesis. A complex interplay between inductive signals, resulting from tissue-tissue interactions, and cell intrinsic factors, as the timely action of TFs, is critical to ensure the correct development of the different eye components as well as maintenance of their fate. Establishing the genetic basis of eye defects in drosophila, zebrafish, chicken, xenopus, mouse and human provided a very important tool to identify the extrinsic and intrinsic determinants in this complex process.

The vertebrate eye comprises tissues from different embryonic origins. The surface ectoderm gives rise to the lens and the cornea, whilst the anterior neural plate will form the retina and epithelial layers of iris and ciliary body. During gastrulation, the developing eye is organized in a single field "eye field" (EF) located centrally in the developing

forebrain. After specification of the EF within the neuroplate, the forming eye tissues undergo a series of complex morphogenetic movements (Figure 1.12) (Fuhrmann, 2010; Graw, 2010). First, the single EF is separated during the establishment of the midline and two bilateral optic grooves become apparent as the neuroepithelium of the ventral forebrain evaginates forming two bulges at each side (by E8.5 in the mouse). As the evagination process occurs, two optic vesicles (OV) are formed contacting at their distal part with the overlying surface ectoderm, which is then induced to form the lens placode (E9). Secondly, resultant of this interaction an invagination step is now initiated with invagination of the lens placode to form the lens, and invagination of the distal OVs leading to the formation of a bilayered optic cup (OC) (in the mouse this process is initiated at E10). The NR develops from the inner layer of the OC, and RPE is derived from the outer layer contacting with the periocular mesenchyme. As morphogenesis proceeds, the presumptive RPE spreads ventrally and circumferentially to completely surround the NR, allowing the closure of the ventral fissure (Fuhrmann, 2010; Graw, 2010). Several molecular players and cellular processes have been identified as playing a role in controlling the eye development and RPE specification and differentiation, and they vary along the multiple steps already mentioned.

1. Eye field

Although the first morphological signs for eye development only occur with the bilateral evagination of the developing forebrain, the early EF is specified earlier during gastrulation. Reports supporting the existence of this single eye field go back till late 1920s when Adelmann's embryological manipulations have shown that transplanted regions of the anterior neural plate demonstrated an eye-forming potential (Adelmann, 1929)**.** Modern genetic evidence showed that the early EF is specified at the neural plate stage by the expression of a set of eye field transcription factors, EFTFs. The EFTFs in *Xenopus* are expressed in a dynamic and overlapping pattern in the EF and include *ET (also known as transcription repression factor Tbx3), Rx1, Pax6, Six3, Lhx2, Tll (also known as Nr2e1)* and *Optx2* (also known as *Six6*). Expression of an EFTF cocktail with *Otx2* was shown to be sufficient to induce ectopic eyes outside the nervous system at high frequency. Together these TFs are organized in a hierarchical network with self-regulating feedback interactions that specifies the vertebrate EF, which is very close to the previously described network of homologous *Drosophila* genes (Chow and Lang, 2001; Zuber et al., 2003).

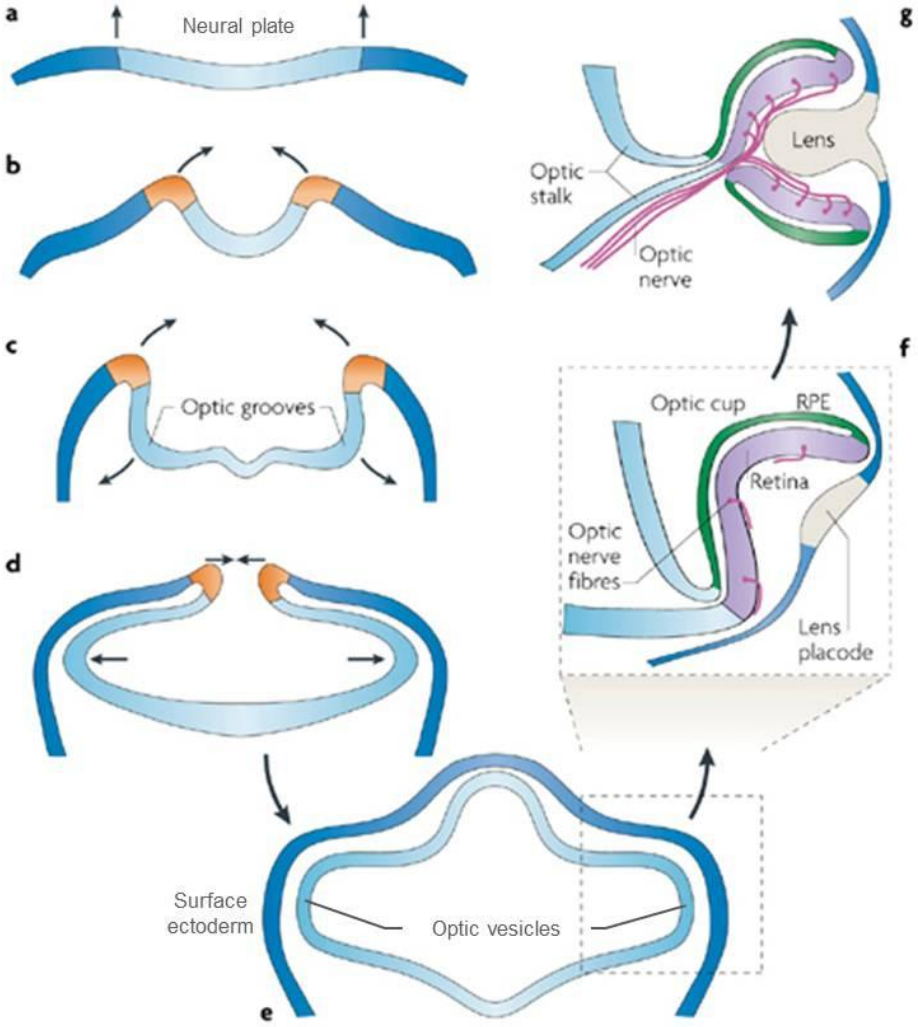

Figure 1.12: Embryonic development of the vertebrate eye cup.

The first signs of the developing eye cup become apparent during neurulation, when the neural plate folds upwards and inwards (a and b). Two lateral optic grooves evaginate (c) and bulge outwards as the lips of the neural folds approach each other (d). At this point the optic grooves have enlarged to form the optic vesicles, which continue to balloon outwards and terminate very close to the surface ectoderm (e). As a result of this interaction, the lens placode is induced and the neuroectoderm folds inward forming the optic cups by invagination. The inner layer of the optic cup gives rise to the retina, whereas the outer layer will form the RPE. Developing retinal ganglion cells send axons out across the retinal surface, growing toward the optic stalk and forming the optic nerve. Lens placode will also invaginate and give rise to the lens (f). The optic cups grow circumferentially, eventually sealing over the choroidal fissure and enclosing the axons of the optic nerve (g). Adapted from (Lamb et al., 2007).

The **orthodenticle protein homolog Otx2** is a member of the *orthodenticle*-related family of TFs, containing a highly conserved *bicoid*-type homeodomain. In

Otx2$^{-/-}$ mice mutants, forebrain and midbrain structures are completely missing. Heterozygous deletion of Otx2 leads to a variable phenotype and mice can be normal, display developmental eye abnormalities including anterior segment malformations, severe eye anomalies such as microphthalmia (eyes with reduced size) or anophthalmia (absence of both eyes), or head defects. Otx2 is expressed throughout the forebrain and midbrain in the developing embryo, specifying the anterior neuroectoderm. Its expression precedes that of the other early EFTFs, and is subsequently down-regulated and absent in the EF defined by them. As mentioned later on, Otx2 also plays a role in subsequent steps of eye development, namely in directing the evagination of the OV to contact the surface ectoderm and in specifying the presumptive RPE (Hever et al., 2006; Martinez-Morales et al., 2001).

An essential role in the early events of eye development has been established for the *paired*-type homeobox gene ***Rax*** **(retina and anterior neural fold homeobox)** after analysis of its expression patterns and loss and gain-of-function phenotypes in mice (Furukawa et al., 1997; Mathers et al., 1997). Rax is first expressed at the anterior neural plate, and following neurulation, it is expressed most abundantly in the OV. At later stages, Rax expression is found only in the developing retina. Post-natally, the expression of Rax is restricted to proliferating cells within the retina, gradually decreasing as proliferation declines. Mouse embryos carrying a null allele of this gene do not form OCs and so do not develop eyes. Similarly, among other species, in zebrafish the ortholog for *Rax* gene is *rx3* which once mutated generates an anophthalmic phenotype. Mutation in the human RAX gene also leads to anophthalmia (Voronina et al., 2004). Rax is one of the molecules that define the EF during early development: anterior neuroectoderm expresses Otx2 that in turn activates transcription of Rax; Rax itself then increases transcription of several EFTFs like Pax6, Six3 and Lhx2. Proliferation of the EF is controlled by Six6 in a Rax-dependent way. Rax also participates in suppressing the canonical Wnt pathway to prevent the induction of posterior fates of the anterior neural plate, and it promotes non-canonical Wnt signalling that controls morphogenetic movements of eye cells. Additionally, Rax performs several functions that are important for the formation of retinal progenitor cells, their proliferation and movement from the midline and outward to contribute to evaginating OV. At subsequent steps of the eye formation, Rax also plays a role in downregulating the transcription of Otx2 in the cells of the presumptive NR. Moreover it has been described that Rax, in combination with other TFs, is

necessary for normal PR gene expression, maintenance, and function (Bailey et al., 2004; Fuhrmann, 2010; Martinez-Morales and Wittbrodt, 2009; Pan et al., 2010).

Pax6, a TF containing paired-box and homeobox motifs, is the paradigm for a master control gene in eye development. Loss of Pax6 function leads to the *eyeless* phenotype in *Drosophila* (Quiring et al., 1994), and the same happens in different organisms as frog, mouse and human. Pioneering work in the nuclear reprogramming field showed that ectopic expression of the mouse *Pax6* induces functional eyes in *Drosophila* antennae or legs (Halder et al., 1995). The small eye (*Sey*) in mouse is a semidominant mutation in which the homozygous animals display no eyes and the heterozygous condition results in multiple ocular abnormalities, such as microphthalmia, lens cataracts and iris defects (Hill et al., 1991). Similar mutations in humans cause the ocular syndrome Aniridia, as well as multiple lens and corneal defects (Ton et al., 2014). Pax6 is first expressed in the early anterior neural plate, followed by expression on the prospective lens field in the surface ectoderm and on the neuroectoderm from where OV evaginates. On the OV stage, expression becomes restricted dorsodistally and in the presumptive lens ectoderm. In the developing OC, Pax6 is initially expressed throughout but then expression is lost in the RPE and only kept at NR level in ganglion and amacrine cells. Besides these cell types, expression is also maintained in lens and cornea on adult eye (Hever et al., 2006). Since Pax6 null mutants fail to develop eyes, conditional gene targeting and chimeric studies provided the way to establish its role in later stages of the eye development. Tissue-specific deletion of one copy of Pax6 using the Cre/loxP system has shown that correct levels of expression in the distal OC are essential for normal iris development. Dosage levels in the surface ectoderm were also shown to be critical for development of the lens and cornea (Davis-Silberman et al., 2005). Moreover, other studies have shown that Pax6 is required for the multipotent state of retinal progenitor cells, once upon Pax6 inactivation these progenitors can lead exclusively to the generation of amacrine neurons and not the other NR fates (Agathocleous and Harris, 2009; Marquardt et al., 2001). Pax6 also participates in the determination of RPE cells as mentioned later on.

Also classified as EFTFs are two closely related members of the *Six/sine oculis* homeodomain family, **Six3 and Six6** (also known as Optx2 or Six9). Loss of function mutations on both genes lead to disorders in humans with severe brain defects, anophthalmia and/or microphthalmia (Aldahmesh et al., 2013; Gallardo et

al., 1999; Wallis et al., 1999). Both genes have expression patterns on mice embryos suggestive of their role in early eye development. Early on, Six3 expression is restricted to the anterior neural plate including areas that later will give rise to ectodermal and neural derivatives. Later, Six3 is expressed throughout the OV and then in the optic stalk, NR and invaginating lens tissues. Six6, when compared to Six3, has an expression pattern quite similar, but more restricted. Six6 is expressed in the anterior neural plate, not necessarily in the EF, and subsequently in the ventral forebrain and ventral portion of the future NR. Thereafter, Six6 is detected in the NR and optic stalk but not in the lens (Jean et al., 1999; Lee et al., 2012; Oliver et al., 1995). Ectopic Six3 expression promotes the formation of ectopic OV-like structures in developing medaka and mouse embryos (Lagutin et al., 2001; Loosli et al., 1999) Furthermore, overexpression of Six3 in zebrafish embryos induces enlargement of the rostral forebrain (Kobayashi et al., 1998). Six3 has been known to play a role in the formation of anterior neural plate structures, and thereafter on NR specification, both through inhibition of Wnt signaling (Lagutin et al., 2003; Liu et al., 2010). Concerning lens specification, Six3 also plays a role, namely through direct activation of Pax6 (Liu et al., 2006). Similarly, Six6 overexpression leads to an enlargement of the eye tissue and transformation of anterior neural plate into retinal tissue in *Xenopus.* Moreover, Six6 has shown to be capable of inducing transdifferentiation of RPE into NR, thus suggesting that Six6 role in eye development lies on NR development (Wawersik and Maas, 2000; Zuber et al., 1999).

Another EFTF is **Lhx2**, a member of the LIM homeobox-containing TFs family. In mice embryos, Lhx2 expression has been observed in the anterior neural plate prior to OV formation. Subsequently, in the OV Lhx2 expression becomes progressively restricted to the NR and its inner nuclear layer. Null embryos display severe forebrain defects and anophthalmia, revealing its role in patterning the forebrain and particularly in eye development. Lhx2 is essential for progression of the OV to the OC stage, since *Lhx2*$^{-/-}$ embryos have normal OV specification but OC and lens placode fails to occur (Porter et al., 1997). Although Lhx2 overexpression *per se* did not induce ectopic eye structure formation, overexpression of various combinations of EFTFs factors other than Lhx2 only induced ectopic eyes when endogenous Lhx2 expression was upregulated (Zuber et al., 2003). Expression of important EFTFs, namely, *Rax, Pax6*, and *Six3*, at the anterior neural plate stage was found to be reduced in *Lhx2* mutants, further indicating requirement of Lhx2 in the earliest stage of optic development. Later on,

Lhx2 is also required for Six6 expression initiation in the OV, cooperating synergistically with Pax6, and thus promoting establishment of definitive retinal identity and cellular proliferation (Tétreault et al., 2009). Recent reports also highlighted an ongoing role of Lhx2 to maintain optic identity across multiple stages, from the formation of the OV to the differentiation of the NR, by continuously suppressing alternative fates (Roy et al., 2013). Furthermore *Lhx2 regulates* OV patterning and lens formation in part by regulating BMP signaling, either in an autocrine or paracrine manner, respectively (Yun et al., 2009).

Nr2e1 (also known as *Tlx*, *Tll*, and *Tailless)* encodes a highly conserved TF known to be a key stem cell fate determinant in both the developing mouse forebrain and retina. In the mouse embryo it is detected in the developing forebrain as soon as E8 in few adjacent cells of the neural epithelium. Its expression is then intensified and spread, including into the evaginating OV. Later on, Nr2e1 expression becomes restricted to the innermost surface of the retina and reaches its maximum intensity at E15.5, suggesting a role for this gene in an early phase of retinogenesis. Notwithstanding brain and behavioural phenotypes, *Nr2e1*-null mice have retinal and optic nerve dystrophy, leading to blindness. The proliferation rate of retinal progenitor cells is affected and increased apoptotic levels in the ganglion cell layer is observed, which results in a marked reduction in thickness of the distinct layers in the adult retina (Monaghan et al., 1995; Schmouth et al., 2012; Young et al., 2002). In *Xenopus*, it has been described that Six3 and Pax6 expressed early in EF can induce Nr2e1 expression. Conversely Nr2e1 is capable of regulating the expression of these TFs and other EFTFs with whom it is not co-expressed, supporting a role in eye formation and maintenance (Zuber, 2010).

Finally, **T-box 3 (Tbx3)** is a member of the T-box gene family, first identified as *ET* (eye T-box) in *Xenopus*. In this animal model, it is expressed in the early EF with a more restricted pattern in the anterior neural plate when compared with the other EFTFs. Misexpression of Tbx3 in frog embryos results in abnormal eye morphogenesis, loss of ventral retinal markers, and when expressed medially, fused retinas. Tbx3 has also been shown to regulate the expression of other EFTFs *in vivo* and *in vitro* and to be a crucial component of a cocktail of EFTFs sufficient to induce ectopic eye formation in *Xenopus* (Zuber, 2010). However, homozygous mutations of Tbx3 are embryonic lethal in mice but with no described eye phenotype, which supports its role in regulating early embryo development, but questions its requirement for eye field specification. Additionally, Tbx3 has been identified as a key regulator of mouse and human ES cell pluripotency and

differentiation, regulating its self-renewal. Moreover, knockdown of TBX3 during differentiation of ES cells reduced neural rosette formation as well as the expression of neuroepithelial and neuroectoderm markers (PAX6, LHX2, and RAX), suggesting a role in promoting neuroepithelial differentiation (Esmailpour and Huang, 2012). Interestingly, Tbx3 significantly improves the quality of iPS cells in reprogramming protocols when it is used along with Oct4, Sox2 and Klf4 (Han et al., 2010).

In summary, in the early embryo several TFs are expressed in the anterior neural plate within a single EF which contains the primordial cells that will give rise to the vertebrate eye. Splitting of the single EF in two occurs in parallel with the introduction of the midline. Sonic hedgehog (Shh) and TGFβ/nodal pathways have been described to be involved in this step preceding OV formation (Chow and Lang, 2001).

2. Optic vesicle

When the splitted EF begins to evaginate, it gives rise to two OV that progressively become closer to the surface ectoderm. Initially, OV cells are indistinguishable and express a common set of TFs. Neuroepithelial cells are bipotential and the presumptive retina is able to develop into RPE cells. Conversely, prospective RPE can differentiate into the retina (Coulombre and Coulombre, 1965; Pritchard, 1981). Due to the evagination process, the distal part of the OV, the prospective NR, is in contact with the surface ectoderm, whereas its dorsal part, the presumptive RPE, faces the extraocular mesenchyme. Exogenous signals originating from these tissues play an instrumental role in influencing the initial patterning of the OV into NR and RPE (Figure 1.13).

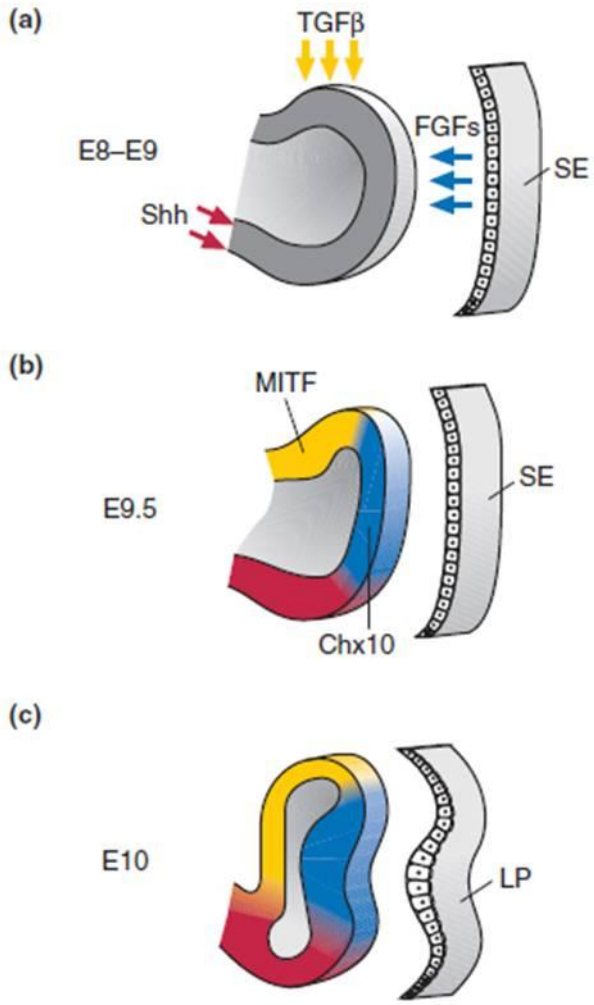

Figure 1.13: Patterning of the OV in the presumptive NR and RPE.

(a) At E8-E9, the initial patterning of the OV into distal NR and proximal RPE domains is mediated by head surface ectoderm (SE) and surrounding mesenchyme. FGFs secreted from the SE (blue arrows) promote NR differentiation while a TGFβ family member secreted from the mesenchyme (yellow arrows) promotes RPE cells' fate. Shh emanating from the ventral forebrain (red arrows) promotes formation of the optic stalk from the ventral portion of the OV. (b) The external signalling clues instruct the regionalization of the OV, and several TFs acquire region-specific expression. Namely, Chx10 (or Vsx2) is upregulated in the NR (blue) and Mitf expression is restricted to prospective RPE (in yellow). (c) The earliest lens structure, the lens placode (LP), is essential for promoting further developmental step with the formation of the OC. Adapted from (Ashery-Padan and Gruss, 2001).

FGF signalling is responsible for the patterning of the retina in the distal OV, as well as for initiation of retinal neurogenesis later on. FGF ligands and receptors are profusely expressed in ocular and extra-ocular tissues and particularly, FGF1 and FGF2 are expressed by the lens ectoderm facing the prospective NR. In chick embryos, inhibition of FGF2 signalling blocked neural differentiation in the presumptive NR, without affecting pigmented epithelial cell differentiation.

Moreover, addition of FGF to the OV causes the presumptive RPE to undergo neuronal differentiation and, as a consequence, a double retina is formed (Pittack et al., 1997). In mouse embryos the ectopic expression of FGF molecules in the proximal region of the OV also resulted in a duplicate NR (Nguyen and Arnheiter, 2000). Additionally, FGF signal is transduced through the tyrosine kinase type FGF receptors that activate a wide variety of signalling transducing cascades, including the MEK – ERK (also known as mitogen-activated protein kinase, MAPK) pathway. Ectopic expression of constitutively active Ras was also sufficient to convert the RPE into NR, highlighting that activation of MAPK pathway may mediate FGF-induced repression of RPE (Zhao et al., 2001). This repression of the RPE phenotype is mediated by a homeobox gene ***Vsx2*** (also known as Chx10), the earliest gene that shows domain-specific expression for the retina. In Vsx2 null mutant mice, FGF can no longer induce transdifferentiation of RPE into the retina. Consistently, loss of Vsx2 activity mimics FGF loss-of-function resulting in a retina-into-RPE transdifferentiation (Horsford et al., 2005). This Vxs2 action may be mediated by directly suppressing transactivation of *Mitf* gene in the distal OV, a critical TF for RPE identity as discussed later on.

Midline tissue-derived **Shh** molecules play critical roles in establishing the bilateral EF, as mentioned before, but also in determining the proximal–distal axis of the eye primordium. Experiments in chick embryos highlighted Shh role in coordinating dorsal-ventral patterning of the eye at OV stage. Shh activity is also required for eye morphogenesis during the transition from the OV to the OC, as well as after initial formation of the double-layered OC (Zhang and Yang, 2001).

On the other hand, members of **TGFβ** family favour the specification of the RPE. In explant cultures of chick OV after removal of surrounding extraocular mesenchyme, RPE development did not occur. Extraocular mesenchyme was shown to be required for the induction and maintenance of expression of the RPE-specific genes (such as Mitf), inhibition of the expression of NR-specific TF Vsx2 and downregulation of EFTFs (Pax6 and Six6). Furthermore, TGFβ family member Activin A was shown to mimic the effects of the extraocular mesenchyme. **Activin** ligands and receptors are expressed in the surrounding mesenchyme and in the OV, respectively (Fuhrmann et al., 2000).

Also belonging to the TGFβ superfamily are **BMP**s. Several BMP ligands and their receptors are expressed in the developing chick and mouse eye and surrounding tissues. BMP treatment of chick OV converts cells of the presumptive optic stalk and NR region into RPE (Mitf expression is induced). By contrast, interfering with

BMP signalling at OV stages inhibits RPE formation and induces NR-specific gene expression in the outer OC (Müller et al., 2007). Thus, TGFβ signalling plays a role in establishing RPE identity, with signals originating from both the extraocular mesenchyme and the surface ectoderm.

Moreover, **Wnt** signals, which are context-dependently transduced via the noncanonical or canonical signalling pathways, were recently shown to mediate RPE specification by a GSK3β-dependent but β-catenin-independent pathway. Wnts (namely Wnt2b) and BMPs are released from the surface ectoderm to specify the RPE cooperatively. Surface ectoderm removal at early OV stages or inhibition of Wnt, but not Wnt/β-catenin, signalling prevents pigmentation and downregulates Mitf expression. This effect is rescued by both activation of BMP or Wnt signaling. Thus, Wnt signalling from the overlying surface ectoderm was proposed to be involved in restricting BMP-mediated RPE specification to the dorsal OV (Steinfeld et al., 2013).

In addition to signalling molecules, patterning of OV is also specified by TFs, in particular **Lhx2**. As mentioned before, in *Lhx2*$^{-/-}$ mouse embryos, eye field specification and OV morphogenesis occur, but development arrests prior to OC formation. This is accompanied by failure to maintain or initiate the expression patterns of OV-patterning. Lhx2 is cell-autonomously required for expression of TFs determinants of RPE and NR in the OV (namely Mitf and Vsx2). Moreover, Lhx2 also influences OV patterning by modulating BMP signalling (Roy et al., 2013; Yun et al., 2009).

Regarding RPE specification, signalling molecules previously mentioned instruct the cells of the dorsal OV towards a RPE fate by activating/repressing a network of TFs. Contrarily to early EF, only a small number of TFs have been proven to be essential to RPE specification: Mitf, Otx1 and Otx2, and Pax6.

Microphthalmia-associated transcription factor Mitf, which encodes a basic helix-loop-helix leucine-zipper (bHLH-LZ) protein at the mouse *microphthalmia* locus, plays important roles in many developmental pathways, including the differentiation of melanocytes of neural crest origin and neuroepithelial-derived RPE. Mice with mutations at this locus display loss of pigmentation, reduced eye size, failure of secondary bone resorption, reduced numbers of mast cells, and early-onset of deafness (Hodgkinson et al., 1993). Mutations in the *MITF* gene, the human counterpart of the *Mitf* gene, are associated with dominantly inherited auditory–pigmentary syndromes, such as Waardenburg syndrome type 2 (WS2),

which are characterized by sensorineural hearing loss and abnormal pigmentation of the hair and skin (Tassabehji et al., 1994). Mitf belongs to the bHLH-LZ family of TFs and thus the basic region permits the binding to the E box motif (CANNTG), and the HLH-LZ region allows it to form homodimers or heterodimers with the related TFs TFE3, TFEB and TFEC. In mice and humans, *MITF* gene encodes a family of at least 10 distinct isoforms generated from the same gene by alternative promoter/exon usage (Bharti et al., 2008; Li et al., 2010b). MITF-M is specifically expressed in melanocytes originating from neural crest and in melanoma cells. Isoforms MITF-A, MITF-H and MITF-J are expressed in variable levels in different cell types, including the RPE. Relevantly, MITF-A is the most abundantly expressed in the RPE. The expression of MITF-D isoform has been found in RPE, macrophages, osteoclasts and mast cells, but not melanocytes and melanoma cells. Isoforms MITF-E and MITF-Mc are specifically expressed in mast cells, whilst MITF-CX has been shown to be expressed in human cervical stromal cells (Amae et al., 1998; Hershey and Fisher, 2005; Li et al., 2010b; Šamija et al., 2010; Shibahara et al., 2000).

During the eye developmental process in the mouse, Mitf is initially expressed throughout the entire OV, but subsequently its expression is restricted to the dorsal portion and downregulated in the distal part when Vsx2 expression is initiated. Moreover, in Mitf mutant embryos, at least the dorsal part of the future RPE becomes thickened, loses expression of a number of specific TFs, gains expression of NR-specific genes (such as Six3, Chx10 and Crx), remains unpigmented and eventually transdifferentiates into a laminated second retina (Nguyen and Arnheiter, 2000). As mentioned earlier on and to summarize, Mitf expression is downregulated by FGF signalling and Vsx2 TF, and upregulated by Activin, BMP and Wnt signalling pathways as well as Lhx2 TF. Moreover, Pax6 and Otx genes also regulate Mitf expression, in the context of OV patterning events (Bharti et al., 2006).

Mitf binds and transactivates the promoter regions of genes involved in the terminal differentiation of the RPE, including the melanosome glycoprotein QNR17, melanogenic enzyme Tyrosinase and the Tyrosinase-related protein TRP-1 and TRP-2. This transactivation occurs through specific binding of Mitf to M-boxes and E-boxes containing the hexameric E-box containing motif present in the promoter regions of these genes (Martínez-Morales et al., 2004; Murisier et al., 2007). Besides cell differentiation, Mitf also plays a role in regulating cell proliferation. Mouse Mitf mutations lead to a thickening of the RPE and increased cell numbers.

At least in melanocytes, Mitf-M isoform has been described to inhibit cell proliferation, through stimulation of the transcription of two negative regulators of the cell cycle: the CIP/KIP family member p21 and Ink4a. Aditionally, Mitf controls cell proliferation indirectly through the regulation of tyrosinase, which catalyzes DOPA synthesis and in turn, DOPA negatively regulates cell proliferation (Bharti et al., 2006; Nguyen and Arnheiter, 2000).

The **orthodenticle-related TF Otx1 and Otx2** are homeodomain TF with an essential role in anterior head formation (as described earlier for Otx2). The two Otx genes appear to cooperate in some aspects of vertebrate brain morphogenesis since a minimum level of OTX protein is required for the patterning of the anterior brain (Suda et al., 1999). In the vertebrate eye, both Otx1 and Otx2 are initially expressed throughout the OV. Later Otx2 becomes specifically restricted to the presumptive RPE territory. After that regional specification of the eye is achieved, a second wave of Otx2 expression was found also in the NR, particularly in postmitotic neuroblasts committed to both neuronal and glia cell types. Studies involving mutant mice revealed that both Otx1 and Otx2 genes are required in a dose-dependent manner for the normal development of the eye. Mice deficient in Otx genes present clear defects in the patterning of the RPE, which is replaced by a NR-like territory. The expression of Mitf and Tyrosinase is largely absent and conversely upregulation of Pax6, Six3 and Pax2 is observed (Martinez-Morales et al., 2001). Furthermore, Otx2 induces a pigmented phenotype, as Mitf, when overexpressed in avian NR cells. Additionally, Otx2 binds specifically to a bicoid motif present in the promoter regions of QNR71, TRP-1, and tyrosinase genes, transactivating them (as is described for Mitf). Both Otx2 and Mitf co-localize in the nuclei of RPE cells, physically interact with each other and operate cooperatively in transactivating the mentioned RPE-specific promoters. Since in Mitf mutants Otx2 is missing, and it is not possible to simply place Otx genes above Mitf genetically, the current hypothesis is that both TF might collaborate at the same hierarchical level to establish the identity of the RPE (Martínez-Morales et al., 2003a).

As already mentioned, **Pax6** plays a fundamental role in the eye developmental process and, if in mice Pax6 is missing entirely, OVs fail to form properly and eye development is aborted. Regarding differentiation of the RPE, it has shown to delay it (delayed or absent pigmentation) whilst not fully preventing it (Collinson et al., 2003). Another member of the paired box family of TF, **Pax2**, has also been implicated in some steps. Pax2 has a similar expression pattern when compared to Pax6 but more restricted: in the OV, Pax6 has a broad distribution covering the

entire structure, whilst Pax2 is expressed mainly in the ventral portion. Pax2, contrarily to Pax6, is not expressed in the lens ectoderm. At the OC stage, Pax6 is initially expressed in all tissues but then expression is lost in the developing RPE. On the other hand, Pax2 expression is restricted to the ventral NR that surrounds the closing optic fissure and the presumptive glia cells of the optic nerve (Baumer et al., 2003). Loss-of-function mutants have revealed crucial roles for Pax2 in the generation of the optic stalk and for Pax6 in the development of the OC, and results point out to the notion that the position of the OC/optic stalk boundary depends on Pax2 and Pax6 expression (Schwarz et al., 2000). Double null mice present small OV with a partial decrease on Mitf expression. It has been proposed a redundant function of both paired box TFs in the RPE specification, supported by their shared ability to bind and transactivate Mitf promoter through the same binding site (Baumer et al., 2003). However, Pax2 contribution has also been questioned and some evidence supports the idea that Pax2 may act as a negative regulator of RPE specification while Pax6 is a positive one (Martínez-Morales et al., 2004).

3. Optic Cup

The distal part of the OV makes contact with the overlying surface ectoderm, resulting in the specification of the lens ectoderm. Subsequently, the invagination of the lens placode and distal OV occurs, giving rise to a bilayered OC, which inner layer will develop into the NR and the outer layer into the RPE. The RPE fate that was initially established at the OV stage is now maintained by a concerted effort of multiple factors (Figure 1.14). At this point, differentiation and maturations steps occur: proliferation in the presumptive RPE ceases, leading to the formation of a single layer of cuboidal cells that become pigmented. Structural and functional changes take place such as formation of tight junctions, expansion of the apical microvilli, invagination of the basal membrane, establishment of polarity and acquisition of the retinoid recycling machinery (Fuhrmann, 2010; Graw, 2010).

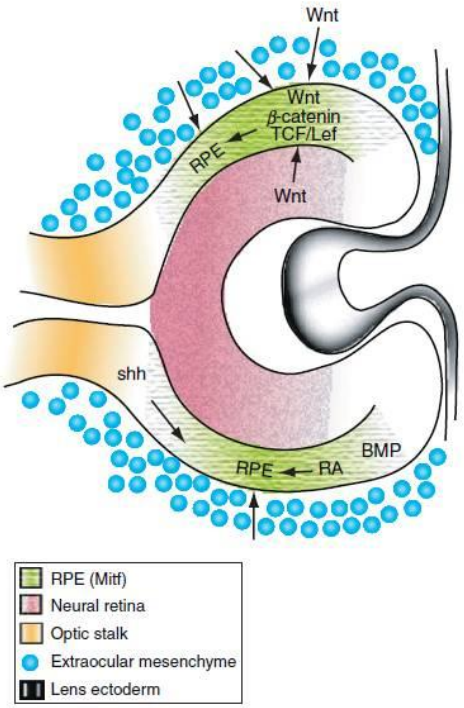

Figure 1.14: Maintenance of RPE phenotype within the OC.

Several signalling pathways, such as retinoic acid (RA), BMP, Shh and Wnt, are implicated in the regulation of cell fate in the presumptive RPE (green). Adapted from (Fuhrmann, 2010).

Interestingly, OC folding can occur independently of the lens (but not the pre-lens ectoderm) or is ectopically induced by Six3 overexpression, suggesting that the invaginating lens may not play a role in the formation of the OC. The folding process may be dependent of the early specification events on OV stage and on the intrinsic properties of the developing epithelial cells. A study conducted in chick indicated that invagination was a Ca^{2+}-dependent process. In medaka, the *ojoplano* mutant was identified displaying defects in OC folding. The mutated gene encodes for a transmembrane protein that localizes to the basal side of the epithelium and might be implicated in the establishment of focal contacts required to allow the transmission of contractile morphogenetic forces (Martinez-Morales and Wittbrodt, 2009). Moreover, a recent breakthrough work reported that the complex process of OC formation was successfully recapitulated in 3D culture of mouse and human ES cells. Floating aggregates of ES cells have been cultured in medium suitable for retinal differentiation and containing extracellular matrix proteins. ES-cell-derived epithelium first evaginates as vesicles and then undergoes invagination into the NR to form OCs. Furthermore, a multilayered NR is generated with 6 different types of retinal cells. Therefore in homogeneous culture medium without

external forces, positional cues or physical constraints, the formation of OCs and the multilayered NR occurs by self-organization, and is driven by an internal program that functions through local intercellular interactions. It is expected that these cytosystems dynamic studies will shed light in our knowledge of the principles by which organ architecture develops (Eiraku et al., 2011; Nakano et al., 2012; Sasai, 2013b).

Upon OC formation, several signalling pathways continue to exert their action contributing to RPE specification (Figure 1.14). The Shh signalling pathway was shown to be required for this step of maintenance of RPE cell fate in the ventral OC. In the mouse, reduced Shh signalling may not affect RPE specification but in further steps results in dorsal-ventral patterning defects, with loss of RPE marker expression and NR-into-RPE transdifferentiation (Huh et al., 1999). Dorso-ventral polarity of the OC is determined by BMPs dorsally and Shh ventrally, which repress each other's action. Two types of TFs seem to be involved in this mutual repression, the T-box protein Tbx5, induced dorsally by BMP4, and the ventral homeodomain proteins Vax1 and Vax2, induced ventro-proximally by Shh (Bharti et al., 2006; Zhang and Yang, 2001; Zhao et al., 2010). BMP signalling is also implicated in the maintenance of the RPE in the ventral OC, since overexpression of BMP antagonist noggin leads to transdifferentiation of the ventral RPE (Adler and Belecky-Adams, 2002). Additionally retinoic acid signalling plays a role at OC stage since once perturbed, Pax6, Tbx5 and Bmp4 are ectopically expressed in the presumptive RPE, while Otx2 and Mitf are not induced, leading to a dorsal transdifferentiation of RPE to NR (Halilagic et al., 2007).

Wnt/β-catenin signalling activation results in cytoplasmic stabilization of β-catenin, which then translocates into the nucleus and associates with TCF/LEF transcription factors. TCF/LEF-responsive reporters have been shown to be activated in the dorsal OV and in the peripheral and dorsal RPE in the OC. Conditional disruption of β-catenin in the mice RPE results in downregulation of Mitf and Otx2 expression which is replaced by that of Vsx2 and in consequent RPE-into-NR transdifferentiation, causing severe ocular defects such as microphthalmia.. Furthermore, β-catenin binds near and activates putative TCF/LEF sites in the Mitf and Otx2 enhancers. These results highlighted an essential role for Wnt/β-catenin signalling, via TCF/LEF activation, in maintaining cell fate in the developing RPE by the direct regulation of Mitf and Otx2 expression. Interestingly, ectopic activation of Wnt/β-catenin in the presumptive retina is not sufficient to promote a change into

the RPE-like tissue alone, but is capable of doing so when in combination with Otx2 (Westenskow et al., 2009, 2010).

Wnt signalling was also implicated in a regulatory loop together with Pax6 and Mitf controlling RPE development. A model has been proposed positioning Pax6 in the center of a bi-stable regulatory loop, and providing an anti-retinogenic role for Pax6 in the developing RPE, besides its retina-promoting activity. In the RPE and together with Mitf or its paralog Tfec, Pax6 suppresses the expression of Fgf15 (positive regulator of retinal development) and Dkk3 (inhibits RPE-promoting Wnt signalling). On the contrary, on a NR context, Pax6 promotes FGF signalling and inhibits canonical Wnt signalling (through Dkk3 action), thus stimulating the expression of retinogenic genes, including Six6 and Vsx2 (Bharti et al., 2012).

Otx2 also interferes with the definition of RPE-NR boundaries at the OC stage, since it prevents the presumptive RPE region from forming the NR by repressing the expression of Fgf8 and Sox2, both inducers of the NR cell fate (Nishihara et al., 2012). Regarding the differentiation and maturation steps, Otx2 cooperates with Mitf in the regulation of the expression of the melanogenic genes, as mentioned earlier, and also of another RPE-specific gene Bestrophin-1 (Masuda and Esumi, 2010). Moreover, Otx2 has been shown to control the expression of several groups of genes involved in other RPE-specific functions, such as retinol metabolism, pH regulation and metal concentration. This regulatory action, in addition to the disruption of PR-RPE cell adhesion, explains the non-autonomous RPE-dependent origin for PR cell degeneration observed after conditional ablation of Otx2 in mice retinas (Béby et al., 2010; Housset et al., 2013).

In conclusion, several molecular and signalling players work in a concerted and integrative way to establish RPE cells over the multistep eye developmental process.

Degenerative disorders involving the RPE

The retina is a complex structure constituted by several cell layers interacting with each other. Importantly, RPE cells are crucial for visual function providing multiple support roles essential to maintain PRs' activity of sensing and transmitting visual information. Therefore, RPE and PR cells are considered a functional unit that interact synergistically. Supporting this idea, multiple diseases have been described resulting from defects on genes usually expressed by PRs and compromising its function, which lead to degeneration of the RPE. Conversely, several studies showed that diseases impairing

any of the known support functions exerted by the RPE will result in degeneration of the PR, and consequently loss of retina´s structure and functionality with associated vision loss (Figure 1.15) (Sparrrow et al., 2010; Strauss, 2005).

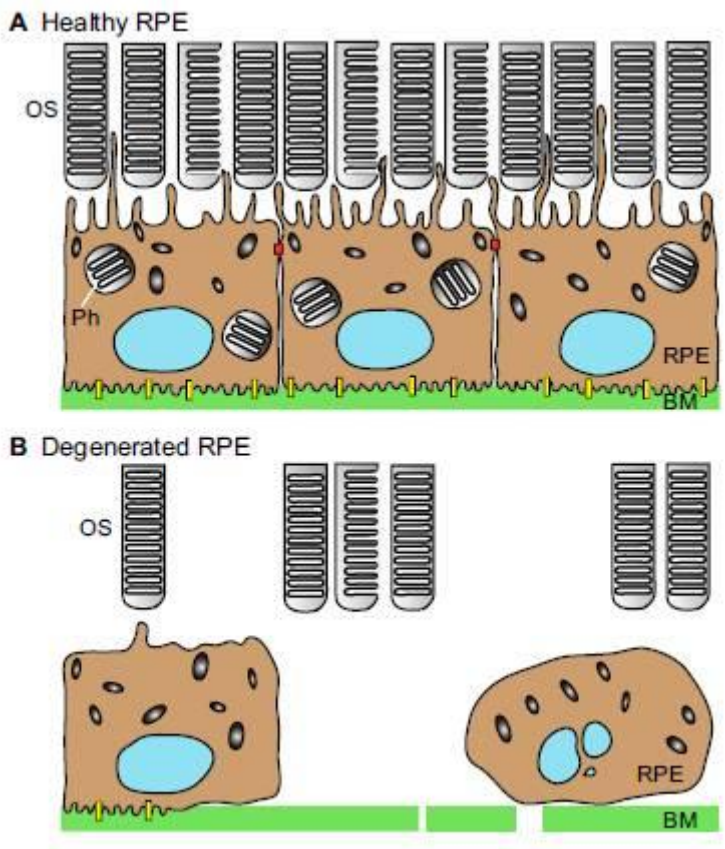

Figure 1.15: Healthy and degenerated RPE: implications for retina's overall structure.

(A) Healthy RPE cell layer in close interaction with Bruch's membrane (BM) and PRs' OS. (B) Degenerated RPE cells lose epithelial phenotype and become a discontinuous layer of cells, with loss of tight junctions between them and loss of adherence to BM. RPE phagosomes (Ph) may be lacking, resulting in inability to phagocytose the daily shed of OS. Consequently, PR cells also degenerate and the complex retina structure imperative for its function is lost. Adapted from (Ramsden et al., 2013).

For example, ABCA4 is a member of the ABCA subfamily of ATP binding cassette (ABC) transporters that is expressed in rod and cone PRs of the vertebrate retina. *ABCA4* gene product was described as a retinylidene-phosphatidylethanolamine transporter that facilitates the removal of potentially reactive retinal derivatives from PRs following photoexcitation. Over 500 mutations in the gene encoding ABCA4 were described as associated with a spectrum of related autosomal recessive retinal degenerative diseases including **Stargardt's macular degeneration**. Stargardt's disease is characterized by a significant loss in central vision in the first or second decade of life, bilateral atrophic

changes in the central retina associated with degeneration of PR and underlying RPE. The clinical picture is of yellow flecks extending from the macula, the central posterior portion of the retina with the densest concentration of PR and responsible for central high-resolution visual acuity. These flecks correspond to abnormal accumulation of the toxic pigment lipofuscin in the PRs and subsequently in the RPE (Allikmets et al., 1997; Molday and Zhang, 2010).

On the other hand, several retinal disorders characterized by PR and associated retinal circuitry degeneration have been described to result from disruption of the various support functions of the RPE, namely protection against photo-oxidative damage, transepithelial transport, visual cycle, phagocytosis of OS and secretion of growth factors (Strauss, 2005). Particularly, **Retinitis Pigmentosa** (RP) refers to a group of inherited retinal degenerations with a very variable clinical course, though most patients report problems with night blindness and progressive peripheral visual field loss, leading to tunnel vision, often followed by blindness. There are over 100 defined mutations that may lead to RP, many of each code for genes in PR (Hartong et al., 2006). However, many RP subtypes begin with primary failure of the RPE, as MERTK-associated autosomal recessive RP. MERTK is required for phagocytosis of PRs' OS by the RPE and once absent, RPEs' phagocytic ability is impaired, resulting in accumulation of subretinal debris and subsequent PR loss via apoptosis and retinal degeneration (Gal et al., 2000).

Another example is **Leber Congenital Amaurosis** (LCA), a rare hereditary retinal degeneration caused by mutations in more than a dozen genes. LCA2 is associated with mutations in RPE65 gene, which is almost exclusively expressed in the RPE and functions as retinoid isomerase involved in the recycling all-*trans*-retinol to 11-*cis*-retinal. Improper functioning or absence of RPE65 results in a lack of 11-*cis*-retinal production and an inability to efficiently form the visual pigments, rhodopsin and cone opsin. Concomitant accumulation of large amounts of all-*trans*-retinyl esters in the RPE is thought to promote PR degeneration (Cideciyan, 2010; Moiseyev et al., 2006).

In addition to genetic disorders, some multifactorial degenerative diseases affecting the retina have also been described, with underlying impairment of RPE functions. **Age-related Macular Degeneration** (AMD) is a major cause of blindness worldwide. With ageing populations in many countries, more than 20% might have the disorder. Damage to the macular region of the retina results in loss of sharp, central vision. AMD is a complex degenerative disorder with a polygenic hereditary component. The major risk factors are cigarette smoking, nutritional factors, cardiovascular diseases, and genetic markers, including genes regulating complement, lipid, angiogenic, and extracellular

matrix pathways. AMD arises as the result of chronic, low-grade inflammatory damage to the macular retina, leading to degeneration of the RPE and the Bruch's membrane. In its early stage, there is formation of drusen, basal laminar and linear deposits located between RPE and Bruch's membrane or inside the later, resultant of accumulation of metabolic end products. Over time, there is also accumulation of the toxic lysosomal protein lipofuscin, consequently to incomplete digestion of the OS discs by the RPE. Bruch's membrane thickness increases, leading to impairment of the import of nutrients and export of metabolic products by the RPE cells. The late stage of AMD is divided into two forms: nonexudative or "dry" form and an exudative/neovascular or "wet" form. In the first, there are atrophic changes in the macula, with the progressive dysfunction of the RPE resulting in PR loss. In exsudative AMD, choroidal neovascularization is present: there is formation of new abnormal blood vessels in the choriocapillaries through the Bruch's membrane. This neovascularisation is driven by the presence of excess VEGF on the apical side of the RPE, which promotes the growth of fenestrated, leaky capillaries that allow the build-up of fluid. These new vessels have a greater tendency of leakage and bleeding into the macula, ultimately leading to irreversible damage to the PRs if left untreated (Ehrlich et al., 2008; Lim et al., 2012).

Moreover, **Diabetic Retinopathy** (DR) is another multifactorial disorder in which RPE dysfunction may play an important role in its pathophysiology. DR is the main cause of blindness in working-age adults in developed countries. It is well known that diabetes duration, poor glycemic control, and hypertension are the primary factors accounting for the risk of developing DR. Genetic factors may also influence either the onset or the severity of DR. Neovascularization due to severe hypoxia is the hallmark of proliferative DR, which is the commonest sight-threatening lesion in type 1 diabetes. In type 2 diabetes, the primary cause of poor visual acuity is diabetic macular edema characterized by vascular leakage due to the breakdown of the blood retinal barrier. Impairment of RPE's functions contributes to the pathogenesis of DR, namely its secretion ability. Overproduction of VEGF plays an essential role in the development of proliferative DR. The pathogenesis of diabetic macular edema remains to be fully understood, but VEGF and proinflammatory cytokines have been showed to be involved in its development. Nonetheless, the balance between angiogenic (i.e., VEGF) and antiangiogenic factors (i.e., PEDF) plays a crucial role in the development of DR (Heng et al., 2013; Simó et al., 2010).

Choroideremia

Choroideremia (CHM) is an X-linked recessive retinal dystrophy characterized by progressive degeneration of the PRs, the RPE and the choriocapillaries. CHM is a rare monogenic disease, with a described prevalence of 1 in 50000 to 1 in 100000 (Moosajee et al., 2014). It is caused by loss-of-function mutations in *CHM/REP1* gene (Xq21.2), which encodes for Rab Escort Protein 1 (REP1), important for the regulation of the intracellular membrane trafficking machinery (van Bokhoven et al., 1994; Cremers et al., 1990).

CHM has an X-linked pattern of inheritance with **affected males** developing night blindness in their first or second decades of life. Usually visual acuity decreases very slowly until subjects reach the fifth decade of age, at which time the rate and extent of vision loss becomes significantly higher. Progressive visual field restrictions with loss of peripheral vision are observed, resulting in tunnel vision and ultimately in complete blindness (Coussa et al., 2012; Roberts et al., 2002). Taking advantage of ophthalmoscopy techniques, fundus autofluorescence and electrophysiological measurements, several studies have revealed a variability of disease severity, whilst some common traits are observed. Moreover, no genotype-phenotype correlation was determined so far (Huang et al., 2012; Mura et al., 2007; Ponjavic et al., 1995; Renner et al., 2006; Zhou et al., 2012).

Despite the maintenance of good visual acuity in CHM patients until the degenerative events affect the central retina, some underlying changes in the retina can be identified on earlier disease stages. Typically, patchy depigmentation, that progressively extents to pigment loss and visibility of yellow white sclera through transparent retina, are observed and constitute a unique feature of CHM, when compared with other retinal dystrophies. Moreover, it has been described a thickening of the retina on earliest stages, whilst still maintaining its normally laminated structure. Further thickening and disorganization of the retina occurs subsequently to the loss of PRs, either independently or associated with RPE depigmentation. Finally, in the subsequent decades, a centripetal thinning of the dysmorphic retina is observed (Jacobson et al., 2006).

The majority of **female carriers** of mutations on *REP1* gene are asymptomatic, with no alterations on visual acuity, notwithstanding some characteristic alterations in fundus autofluorescence are detected (Coussa et al., 2012; Preising et al., 2009; Renner et al., 2009). However, fundus alterations and retina dysfunction can progress over time and, in some rare cases, female carriers are severely affected with findings similar to those in males (Bonilha et al., 2008; Huang et al., 2012;

Renner et al., 2009). Mosaic distribution of abnormal retina areas was also observed, which was attributed to random X-chromosome inactivation leading to variability in the inactivated and activated gene copy in each cell (Rudolph et al., 2003; Vajaranant et al., 2008). Disease manifestations in females may also be due to X-autosomal translocations involving Xq21, which lead to disruption of *CHM* gene (Lorda-Sanchez et al., 2000; Mukkamala et al., 2010).

Loss-of-function mutations of *CHM* gene underlie CHM. This gene spans a genomic sequence of approximately 150 kb on chromosome Xq21.2, containing 15 exons and encoding a ubiquitously expressed protein of 653 amino acids: the **REP1 protein**. REP1 plays a crucial role as a regulator of Rab GTPases' activity. More than 60 different Rab proteins belonging to Ras superfamily of small GTPases have been described so far, functioning as regulators of intracellular vesicular transport and organelle dynamics. Rab GTPases regulate vesicle budding, vesicle tethering and fusion in vesicular transport, as well as vesicle motility given their role in recruiting molecular motors to organelles. Additionally, they coordinate intracellular signalling events with membrane traffic and define organelle identity through attribution of functionally distinct subdomains within a particular membrane (Seabra and Wasmeier, 2004; Seabra et al., 2002; Stenmark, 2009).

Rab GTPases act as molecular switches, cycling between an active GTP-bound and an inactive GDP-bound state, which correlates with phases of association and of dissociation with the target membrane. The GTP/GDP switch along with the membrane association/dissociation cycle allows both spatial and temporal control of Rab proteins' activity and is coordinated by several factors (Figure 1.16).

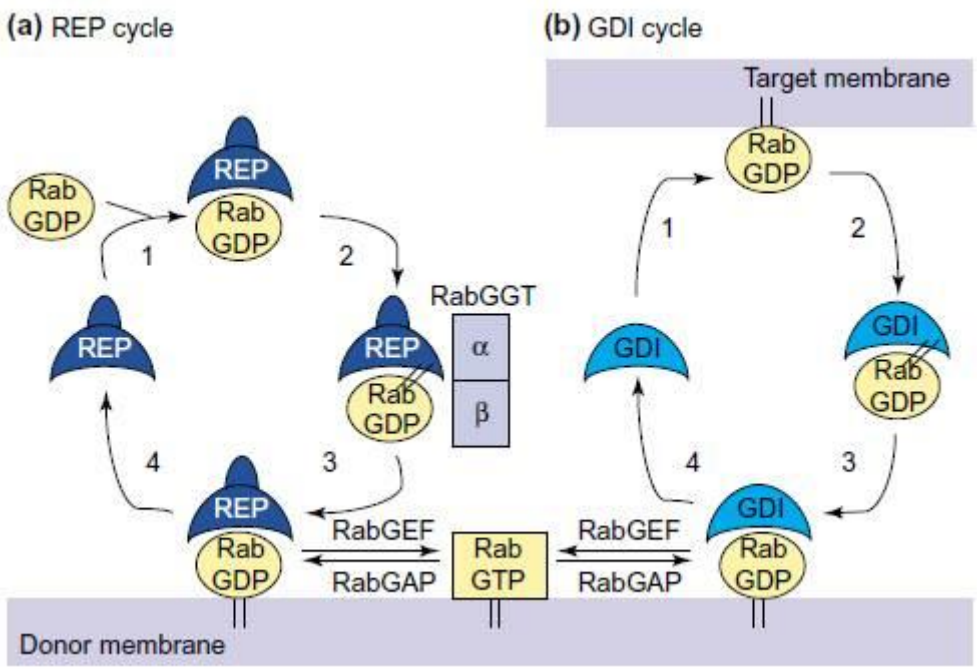

Figure 1.16: Rab proteins' cycle showing membrane recruitment and activation.

(a) Newly synthetized Rab GTPases associate with REP protein forming a stable complex (1), essential for the recognition of Rab proteins by heterodimeric Rab geranylgeranyl transferase (RabGGT or GGTase II). This enzyme is responsible for attaching geranylgeranyl groups to C-terminal cysteines in Rab proteins (2). Following this lipid transfer, REP protein is thought to deliver the prenylated Rab to the donor membrane (3) and then recycles to bind other nascent Rab protein (4). (b) Equivalent role is played by Rab GDP-dissociation inhibitor (GDI) in the case of recycling Rabs. RabGDI is thought to retried Rab proteins from target membranes (1) and maintain them in the cytosol in a stable complex (2). GDP-bound Rab is eventually delivered to the donor membrane by the RabGDI (3), which then recycles back to the cytosol. Both REP and RabGDI proteins specifically bind to the GDP-bound state of Rab proteins. After dissociation of the soluble regulator (REP or GDI), specific Rab guanine nucleotide exchange factors (GEF) are responsible for the exchange of the bound GDP for GTP, activating the Rab and stabilizing it on the membrane. Activated GTP-bound Rabs recruit a wide variety of downstream effector molecules to the membrane, which reflects the diverse functions Rabs play in membrane traffic. GTP hydrolysis catalyzed by a GTPase- activating protein (GAP) returns Rab proteins to their inactive GDP-bound state. Adapted from (Seabra et al., 2002).

Rab proteins are intrinsically soluble proteins, requiring post-translation modifications in order to associate with cellular membranes. Rab GTPases are lipid modified on the C-terminus in a process termed prenylation and consisting of the covalent attachment, via thioether linkage, of C20 (geranylgeranyl) isoprenoid groups to C-terminal cysteine residues in the context of a prenylation motif. Rab proteins exhibit a variety of prenylation motifs at their C-termini, containing either one or, more frequently, two cysteine residues, both of which are modified by geranylgeranyl groups. This prenylation reaction is catalysed by Rab geranylgeranyl transferase (Rab GGTase or GGTase II), a heterodimeric enzyme composed of α and β subunits. However, prenylation motifs of Rab proteins are

insufficient for GGTase II recognition, requiring prior binding of newly synthetized Rabs to REP protein (previously designated as component A of GGTase) (Leung et al., 2006; Seabra et al., 1992; Shen and Seabra, 1996). Rab:REP complex functions as GGTase II substrate and, after the transfer of one or two isoprenoid groups, the ternary complex remains associated until the binding of a new geranylgeranyl diphosphate (GGpp) molecule. This, in turn, stimulates the release of the GGTase II:REP complex. REP then escorts the prenylated Rab protein to its target membrane.

Closely related to REP protein, both in sequence and structure, is Rab GDP-dissociation inhibitor (GDI) protein. Functionally however, RabGDI protein has a distinctive role as an important regulator of the recycling of Rab proteins by mediating their reversible association with membranes. This important distinction is based on RabGDI inability to assist lipid modification of Rab proteins by GGTase II. Crystal structures of REP:GGTase II complex revealed that features observed in a small number of critical residues located at the interface of the two proteins are critical for their interaction. A highly conserved phenylalanine in REP, which is absent in RabGDI, is critical for the ability of REP to interact with GGTase II and form a complex. However, a geranylgeranyl binding site conserved in REP and RabGDI has been identified. Structural data of Rab7:REP complex also revealed a remarkable structural similarity with crystal structure of a complex between yeast RabGDI and Ypt1 (the yeast homologue of Rab1) (Pylypenko et al., 2003; Rak et al., 2004).

In CHM, over 130 unique **mutations** of *CHM/REP1* gene have been reported so far, including deletions, insertions, duplications, translocations, nonsense, splice-site, frameshift and missense mutations. Full and partial gene deletions along with nonsense mutations resulting in truncated and therefore non-functional forms of REP1, account for 55-80% of all cases. Two missense mutations have been reported, being responsible for tertiary structure destabilization or inability to interact with GGTase II (Esposito et al., 2011; van den Hurk et al., 1997a; Moosajee et al., 2014; Sergeev et al., 2009).

Notwithstanding the underlying *CHM* loss-of-function mutations, the molecular pathogenesis of CHM remains speculative. Two REP proteins are found in mammals, sharing 75% amino acid identity, and both are ubiquitously expressed in many tissues, including the several retinal layers (Keiser et al., 2005). **REP2 protein**, a REP1 homolog, is encoded by autosomal *CHML* (*CHM-like*) gene. In an individual with CHM, REP2 is assumed to partially compensate for the loss of

REP1 function in all cells except in the eye, thus leading to the slow-onset retinal degeneration characteristic of CHM and the limited nature of CHM clinical manifestations (Cremers et al., 1994; Seabra, 1996). However, REP2 compensation is only partial since peripheral cells of CHM patients (like skin fibroblasts and monocytes) have been shown to display increased pH levels in lysosomes, reduced rates of proteolytic degradation and altered secretion of cytokines when compared to normal cells. Moreover, it has been proposed that these changes could be monitored and potentially correlated with disease severity (Strunnikova et al., 2012, 2009).

Previous studies suggested that the molecular basis of CHM could reside in the existence of some **Rabs that are selectively underprenylated** in the absence of REP1. One such candidate is Rab27a, which was found to be underprenylated in lymphoblasts of CHM patients. Rab27a is highly expressed in the RPE and choroid, two cell layers usually affected in CHM (Seabra et al., 1995). Its underprenylated status may be due to relying only in the less efficient REP2 prenylation reaction. Rab27a has been shown to bind equally well to both REP1 and REP2, but with REP2-Rab27a complex displaying a lower affinity for GGTase II when compared with REP1-Rab27a. Moreover, Rab27a has a relatively low GTPase activity, resulting in a higher proportion of the inactive form of this molecule and concomitantly decreasing the affinity of the REP interaction *in vivo* (Larijani et al., 2003). Additionally, in CHM all prenylation reactions are provided by the REP-2 protein, with Rab molecules with a higher affinity for REP2 (Rab7 and Rab1A) competing with Rab27A for prenylation (Rak et al., 2004). However, CHM patients do not present absence of the pigmentation and immune system defects characteristic of type I Griscelli syndrome. This syndrome is caused by a defect in the *RAB27A* gene, indicating that loss of REP1 in CHM does not result in complete loss of Rab27a function in all tissues. Thus, it is likely that a more generalized effect of REP1 deficiency on multiple Rab proteins accounts for the retinal phenotype of CHM (Seabra et al., 2002). For instance, recent results point out to the possibility that impairment of Rab27b and Rab38 prenylation rate could contributing to CHM pathogenesis (Köhnke et al., 2013).

Alongside with the still controversial molecular mechanism underlying CHM **pathogenesis**, it is still debatable if the degeneration of the PRs, the RPE and the choroid occur independently or sequentially layer-by-layer. Around the 1950s, McCulloch and colleagues proposed that choroid atrophic alterations resulted in secondary loss of RPE and PR layers (MacDonald et al., 2009). At late 80's, two

contradictory theories were proposed: the primary cause of CHM, as suggested by the name itself, was a degeneration in the vasculature as supported by the finding of vascular endothelial cell abnormalities throughout the uveal tract, including the posterior choroid with loss of the RPE and NR but also the anterior uveal tract (Cameron et al., 1987). Contrarily, observations on a CHM carrier revealed areas of abnormal RPE associated with shorter or absent outer segments of the PR cells. Later, it was also suggested that the primary defect of CHM was at the level of the RPE, due to a probable impairment of its phagocytic ability (Flannery et al., 1990). The possibility that the primary event was a degeneration of the rod PRs was also raised (Syed et al., 2001).

Upon the model of CHM disease progression, it was proposed that the early stage of thickened yet normally laminated retina was resultant of Müller cell activation and hypertrophy due to PR stress. However, it was not conclusively determined if this PR damage was a primary or secondary event to RPE dysfunction (Jacobson et al., 2006). In other studies involving young CHM patients it was observed that in areas where the RPE was preserved or mildly altered, retinal lamination and thickness remained remarkably normal. In contrast, areas of RPE and choriocapillaries atrophy were observed with overlying preservation of retinal thickness albeit with impaired lamination, suggesting that RPE changes could precede retinal damage (MacDonald et al., 2009; Mura et al., 2007). Recent studies using high-resolution retinal imaging demonstrated abnormalities of fundus autofluorescence, retinal layer morphology, and cone morphology and spacing in CHM patients and carriers. The pattern of PR degeneration is different from what is observed in patients with primary PR degenerations, such as Retinitis Pigmentosa. In CHM, both RPE and PR cells were affected, supporting the idea that these cell types may degenerate simultaneously (Syed et al., 2013).

In order to provide some useful insights for understanding CHM pathogenesis, **animal models** of CHM were generated. The current hypothesis that CHM retinal degeneration is independent of a primary cell type or retinal layer is supported by data obtained from such models. Null mutations of the X-linked *Chm* gene in mice revealed to be embryonically lethal in males, and also in heterozygous females when the mutation is of maternal origin. Observed lethality is due to defects in trophoblast development and vascularization in mouse extra-embryonic tissues. In heterozygous females, preferential inactivation of the paternal X chromosome in murine extra-embryonic membranes is observed, resulting in expression of the maternal (mutant) copy. Nevertheless, it was observed that the eyes of chimeric

males showed patchy areas of PR degeneration with normal RPE (van den Hurk et al., 1997b; Shi et al., 2004). In order to avoid embryonic lethality and to circumvent breeding problems caused by the inability to transmit the null allele from carrier females, a conditional mouse knockout (KO) of the *Chm* gene was created. Taking advantage of the Cre/ loxP site-specific recombination system, spatial and temporal control of the actual KO event was achieved. Heterozygous-null females exhibited characteristic hallmarks of CHM: progressive degeneration with diminished thickness of the PR layer, patchy depigmentation and thinning of the RPE cell layer, and Rab prenylation defects. By histological analysis, no correlation was observed between areas of RPE and/or PR degeneration (Tolmachova et al., 2006). Furthermore, elegant experiments creating separate tissue-specific KO of the *Chm/Rep1* gene in PR and in RPE did not result in corresponding loss of RPE and photoreceptors, respectively, suggesting that the degeneration of these layers occurs independently. However, when both PRs and RPE are impaired, PR functional deficit and cell death manifest much earlier, suggesting that the diseased RPE accelerates PR damage (Tolmachova et al., 2010).

In zebrafish, loss of *rep1* gene results in lethality at larval stages (Moosajee et al., 2009; Starr et al., 2004). Studies in zebrafish carrying recessive nonsense mutations on *rep1* gene lead the authors to propose a noncell-autonomous degeneration of PR, contrarily to results with rodent models. However, the zebrafish model possesses an inherent limitation for replicating the human condition, since the zebrafish does not have a second gene parallel to *CHML* to compensate for the lack of *rep1*. Nevertheless, helpful insights were withdrawn for these experiments since mutant RPE cells were not able to effectively eliminate PR outer segments, suggesting a defective phagocytosis in CHM. It was also observed anomalies in the maturation, size, and density of melanosomes on the RPE cell layer, likely reflecting the lack of rep and its role in the prenylation of Rab proteins involved in the trafficking of melanin into the melanosomes (Krock et al., 2007). Similar observations were made in the RPE-specific *Chm* KO mice, which displayed reduced numbers of melanosomes in the apical processes and delayed phagosome degradation. Moreover, disorganised basal infoldings of the RPE cell layer were also described (Tolmachova et al., 2010). In human fetal RPE cells, siRNA silencing of the *REP1* gene lead to reduced degradation of PR outer segments, most likely because of the inhibition of phagosome-lysosome fusion events, and increased constitutive secretion of inflammatory molecules, such as MCP-1 and IL-8 (Gordiyenko et al., 2010).

Abnormal melanin granule distribution, absence of basal microvilli and infoldings as well as lack of phagocytosis of outer segments by the RPE cell layer have also been reported in studies with CHM patients and carriers (Bonilha et al., 2008; Ghosh and McCulloch, 1980; Syed et al., 2001). Additionally, inflammatory cells (T-lymphocytes) at the active lesion have been identified, implying a local immune response. Altogether these data point out for striking similarities between the mentioned observations and some of the phenotypes reported in AMD (MacDonald et al., 2009). Moreover, loss of the CHM gene causes premature accumulation of features of aging in the RPE, suggesting that membrane traffic defects may also contribute to the pathogenesis of AMD (Wavre-Shapton et al., 2013).

Current **treatment** options for CHM are still very limited. Periodic ophthalmologic examination to monitor progression of CHM is recommended. A diet rich in fresh fruit and leafy green vegetables, antioxidants, omega-3 fatty acids and/or vitamin A supplementation have been proposed (MacDonald et al., 2003).

A more definitive intervention for the treatment of CHM is currently under study. As a slowly progressing monogenic disorder, CHM is potentially treatable by gene addition therapy. Also in the favour of this approach is the fact that nearly all reported cases of CHM so far have been attributed to functionally null mutations and the small size of the CHM protein coding sequence (1.9 kb). Preclinical studies had very hopeful results, with the gene therapy vector targeting both RPE and PR layers, the first layers to degenerate. Earlier studies using a lentiviral vector showed a strong and stable expression of the human CHM/REP1 cDNA transgene in the RPE cells but with limited transduction of the NR cell layer (Tolmachova et al., 2012). Serotype 2 adeno-associated viral (AAV2) vectors have been shown to efficiently target RPE and PR, with no long-term retinal toxicity. They were used to provide strong CHM/REP1 cDNA transgene expression in CHM patient fibroblasts and CHM mouse RPE cells *in vitro* and *in vivo*, as well as in human PRs, with no observed toxic effects resulting from the REP1 overexpression (Tolmachova et al., 2013). Gene therapy using AAV vector encoding REP1 protein is currently being studied in a multicentre clinical trial, which includes six male patients with CHM. After 6 months, the initial results of this retinal gene therapy trial were very optimistic and consistent with improved rod and cone function, overcoming any negative effects of retinal detachment (MacLaren et al., 2014).

Cell-based therapies for RPE disorders

RPE defects have a causative role in several retinal degenerative disorders, for which the therapeutic options are still very limited and often not curative. These disorders have an expected escalating burden among the overall human diseases, given the observed increasing longevity of the human population. The search for new therapies is thus of paramount importance and the potential use of cell replacement strategies have been extensively investigated.

In such a regenerative medicine approach, the goal is to replace lost or abnormal cells (RPE cells alone and/or PR) for functional cells that would integrate properly into the already damaged retina structure, with corresponding increase in functionality to ameliorate the effects of cell loss on vision. The retina may be an ideal target for cell replacement therapies since the eye is easily surgical accessible, and imaging and functional monitoring in real time during and after intervention are facilitated by its intrinsic transparency. Potential improvements of visual function can be accurately and rapidly measured, and compared to the contralateral eye. Furthermore, the blood-retina barrier confers a degree of immune-privilege in the healthy eye, which may also be advantageous in the case of transplants in diseased eyes. The required number of cells may also be very small since it was estimated that 60 000 RPE cells would be sufficient to cover the macular region and improve visual function (Borooah et al., 2013; Ramsden et al., 2013).

Proof-of-principle for the replacement of diseased RPE cells has been provided by experimental surgeries performed as early as the 1990's. In the case of AMD, macular translocations surgeries in which the macula was moved to the non-diseased periphery of the retina and repositioned on top of an area of healthy RPE were performed as well as grafting healthy RPE cells from the periphery under the macula. Despite being complex and lengthy surgical procedures with high rate of complications, they provided evidence that such cell replacement approaches would benefit patients suffering from retinal degenerations (Machemer and Steinhorst, 1993; MacLaren et al., 2007).

Replacement cells could also potentially come from endogenous progenitors. Early studies of retinal regeneration in amphibians have demonstrated that a small zone of mitotically active cells at the peripheral margin of the retina, the ciliary marginal zone (CMZ), responds to retinal damage by upregulating its production of new neurons. Additionally to this contribution by the CMZ, the RPE serves as the primary source for the formation of an entirely new retina by a process of transdifferentiation. In fishes and birds, Müller glia spontaneously re-enter the cell cycle after retinal damage, and they re-

express embryonic retinal progenitor genes, generating all or only a few types of retinal neurons. However, the mammalian retina has a more limited regeneration potential with no significant persistent neurogenic sources in the adult CMZ, and Müller glia not spontaneously re-entering the mitotic cycle after retina damage. Nevertheless, despite the progressive decline in regenerative potential during vertebrate evolution, there are reasons for optimism in the possibility that such endogenous repair mechanisms can be stimulated in this system in higher vertebrates (Lamba et al., 2008). However, in genetically determined retinal degenerations, the endogenous progenitors would carry the same underlying genetic alteration thus probably compromising this approach. Recently, it was reported that a subpopulation of adult human RPE cells could be activated *in vitro* to a self-renewing cell, the RPE stem cell, with multipotent capacity to generate both neural and mesenchymal progeny (Salero et al., 2012). More studies to confirm the applicability of such cells are in order.

Additional described cell sources for retinal replacement therapy comprise human foetal stem cells, umbilical tissue-derived stem cells and bone marrow-derived haematopoietic and mesenchymal stem cells. Subretinal or intravitreal injections of such cells on a rat model of AMD (RCS, Royal College of Surgeons) or a mouse model of RP have been performed, with observed improvement in the visual function. Since no definite evidence for the attainment of RPE cell morphology and/or functionality was observed in such cases, a paracrine rather than a replacement mechanism of repair is presumed to occur, with improvements on circulation and secretion of growth factors (Ramsden et al., 2013; Stern and Temple, 2011) .

In recent years, pluripotent stem cells (ES cells and more recently iPS cells) have attracted much attention from the scientific community as a potential cell source in such retinal replacement therapies. The first account of the rescue of visual function by ES cells was that of primate ES cells-derived RPE transplanted into RCS rats. ES cells were differentiated into RPE cells prior to transplantation by a co-culture system with stromal cells (PA6) to induce neural differentiation. Large patches of polygonal pigmented cells expressing PAX6 and RPE-specific genes were observed (Haruta et al., 2004).

Other approaches to obtain RPE cells from differentiation of pluripotent cells have been developed. Overgrowth of human stem cell colonies was observed to result in spontaneous differentiation of RPE cells following removal of FGF from the culture medium. After a few weeks, pigmented foci develop, from which the RPE-like cells were derived (Klimanskaya et al., 2004; Vugler et al., 2008). Later on, the same protocol was also successfully applied to human iPS cells (Buchholz et al., 2009; Carr et al., 2009). Spontaneous differentiation of both human ES cells and iPS cells to RPE-like cells can

also be achieved using embryoid bodies (EB) grown in suspension that are plated out as adherent colonies in neural differentiation medium (Meyer et al., 2009).

Directed differentiation protocols were also implemented with the addition of exogenous factors to first promote ES cells and iPS cells into neuroectodermal lineage, following by a step of guided differentiation into RPE-like cells. These stepwise differentiation methods begin with serum-free EB culture system in media containing proteins known to control specification of neuronal lineage, the WNT and Nodal antagonists, Dickkopf 1 (DKK-1) and left-right determination factor (Lefty-A), respectively. A retinal precursor fate is induced, resulting in the expression of the early EFTFs and RPE-specific genes. Fully formed pigmented RPE cells arise from replated EBs after several days in culture (Hirami et al., 2009; Ikeda et al., 2005; Osakada et al., 2009). Alternative methods include sequential incubation with nicotinamide and then activin A, mimicking the TGFβ signalling from the extraocular mesenchyme during OV patterning and which addition has shown to promote the appearance of pigmented cells (Idelson et al., 2009).

Following differentiation of pluripotent cells in RPE-like cells, a thorough step of characterization of the obtained cells is necessary to confirm the molecular and functional identity of RPE cells (a summary of these criteria was reviewed by (Bharti et al., 2011). ES or iPS cell-derived RPE cells have been shown to acquire a pigmented and polarized monolayer phenotype and to express RPE-specific genes and proteins with known roles on the several RPE functions. Phagocytic ability was also detected. *In vivo* functionality was also confirmed after transplantation into RCS rats or mouse models of RP, with observed improvement of visual function (Carr et al., 2009; Li et al., 2012; Meyer et al., 2009).

Delivery of the pluripotent cells-derived RPE has been attained by injection of a single-cell suspension or alternatively, as a preformed monolayer. Preliminary results of a clinical trial in which single-cell suspension of human ES cells-derived RPE were very optimistic, reporting no evidence for teratoma formation, no vision loss and observed new pigmentation near the injection site (Schwartz et al., 2012). However, this delivery method has raised some concerns since single-cells might not develop into monolayers and likely will raise issues with immune rejection. In order to overcome the disorganised fashion in which RPE cells adhere to Bruch's membrane when injected as a suspension, ES cell-derived RPE cells have also been cultured as a monolayer on a thin sheet of plastic polymer. This polymer was designed to act as a replacement for the aged and thickened Bruch's membrane, providing an anchor for the cells as well as aiding in surgical delivery. A clinical trial with this RPE patch graft is already underway (Carr et al., 2013).

In addition to these two phase I clinical trials using ES cell-derived RPE, several others using different cellular sources, including iPS cells, are in earlier stages of development. The scientific community is actively discussing and developing guidelines related with tissue sourcing and GMP manufacturing in order to more efficiently and economically move stem cell-based therapies for retinal degenerative diseases toward the clinic (Bharti et al., 2014).

In several retinal degenerations, PR loss occurs as a consequence of dysfunction of the diseased RPE. In late stages of such degenerative process, a dual replacement of PR and RPE cells is likely to be a promising therapeutic strategy. Similarly to RPE cells, direct differentiation of ES cells and iPS cells into PR has also been reported (Hirami et al., 2009; Lamba et al., 2009, 2010). Furthermore, recent developments have demonstrated the self-formation of entire OC from mouse and human ES cells. The obtained 3D structures possess a stratified neural retina and RPE which may also be a potential route to develop a dual RPE/PR graft that can be used in individuals at later stages of the disease with severe neural retina and RPE loss (Eiraku et al., 2011; Nakano et al., 2012).

On the case of iPS cell-based therapies developed for monogenic diseases, gene defects must be corrected on iPS cells prior to differentiation and transplantation. Proof of principle for this approach was reported by Meyer and colleagues. Human iPS cells derived from a patient with gyrate atrophy, a retinal degenerative disease affecting the RPE, were differentiated into RPE cells exhibiting a disease-specific functional defect. Such phenotype was no longer observed in RPE cells derived from genetically corrected iPS cells (Meyer et al., 2011). This study and others, in which retinal degenerative disease-specific iPS cells were generated, also highlight the potential use of this reprogramming technology to facilitate the study of human retinal development and disease (Jin et al., 2011; Singh et al., 2013).

Main goals and thesis overview

Cellular reprogramming emergent technologies have opened new opportunities for the establishment of novel approaches for regenerative medicine, as well as for disease modelling, drug discovery and toxicity assessment. Several retinal degenerative disorders affect millions of individuals worldwide, ultimately leading to social-impairing blindness. Genetic and multifactorial diseases not yet fully characterized and mostly without a definitive cure, with underlying defects on the RPE cell layer, cause degeneration of the complex retina structure with its consequent loss of function.

Given the key advantages of prospective RPE transplantation in these pathological cases, and also the need for a proper model to further investigate the underlying molecular and pathological events, the work described in this thesis aimed at exploiting the potential of cellular reprogramming approaches to overcome these lacunas.

The main goals of the work presented here are:

1. Implement a methodology for obtaining iPS cells from wild-type mouse somatic cells, properly characterized to confirm self-renewal and pluripotency traits (Chapter 3).

2. Obtain disease-specific iPS cells from a model of a specific retinal degeneration, CHM (Chapter 4).

3. Differentiate pluripotent cells (WT and CHM) into RPE cells, in order to establish an *in vitro* disease model or ultimately to provide cells for prospective transplantation procedures (Chapter 4).

4. Implement a novel methodology to directly reprogram fibroblasts into RPE cells by lineage conversion (Chapter 5).

Chapter 2 Materials and methods

Chapter 2 : Materials and methods

Materials

Standard laboratory chemicals were obtained from Sigma-Aldrich, VWR and Cayman Europe, unless stated otherwise. Recombinant proteins were acquired from R&D Systems.

Antibodies

Table 2.1: List of antibodies used throughout this work, either for Immunofluorescence (IF) or western blot (WB) applications.

Antigen	Host specie	Isotype	Working dilution (application)	Supplier	Catalog number
Oct-3/4	mouse	IgG_{2b}	1:100 (IF), 1:500 (WB)	Santa Cruz Biotechnology	sc-5279
Sox2	mouse	IgG_{2a}	1:100 (IF), 1:300 (WB)	R&D Systems	MAB2018
Klf4	rabbit		1:100 (IF), 1:300 (WB)	Santa Cruz Biotechnology	sc-20691
c-Myc	rabbit		1:100 (IF), 1:300 (WB)	Millipore	#06-340
Nanog	goat		1:100 (IF), 1:500 (WB)	R&D Systems	AF2729
SSEA-1	mouse	IgM	1:100 (IF)	R&D Systems	MAB2155
PAX6	rabbit		1:1000 (IF)	Millipore	Ab2237
RPE65	mouse	IgG1	1:200 (IF), 1:1000 (WB)	Abcam	Ab13826
Smooth Muscle Actin (SMA)	mouse	IgG2ak	1:100 (IF)	Dako	M0851
Alpha-1-Fetoprotein (AFP)	rabbit		1:100 (IF)	Dako	A0008
Pan-REP (REP1 and REP2)	rabbit serum		1:500 (WB)		J906
Calnexin (Canx)	goat		1:2000 (WB)	Sicgen	AB0041
GFP	goat		1:1000 (WB)	Sicgen	AB0020
V5	mouse	IgG2aκ	1:1000 (IF, WB)	Life Technologies	R960-25

Animals

Wild-type (WT) animals mentioned throughout this work correspond to C57BL/6 mice, which were bred and maintained in the Faculdade de Ciências Médicas' Animal House (Alvará de utilização de animais ao abrigo da Portaria nº 1005/92 de 23 de Outubro).

The Chm conditional KO mouse *Chm^{flox}, MerCreMer^{+}* that carries a tamoxifen (TM) responsive Cre-recombinase transgene was previously generated (Tolmachova et al., 2006). These animals were bred and maintained at the Imperial College London's Animal House. They were treated humanely in accordance with Home Office guidance rules under project licence 70/6176 and 70/7078, adhering to the ARVO Statement for the Use of Animals in Ophthalmic and Vision Research.

Non-obese diabetic/ severe combined immunodeficiency (NOD.Scid) mice were obtained from the Instituto Gulbenkian de Ciência Animal House Facility where they were also bred and housed. Animal handling was conducted according with institutional animal care guidelines and committee-approved protocols.

Cells and cell culture conditions

Commercially available cell lines were used when referred. However, most of the cellular systems employed were either primary cultures of adult somatic cells or pluripotent stem cell lines established under the scope of this work.

All cell lines were maintained at a humidified cabinet at 37ºC and 5% CO_2.

Growth and maintenance of mammalian cell lines

Human embryonic kidney HEK-293A and HEK-293FT were obtained from Life Technologies. STAR-Rdpro cells were obtained from the European Collection of Cell Cultures (ECACC). Mouse RPE cell line (B6-RPE07) was kindly provided by Dr. Heping Xu (Queen's University Belfast, Ireland) (Chen et al., 2008). These cell lines were cultured in Dulbecco's Modified Eagle Medium (DMEM) (Lonza) supplemented with 10% Fetal Bovine Serum (FBS) (Life Technologies), 100 U/mL penicillin and 100 µg/mL streptomycin (Pen Strep) (Life Technologies) (DMEM complete).

Human RPE cell line ARPE19 was obtained from American Type Culture Collection (ATCC). This cell line was cultured in 1:1 mixture of DMEM and Ham's F12 nutrient mixture (DMEM/F12) (Lonza) containing 10% FBS and Pen Strep.

Bl6 (Black6) Ink4a -/- Melanocytes (Melan Ink4a) (kind gift of Dr Sviderskaya, St Georges Hospital, London) (Sviderskaya et al, 2002) were cultured in RPMI 1640 (Life Technologies) supplemented with 10% FBS, 2 mM L-glutamine and Pen Strep. PMA (Phorbol-1,2-myristate 1,3-acetate) and cholera toxin were added fresh to the medium to the final concentration of 200 nM and 200 pM, respectively.

Growth and maintenance of pluripotent stem cells

Culture of pluripotent stem cells implies distinctive conditions that promote and maintain the self-renewal and undifferentiated phenotype *in vitro*. Since the first reports describing establishment of mouse ES cell lines (Evans and Kaufman, 1981), extensive work was dedicated to optimize the culture conditions of ES cells. Classically, murine ES cells are cultured in serum-containing media and on top of a mitotically inactivated fibroblast layer ("feeder cells") to promote their proliferative and undifferentiated status. Alternatively, recombinant cytokine Leukemia Inhibitory Factor (LIF) can be added to the culture medium as a substitute of self-renewal feeders' function (Williams et al., 1988b), given its capability to activate JAK-STAT signalling (Matsuda et al., 1999).

More recently, evidence for a metastable pluripotency level has been shed into light and two pluripotent states have been described: a primed committed state and a naïve or ground state (Nichols and Smith, 2009). Culture conditions to favour naïve pluripotency have been optimized, involving the use of the small molecules MEK/ERK and GSK3 signalling inhibitors (Silva et al., 2008). This so called 2i/LIF culture conditions have been shown to provide an optimal culture environment for mouse ES cells and to promote the acquisition of naïve pluripotent status when reprogramming somatic cells into iPS cells.

Pluripotent stem cells used in this work comprise several established iPS cell lines (summarized in Table 2.2) and a mouse embryonic stem cell line ES-CJ7 kindly provided by Moises Mallo (Instituto Gulbenkian Ciência, Oeiras, Portugal). Cells were maintained in ES medium composed of DMEM supplemented with 15% FBS, Pen Strep, non-essential aminoacids (Life Technologies), 0.1mM 2-mercaptoethanol (Fluka), and 1000 U/mL of LIF (Millipore). Before use, 1 µM of MEK inhibitor PD 0325901 and 3 µM of GSK3 inhibitor CHIR99021 (both from Cayman Europe) were added fresh to the medium (2i/LIF conditions). Pluripotent stem cells were cultured in gelatin-coated dishes, with or without feeders (see details for preparation of feeder layer subsequently). Morphology in culture was observed carefully and frequently to avoid appearance of colonies with non-defined edges and flatten structure, reminiscent of loss of undifferentiated state. Cells were sub-cultured before large colonies start to contact with each other. TrypLE™

Express (Life Technologies) was used as cell dissociation agent and dilution factors ranged from 1:5 to 1:20.

Table 2.2: Established iPS cell lines mentioned in this work and corresponding genotype, according to *Chm* alleles and *MerCreMer* transgene presence/absence.

iPS cell line	Genotype	
	Chm	***MerCreMer***
i2#1	*WT*	Negative
i2#2	*WT*	Negative
j2#2	*WT*	Negative
j2#3	*WT*	Negative
k2#1	*WT*	Negative
k3#2	*WT*	Negative
j5#1	*Null*	Positive
j5#2	*Null*	Positive
j5#9	*Null*	Positive
j6#4	*Null*	Positive
j6#5	*Null*	Positive
j6#6	*Null*	Positive
k5#4	*Null*	Positive
k6#10	*Null*	Positive
k6#3	*Null*	Positive
k6#7	*Null*	Positive
k6#9	*Null*	Positive
j8#1	*Flox*	Positive
j8#2	*Flox*	Positive
j9#3	*Flox*	Positive
k8#1	*Flox*	Positive
k8#6	*Flox*	Positive
k9#2	*Flox*	Positive

To prepare gelatin-coated dishes, culture petri dishes or multiwell plates' bottom were covered with 0.1% porcine gelatin in phosphate buffered saline (PBS; 137 mM NaCl, 2,7 mM KCl, 10 mM Na_2HPO_4 and 2 mM KH_2PO_4) and incubated at 37ºC for at least 30 min. Before using, excess of gelatin solution was aspirated.

Mouse Embryonic Fibroblast (MEF) isolation and culture

Primary MEFs were obtained from WT or *Chm*$^{flox/flox}$ *MerCreMer* $^{+}$ pregnant female mice on Embryonic day 13.5 (E13.5) according to the protocol described in (Takahashi et al., 2007b). Briefly, pregnant mice were sacrificed by cervical dislocation and uteri was exposed, isolated and washed with PBS twice. Embryos were separated from placenta and surrounding membranes and further processed in combination (WT animals) or each embryo individually (Chm animals). Head, visceral tissues and gonads were removed from isolated embryos. For Chm animals, each embryo's head was used for genotyping purposes. Eventually embryonic eyes were isolated and kept for RT-PCR purposes. Remaining bodies were hashed out with scissors in order to provide mechanical dissection of the tissues. Enzymatic digestion was followed using 0.12% trypsin/0.1 mM Ethylenediaminetetraacetic acid (EDTA) solution (3 mL *per* embryo), and incubation at 37ºC for 20 min. Additional 3 mL of same solution *per* embryo were added, followed by another 20 min incubation period. Enzymatic activity was stopped by adding 6 mL of DMEM complete *per* embryo. Cell debris were allowed to deposit for 5 min at room temperature (RT). Supernatant was carefully removed and centrifuged at 260 x *g* for 5 min. Cell pellet was resuspended in DMEM complete and cells were plated in gelatin-coated dished (Passage 0, P0). Medium was changed on the following day, after washing with PBS to remove floating/death cells. On reaching confluency, cells were passaged with 1:3 or 1:4 dilutions. For reprogramming experiments, MEFs were used within 3 or 4 passages to avoid replicative senescence.

Preparation of feeder cells to culture pluripotent stem cells

WT MEFs were used as feeder layer to culture pluripotent stem cells, after mitotic inactivation using mitomycin C. MEFs cultured in 10 cm petri dishes (within 5-6 passages) were incubated with 0.012 mg/mL mitomycin C in DMEM complete medium for 2h30 at 37ºC, 5% CO_2. Culture medium was removed and cells washed twice with PBS. For cell dissociation, cells were incubated with TrypLE™ Express for 5 min at 37ºC, 5% CO_2. Then cells were resuspended and pelleted by centrifugation at 260 x *g*

for 5 min. The pellet was resuspended in fresh medium and the cell number was determined. Mitotically-inactived MEFs (feeders) were plated on gelatin-coated dishes, approximately $1.5x10^4$ cells /cm^2. On the following day, cells were nicely spread with little gaps in between and ready to be used for pluripotent stem cell culture.

Mouse RPE primary cells' isolation and culture

Three-week old WT mice were sacrificed by cervical dislocation and eyes were collected in PBS. Eyes were dipped in 70% ethanol and then placed in DMEM, without serum and antibiotics. Eyes were then incubated in 2% dispase (Life Technologies) in DMEM for 30 min at 37ºC for gentle dissociation of tissues. DMEM complete medium was used to stop enzymatic activity. Cornea, lens and vitreous were removed by piercing with the scalpel and cutting the front. Eye cups were subsequently incubated in DMEM complete for 8 minutes at 37ºC, 5% CO_2. Gentle pressure on the eye cup allowed detachment of NR. For release of RPE sheets and individual cells, eye cups were flushed with 70 µL pulses of DMEM complete. Medium and cells were spinned down at 260 x *g* for 4 min. Cell pellet was resuspended in DMEM supplemented with 5% FBS, Pen Strep, 50 ng/mL Amphotericin B and 2.5 mg/mL Gentamycin and plated in 96-well plates. Medium was changed after 48 h and everyday afterwards.

Constructs and generation of new molecular tools

pLenti-TetO-OSKM (#2544) and pLenti-M2rtTA (#2545) mentioned in this work were acquired from Addgene and correspond to TetO-FUW-OSKM plasmid 20321 and FUW-M2rtTA plasmid 20342, respectively. pLenti-TetO-OSKM encodes for 4 genes (Oct4, Sox2, Klf4 and c-Myc) separated by self-cleaving 2A sequences (P2A, T2A and E2A) and included in a polycistronic unit. When cloned in between different cDNAs, self-deleting 2A peptide sequences (~20 amino acids long) from the foot-and-mouth disease virus (FMDV) or other picornaviruses allow ribosomes to continue translating the downstream cistron after releasing the first protein with its carboxyl terminus fused to 2A. This results in the expression of almost stoichiometric amounts of each protein encoded by the polycistron (Radcliffe and Mitrophanous, 2004) (Figure 2.1).

Figure 2.1: Schematic representation of Lenti-TetO-OSKM.
Adapted from (Carey et al., 2009)

Expression of the 4 genes is controlled by the tetracycline operator minimal promoter (TetO) providing tetracycline-inducible expression when cells are co-transduced with Lenti-M2rtTA viral particles, which constitutively express reverse tetracycline-controllable transactivator (M2rtTA). DOX is used as the inducing drug.

For generation of pAd-OSKM (#3079C2), polycistronic open reading frame encoding for Oct4, Klf4, Sox2 and c-Myc (OSKM) was excised from Lenti-TetO-OSKM using *Eco*RI restriction sites. The open reading frame was inserted into *Eco*RI-linearized pcDNA-ENTR-BP 1848, which was prepared by removing Emerald Green Fluorescent Protein (EmGFP) from pcDNA™ 6.2/C-EmGFP-GW (Invitrogen) and cloning the polylinker with *Dra*I/*Xho*I. The polylinker was generated by oligonucleotide annealing. This vector includes features from the Gateway® Technology (Invitrogen) which takes advantage of the site-specific recombination properties of bacteriophage Lambda to provide a rapid and efficient way to move the DNA sequence of interest into multiple vector systems. This universal cloning method comprises 2 recombination reactions of an entry vector encoding the gene of interest to create a desired destination vector. After confirmation of correct orientation of OSKM by Polymerase Chain Reaction (PCR) and *Nhe*I digestion, polycistronic expression cassette was shuttled first into Gateway® pDONR™221 vector and then into pAd/CMV/V5-DEST™ vector, through BP and LR recombination reactions, according to manufacturer's protocols. Resulting pAd-OSKM was used to produce adenoviral particles as described on proper section.

To prepare lentiviral expression vectors encoding for 10 different Eye TFs, a Gateway® Technology-based cloning workflow was used. First, pLenti6/V5-DEST™ Gateway® vector was modified to allow inducible expression of target genes. Constitutive CMV promoter was removed by *Cla*I/*Spe*I restriction and substituted by TetO promoter, prepared by PCR amplification from pLenti-TetO-OSKM using flanking primers containing corresponding restriction sites. Obtained pLenti6/TetO/DEST was used in BP/LR recombination reactions with an entry clone encoding for Green Fluorescent Protein (GFP) (pcDNA ENTR BP GFP, previously cloned) in order to produce lentiviral control plasmid pLenti-TetO-GFP (#3149C144).

Regarding cloning of the chosen 10 Eye TFs, complementary DNA (cDNA) libraries were produced by amplification through RT-PCR from total RNA isolated from mouse embryonic eye (isolated on E13.5), RAW 264.7 macrophages or Melan Ink4a cells. Subsequently, cDNAs encoding for the Eye TFs were PCR amplified from the cDNA libraries. Some of the coding sequences were PCR amplified from commercially available expressed sequence tags. All PCR amplifications were performed using Phusion polymerase (New England Biolabs) and flanking primers containing either *Eco*RI/*Sal*I restriction sites or *Xho*I/*Kpn*I. The digested products were cloned into adequate pcDNA ENTR BP V5 vectors, prepared with the corresponding endonucleases. C2 or C1 vectors were used in order to obtain entry vectors encoding for the Eye TFs with in frame N-terminus V5 tag sequences. Then, BP/LR reactions were performed using the 10 different entry vectors and pLenti6/TetO/DEST to produce 10 inducible lentiviral plasmids, each one encoding for a V5-tagged version of the corresponding Eye TF.

For the generation of lentiviral reporter systems, pLenti6/V5-DEST™ Gateway® vector was modified to substitute CMV promoter for RPE-specific promoters. Tyrosinase (monophenol monooxygenase) is the essential enzyme in melanogenesis and is expressed in pigmented cells, like skin melanocytes and RPE cells. Tyrosinase (Tyr) promoter (a 2.2kb genomic fragment containing upstream regulatory sequence of mouse tyrosinase gene) was obtained from pTYBS by *Cla*I/*Spe*I restriction (Yokoyama et al., 1990). Constitutive CMV promoter of pLenti6/V5-DEST™ Gateway® vector was removed by *Cla*I/*Spe*I restriction digestion and substituted by the Tyr promoter. Obtained pLenti6/Tyr/DEST was used in BP/LR recombination reactions with an entry clone encoding for GFP (pcDNA ENTR BP GFP, previously cloned) in order to produce reporter lentiviral plasmid pLenti-Tyr-GFP (#3147C32).

pLenti-Rpe65-GFP reporter plasmid was obtained similarly. RPE65 protein plays a crucial role in RPE's visual cycle, particularly in retinal isomerization. The upstream region of *Rpe65* gene has been shown to confer RPE-specific expression (Boulanger et al., 2000). A fragment containing bases -655 to +52 of the 5' flanking region of the mouse *Rpe65* gene was PCR amplified from mouse genomic DNA. Resulting Rpe65 promoter was cloned in pLenti6/V5-DEST vector using *Cla*I/*Spe*I restriction sites, to generate pLenti6/Rpe65/DEST. pLenti-RPE65-GFP (#3681C27) was produced by BP/LR recombination reactions as above described.

All generated constructs were confirmed by adequate restriction enzyme digestion and sequencing. See supplementary experimental procedures for information regarding primer sequences.

Transfection of HEK-293FT Cells with plasmid DNA

Cells were transfected at 70-80% confluence in 6-well plates. Cationic lipid-based Lipofectamine™ 2000 (Life Technologies) was used as transfection reagent and 3 µL were added to 250 µL of Opti-MEM I (Life Technologies). To allow the formation of DNA-lipid complexes, 1 µg of each plasmid to be transfected was first added to 250 µL of Opti-MEM I and then mixed gently with the Lipofectamine solution. Transfection mix was incubated for 45 min at RT. Growth medium was removed from the cells to be transfected prior to PBS wash and gently replaced by the transfection mix (500 µL final volume). Cells were incubated at 37°C 5% CO_2 for 5-6h before the transfection mix was replaced with DMEM complete. Cells were incubated for additional 18-24h before harvesting.

Preparation and use of lentiviral transduction particles

For producing lentiviral particles, besides the lentiviral vector plasmid (transfer vector), packaging plasmid(s) and envelope plasmid are needed in order to properly assembly of the viral capsid to occur.

Third Generation Packaging System plasmids (available from Addgene) pMD2.G, pMDLg/pRRE and pRSV-Rev can be used and co-transfected with transfer vector. Alternatively, STAR-Rdpro cells that stably express synthetic HIV Gag-Pol, HIV tat and HIV rev sequences and RD114 envelope protein can also be used. To increase efficiency of the viral production, both systems were used in combination.

Star-Rdpro cells were plated the day before transfection in DMEM complete and transfected at 80-90% confluency. For a 10 cm petri dish, 3 µg of transfer vector, 3 µg of pMD2.G, 4 µg of pMDLg/pRRE and 2 µg of pRSV-Rev were mixed in 500 µL of Opti-MEM I. Polyethylenimine (PEI) 1 µg/µL was used as transfection reagent, and 36 µg were added first to 500 µL of Opti-MEM I and then to plasmid DNA - Opti-MEM I mix. To allow formation of DNA-lipid complexes, transfection mix was incubated 45 min RT. Star-Rdpro cells were washed with PBS twice and 3 mL Opti-MEM I was added. Then transfection mix was added dropwise to cells. After 6-7 h incubation at 37ºC 5% CO_2, 4 mL of DMEM without serum and antibiotics were added, followed by an overnight incubation. On the following day, the medium was replaced by fresh DMEM complete.

Viral particles were harvested 72 h post-transfection. Supernatant was spun at 4000 x *g* for 10 min to remove cell debris, and used fresh for direct reprogramming experiments. In Chapter 5, supernatant was additionally filtered through a 0.45-µm filter and

concentrated through ultracentrifugation at 100 000 x *g* for 3 h at 4ºC. The resultant viral pellet was resuspended in DMEM complete.

Lentiviral transductions were performed for 24 h or 48 h in the presence of 6 µg/mL Polybrene® (hexadimethrine bromide). This cationic polymer increases gene transfer efficiency through neutralization of the negative electrostatic repulsion between the cell surface and the virus particles, facilitating viral adsorption (Davis et al., 2004).

For selection of lentiviral transduced cells, blasticidin was used on appropriate conditions for each cell line (concentration and exposure time) as optimized by a MTT-based cell viability assay.

Preparation of adenoviral transduction particles

Plasmid DNA of pAd-OSKM was isolated using QIAGEN Plasmid Midi kit (Qiagen) and 5 µg of DNA were digested with *Pac*I according to manufacturer's protocols, followed by purification by phenol/chloroform extraction and isopropanol precipitation.

On the day before transfection, HEK-293A cells were plated in T25 flasks in DMEM complete to reach 80% confluence on the next day. Transfection was executed as described previously for HEK-293FT cells, using Lipofectamine™ 2000 Reagent. Cells were cultured until viral production was observed by monitoring cytopathic effect with plaque formation and cell death (approximately 10-15 days post-transfection). The supernatant was collected and 3 freeze-thaw cycles were performed, followed by a 10 min 4000 x *g* centrifugation to remove cell debris. A portion (500 µL approximately) of this initial supernatant was used to transduce confluent HEK-293A cells in a 10 cm petri dish. With this re-amplification step, the cytopathic effect occurs much sooner and collected supernatant (prepared as described) has higher viral titer. Viral aliquots were maintained at -80ºC for storage.

Reprogramming somatic cells into pluripotency

Generation of iPS cells was performed according to available protocols (Carey et al., 2009; Takahashi et al., 2007b) with minor modifications. Passage 3 or 4 MEFs, either WT, Chm^{null} or Chm^{flox}, were plated on gelatin-coated 6-well plates ($1x10^5$ cells *per* well). On the following day, 250 µL of both Lenti-TetO-OSKM and Lenti-M2rtTA freshly prepared lentiviral supernatants were added to each well, in the presence of Polybrene®. On day 1 post-transduction (dpt), 1 mg/mL DOX was added to the medium (except

control wells referred as "- DOX") to induce lentiviral expression of the 4 TFs. DMEM complete medium was changed on 2 dpt to remove lentiviral particles (48 h of viral transduction). Cells were cultured in ES medium (first without 2i), with or without DOX accordingly, from 3 dpt and forward. Medium was changed every other day, until on 14 dpt 1 µM of MEK inhibitor PD 0325901 and 3 µM of GSK3 inhibitor CHIR99021 were added (LIF/2i). These conditions were used to promote conversion of pre-iPS cells into fully reprogrammed cells and achievement of a naïve pluripotent state (Silva et al., 2008). Lastly, from 21 dpt forward, DOX was removed from culture medium in all culture wells, to select clones that have acquired transgene independence.

After 4 weeks of reprogramming protocol, ES cell-like colonies were manually "picked". Culture medium was changed into PBS and dome-shaped colonies were aspirated using a P-10 micropipette. Aspirated cells were up-and-down homogenized in a 96-well plate, before being plated in 24-well plate wells previously prepared with a feeder layer (P0). From this point further iPS cells were always cultured in ES medium, in which 2i were added freshly. After 2-3 passages, established iPS cell lines were successfully adapted to feeder-free culture conditions.

For the adenoviral-based reprogramming protocol, same conditions were employed with minor adjustments. Briefly, Ad-OSKM supernatant was used to transduce MEFs plated on the previous day. On 1 dpt, medium was changed to remove adenoviral particles. ES medium (without 2i) was used from 3 to 14 dpt, when 2i were added.

Characterization of pluripotent stem cells

Alkaline phosphatase staining

Undifferentiated state of pluripotent stem cells in culture is characterized by high level of alkaline phosphatase (AP) expression (Pease et al., 1990). iPS cell lines and ES cells were plated on 6-well plates prepared with feeders with low density and allowed to grow for 3-4 days (small colonies are preferred to detected AP activity). AP Detection kit (Millipore) was used according to manufacturer's protocol to confirm enzymatic activity of AP through a colorimetric reaction. ES cells were used as positive control, and feeder cells in each well control for false positive results.

Embryoid Bodies' differentiation assay

EB formation followed by *in vitro* spontaneous differentiation is commonly used to confirm pluripotency capacity and differentiation potential of pluripotent stem cells (Kurosawa, 2007). Feeder-free cultures of iPS cell lines and ES cells were used and $2.75x10^6$ cells of each line were plated in bacterial-grade petri dishes (low attachment conditions). EB medium (DMEM supplemented with 15% KnockOut™ Serum Replacement (Life Technologies), non-essential amino acids, Pen Strep and GlutaMAX™-I (Life Technologies)) was used and cells were incubated at 37ºC 5% CO_2 for 3 days to allow formation of floating EBs. Growth medium was replaced daily. After 3 days, EBs were spun at 100 x g for 5 min prior to being plated in gelatin-coated dishes in EB medium supplemented with 10% FBS. After overnight incubation to allow EBs to adhere, medium was changed into EB medium (without FBS). Cells were washed with PBS every other day and medium was changed. At day 7 and 14 of differentiation, RNA was collected for RT-PCR analysis. Alternatively, cells were fixed for IF staining to confirm the presence of endodermal, mesodermal and ectodermal markers.

Teratoma formation assay

One of the hallmarks of pluripotent stem cells is their ability to differentiate into cells from the three germ layers: endoderm, mesoderm and ectoderm. Besides performing *in vitro* differentiation assays, the confirmation of this property can be achieved in a more stringent way through an *in vivo* teratoma formation assay. Teratomas are benign tumours composed of differentiated tissues derived from all three germ layers. When transplanted into immunodeficient animals, pluripotent stem cells form teratoma-like outgrowth masses (Gropp et al., 2012).

iPS cell lines to be tested were cultured in feeder-free conditions and subjected to a shorter trypsinization period in order to obtain small aggregates of cells. Single cell dissociation was avoided since it has been described that injection of small clusters of cells increases teratoma formation efficiency (Zhang et al., 2012). One million cells of each cell line was resuspended in 100 µL of PBS and injected subcutaneously into a NOD.Scid mouse. Immunodeficient mice are used to avoid immune rejection that occurs in non-immunocompromised animals. ES cells were also injected (positive control), as well as MEFs (non pluripotent cells) or PBS (negative controls). All animals were kept in parallel and each experimental group was composed of 2-4 animals. Five to seven weeks later, mice developed tumours, which were removed, immediately rinsed with PBS, fixed, and embedded in paraffin. Tissue sections were cut and processed for

hematoxylin-eosin staining. The histological analysis was performed by a pathologist and a tumour was defined as a teratoma only if it contained tissues representing all three germ layers.

Differentiation of pluripotent stem cells into retinal lineages

Differentiation protocol adapted from Zhu *et al.*

iPS cell lines and ES cells were subjected to the protocol described by (Zhu et al., 2013), with minor modifications. Briefly, undifferentiated cell colonies were partially lifted by dispase. Detached cell aggregates (diameter: 50–100 µm) from one confluent well of a 6-well plate were embedded in 100 µL of Matrigel™ Basement Membrane Matrix (BD Biosciences) and plated in 24-well plates. After gelling at 37ºC for 10 min, cells embedded in the Matrigel layer were cultured in neural induction medium N2B27 which consisted of DMEM/F12+GlutaMAX (Life Technologies), neurobasal medium (Life Technologies), 0.5x B27 supplement (Life Technologies), 0.5x N2 supplement (Life Technologies), 0.1 mM 2-mercaptoethanol and 0.2 mM L-Glutamine. In separate experiments, IGF-1 recombinant protein was added to the medium to a final concentration of 10 ng/mL.

Differentiation protocol adapted from Eiraku *et al.* and Gonzalez-Cordero *et al.*

iPS cell lines and ES cells were subjected to the protocol described by (Eiraku and Sasai, 2012; Eiraku et al., 2011; Gonzalez-Cordero et al., 2013) with some modifications. Briefly, cells were dissociated to single cells with TrypLE™ Express and $2x10^6$ cells were plate in bacterial-grade 10 cm petri dishes in Early retinal differentiation medium. This medium was composed of Glasgow minimum essential medium (GMEM) (Life Technologies) supplemented with 1.5% (vol/vol) KSR + 0.1 mM non-essential amino acids + 1 mM pyruvate + 0.1 mM 2-mercaptoethanol. Growth factor–reduced Matrigel (BD Biosciences) was added to the culture medium to a final concentration of 2% (v/v) on the following day.

Differentiation protocol adapted from La Torre *et al.* and Osakada *et al.*

iPS cell lines and ES cells were subjected to a differentiation protocol adapted from the reports of (Osakada et al., 2009; Torre et al., 2012). Cells were dissociated to single cells with TrypLE™ Express and $2x10^6$ cells were plate in bacterial-grade 10 cm petri dishes

in Retinal induction medium. This medium was constituted of DMEM/F12+GlutaMAX, neurobasal medium, 0.5x B27 supplement, 0.5x N2 supplement, 0.1 mM 2-mercaptoethanol and 0.2 mM L- Glutamine. Recombinant proteins Dkk-1, IGF-1 and Noggin were also added to a final concentration of 10 ng/mL each. After 3 days, on some experiments, floating aggregates were plated in 12-well plates coated with Growth factor–reduced Matrigel (P conditions).

Cell viability assay

The MTT (3-[4,5-dimethylthiazol-2-yl]-2,5 diphenyl tetrazolium bromide) assay is a colorimetric assay based on the reduction of MTT into formazan crystals by mitochondrial succinate dehydrogenase. Water soluble MTT enters cells and, in the mitochondria, it is reduced into an insoluble, coloured (dark purple) formazan product. After solubilisation with an organic solvent, the dissolved material is measured spectrophotometrically. Since for most cell populations the total mitochondrial activity is related to the number of viable cells, this assay is broadly used to measure the cell viability, cell proliferation or *in vitro* cytotoxic effects of drugs on cell lines or primary cells (Carmichael et al., 1987).

MEFs were plated in a 48-well plate ($1x10^4$ cells/ well) and treated with different concentrations of TM, blasticidin, or lentiviral supernatants. Cell viability was assessed after 72 and 96 h (for TM), 48 and 72 h (for blasticidin) or 96 h (lentiviral supernatants). Cell culture medium was removed, 100 µL of 0.5 mg/mL MTT solution in DMEM without phenol red (Life Technologies) were added to the wells and samples were incubated for 3 h at 37ºC. Removal of MTT solution preceded addition of 100 µL of acidic isopropanol (0.04 M HCl in absolute isopropanol) for solubilization of formazan salts. Absorbance was measured at 595 nm (iMark, BioRad). Percentage of cells' survival was determined relative to untreated cells, after correction for the background (absorbance of the dissolution vehicle). For each condition, including the controls, 3 independent assays were carried in quadruplicates.

For ARPE-19 cells, cell viability was assessed similarly, just adjusting cell density to $3x10^4$ cells/ well.

A MTT-based cell viability assay was also used to infer proliferation and growth rates of iPS cell lines. For that purpose, several plating densities were tested in a 96-well plate format (1, 2, 5, 10 and $20x10^4$ cells/ well). The MTT assay was performed after 24 h as previously described using 50 µL of MTT solution and acidic isopropanol. Subsequently,

cells were plated with the chosen density ($1x10^4$ cells/ well) and MTT reduction assay performed every day, for a total of 4 days.

PCR Genotyping

For genotyping of embryos (when isolating MEFs primary cultures), a portion of the embryonic head was isolated from each sample. For genotyping of cells in culture, at least $2x10^4$ cells were used and pelleted after tripsinization. All samples were digested overnight in GNTK buffer (50 mM KCl, 1.5 mM $MgCl_2$, 10 mM Tris-HCl, pH 8.5, 0.01% gelatin, 0.45% Nonidet P-40, 0.45% Tween-20) supplemented with 50 µg/mL proteinase K (Invitrogen) at 55°C. Proteinase K was heat inactivated (94ºC for 15 min) and samples were spun at 16000 x *g* for 5 min before 1–3 µL of the supernatant was used in PCR.

PCR primers and conditions were described previously by (Tolmachova et al., 2006) (Table 2.3).

Table 2.3: PCR primers used for genotyping.

Primer	Sequence (5'- 3')	Product size (bp)	Allele
H7	AGAGTATCTCAGCAGTAGCTCTCC	780 / 860 / 330	Chm^{WT} / Chm^{flox} / Chm^{null}
H9	CCAGAGAACACTGAGGGTTAGAGC		
Cre1	TCCCGCAGAACCTGAAGATGTTC	510	*MerCreMer*
Cre2	GGATCATCAGCTACACCAGAGACG		

RNA isolation and Reverse Transcriptase (RT) - PCR

Total RNA was isolated from cells using an RNeasy Mini kit (Qiagen) according to manufacturer's protocols. One µg of total RNA was converted into cDNA using SuperScript® II (Life Technologies) and random primers. cDNA was diluted 10x before further analysis.

Conventional RT-PCR reactions were performed using Taq polymerase (Promega) and the following PCR program: 2 min initial denaturation step at 95ºC; 32 cycles of 20 seconds denaturation step at 95ºC, 30 seconds annealing step at 58ºC and 1 min/kb at 72ºC; 10 min final extension step at 72ºC.

Quantitative RT-PCR reactions were performed using an ABI Prism 7900HT system (Applied Biosystems) using SybrGreen Master Mix. Five µl of SybrGreen, 4 µl of cDNA sample together with 1µl of adequate primers were used *per* well, in quadruplicate conditions. The relative transcript levels of the target genes were calculated relative to control wells and standardized using *Gapdh* as a housekeeping gene; quantification was performed using the delta-delta Ct method (Livak and Schmittgen, 2001).

PCR primers used to assess gene expression levels are summarize in supplementary experimental procedures (Table 2.5). *Ecat*, *Esg1*, *Eras*, *Zfp42* and *Utf1* primers were described by (Takahashi et al., 2007b).

Immunofluorescence (IF)

Cells were seeded on gelatin-coated coverslips at appropriate cell density. When ready, cells were washed 2x with PBS, and fixed with 4% (v/v) paraformaldehyde (PFA) in PBS for 15 min at room temperature. Cells were washed 2x in PBS and permeabilized for 45 min with 1% Bovine Serum Albumin (BSA) 0.1% Triton X-100 in PBS. Incubation with primary antibodies followed, diluted in the same solution, for 1 h RT or overnight at 4ºC. After washing 4x with PBS, samples were incubated for 1 h RT with Alexa 488-conjugated and Alexa 547-conjugated secondary antibodies (Life Technologies, 1:1000). Samples were mounted using ProLong Gold Antifade Reagent with DAPI (4',6-diamidino-2-phenylindole) (Life Technologies) and visualized either on an inverted microscope (Olympus IX51 U-RFL-T) or on a confocal microscope (Leica TCS SP5 microscope, Leica Microsystems, using an 63x immersion oil lens; objective type: HCX PL APO CS, NA: 1.40 - 0.60).

Image acquisition and analysis

Brightfield and fluorescent images of cells in culture were acquired using an inverted microscope (Olympus IX51 U-RFL-T). When necessary, images were post-processed for overall brightness and contrast using Fiji (NIH) software.

For determination of the percentage of cell transduction, number of Oct4 positive cells was counted by applying the Otsu or Moments threshold filter in each image using Fiji. The resulting number was divided by the corresponding number of cells, counted as the number of nuclei (DAPI staining). At least 1000 cells were analysed for each replicate for each condition.

Flow cytometry

In order to determine lentiviral-driven GFP expression using flow cytometry, transduced MEFs cells were washed in 0.1% BSA in PBS once after tripsinization. Cells were then fixed in 0.4% PFA 0.1% BSA in PBS and kept at 4ºC until acquisition.

Samples were analyzed using FACSCalibur ™ (BD Biosciences) or Attune® Acoustic Focusing Cytometer (Life Technologies) with acquisition of at least 30 000 events on gated population (cells). Attained results were processed using FlowJo software (Tree Star). Due to MEFs' autofluorescence particularly after several days in culture, flow cytometry plots were analysed as FL1/BL1 versus FL2/BL2 plots to determine percentage of cells expressing GFP. In some cases, Median Fluorescent Intensity (MFI) values were also determined.

Preparation of protein lysates and western blotting analysis

Cells were seeded on 6-well plates and homogenized in RIPA buffer (50 mM Tris-HCl pH 7.4 containing 150 mM NaCl, 1% Triton X100, 0.1% sodium dodecyl sulphate (SDS), 0.5% sodium deoxycholate, 1 µg/mL leupeptin and TPCK). Lysates were subsequently cleared by centrifugation and bicinchoninic acid (BCA) colorimetric method was used according to the manufacturer's instructions (Pierce) to quantify protein content. For each sample, a fraction of proteins was combined with Laemmli buffer (2% SDS, 5% 2-mercaptoehtanol, 10% glycerol, 0.002% bromophenol blue, 0.065 M Tris HCl in final solution) before subjected to separation based on molecular weight by SDS - Polyacrylamide Gel Electrophoresis (SDS-PAGE). Acrylamide gels (12.5%) were used and proteins were subsequently transferred to Immobilon polyvinylidine fluoride (PVDF) membranes (Millipore). Membranes were blocked in 4% non-fat dried milk in 0.02% Tween® 20 in PBS (PBST buffer) for 60 minutes at RT. Incubation with primary antibodies for at least 1 h RT followed, prior to incubation with appropriate Horseradish Peroxidase (HRP)-conjugated secondary antibodies (1:10000) for 1 h RT in 4% non-fat milk in PBST. Membranes were incubated with ECL Plus (GE Healthcare) and chemiluminescence was detected using ChemiDoc (BioRad). Western blot analysis was performed using Fiji software. Quantification plots show the relative density, which is optical density normalized to the calnexin signal in the same lane (relative density = optical density x 100 / optical density for calnexin).

Statistics

Unless stated otherwise, data are presented as mean values from at least 3 independent experiments and error bars indicate ± SD. The results' statistical analysis was carried out using the Graph Pad Prism software version 5 (GraphPad Inc., San Diego, CA, USA). Two-tailed Student's t Test, one-way analysis of variance (ANOVA) or two-way ANOVA were used accordingly. The significance level is indicated as *** for $p<0.001$, ** for $p<0.01$, * for $p<0.05$ and NS for $p>0.05$.

Supplementary experimental procedures

Primers used for pcDNA-ENTR-BP1848 polylinker generation:

Forward:

5´AAAGCTAGCGATCTCGAGCTCAAGCTTCGAATTCTGCAGTCGACGGTACCGCGG GCCCGGGATCCAGCGGCCGCTCTAGATAACTGATCA 3´

Reverse:
5´TCGATGATCAGTTATCTAGAGCGGCCGCTGGATCCCGGGCCCGCGGTACCGTCG ACTGCAGAATTCGAAGCTTGAGCTCGAGATCGCTAGCTTT 3´

Primers used for amplification of TetO promoter region:

Forward: 5' ATTCAATCGATAATCGGGTTTATTACAGGGACAGCAGAG 3' (PR1493)

Reverse: 5' GGCGACTAGTGGGCCGCGGAGGCTGGATCGGTCCCG 3' (PR1494)

Primers used for amplification of Rpe65 promoter region

Forward: 5' GCATATCGATGTCTCTGAGTGCAGAACAAA 3' (PR1949)

Reverse: 5' GGATACTAGTTTTCTTCCAGTGAAGATTAGAGAGAGTT 3' (PR1950)

Table 2.4: Cloning details of Eye TFs' constructs.

Gene	cDNA origin	Primer #	Sequence (5'- 3')	Restriction Sites	Product size (bp)	Entry vector #	Inducible lentiviral vector #
Mitf var1	Raw264.7	PR1495	AGAGGAATTCATGCAGTCCGAATCGGGAATCGTGGCGG	EcoRI	1601	#2939C151	#3470C61
		PR1496	GGCAGTCGACCTAACACGCATGCTCCGTTTCTTCTGCG	SalI			
Otx1	Embryonic eye	PR1497	GGCTGAATTCATGATGTCTTACCTCAAACAACCCCCAT	EcoRI	1088	#2927C52	#3417C11
		PR1498	CCTCGTCGACTCACAAGACCTGGAACCGCCACG	SalI			
Otx2	Embryonic eye	PR1499	CAACGAATTCATGATGTCTTATCTAAAGCAACCGCCTT	EcoRI	890	#2921C69	#3418C38
		PR1500	CTACGTCGACTCACACAAAACCTGGAATTTCCATGAGGAC	SalI			
Pax6	Embryonic eye	PR1501	CCAACTCGAGCCAGCATGCAGAACAGTCACAGCGGAGT	XhoI	1346	#2930C102	#3419C31
		PR1502	CATGGGTACCCCTTCTCTCTTTACTGTAATCGAGGCCA	KpnI			
Six6	Embryonic eye	PR1503	CGCAGAATTCATGTTCCAGCTGCCCATTTTGAATTT	EcoRI	761	#2922C76	#3420C89
		PR1504	AGTGGTCGACTCAGATGTCGCACTCACTGTCGCTGGAT	SalI			
Six3	pYxAsc mSix3 EST	PR1505	GGTGAATTCATGGTATTCCGCTCCCCCCTAGAT	EcoRI	1022	#2943C29	#3471C77
		PR1506	GCCTGTCGACTCATACATCACATTCCGAGTCGCTGGAG	SalI			
Nr2e1	Embryonic eye	PR1507	GGGACTCGAGGCATGAGCAAGCCCGCCGGATCAACAAGCC	XhoI	1186	#2929C86	#3421C124
		PR1508	GTGGGGTACCGAGCCCTTAGATGTCACTGGATTTGT	KpnI			
Lhx2	Embryonic eye	PR1509	CCGCGAATTCGGTCCCGCCGCGATGCTGTTCCACAGTCTG	EcoRI	1253	#2926C34	#3422C140
		PR1510	TGGCGTCGACTTAGAAAAGGTTGGTAAGAGTCGTTTGT	SalI			
Tbx3 var1	Melan ink4a	PR1511	TGTCCTCGAGGGATGAGCCTCTCCATGAGAGATCCGGTTA	XhoI	2251	#2940C23	#3423C167
		PR1512	GTTTGGTACCTTTTTAAGGGGACCCGCTGCAAGACCTG	KpnI			
Rax	pCMV Sport6 mRax	PR1515	AGTGGAATTCCTCCCTCTCCATGCACCTGCCGGGCTGCG	EcoRI	1061	#2928C8	#3469C46
		PR1516	CTCCGTCGACCCTCTAGAGGGCTTGCCAGGGCTTTCCGAT	SalI			

Table 2.5: RT-PCR primers.

Gene	Primer #	Sequence (5'- 3')	Product size (bp)
P2A-Sox2	PR1452	GCGCCACAAACTTCTCTCTGCTAA	96
	PR1453	GCTTCAGCTCCGTCTCCATCATGTTA	
Total Oct4	PR1454	TGGAGGAAGCCGACAACAATGAGA	171
	PR1455	TGGCGATGTGAGTGATCTGCTGTA	
Endo Oct4	PR1456	CCATGCATTCAAACTGAGGCAC	169
	PR1457	ACAGCATCACTGAGCTTCTTTCCC	
Nanog	PR1458	AGCAGAAGATGCGGACTGTGTTCT	173
	PR1459	CCGCTTGCACTTCATCCTTTGGT	
Fgf4	PR1460	CAAGCTCTTCGGTGTGCCTTTCTT	82
	PR1461	TTCGTAGGCGTTGTAGTTGTTGGG	
Ecat1	PR2251	TGTGGGGCCCTGAAAGGCGAGCTGAGAT	164
	PR2252	ATGGGCCGCCATACGACGACGCTCAACT	
Esg1	PR2253	GAAGTCTGGTTCCTTGGCAGGATG	376
	PR2254	ACTCGATACACTGGCCTAGC	
Eras	PR2255	ACTGCCCCTCATCAGACTGCTACT	210
	PR2256	CACTGCCTTGTACTCGGGTAGCTG	
Zfp42	PR2257	ACGAGTGGCAGTTTCTTCTTGGGA	287
	PR2258	TATGACTCACTTCCAGGGGGCACT	
Utf1	PR2259	GGATGTCCCGGTGACTACGTCTG	344
	PR2260	GGCGGATCTGGTTATCGAAGGGT	
Pax6	PR2030	ACCCCTCCGCACATGCAAACA	185
	PR2031	CTCTCTCGATCACATGCTCTCTCCT	
Col1a1	PR1861	CACTGCCCTCCTGACGCATGG	148
	PR1862	CACGTCATCGCACACAGCCG	
GATA6	PR2367	GCCAACTGTCACACCACAAC	285
	PR2368	TGAGGTGGTCGCTTGTGTAG	
Gapdh	PR1877	AGTGCCAGCCTCGTCCCGTA	71
	PR1878	CAGGCGCCCAATACGGCCAA	

Gene	Primer #	Sequence (5'- 3')	Product size (bp)
Rep1	PR1992	TTCGCCATTCAGTACAGTGCCTTG	167
	PR1993	TGCCCTGGAAATTTGCCTGTACTGT	
Rax	PR1844	GAAGCATCGACGCAACCGCAC	183
	PR1845	TCCTGGCGCCTCCACTTAGCC	
Six3	PR2191	CTGGTTTAAGAACCGGCGAC	369
	PR2192	TGTCTGTGTATCCTGATTTCGGT	
Six6	PR2195	GCAGCTGCAGCCAAAAACAG	214
	PR2196	ATTCTAAGTGTGATGAGTGGGCA	
Otx1	PR2186	TAGATGGTGAAAAGCCGCGA	180
	PR2187	TTCATGCCGTATGGGGGTTG	
Otx2	PR2189	CGCCTCCAAACAACCTTAGC	145
	PR2190	CTCTCCCTTCGCTGTTTCCG	
Mitf	PR1846	CCGAATCGGGAATCGTGGCGG	130
	PR1848	GGCTTGGAGGCCCCAGAATGC	
Tyr	PR1853	TCCCAAGTACAGGGATCGGCCA	100
	PR1854	AAAGAGGGCGGTGCCTTCGC	
Rpe65	PR1859	ATTGAACACCCTGCTGGTGGCTA	127
	PR1860	GCCCACATCGGAGGAGACTGC	
Rgr	PR2042	CTGCCTGCTGGTTTGGGGGAA	143
	PR2043	AGCAGGTTGCTGGGAGTCCGC	
Rlbp1	PR1857	CAGCTGCCCCGCCACACTTT	74
	PR1958	ACCGCTTCCTCCCGGGTCTC	
Mertk	PR1855	CTACCCGCGCTCTGGAGTGGA	132
	PR1856	CCGGCTGGAGTGAGGAGCAGA	
Best1	PR2036	TGCTTCTGCCAGGTCTCGCC	103
	PR2037	CGTGTCAGCCTCCTCTTTTGACCA	
Mitf-A	PR1846	AAGCAGTGGAAGGCGGGCAAG	166
	PR1847	GGCTTGGAGGCCCCAGAATGC	

Chapter 3 Induced Pluripotent Stem cell technology

Chapter 3 : Induced Pluripotent Stem cell technology

Summary

Reprogramming of somatic cells into pluripotency can be achieved using a transcription factor-mediated approach. Obtained iPS cells display morphology, self-renewal and pluripotency properties similar to ES cells. Uses for this pioneering technology are wide, including a better understanding of pluripotency and developmental biology, generation of patient- and disease–specific cell lines, drug and toxicology screenings and clinical applications in regenerative medicine approaches (Takahashi & Yamanaka 2013).

Since Yamanaka's seminal discovery in 2006 (Takahashi & Yamanaka 2006), numerous scientific advances were made trying to overcome major limitations of the reprogramming protocol, namely low efficiency, insertional mutagenesis, oncogenic transformation and epigenetic memory of obtained cells.

Several methods have been described, using different initial somatic cell types, delivery systems and combinations of reprogramming factors. Culture conditions for the derivation procedure as well as the possibility of combining TFs with small molecules were also studied and optimized (Maherali & Hochedlinger 2008).

Here we describe our strategy to implement iPS cell technology in the laboratory. Inducible lentiviral and adenoviral vectors were tested to force the expression of the 4 classical Yamanaka factors in MEFs isolated from WT animals. Contrarily to an adenoviral-based approach, a lentiviral strategy was successfully implemented. Several iPS cell clones were isolated, expanded and characterized, displaying morphological, molecular and functional properties similar to ES cells, particularly in terms of self-renewal and pluripotency.

Results

Lentiviral molecular tools efficiently transduce MEFs and allow expression of reprogramming factors

Inducible polycistronic lentiviral systems can be used to reprogram somatic cells into pluripotency, as described by Carey and colleagues (Carey et al., 2009). In this system, a viral vector encodes for the 4 reprogramming genes *Oct4*, *Sox2*, *Klf4* and *c-Myc* separated by 2A "self-cleaving" peptides. Therefore, efficient polycistronic expression is achieved from a single promoter, in this case a tetracycline-operator minimal promoter

(TetO). In the presence of DOX, cells co-transduced with the polycistronic vector (Lenti-TetO-OSKM) and a constitutive lentivirus encoding for the tetracycline controllable transactivator (Lenti M2rtTA) express the 4 TFs.

In order to implement a reprogramming protocol and to confirm the efficiency of the delivery system, primary cultures of MEFs isolated from E13.5 pregnant WT C57BL/6 mice were established and transduced with viral particles of both polycistronic and transactivator lentiviruses. As depicted in Figure 3.1, forced expression of the 4 TFs was attained when cells were cultured in the presence of DOX at 4 dpt, despite some observed residual expression in the absence of the inducing drug justified by the described leakiness of the promoter (Goverdhana et al., 2005).

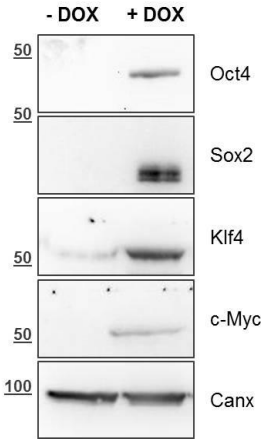

Figure 3.1: MEFs transduced with inducible lentiviral particles express the 4 reprogramming factors, in the presence of DOX.

MEFs were co-transduced with Lenti-TetO-OSKM and Lenti M2rtTA viral particles and were cultured in the absence (-) or presence (+) of DOX. Protein expression of Oct4, Sox2, Klf4 and c-Myc is observed in the second condition. Protein lysates collected 4 dpt were subjected to western blot analysis with the indicated antibodies; Canx was used as loading control.

Transduced cells were also analysed by IF in order to determine the efficiency of transduction (Figure 3.2). Considering the quantification of Oct4 expressing cells, approximately 25% of WT fibroblasts were shown to be transduced.

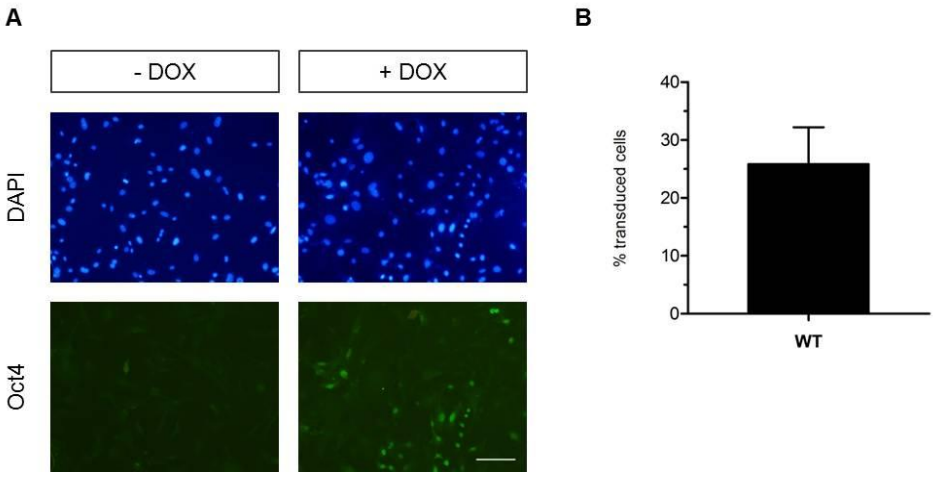

Figure 3.2: MEFs are transduced by the reprogramming lentiviral particles with 25% of efficiency.

(A) Presence (+) of DOX induces expression of Oct4 as assessed by IF at 4 dpt; nuclei were counterstained with DAPI and used to quantify the total number of cells; scale bar 50 µm. (B) Quantification of transduced cells, calculated by dividing Oct4 positive cells for the total number of cells and expressed in percentage; mean ± SD, n=5.

Lentiviral transduced cells display morphology and gene expression alterations during reprogramming protocol

In addition to an efficient delivery system for the selected set of TFs, reprogramming to pluripotency is highly dependent on culture conditions, which may also to be tested and subjected to optimization. Standard culture conditions for the derivation and propagation of mouse ES cells were adopted since these conditions have been described to favour generation of mouse iPS cells from fibroblasts (Maherali and Hochedlinger, 2008).

A schematic representation of the implemented protocol is depicted on Figure 3.3A. MEFs were co-transduced with abovementioned lentiviral particles and DOX was added to the culture medium on the following day, except to control wells (- DOX). At 3 dpt, cell culture medium was changed into an ES cell medium containing serum and LIF. On day 14, ES cell medium was also supplemented with 1 µM of PD0325901 and 3 µM of CHIR99021, which inhibit MEK/ERK and GSK3 signalling, respectively. These dual inhibitors (2i) combined with the self-renewal cytokine LIF were described to induce a complete reprogramming event and promote the generation of ground state pluripotent cells (Silva et al., 2008). On the 4th and final week of the protocol, DOX was removed from culture in order to facilitate identification and isolation of fully reprogrammed cells. Given the inducible nature of the lentiviral delivery system, upon DOX withdrawal, cells that rely on exogenous expression of the pluripotent TFs are eliminated, providing a useful selection system.

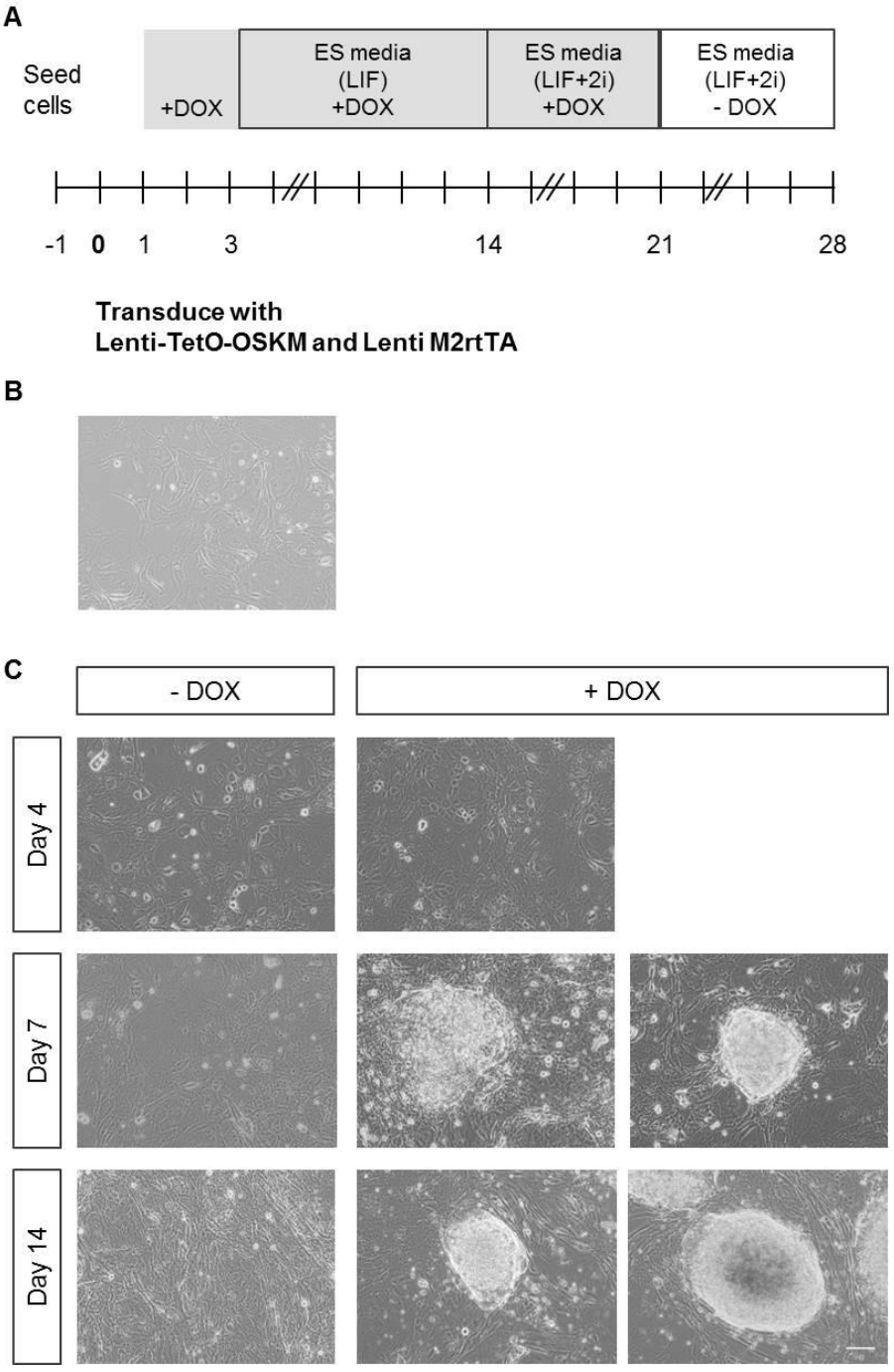

Figure 3.3: MEFs subjected to reprogramming protocol display typical morphological alterations.

(A) Scheme representing protocol outline. (B) Initial morphology of MEFs prior to lentiviral transduction. (C) Representative bright-field images of transduced MEFs cultured in the presence (+) of DOX showing that approximately 7 dpt typical ES-like colonies start to appear, composed of small and compacted cells. At day 14, colonies have a more condensed and well defined structure in culture. In the absence (-) of DOX, transduced cells maintain a fibroblast-like morphology, despite becoming more confluent. Scale bar 25 µm.

Several independent experiments were performed and typical morphological alterations were observed consistently. On 4 dpt transduced cells still display a fibroblast-like morphology, similar to initial cells and control cells cultured in the absence of DOX (Figure 3.3B and C). After approximately 7 dpt, colonies that resemble ES cells start to arise, with their distinctive refractive appearance. Progressively, some colonies gained more tight and well-defined borders, which are known to be correlated with fully reprogrammed iPS cell colonies (colony depicted on bottom right panel of Figure 3.3C for example).

To confirm the identity and significance of the observed morphological alterations, expression of key pluripotency markers was analysed during the protocol time course. Interestingly, on 7 dpt, IF technique using antibodies against Oct4 and Sox2 revealed that cells corresponding to nascent ES-like colonies expressed these TFs (Figure 3.4A), despite exogenous (viral) or endogenous expression cannot be distinguished. Importantly, at 14 dpt, pluripotency TF Nanog and specific surface marker SSEA-1 were expressed by the arising colonies, confirming the activation of an endogenous pluripotent expression profile (Figure 3.4B). AP staining was also performed, with positive pink colonies (Figure 3.4C). In some cases, colonies were overgrown after 28 days in culture and cells in the middle of the colony start to die and lose their AP content, as seen on lower panel of Figure 3.4D.

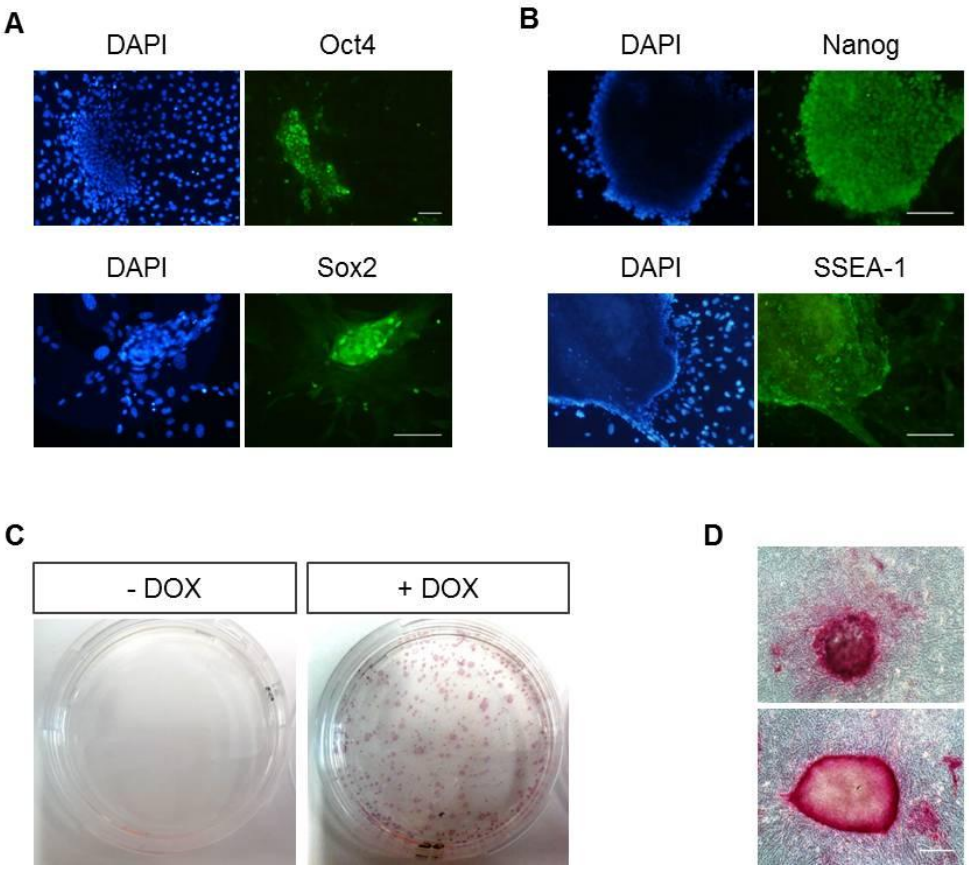

Figure 3.4: Stem cell-like colonies arise during the reprogramming protocol and express typical pluripotency markers.

(A) At 7 dpt, cells that start to display morphological alterations express Oct4 and Sox2. (B) Nanog and SSEA-1 expression is also observed in the arising colonies around 14 dpt. (A-B) IF staining using the indicated antibodies, DAPI used to counterstain cell nuclei; scale bar 50 µm. (C) Cell culture dishes (6 cm) of transduced cells stained for AP 28 dpt show positive colonies in the presence (+) of DOX. (D) Representative images of AP-positive colonies are shown; scale bar 50 µm.

In order to further characterize the reprogramming events that were being observed, total RNA samples collected during the 28 days' time course were analysed by quantitative RT-PCR. Using primers for viral specific transcripts (*P2A-Sox2*), robust and stable induction (6- to 10-fold increase) was observed in cells cultured with DOX as compared to control conditions (- DOX). Of interest is to notice that viral transcripts were no longer expressed when inducing drug was withdrawn from culture media after day 21 (Figure 3.5A). Additionally, *Oct4* primers that cannot discriminate between viral or endogenous transcripts (Total *Oct4*) were used, showing that transduced DOX-induced MEFs expressed *Oct4* with similar levels when compared to ES cells. *Oct4* endogenous expression was also confirmed using a specific primer pair.

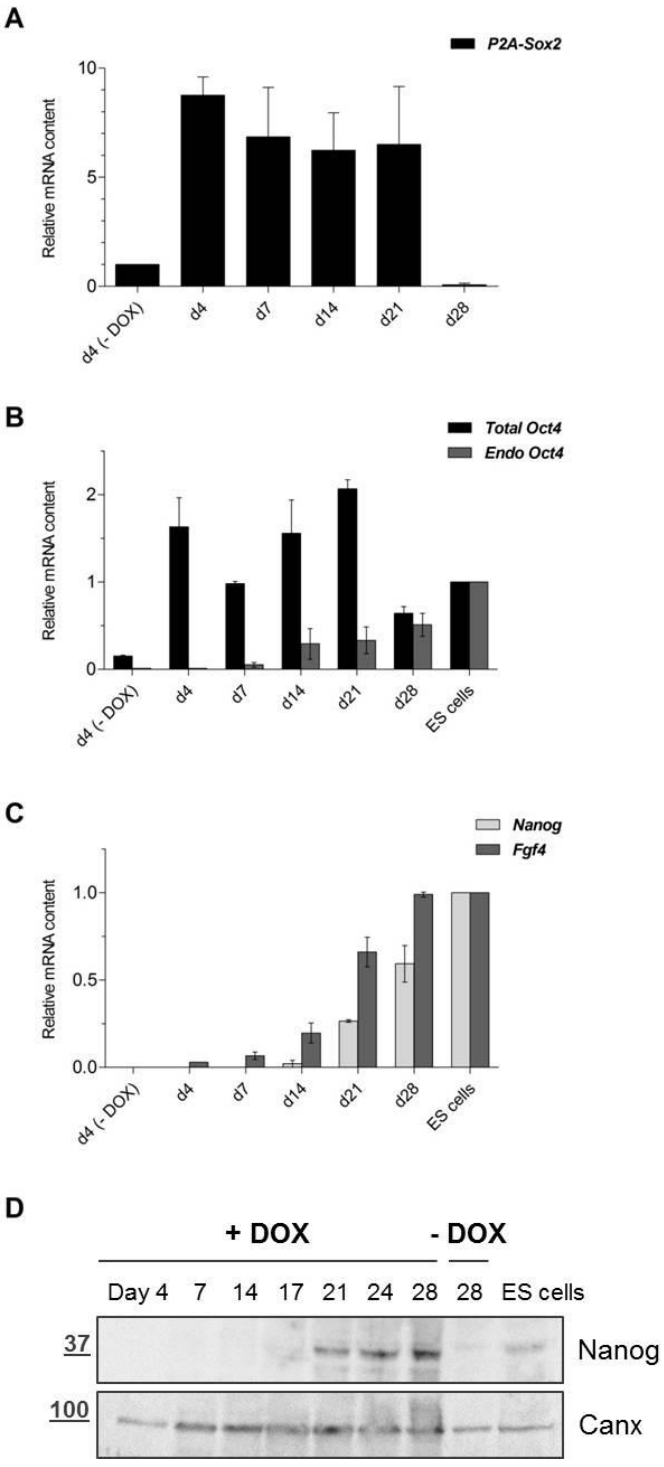

Figure 3.5: Reprogramming procedure induces consistent temporal alterations in terms of gene and protein expression.

(A-C) RT-qPCR analysis of total RNA content of transduced cells reveals expression of *P2A-Sox2* (viral transcript) when cultured in the presence of the inducing drug (DOX). Total *Oct4* levels correlate with this result. Pluripotency genes, like endogenous *Oct4*, *Nanog* and *Fgf4*, are transcribed at detectable levels starting at day 7, 14 or 4, respectively. *Gapdh* is used as endogenous control; results are normalized to d4 (-DOX) in (A) or to ES cells (B-C); mean ± SD, n=3. (D) Protein lysates were collected at different timepoints and subjected to western blot analysis. Nanog protein expression is observed starting on 21 dpt.

As shown in Figure 3.5B, endogenous *Oct4* was detected on day 7 and it kept increasing during cellular reprogramming, even after DOX withdrawal. At day 28, Total and Endo *Oct4* levels were similar given that viral transcripts were no longer present. *Nanog* and *Fgf4* transcript levels were also determined and expression of these pluripotent markers was also detected on day 14 or 4, respectively. It was observed that *Nanog* and *Fgf4* expression also increased during the protocol time course (Figure 3.5C). Importantly, Nanog protein expression was confirmed by western blot analysis and observed in high levels since day 21 (Figure 3.5D).

At the end of the reprogramming procedure, several colonies were observed on the culture wells. The number of colonies emerging in each individual experiment was quite variable, ranging from 50 to 300 colonies arising from $1x10^5$ initial MEFs. Given the determined 25% of transduction efficiency, we calculated that the reprogramming efficiency varied between 0.2 and 1.2%, which is in agreement with the literature (Silva et al., 2008). It was also observed in some experiments that colonies were present but with a flatter morphology and undefined borders, characteristic of partial reprogramming to pluripotency. These episodes, as well as experiments with lower efficiencies, could be related with not so freshly prepared culture media, in particular in terms of LIF, and variations in serum lots. Additionally, the number of arising colonies when transducing MEFs could be increased with higher volumes of lentiviral preparations (with expected increase in transduction efficiency). However, the final objective of isolating single colonies/clones was progressively more challenging as the colonies became closer to each other. Hence we decided to maintain the protocol as described.

On each reprogramming experiment, several colonies were manually “picked” and further cultured in the same culture media (ES media + LIF + 2i) and in the presence of feeder cells (mitomycin C mitotically inactived MEFs). Some colonies didn’t survive or grow after subculture as expected. However the vast majority could be submitted to successive culture passages and expanded. Isolated iPS cell clones were now ready for complete characterization in terms of morphology, self-renewal and pluripotency attributes, which will be described later on. A diagram representing this established workflow is depicted on Figure 3.6.

Despite success on generating colonies and isolated iPS clones with the lentiviral delivery system, alternative systems were also tested as described subsequently.

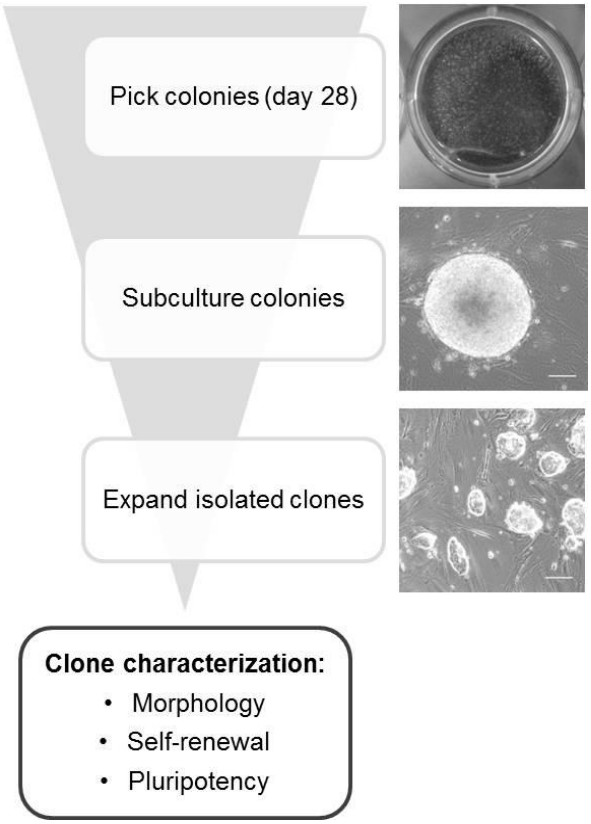

Figure 3.6: Stem cell-like colonies are isolated, subcultured and expanded to generate iPS cell clones that will be further characterized.

Scheme representing typical workflow subsequent to described reprogramming protocol.

Adenoviral molecular tools efficiently transduce MEFs and allow expression of reprogramming factors

The generation of iPS cells using lentiviral vectors poses an obstacle to its potential use as therapeutic tools, given the integrative nature of lentivirus that can lead to insertional mutagenesis. Different delivery strategies were envisioned and studies describing non-integrating viral vectors usage, such as adenovirus, for inducing pluripotency soon were published (Stadtfeld et al., 2008).

Aiming at establishing an adenoviral-mediated delivery of the reprogramming factors whilst maintaining the same set of TFs, the polycistronic OSKM unit was subcloned into an adenoviral vector (Ad-OSKM) (see Chapter 2 for details). One prospective advantage of this approach would be to transduce all cells concomitantly with all 4 TFs, since co-transduction with the 4 TFs in separate vectors is very inefficient, difficult to control and to optimize. In order to confirm the efficient delivery of the 4 TFs, cells were transduced with increasing quantities of adenoviral preparation and total protein content was

analysed by western blot technique. Results showed that all 4 TFs were expressed at protein level (Figure 3.7).

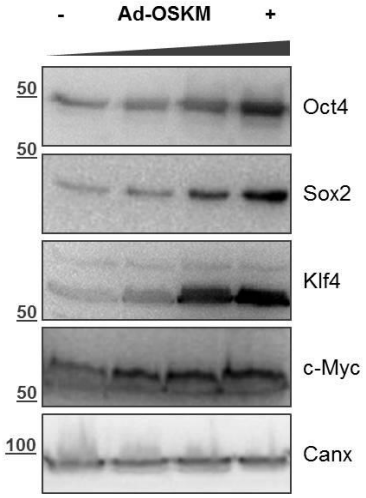

Figure 3.7: Adenoviral transduced cells express the 4 reprogramming factors.

HEK-293FT cells were transduced with Ad-OSKM in increasing quantities of viral supernatant preparation. Protein expression of Oct4, Sox2, Klf4 and c-Myc is observed and is intensified with the correspondent increase in the quantity of viral particles (+). Protein lysates collected 1 dpt were subjected to western blot analysis with the indicated antibodies; Canx was used as loading control.

For the sake of comparing results with the successful lentiviral protocol, several volumes of adenoviral preparations were used to transduce MEFs. Transduction efficiencies were quantified by IF as the percentage of Oct4 positive cells *per* total number of initial cells. We observed that 100 µL of viral supernatants showed to provide a transduction efficiency of approximately 24%, which was similar to the one obtained for the lentiviral co-transductions (Figure 3.8 and recall Figure 3.2).

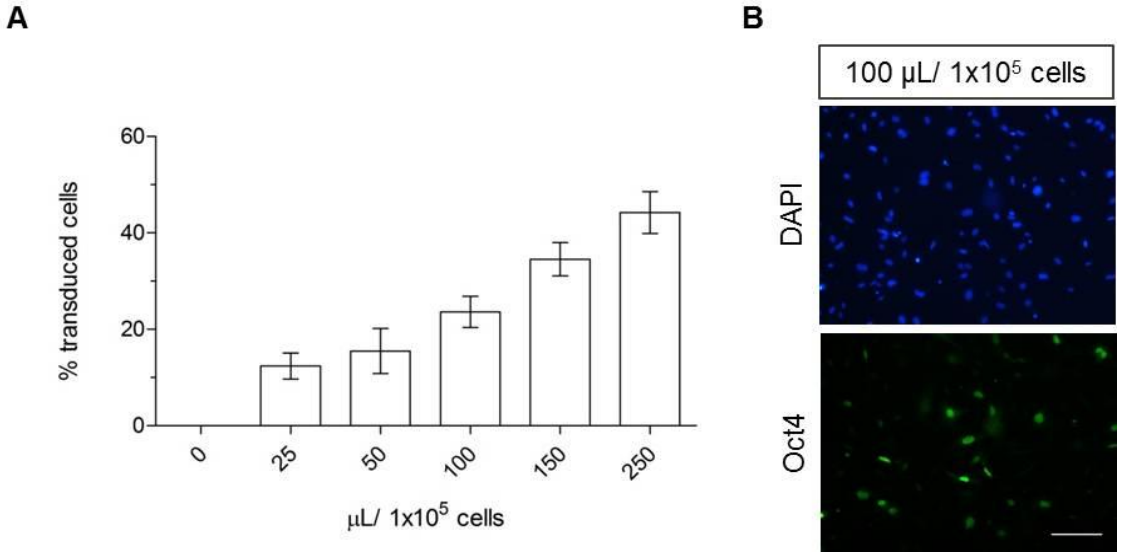

Figure 3.8: MEFs are efficiently transduced by Ad-OSKM depending on the volume of transducing viral particles.

(A) Increasing volumes of adenoviral preparation were added to MEFs and the percentage of transduced cells was calculated by dividing Oct4 positive cells for the total number of cells; mean ± SD (n=3). (B) Representative images of 100 µL of viral preparation added to $1x10^5$ initial cells; after quantification, these conditions correspond to approximately 24% of transduction efficiency. IF analysis against Oct4 was performed at 1 dpt. Nuclei were counterstained with DAPI and used to quantify total number of cells; scale bar 50 µm.

To further characterize adenoviral forced expression of the exogenous TFs and compare it with the lentiviral system, western blot analysis of total protein content of transduced cells at 4 dpt was performed, as depicted in Figure 3.9. When comparing transduction conditions that provide the same level of transduction efficiency (approximately 24%), it was observed that Oct4 protein levels attained with 100 µL of Ad-OSKM are diminished than the levels promoted by the lentiviral system. Using the inducible lentiviral system, protein expression was only observed at this point due to the lentiviral mechanism of action and the use of an inducible promoter. Since adenoviral vectors do not integrate into the host genome, viral copies are known to diminish along with cell divisions, which may already have occurred at this timepoint and might explained the observed difference on Oct4 protein levels. However, with increasing volumes of transduction adenovirus, this difference was attenuated until equivalent Oct4 protein levels was attained with 250 µL of Ad-OSKM (Figure 3.9B).

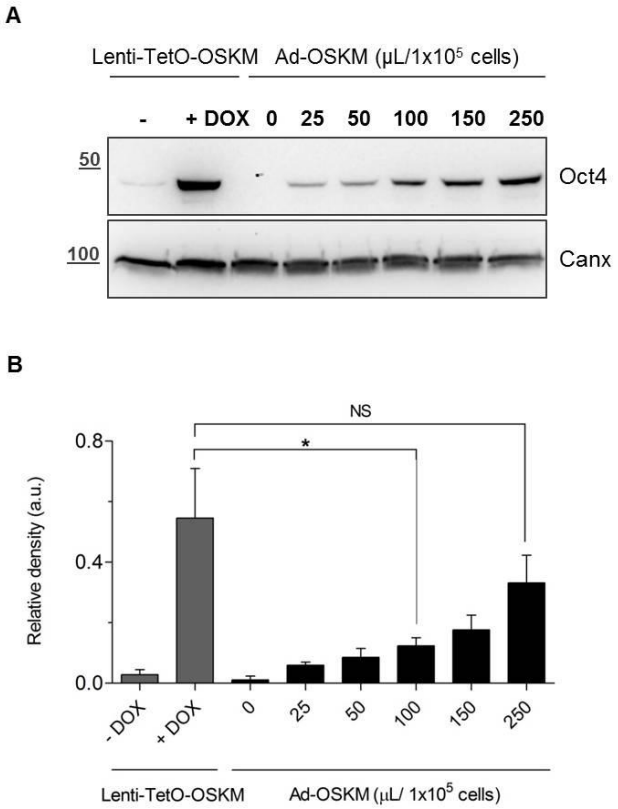

Figure 3.9: MEFs transduced with lentiviral and adenoviral particles used for delivery of reprogramming factors express Oct4 protein.

(A) Protein lysates of transduced MEFs were collected at 4 dpt and subjected to western blot analysis with the mentioned antibodies. Lentiviral co-transduction was performed with the volumes of viral preparations used in previous section. Ad-OSKM transduction was performed with increasing volumes of viral supernatant. (B) Relative density of Oct4 protein bands using Canx as loading control, in arbitrary units (a.u.). When comparing lentiviral co-transduction (+ DOX) and transduction with 100 µL of Ad-OSKM, the difference between the relative densities of Oct4 protein is statistically significant. However, no statistical significant difference is found when comparing with 250 µL of Ad-OSKM preparation (unpaired t-test, NS $p>0.05$, * $p<0.05$). Quantification of densitometry was performed using Image J software; mean ± SD, n=3.

Adenoviral transduced cells do not display typical morphological and gene expression alterations during reprogramming protocol

The optimized lentiviral protocol, in terms of timeline and culture media, was applied to MEFs transduced with Ad-OSKM viral particles, as schematized in Figure 3.10. Cells were transduced with different numbers of viral copies *per* initial cells (termed multiplicity of infection, MOI). Viral volumes ranging from 25 to 500 µL *per* 1x10^5 initial cells were used either in a single or in several transduction events. The rationale behind this multiple transduction strategy was to try to overcome dilution of adenoviral intracellular copies due to cell division. Additionally, this strategy could allow the maintenance of high

protein levels of exogenous factors essential to promote reprogramming events and activation of endogenous pluripotency program.

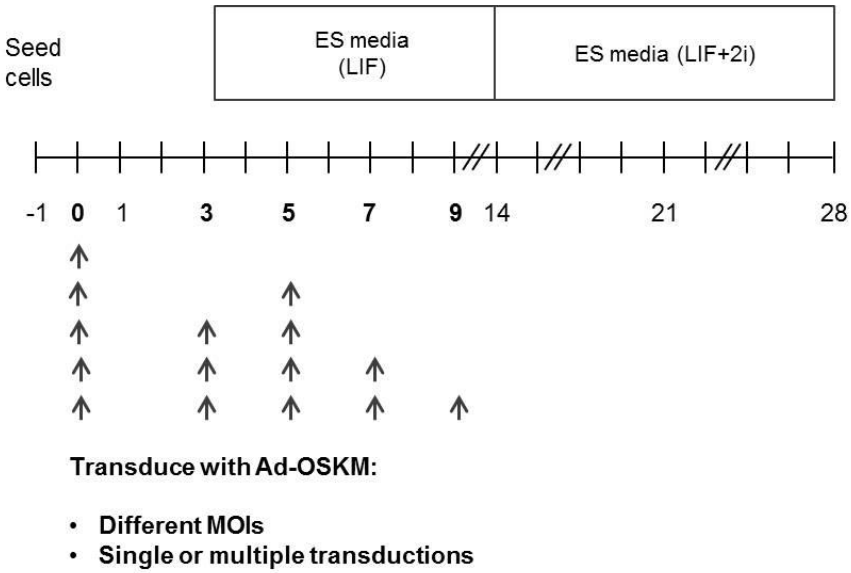

Figure 3.10: Timeline representing reprogramming protocol adapted for adenoviral delivery of reprogramming TFs.

Transduction of MEFs with Ad-OSKM viral particles was tested using different volumes of viral preparation *per* initial number of cells (different MOIs). Single or multiple transductions were also tried, with distinctive temporal combinations; vertical arrows indicate transduction days.

Several independent experiments were performed but no typical morphological alterations were observed, as for the lentiviral protocol executed in parallel to control for the proper experimental conditions. In some cases, few colonies were observed and manually "picked" despite not displaying fully reprogrammed morphological appearance. Nevertheless these cells failed to proliferate in an ES cell-like manner and no clones were successfully established.

In order to dissect the absence of reprogramming events at a molecular level, quantitative RT-PCR analysis of total RNA of adenoviral transduced cells was performed during the protocol time course. A volume of 100 µL viral particles *per* $1x10^5$ MEFs was used to obtain transduction efficiencies equivalent to the lentiviral protocol. Specific viral transcripts (*P2A-Sox2*) were detected on the first weeks after the single transduction event (Figure 3.11A). Similarly, *Total Oct4* (viral+endogenous) levels of transduced MEFs were comparable to ES cells, at least on day 4 and 7, but afterwards it started to decrease (Figure 3.11B). No expression of endogenous pluripotency genes, like *Endo Oct4*, *Nanog* and *Fgf4*, was observed (Figure 3.11C). In a gene expression perspective,

there was no evidence of an activation of a pluripotency profile, contrarily to what was observed with the lentiviral delivery system.

These gene expression results were in agreement with the observed absence of morphological alterations. Therefore, the objective of implementing a non-integrative delivery system to reprogram cells to pluripotency was not fulfilled.

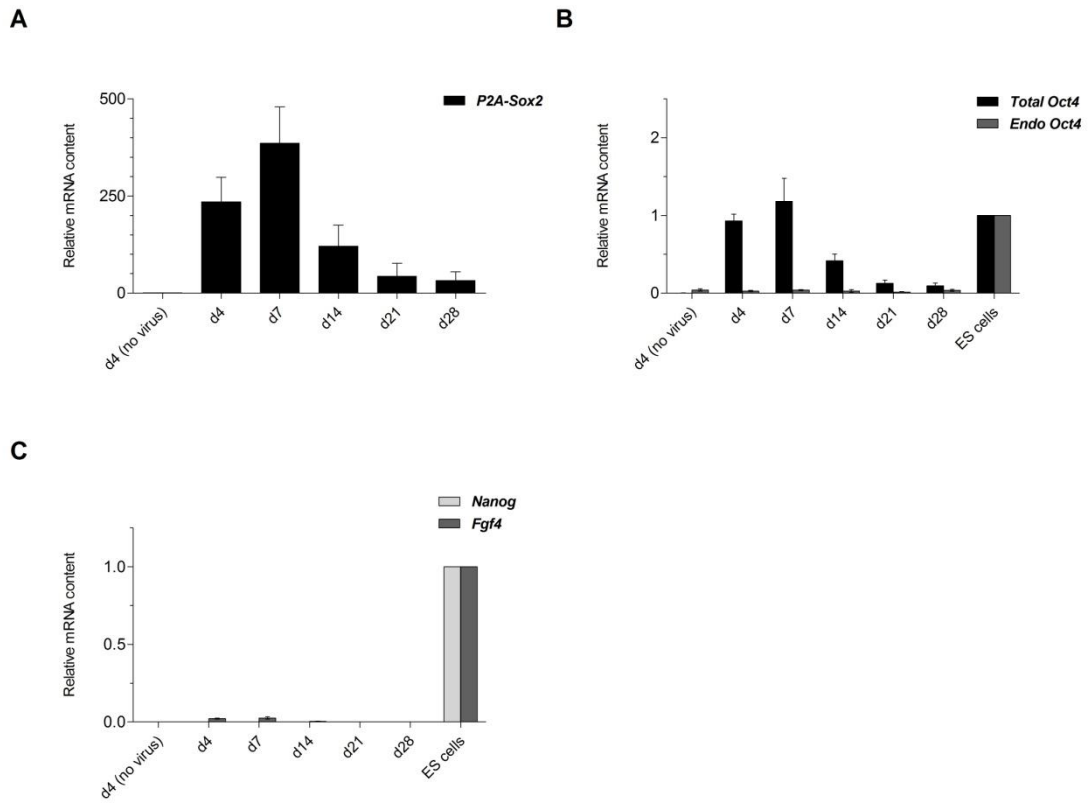

Figure 3.11: Protocol using adenovirus does not induce alterations of pluripotency genes' expression consistent with a reprogramming event.

(A-C) RT-qPCR analysis of total RNA content of transduced cells reveals expression of *P2A-Sox2* (viral transcript) on the initial days but with a gradual decrease over time. Total *Oct4* levels follow the same trend. Pluripotency genes, like endogenous *Oct4*, *Nanog* and *Fgf4*, are only expressed in residual levels. MEFs were transduced with 100 µL of adenoviral preparation *per* $1x10^5$ initial cells. *Gapdh* is used as endogenous control; results are normalized to d4 (no virus) in (A) or to ES cells (B-C); mean ± SD, n=3.

Lentiviral iPS cell clones exhibit typical morphology in culture, self-renewal properties, and expression of key pluripotency markers

Despite no success in replicating adenoviral-mediated reprogramming to pluripotency, a lentiviral-based protocol was efficaciously established, providing several iPS cell clones

that were further characterized. All iPS cell lines mentioned from this point forward were obtained using the described lentiviral delivery system and protocol.

Several clones from different independent experiments were established and expanded. To confirm that a fully reprogrammed state was achieved, iPS cell lines must first demonstrate morphology similar to ES cells (considered as a positive control) and unlimited self-renewal capacity. The obtained representative results are shown in Figure 3.12. Clones were established first in feeder culture conditions, but they could also be passaged into feeder-free cultures, maintaining colonies' appearance and growth rates (Figure 3.12A). In terms of self-renewal, iPS clones were subjected to enzymatic passaging every 2-3 days for at least 15-20 passages, still maintaining their phenotype. AP staining was also performed with positive results (Figure 3.12B).

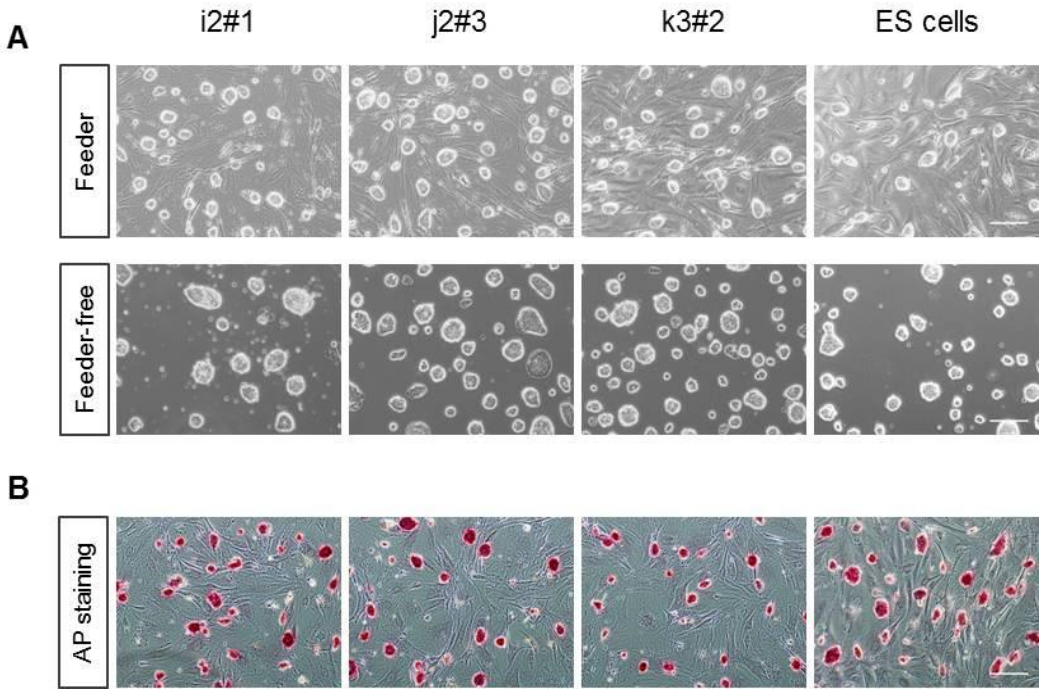

Figure 3.12: iPS cells clones demonstrate morphology in culture and AP positive staining, similar to ES cells.

(A) Three representative iPS cell lines, i2#1, j2#3 and k3#2, show a typical ES cell-like morphology when cultured in feeder and feeder-free conditions. (B) All clones also stain positively for AP. Scale bar 50 µm.

Secondly, iPS clones must be characterized in a molecular level to confirm expression of key pluripotency factors. By conventional RT-PCR, iPS cell lines were analysed and expression of a selection of ES cell marker genes (such as *Oct4*, *Nanog*, *Eras*, *Fgf4*, *Ecat1*, *Zfp42* and *Esg1*) was positively confirmed (Figure 3.13). Moreover, all clones

were negative for *P2A-Sox2* viral transcript expression, confirming that they no longer depend on exogenous TFs' expression.

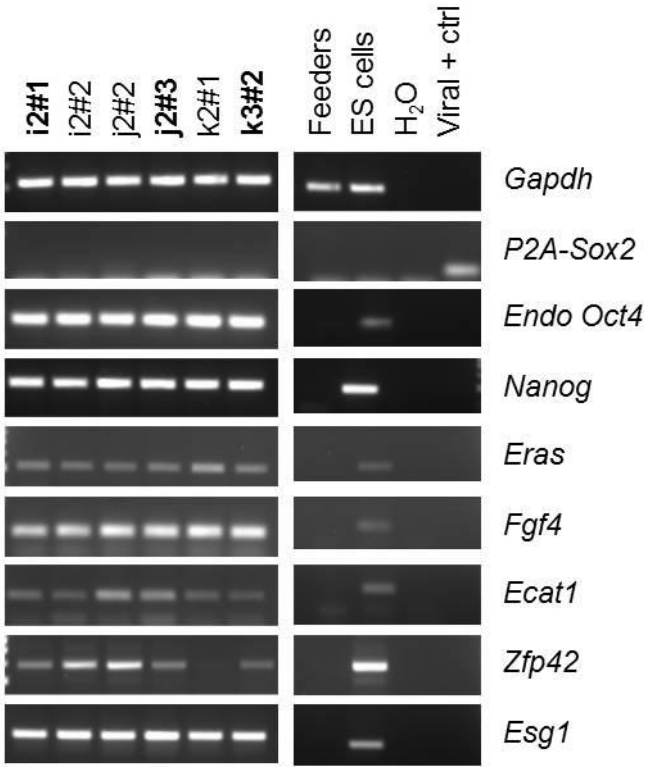

Figure 3.13: iPS cell lines express endogenous pluripotency markers.

Total RNA content of 6 different clones was isolated, cDNA was produced and analysed by RT-PCR, using the indicated pairs of primers. iPS cell lines express pluripotency genes, in a transgene independent manner, since no expression of viral transcript *P2A-Sox2* is detected. ES cells are shown as a positive control, feeders as a negative control, and *Gapdh* as endogenous control.

Furthermore, expression of Oct4 and Nanog was assessed at a protein level, as depicted in Figure 3.14. Three different clones are shown, all being positive for the expression and cellular localization of the mentioned TFs. Also, an undifferentiated ES cell surface antigen SSEA-1 staining was also detected in all clones.

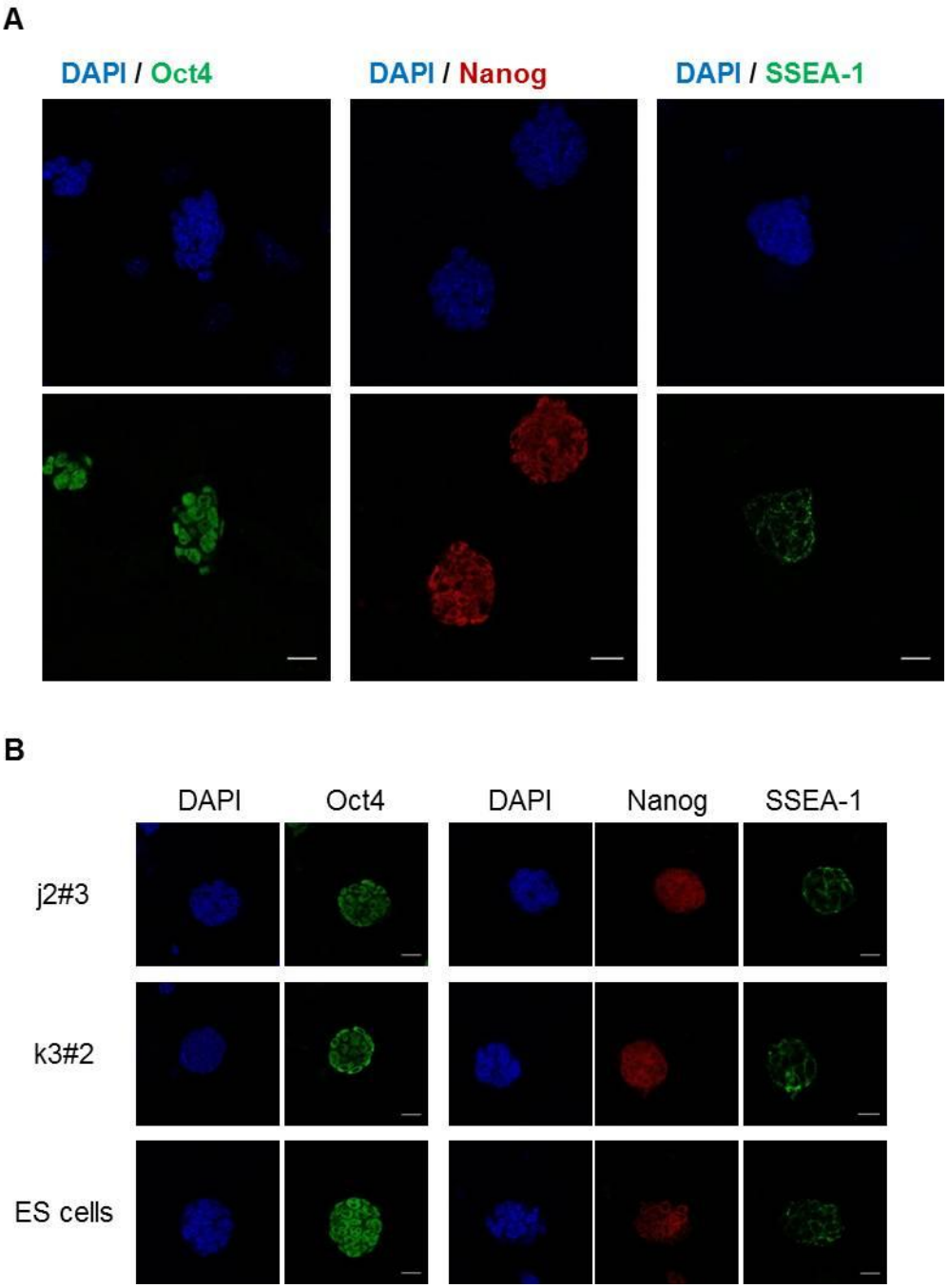

Figure 3.14: iPS cell lines express ES cell characteristic TFs and surface markers.

(A) Confocal images of i2#1 cells subjected to immunostaining using mentioned antibodies and DAPI for nuclei counterstaining. iPS cells express Oct4, Nanog and SSEA-1, at a protein level and with a nuclear (Oct4 and Nanog) or cell surface localization (SSEA-1). (B) Same IF study is shown for 2 more clones, j2#3 and k3#2, and for ES cell as a positive control. Scale bar 20 µm.

Thus, isolated iPS cell clones proved to recapitulate ES cells properties, both at morphological and molecular levels. Subsequently, functional confirmation of attainment of a naïve pluripotent state was assessed.

Established iPS cell lines demonstrate a functional pluripotent capability

Pluripotency is usually defined as the ability of germ cells to differentiate into all three germ layers such as endoderm, mesoderm and ectoderm. This capability of differentiation is regulated by a complex network of TFs and signalling pathways. Besides demonstrating expression of these key pluripotent TFs, one needs to prove iPS clones' functional pluripotency.

Different assays with variable levels of stringency can be used to test for iPS cell lines developmental potential. For that purpose, *in vitro* differentiation assay using EBs was used. Clones were grown in low attachment culture dishes to promote EB formation in suspension cultures. Afterwards, obtained EBs were transferred for attachment conditions and culture media without LIF and 2i, and allowed to differentiate spontaneously for 14 days in total. Results for EB assay for 3 clones and ES cells are depicted in Figure 3.15.

As shown, after differentiation of all 3 clones, expression of genes from ectoderm, mesoderm and endoderm was detected: *Pax6*, *Col1a1* and *Gata6* respectively. In some cases expression was detected as soon as 7 differentiation days, while for others 14 days were needed. Protein levels were also assessed by IF, and positive cells for Pax6 (ectoderm), SMA (mesoderm) and AFP (endoderm) were detected for all clones (see representative images of one clone in Figure 3.15B).

In order to confirm iPS clones *in vivo* differentiation potential, cells from i2#1, j2#3 and k3#2 iPS cell clones were also injected subcutaneously into immunodeficient mice. These cells induced teratomas, with all 3 germ layers being identified after histopathological analysis, therefore confirming the pluripotency of the generated iPS cell lines (Figure 3.16).

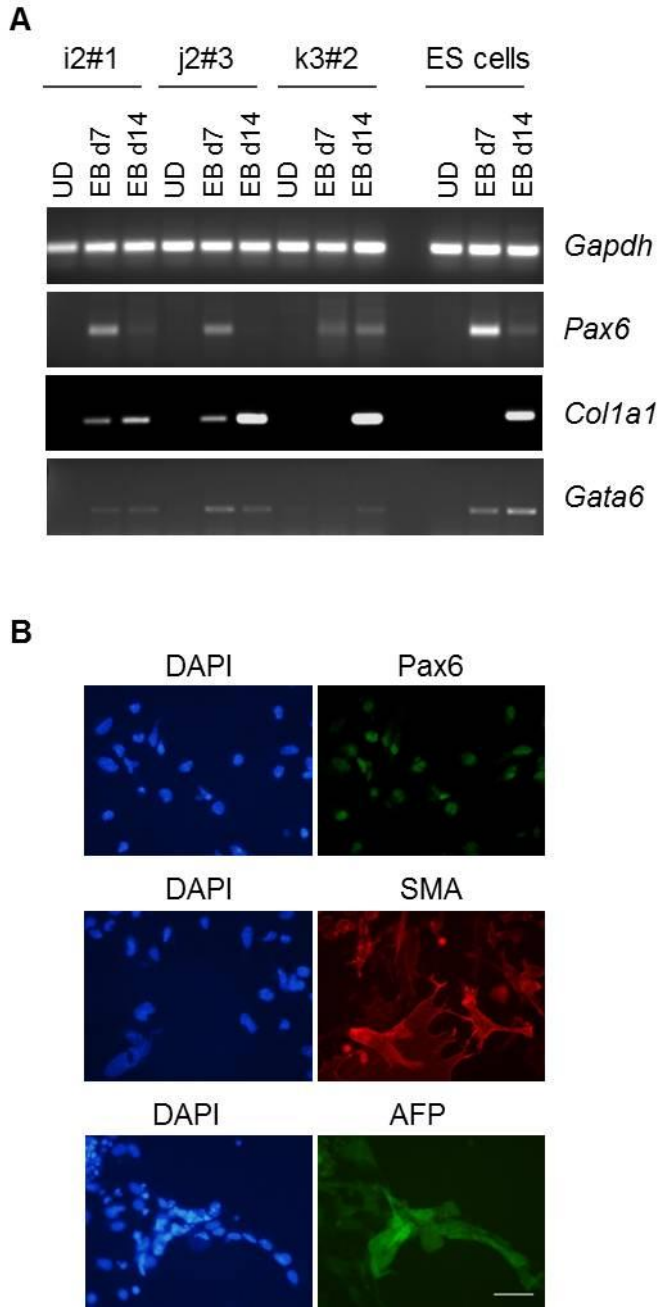

Figure 3.15: iPS cell clones demonstrate their functional pluripotency in *in vitro* differentiation assay.

(A) RT-PCR analysis of iPS cell clones in undifferentiated (UD) state or after 7 or 14 days of EB differentiation. ES cells were used as positive control and primers designed to specifically amplify transcripts from ectodermal (*Pax6*), mesodermal (*Col1a1*) and endodermal (*Gata6*) lineages. (B) Representative images of immunostaining of j2#3 cells after 14 days of EB differentiation assay. Protein expression of markers for the 3 lineages is observed, when the mentioned antibodies are used. Scale bar 25 µm.

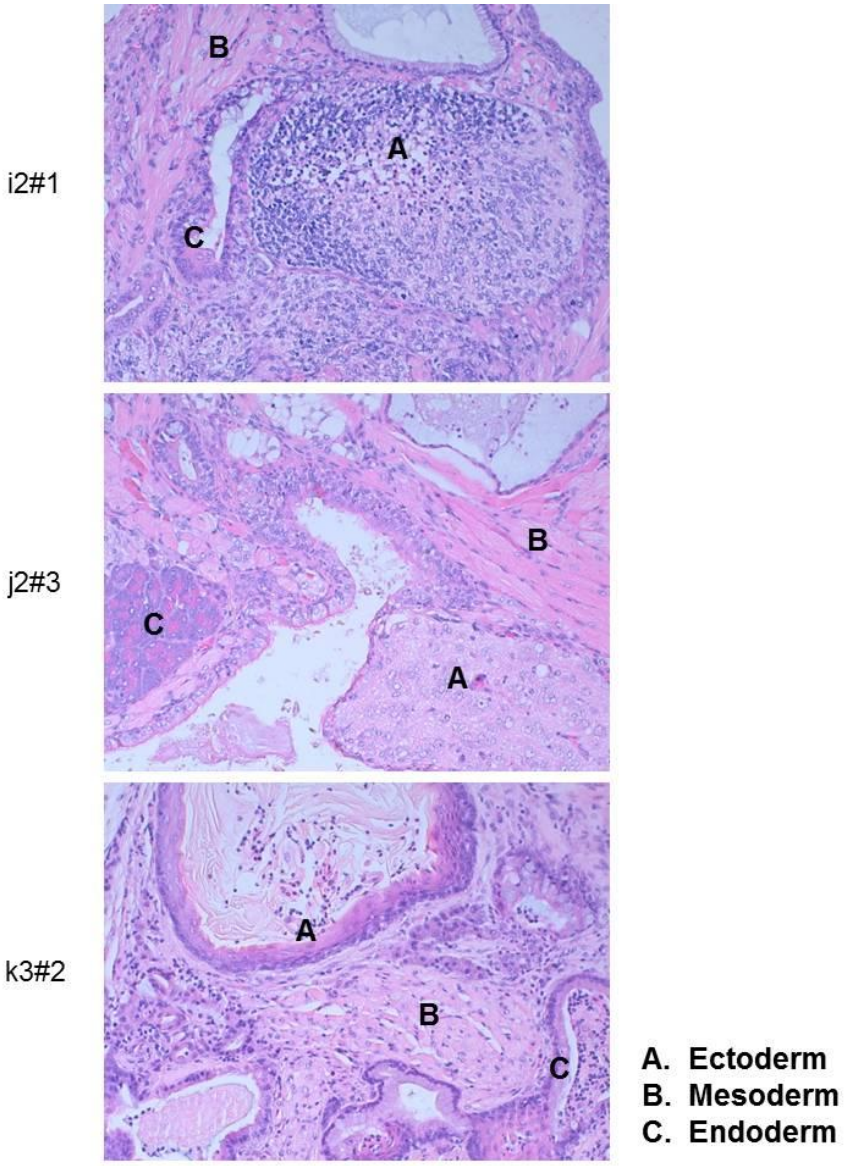

Figure 3.16: Established iPS cell lines give rise to tissues from the three germ layers, in *in vivo* differentiation assay.

iPS cell lines (i2#1, j2#3 and k3#2) were subcutaneously injected into NOD.Scid mice. Resultant teratomas were collected after 5 to 7 weeks and subjected to histological analysis after hematoxylin-eosin staining. In each teratoma, characteristic tissues from ectoderm (A), mesoderm (B) and endoderm (C) lineage are observed, as illustrated on representative images.

Discussion

Forced expression of defined factors can induce reprogramming of somatic cells from different tissues and species into a pluripotent state, generating iPS cell lines (Takahashi and Yamanaka, 2006; Takahashi et al., 2007a). Different technological improvements have been made over the years in order to increase the efficiency of the reprogramming

process and diminish the genomic alterations required to complete the process. The choice of the appropriate donor cell type, reprogramming cocktail and delivery system varies according to the ultimate goal of the study, for instance, basic biology studies or clinical applications (González et al., 2011).

At the time that this study was initiated and until now, delivery of the 4 classical Yamanaka TFs (Oct4, Sox2, Klf4 and c-Myc) by an inducible lentiviral system is still the gold-standard procedure for the generation of iPS cells. However, the lentiviral delivery system raises some concerns related with lack of safety for prospective clinical applications. It induces genomic transgene integration, with the consequent possible caveat of insertional mutagenesis. Exogenous expression of a reprogramming cocktail, that includes the known oncogene c-Myc, contributes to the tumorigenic risk of iPS cells, though minimized by withdrawal of the inducing drug. Nevertheless, the efficiency, robustness and reproducibility of the inducible lentivirus-mediated reprogramming process makes it an ideal approach for the implementation of such technology in a laboratory for the first time (Bayart and Cohen-Haguenauer, 2013; González et al., 2011).

Here, we reported the generation of mouse iPS cells using a lentiviral system. MEFs isolated from WT animals were used and forced expression of the 4 TFs was achieved by transduction with an inducible lentiviral system encoding for a polycistronic OSKM. The polycistronic unit allows the expression of several cDNAs from the same promoter, thus minimizing the number of genomic insertions compared with single-factor-expressing viruses. Additionally, the inducible nature of the lentiviral system permits the expression of the reprogramming factors in a controllable manner (Carey et al., 2009). Initially, the efficient transduction of the initial cells was confirmed, as well as the inducible expression of the 4 TFs. Cellular reprogramming of MEFs was attempted in typical ES cell culture conditions (serum and LIF), with subsequent addition of 2i to the culture medium in order to promote conversion of pre-iPS cells into fully reprogrammed cells, in a naïve pluripotent state (Silva et al., 2008). Morphological alterations of the initial cells were observed, with elongated fibroblasts becoming rounded and aggregated in small clusters characteristic of MET described to occur on early reprogramming events (Li et al., 2010a). Alterations on gene and protein expression were also observed with the reactivation of endogenous pluripotency markers, such as Oct4, Nanog, Fgf4, SSEA-1 and AP. Such expression was maintained even when the inducing drug was withdrawn from the system, highlighting that reprogrammed cells were already on a transgene independent phase of the reprogramming process (Federation et al., 2013).

In order to establish a reprogramming protocol suitable for clinical applications, similar conditions (donor cell type and culture media) were employed but using a non-integrative viral delivery system. The same polycistronic cassette encoding for OSKM was cloned into an adenoviral vector, which was shown to efficiently transduce MEFs. However, the morphological and molecular alterations, occurring during the lentiviral protocol, were not observed. One possible explanation could be related with Oct4 essential role on reprogramming events, on a dose dependent manner. It has been shown that high expression of transgenic Oct4 in somatic cells and reprogramming intermediates is necessary for successful reprogramming, probably because Oct4 protein may assist in opening chromatin, increasing the chances of reactivating early pluripotency genes (Radzisheuskaya and Silva, 2013). Given the reduced level of Oct4 protein when comparing with equivalent conditions of the lentiviral system (Figure 3.9), one can speculate that Oct4 levels were insufficient for the initial reprogramming events. Additionally, an ES cell level of Oct4 must be achieved at the late stages of reprogramming for cells to enter the pluripotent cell state, which did not occur with the adenoviral system (Radzisheuskaya et al., 2013). It was observed that, on 14 dpt, Oct4 levels were not equivalent to ES cells, contrarily to what was found for the lentiviral approach (Figure 3.11B and Figure 3.5B). However, increased volumes of viral preparations (thus with higher percentage of transduced cells) and/or multiple transductions (attempting a more robust expression over time) were also tested unsuccessfully. In some rare cases, some colonies arose in culture but could not successfully originate an expandable iPS cell line. Importantly, since the first reports of adenoviral-mediated delivery of the reprogramming factors, only a few authors claimed to reproduce it and with different donor cells (Fink et al., 2013). Moreover, additional and more appealing non-integrative approaches have been developed, such as the highly efficient RNA delivery (Warren et al., 2010), which will be explored in the near future.

Contrarily to the adenoviral delivery, inducible lentiviral system efficiently allowed the reprogramming of MEFs into pluripotency. Emerging colonies were identified by their morphology, and subsequently isolated and sub-cultured, generating several iPS cell lines that could be expanded and characterized. Such cells must demonstrate self-renewal and pluripotency properties similar to ES cells, in order to confirm that a pluripotent state has been achieved by the reprogramming process. Obtained iPS cell lines demonstrated unlimited propagation *in vitro* (self-renewal property), whilst displaying a typical ES cell-morphology. Molecularly, iPS cells exhibited expression of key pluripotency markers at a transcriptional and protein level, confirming the reactivation of the endogenous pluripotent program. Of particular relevance is the

observed expression of Oct4 and Nanog, members of the core circuitry responsible for activating expression of genes involved in pluripotency maintenance and inhibiting early lineage differentiation genes (Young, 2011). Additionally, iPS cell lines expressed other pluripotency factors, such as *Eras*, *Ecat1*, *Esg1*, *Fgf4* and *Zfp42* (Takahashi et al., 2007b), were positive for AP staining and displayed characteristic SSEA-1 surface marker. Expression of Nanog and *Zfp42* (also known as *Rex1*) further confirms the attainment of naïve pluripotency. This “ground state” has been known to be promoted by dual inhibition of MEK and GSK3 signalling pathways with the addition of 2i small molecules to the culture medium of ES cells and iPS cells. Nanog and Zfp42 are usually heterogeneously expressed by pluripotent cells, except in this 2i culture conditions that promote a more homogeneous level of expression within the cell population (Wray et al., 2010). In accordance, Nanog protein was found to be homogeneously expressed by generated iPS clones (Figure 3.14).

Another feature of naïve pluripotency is the capacity to give rise to all cell types of an organism except extraembryonic tissues. To confirm such property, several functional tests have been implemented. Generated iPS cell lines were first subjected to an *in vitro* differentiation assay, in which EB grown in suspension are plated out as adherent colonies and allowed to differentiate spontaneously. Expression of markers from ectoderm, mesoderm and endoderm lineages was observed for the tested iPS cell lines thus providing the first evidence for the pluripotent developmental potential. Secondly, a more stringent confirmation of such property was provided by an *in vivo* differentiation assay. After injection on immunodeficient mice, iPS cells formed teratomas, which were composed by tissues from the 3 germ layers.

According to the requirements of the downstream goal, iPS cell lines might be more extensively characterized, namely in the case of prospective therapeutic application. Functionally, iPS cell lines can further demonstrate definite pluripotency by chimera formation with germline transmission and generation of entirely iPS cell-derived mice by tetraploid complementation (Kang et al., 2009; Okita et al., 2007). Additionally, genetic and epigenetic alterations have been detected on iPS cell lines, with consequent immunogenicity and tumorigenicity concerns, which might impair their use for cell replacement therapies. On such case, genome-wide sequencing, expression analysis, and DNA and histone modification analysis have been used for a more comprehensive genetic and epigenetic profiling of iPS cell lines (Liang and Zhang, 2013; Peterson and Loring, 2014).

In conclusion, an inducible lentiviral approach was successfully undertaken with the generation of several iPS cell lines. These cells demonstrated self-renewal and naïve

pluripotency properties, both molecular and functionally. Importantly, in addition to possible therapeutic intervention on regenerative medicine field, these iPS cells can be used for disease modelling, drug or toxicity screening and basic biology studies. Thus, implementation of such Nobel awarded technology in a laboratory opens new avenues for the progress of scientific discoveries.

Chapter 4 Induced Pluripotent Stem cell-based applications for Choroideremia

Chapter 4 : Induced Pluripotent Stem cell-based applications for Choroideremia

Summary

Choroideremia (CHM) is an X-linked form of retinal degeneration of slow onset and progression, with affected males suffering blindness by middle age. CHM is caused by loss of function of REP-1, which is a regulator of Rab GTPase activity, essential for intracellular trafficking processes. In CHM, the RPE and other components of the retina, like photoreceptors and choriocapillaries, deteriorate progressively causing visual impairment. Using mouse models, we showed recently that the RPE plays a central role in the pathogenesis of CHM, suggesting that rescue of RPE function may be of great benefit to CHM patients (Tolmachova et al., 2013). For patients with extensive retinal degeneration, only regenerative approaches will enable restoration of vision. In recent years, this area of research has seen tremendous technological developments, which have offered new hope that this approach may yield results in the short term.

iPS cells appear to be particularly attractive, given the potential to reprogram adult somatic cells to pluripotency, gene correction and differentiation into the desired cells, and therefore to generate patient-specific cells to replace damaged tissue. Alternatively, and more straightforwardly, iPS cells can also be used, after differentiation into a functional RPE, as an *in vitro* model of CHM to study the still unclear pathophysiological and molecular events that trigger retinal degeneration in this disorder. This is particularly relevant for CHM given the lack of proper *in vitro* models, namely due to limited cell availability of RPE primary cultures from *Chm* mouse model.

Here, we report the generation and characterization of iPS cells from fibroblasts derived from a mouse model with conditional *Chm/Rep1* KO (Tolmachova et al., 2006). MEFs were reprogrammed using a polycistronic lentivirus coding for Yamanaka's transcription factors (Oct4, Sox2, Klf4 and c-Myc) (Carey et al., 2009; Takahashi and Yamanaka, 2006). Several iPS cell clones were isolated and characterized in terms of morphology, self-renewal and expression of key pluripotency markers. *In vitro* and *in vivo* differentiation assays were executed to further confirm the pluripotency status of the obtained pluripotent cell lines. Subsequently, differentiation into RPE of iPS cell lines was attempted in order to provide a proof of concept of their prospective use in disease modelling studies and transplantation procedures.

Results

Chm MEFs primary cultures can be used as an *in vitro* model of *Rep1* KO

Conditional mouse models of *Rep1* KO have been generated in order to study CHM pathophysiology and to test new therapeutic approaches (Tolmachova et al., 2006). Null mutations of *Chm/Rep1* have shown to be embryonically lethal in males and heterozygous females that have inherited the mutation from their mothers, due to defects in trophoblast development and vascularization of extra-embryonic tissues (Shi et al., 2004). Therefore conditional approaches were undertaken to circumvent this described lethality and breeding problems of transmitting the Chm^{null} allele from carrier females.

Tamoxifen (TM)-induced conditional mouse model, which features a temporal control of the *Cre/loxP* site-specific recombination event that triggers actual *Rep1* KO, can be used to obtain somatic cells for reprogramming experiments. These animals carry a modified *Chm* allele with its exon 4 flanked by 2 *loxP* sites (Chm^{flox}), and, in some cases, also a *MerCreMer* transgene that provides TM responsiveness.

In order to obtain Chm MEFs, a breeding scheme was established, as depicted in Figure 4.1, with $Chm^{flox/flox}$ $MerCreMer^{+}$ females being mated with Chm^{flox}/Y $MerCreMer^{-}$ males. At E13.5, primary cultures of MEFs were established from each embryo separately. All primary cultures were characterized in terms of genotype and a representative PCR result is shown in Figure 4.1B. As expected, all primary cultures are Chm^{flox}, however only approximately half of them possess the *MerCreMer* transgene (in this illustrative case, embryos E12, E13 and E16-19 are positive). From 10 successful matings, 68 embryos were isolated, and 33 were positive for *MerCreMer* transgene.

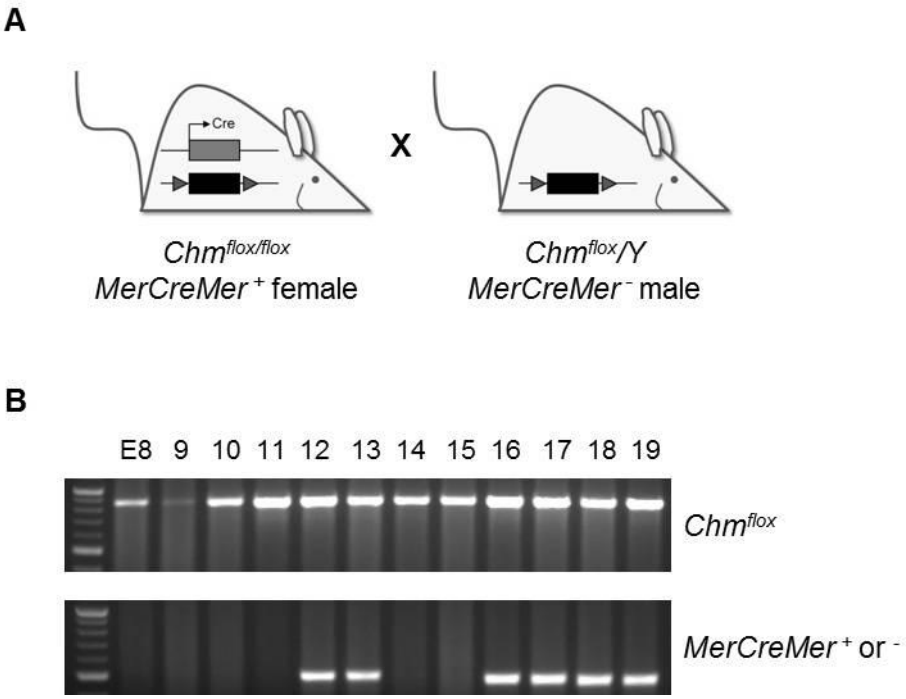

Figure 4.1: Breeding of *Chm*^{flox} animals allows isolation of MEFs suitable as Chm model.

(A) Chm$^{flox/flox}$ *MerCreMer*$^{+}$ females were mated with *Chm*$^{flox/Y}$ *MerCreMer*$^{-}$ males, and pregnant females were sacrificed for establishment of MEF primary cultures. (B) PCR genotyping of isolated embryos (E) 8 to 19 allows characterization in terms of *MerCreMer* transgene presence or absence (bottom panel; 510 bp). Primers to confirm *Chm*^{flox} genotype and genomic DNA (gDNA) integrity were also used (top panel; 860 bp).

When *Chm*^{flox} *MerCreMer*$^{+}$ primary cultures are treated with TM, *Rep1* KO is expected to occur. *MerCreMer* positive cells express Cre recombinase as a fusion protein with 2 copies of TM-responsive estrogen receptor. Upon TM treatment, *MerCreMer*, usually sequestered in the cytoplasm, is translocated into the nucleus and catalyzes recombination between the 2 *loxP* sites flanking *Rep1* exon 4. On resulting *Chm*^{null} cells, a frameshift mutation occurs, leading to a premature stop codon, resulting in a non-functional Rep1 protein (Figure 4.2A).

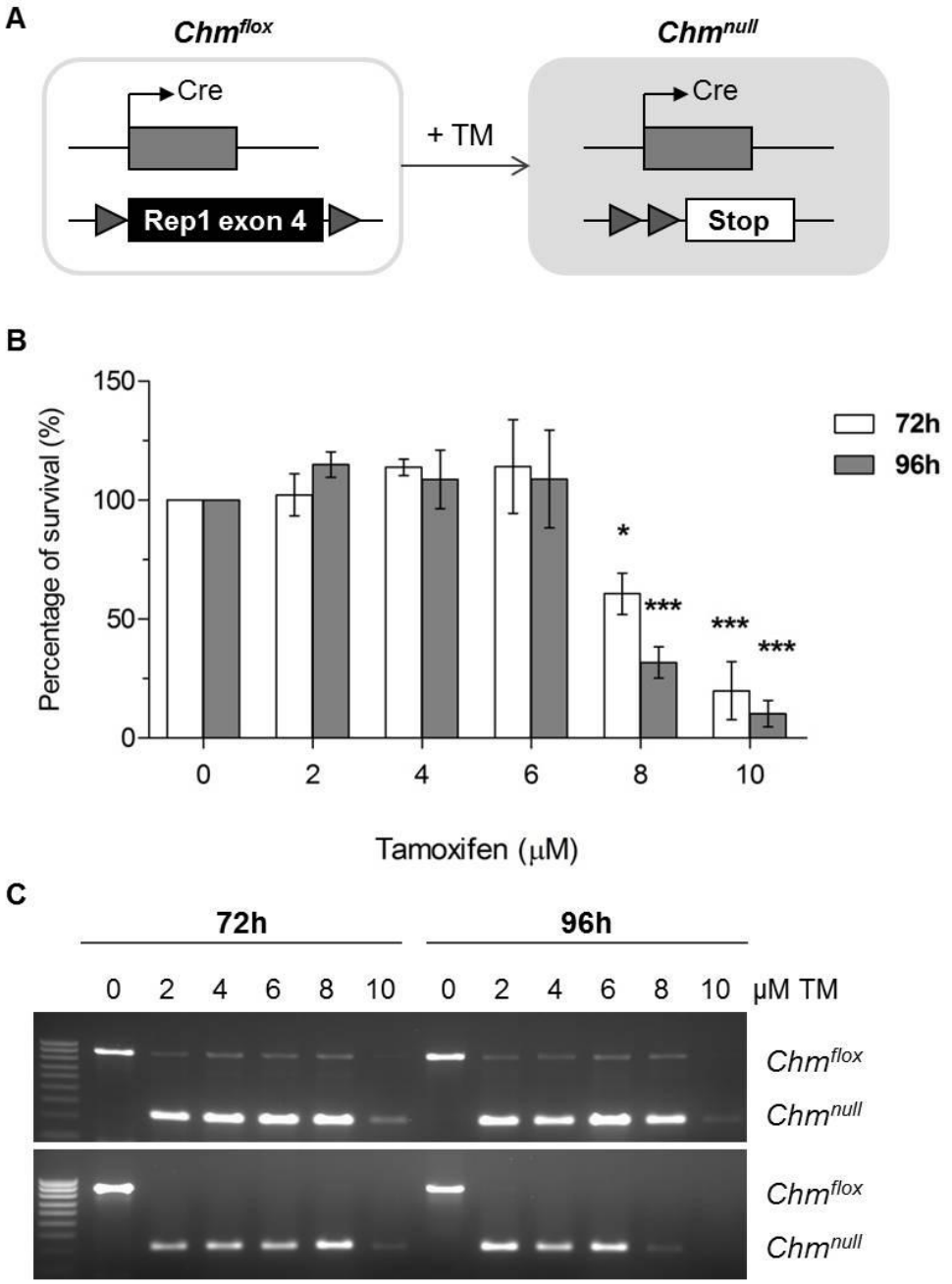

Figure 4.2: Treatment with 6 μM TM for 96 h induces genomic recombination in Chm MEFs without affecting cell survival.

(A) Scheme of TM treatment of *Chm*^{flox} cells inducing genomic recombination between loxP sites (grey triangles) flanking exon 4 of *Rep1* gene. A stop codon is created and *Chm*^{null} cells will not express functional Rep1 protein. (B) MTT assay was used to asses cell survival of MEFs treated with increasing concentrations of TM, for 72 or 96 h. For both exposure periods, 6 μM of TM can be used without affecting the percentage of survival. Mean ± SD, n=3. Statistically significant values relative to control for each exposure time (0 μM) are indicated (one-way ANOVA with Dunnett's multiple comparison test); * $p<0.05$, *** $p<0.001$. (C) MEFs were subjected to increasing concentrations of TM for periods of 72 h or 96 h, and genomic DNA was isolated and analysed by PCR. Two representative *Chm*^{flox} (860 bp) cultures are shown and, in the presence of TM, genomic recombination occurs and *Chm*^{null} alleles (330 bp) are now detected. In the top panel, *Chm*^{flox} (860 bp) alleles are visible even when higher concentrations of TM were used. For 8 or 10 μM, bands are fainter probably due to cell death, as expected according to MTT results.

TM exposure conditions were optimized in terms of concentration and exposure time in order to maximize genomic recombination events without compromising cell viability. MEFs were treated with increasing concentrations of TM (ranging from 0 until 10 µM) for periods of 72 or 96 h. Cell viability, evaluated by MTT assay, was not affected with concentrations up to 6 µM, for both periods of time (Figure 4.2B). These conditions promoted genomic recombination with excision of exon 4 of *Rep1* gene, as a shorter Chm^{null} allele was now detected by PCR (Figure 4.2C). Despite some variability between MEFs and presence of residual amounts of Chm^{flox} allele in some cases, recombination occurred at great extent when cells were treated with TM 6 µM for 96 h. It was also observed that increasing TM concentration or exposure time would affect cell viability, without necessarily increasing recombination efficiency. Specifically, when comparing 6 versus 8 µM treatment and 72 h versus 96 h, maintenance of residual Chm^{flox} allele was observed. (Figure 4.2B and C).

Although treating cells with 6 µM TM for 96 h was shown to be sufficient to induce genomic recombination, it was essential to determine expression levels of *Rep1* gene to confirm that an efficient Rep1 KO has occurred. Therefore, all primary cultures used in reprogramming experiments were always characterized in terms of genotype and *Rep1* expression. In Figure 4.3A, genotyping results of 3 representative cultures are shown and 3 different types of cells were used throughout these studies: Chm^{null} (generated from Chm^{flox} cells subjected to TM treatment), Chm^{flox} (untreated) and WT primary cultures. The later correspond to WT MEFs as described on previous chapter (thus are $MerCreMer^{-}$) and were used in parallel as a positive control for reprogramming events.

In concordance with their genotypes, *Rep1* expression levels of Chm^{null} primary cultures were significantly reduced when compared with Chm^{flox} or WT MEFs, as determined by RT-qPCR (Figure 4.3B). Therefore, an efficient KO of *Rep1* gene was successfully obtained in Chm^{null} primary cultures. Chm^{null} cells can be used to model Chm, directly or after reprogramming into a pluripotent state with the obtention of Chm iPS cells, as is shown afterwards.

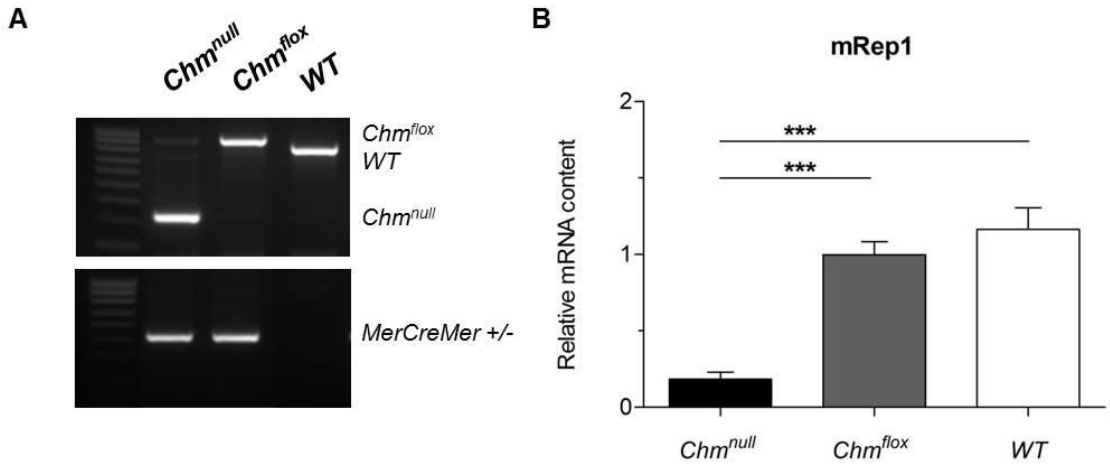

Figure 4.3: Primary cultures of *Chm*^{null} MEFs have reduced levels of *Rep1* expression.

(A) gDNA of 3 different types of MEFs cultures was collected and analysed by PCR genotyping: WT, *Chm*^{null} (*Chm*^{flox} treated with TM) and *Chm*^{flox} cells. On top panel, primers that amplify *Chm* gene were used and, given the size difference, *Chm*^{WT} (780 bp), *Chm*^{null} (330 bp) and *Chm*^{flox} alleles (860 bp) are distinguished. On bottom panel, PCR using primers that amplify *MerCreMer* transgene (510 bp) is shown. (B) Quantitative RT-PCR analysis of MEFs was performed to evaluate *Rep1* expression. *Chm*^{null} cells exhibit at least 80% KO of *Rep1* expression when compared with WT or *Chm*^{flox} MEFs. *Gapdh* was used as endogenous control; mean ± SD, n=3. Statistically significant values relative to control are indicated (one-way ANOVA with Dunnett's multiple comparison test); *** p<0.001.

Chm MEFs can be reprogrammed into pluripotency using a lentiviral based protocol

Somatic cells from Chm mouse model were subjected to established lentiviral reprogramming protocol (see Chapter 3 for details). As WT MEFs were used to implement and optimize the protocol, these cells were used as a reprogramming control in experiments involving Chm cells.

The first step was to assess the transduction efficiency with lentiviral reprogramming tools by immunostaining against Oct4 (Figure 4.4A). Co-transduction with Lenti-TetO-OSKM and Lenti-M2rtTA was shown to promote exogenous expression of Oct4, 4 dpt, in the presence of DOX. This also occurred with *Chm*^{null} and *Chm*^{flox} cells, with no significant difference in terms of percentage of transduced cells (29 and 26%, respectively) when comparing both cells types with each other or with WT MEFs (Figure 4.4B). Inducible nature of lentiviral system was confirmed by western blot analysis, with Oct4 protein levels only being detected in the presence of DOX, in all 3 types of MEFs (Figure 4.4C).

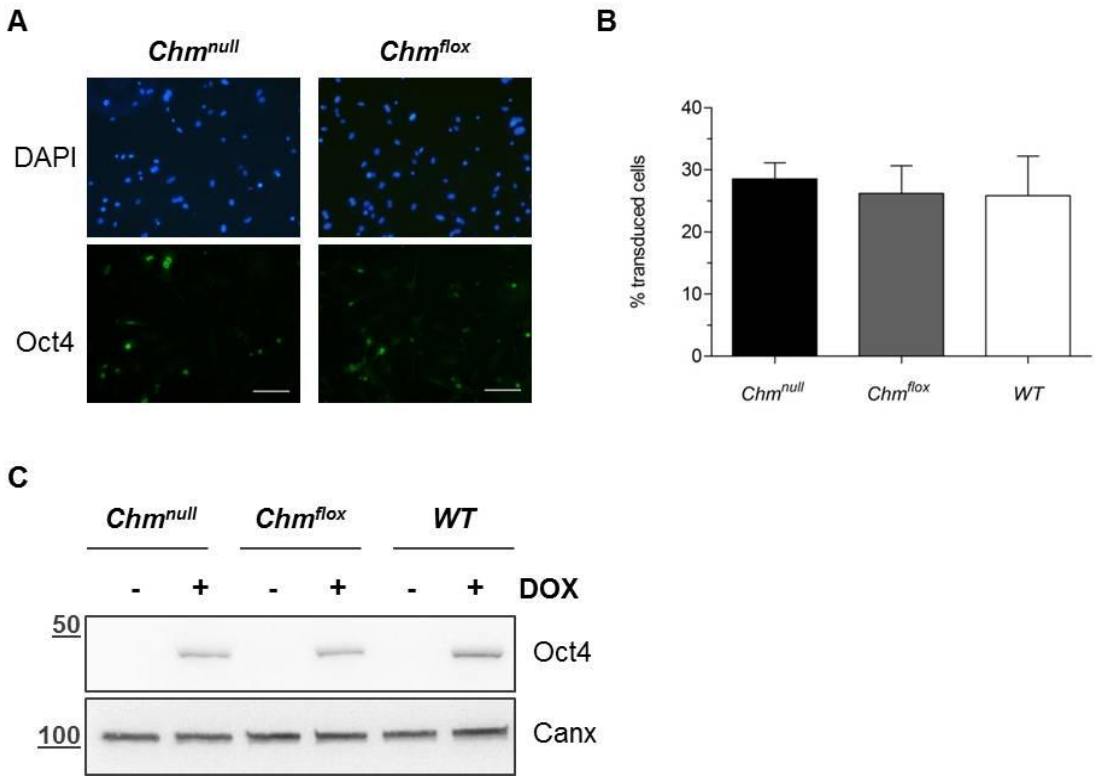

Figure 4.4: Lentiviral reprogramming particles efficiently transduce Chm MEFs.

(A) Transduced *Chm*^{null} and *Chm*^{flox} MEFs express Oct4, in the presence of DOX, as assessed by IF at 4 dpt; nuclei are counterstained with DAPI and used to quantify total number of cells; scale bar 50 µm. (B) Quantification of transduced cells, expressed as percentage of Oct4 positive cells *per* total number of cells, shows no statistically significant difference between 3 cell types (one-way ANOVA with Bonferroni's multiple comparison test, NS $p>0.05$); mean ± SD, n=4. (C) Protein lysates were subjected to western blot analysis and exogenous expression of Oct4 occurs only in the presence (+) of DOX. Canx antibody was used as loading control.

Transduced cells were subjected to same culture conditions as described on Chapter 3 (schematic protocol in Figure 4.5A). The morphological alterations observed for WT cells also took place when reprogramming *Chm*^{null} and *Chm*^{flox} cells (Figure 4.5B). Moreover, ES cell-like colonies emerged around 7 dpt in the presence of DOX, in both cases and as shown for *Chm*^{null} cells.

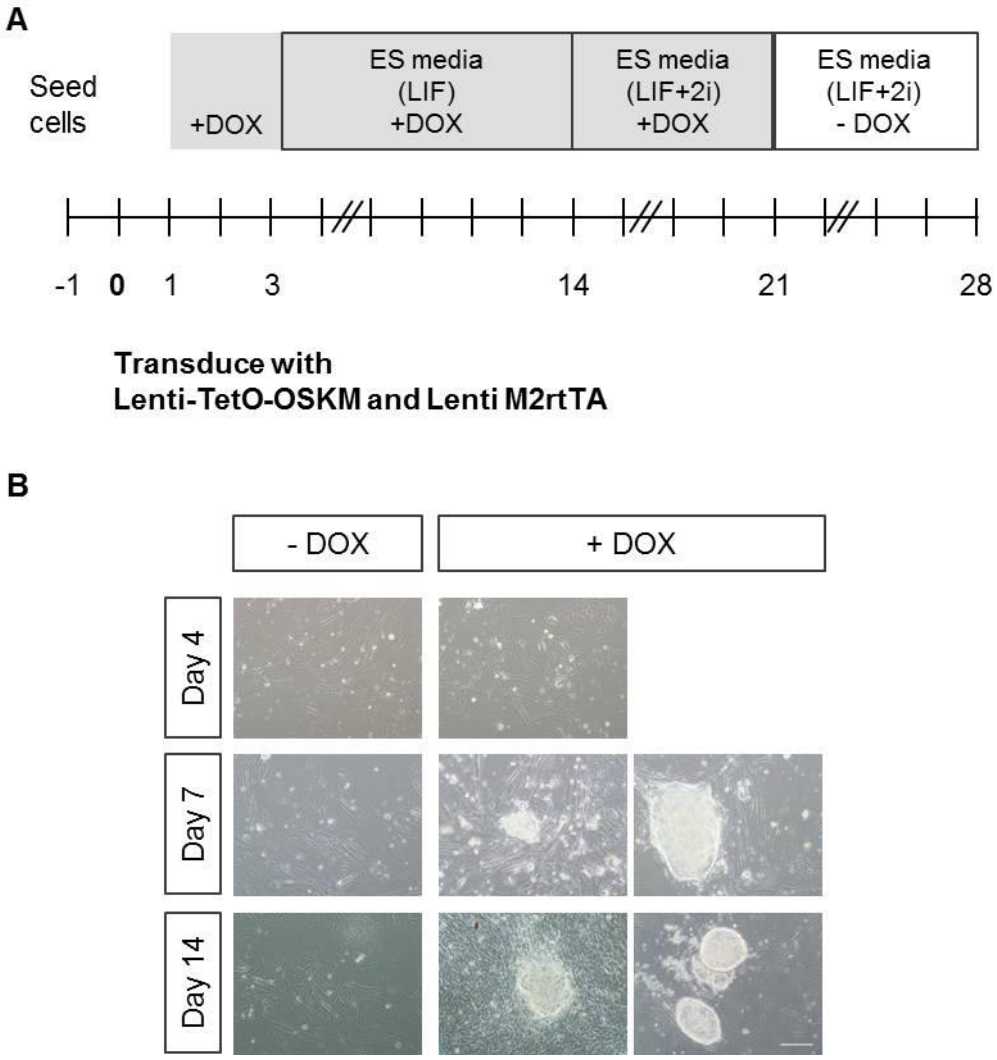

Figure 4.5: *Chm*^{null} MEFs subjected to reprogramming protocol display typical morphological alterations.

(A) Schematic representation of established protocol. (B) Representative brightfield images of transduced *Chm*^{null} MEFs cultured in the presence (+) of DOX showing that approximately 7 dpt typical ES-like colonies start to appear. At day 14, colonies have a more condensed and well-defined structure in culture. In the absence (-) of DOX, transduced cells maintain a fibroblast-like morphology. Scale bar 50 µm.

Several independent experiments were performed, given rise to numerous colonies from *Chm*^{null} and *Chm*^{flox} cells that were manually "picked" and subcultured at 28 dpt (at least 24 colonies of each cell type *per* experiment). As stated before for WT cells, not all colonies generated an expandable cell line. Nevertheless, several iPS cell lines were established from each cell type and further characterized.

Chm iPS cell lines display morphology, self-renewal and pluripotency attributes

Morphological, molecular and functional characterization of iPS cell lines is required in order to confirm self-renewal and pluripotency properties similar to ES cells. Established Chm iPS cell lines were cultured in feeder and feeder-free conditions and submitted to enzymatic passaging every 2-3 days during at least 15-20 subcultures, whilst maintaining typical ES cell-like morphology in both culture conditions. In addition to mentioned self-renewal capability, Chm iPS clones were also positive for AP staining. In Figure 4.6, representative images of ES cell-like morphological appearance and positive AP staining of 3 *Chm*^{null} (j5#2, j6#5, k6#10) and 3 *Chm*^{flox} (j9#3, k8#6, k9#2) iPS cell clones are shown. Identical results were obtained for several clones of each genotype.

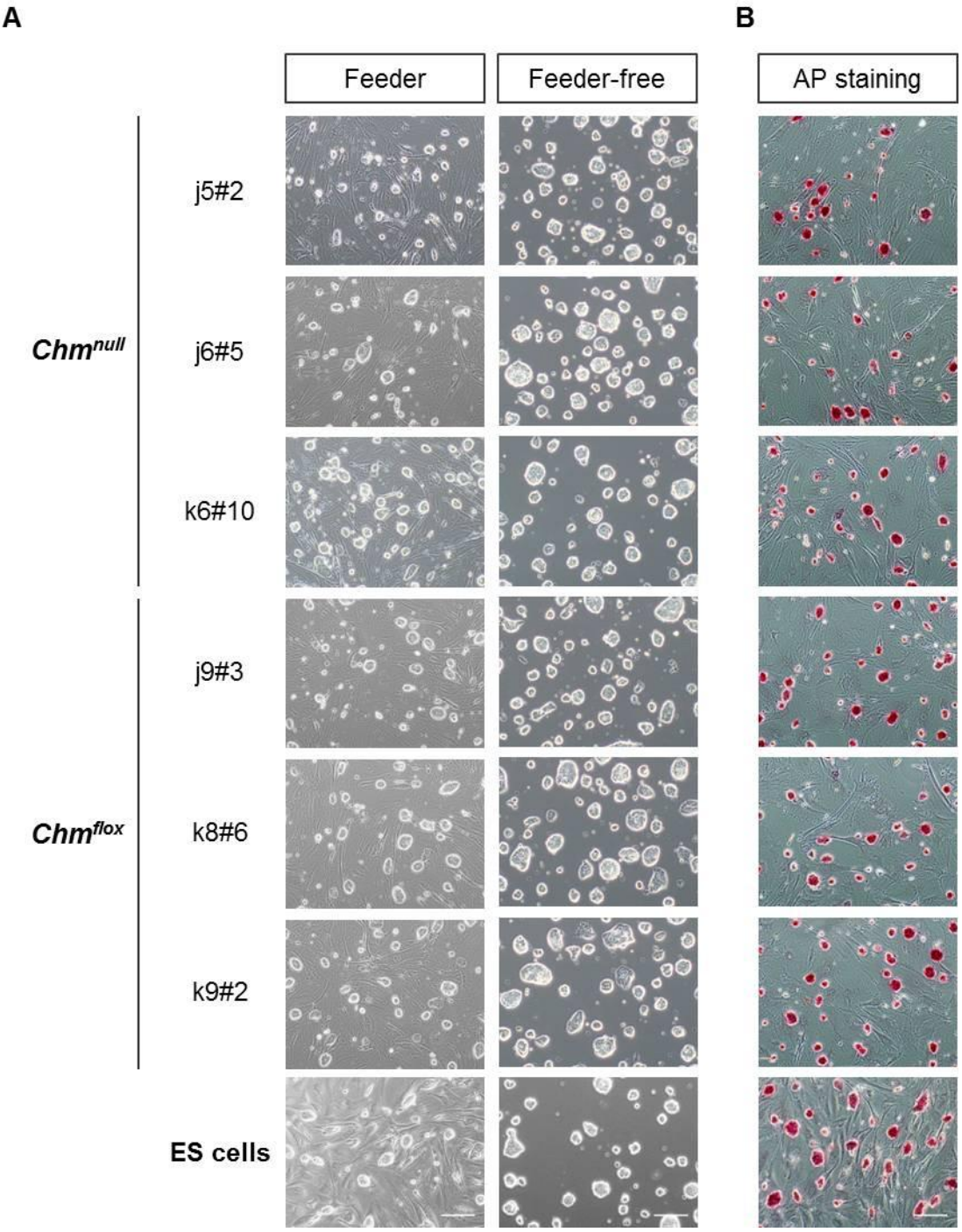

Figure 4.6: *Chm*^{null} and *Chm*^{flox} iPS cell clones demonstrate morphology in culture and AP positive staining similar to ES cells.

(A) Three representative iPS cell lines from each genotype (*Chm*^{null}: j5#2, j6#6, k6#10; *Chm*^{flox}: j9#3, k8#6, k9#2) show a typical ES cell-like morphology when cultured in feeder and feeder-free conditions. (B) All iPS cell clones and ES cells stain positively for AP. Scale bar 50 µm.

At a molecular level, iPS clones were characterized by conventional RT-PCR to determine expression of key pluripotency markers (Figure 4.7). No expression of viral transcript *P2A-Sox2* was observed for several *Chm*^{null} and *Chm*^{flox} clones, which demonstrates their transgene independence. Most of *Chm*^{null} and *Chm*^{flox} clones endogenously express all pluripotency genes tested (for *Oct4*, primers that specifically amplify endogenous transcripts and not viral ones were used).

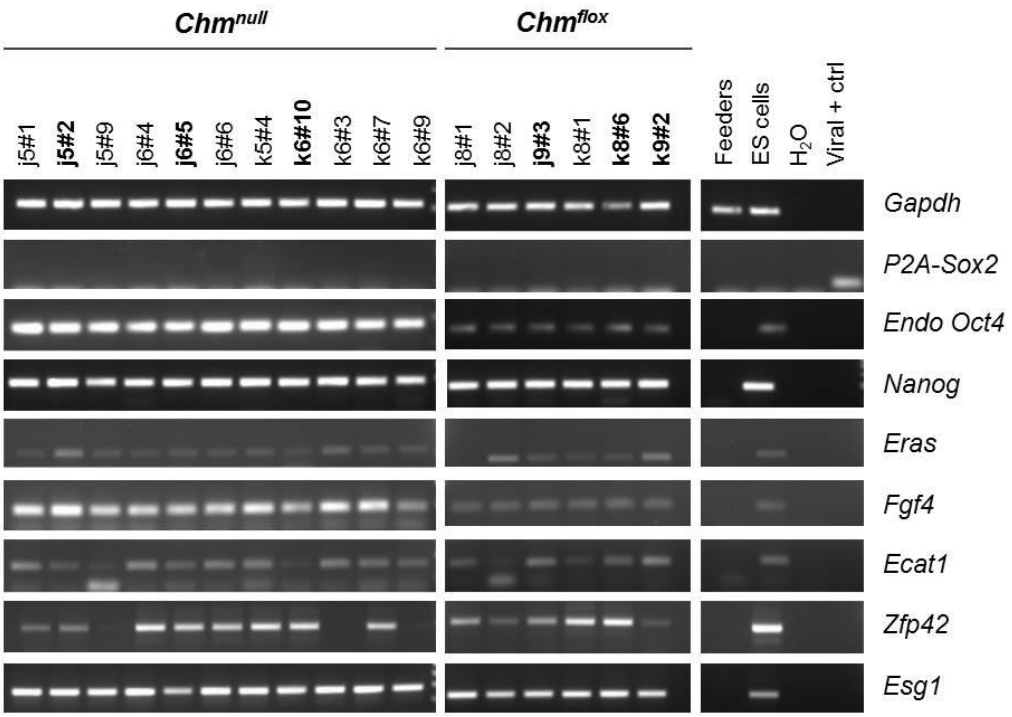

Figure 4.7: iPS cell lines express endogenous pluripotency markers.

Total RNA content of 11 different *Chm*^{null} and 6 *Chm*^{flox} iPS cell clones was isolated. cDNA was produced and analysed by RT-PCR, using the indicated pairs of primers. iPS cell lines express pluripotency genes, in a transgene independent manner, since no expression of viral transcript *P2A-Sox2* is detected. ES cells are shown as a positive control, feeders as a negative control, and *Gapdh* as endogenous control.

Further characterization was undertaken for 3 *Chm*^{null} (j5#2, j6#5, k6#10) and 3 *Chm*^{flox} (j9#3, k8#6, k9#2) iPS cell clones. Expression of pluripotency markers, such as Oct4, Nanog and SSEA-1, was confirmed at a protein level by IF and all clones displayed positive staining as representatively illustrated (Figure 4.8).

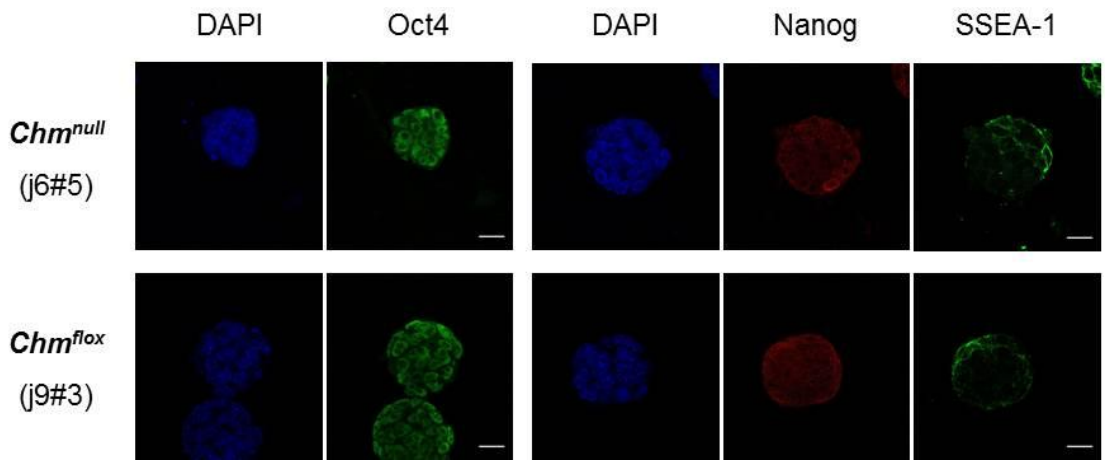

Figure 4.8: iPS cell lines express ES cell characteristic TFs and surface markers.

Chm^{null} and *Chm*^{flox} iPS cells were subjected to immunostaining using Oct4, Nanog and SSEA-1 antibodies and DAPI for nuclei counterstaining. Confocal images for two representative iPS clones are shown. Scale bar 20 µm.

Moreover, functional pluripotency was assessed by *in vitro* differentiation assay, and all mentioned clones have demonstrated the ability to differentiate into cells from the 3 germ layers (Figure 4.9). After 7 or 14 days of differentiation of EB, ectodermal (Pax6), mesodermal (*Col1a1* or SMA) and endodermal (*Gata6* or AFP) markers were expressed as evaluated by RT-PCR and IF.

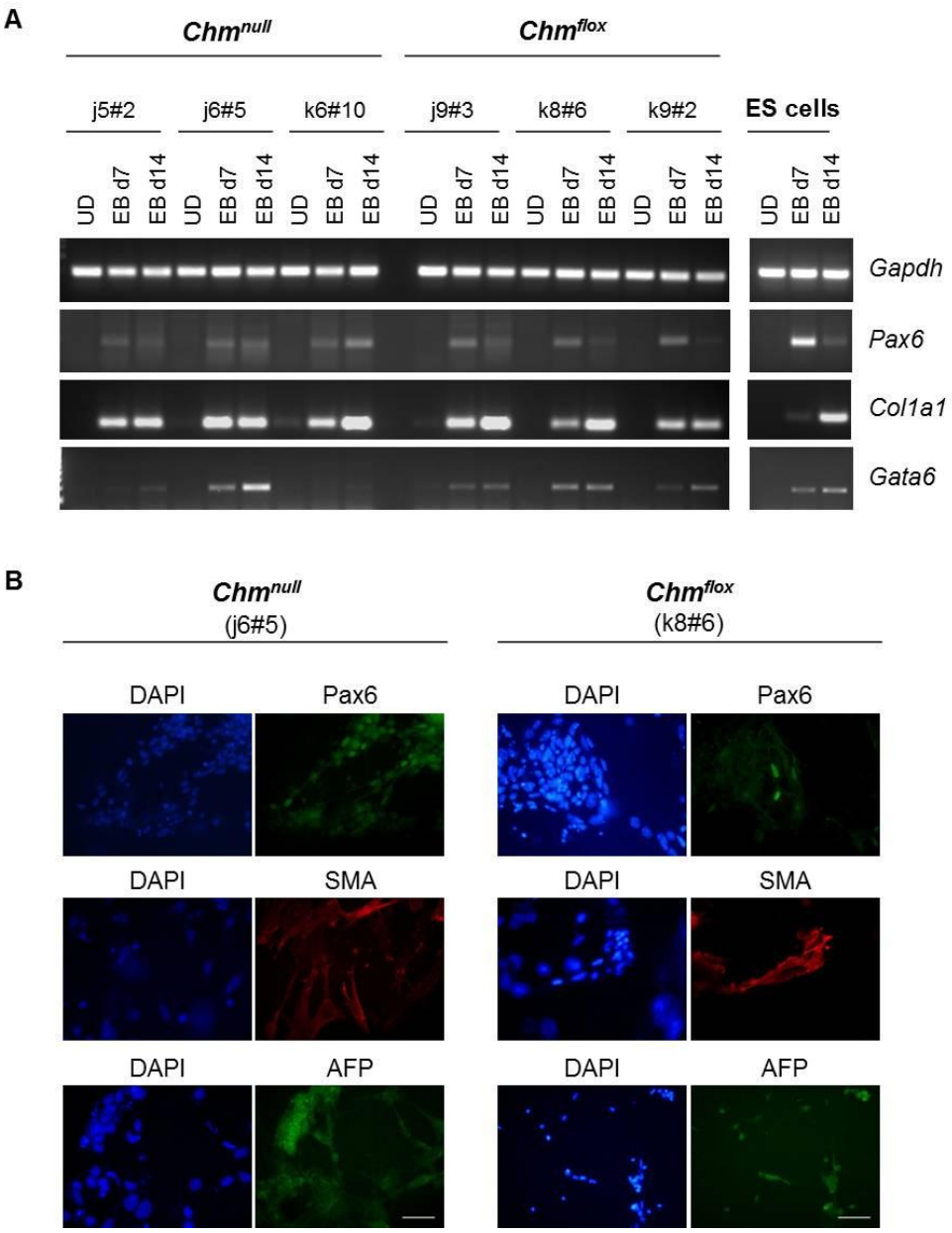

Figure 4.9: *Chm*^{null} and *Chm*^{flox} iPS cell clones demonstrate their functional pluripotency in *in vitro* differentiation assay.

(A) RT-PCR analysis of iPS cell clones in undifferentiated (UD) state or after 7 or 14 days of EB differentiation. Three clones from each genotype are shown as a representative result. Primers designed to specifically amplify transcripts from ectodermal (*Pax6*), mesodermal (*Col1a1*) and endodermal (*Gata6*) lineages were used. ES cells were used as positive control (B) Representative images of immunostaining of j5#2 and k8#6 iPS cell clones after 14 days of EB differentiation assay. Protein expression of markers for the 3 lineages (ectoderm, mesoderm and endoderm) is observed, when the mentioned antibodies (Pax6, SMA and AFP, respectively) are used. Scale bar 25 µm.

In a more stringent and definitive way, pluripotency was confirmed by an *in vivo* differentiation assay. Three *Chm*^{null} (j5#2, j6#5, k6#10) and 3 *Chm*^{flox} (j9#3, k8#6, k9#2) iPS cell lines were subcutaneously injected in immunodeficient NOD.Scid mice. In all cases tumours arose and were collected at appropriate timepoints, followed by histopathological characterization to confirm that the tumours were teratomas (Figure 4.10).

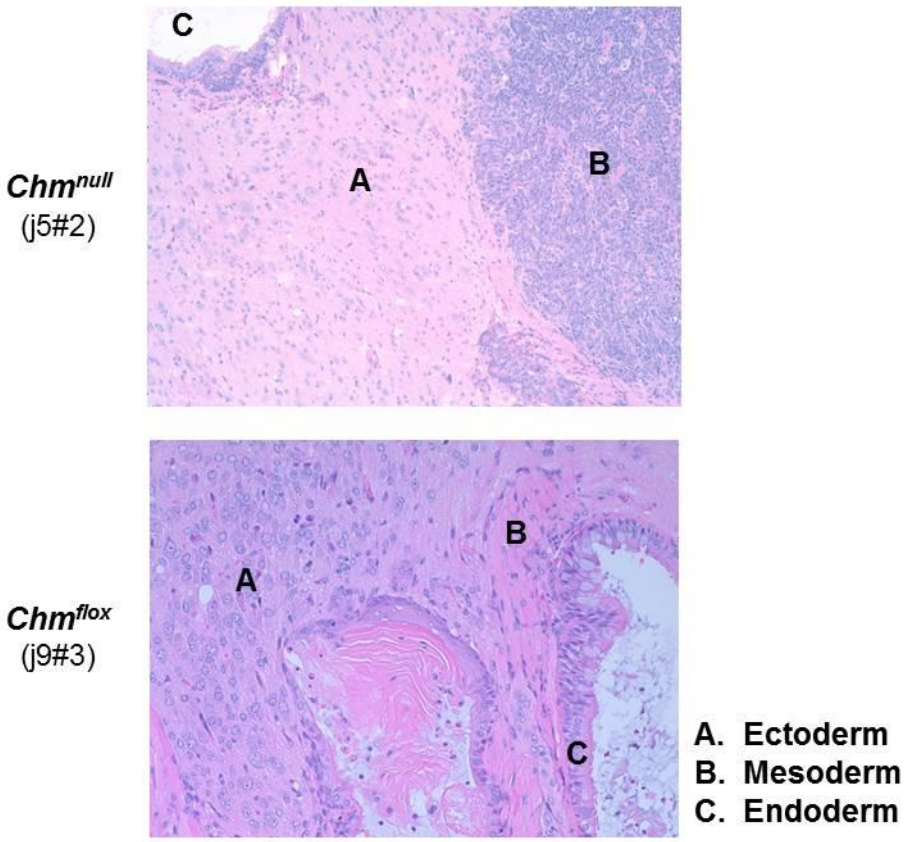

Figure 4.10: *Chm*^{null} and *Chm*^{flox} iPS cell clones demonstrate their functional pluripotency in *in vivo* differentiation assay.

Chm iPS cell lines were subcutaneously injected into NOD.Scid mice. Resultant teratomas were collected after 5 to 7 weeks and subjected to histological analysis after hematoxylin-eosin staining. In each teratoma, characteristic tissues from ectoderm (A), mesoderm (B) and endoderm (C) lineage are observed, as illustrated on representative images for one *Chm*^{null} and one *Chm*^{flox} iPS clone.

Chm iPS cell lines generated from *Chm*^{null} fibroblasts display efficient Rep1 KO

Besides demonstrating that generated iPS cell clones display features similar to ES cells, characterization in terms of *Chm/Rep1* gene is essential in order to establish these clones as suitable Chm models.

Clones of both types were subjected to PCR genotyping using primers to confirm identity of *Chm* alleles and presence/absence of *MerCreMer* transgene (Figure 4.11A). As expected, iPS cells demonstrated the same genotype as the initial somatic cells: j5#2, j6#5 and k6#10 iPS cells are Chm^{null}, and j9#3, k8#6 and k9#2 iPS cells are Chm^{flox}. All clones are positive for the *MerCreMer* transgene.

Interestingly, all clones isolated from Chm^{null} MEFs submitted to reprogramming also maintained the same genotype as the initial cells. As mentioned before, TM treatment of Chm^{flox} cells does not allow a totally efficient recombination event, as some residual Chm^{flox} allele was occasionally detected, probably meaning that a small population of Chm^{flox} cells is maintained (recall Figure 4.2). Nevertheless, all clonaly isolated iPS colonies from Chm^{null} MEFs have proven to be Chm^{null} after PCR genotype.

In terms of *Chm/Rep1* expression RT-qPCR analysis demonstrated that Chm^{null} iPS cells have reduced *Rep1* expression when compared to Chm^{flox} clones (Figure 4.11B). Furthermore, Rep1 KO was also confirmed at a protein level using an antibody that detects both Rep1 and Rep2 proteins. Concordant with the fact that only *Chm/Rep1* gene was modified and targeted for deletion in the Chm mouse model, Rep2 protein expression was detected on both Chm^{flox} and Chm^{null} iPS cell lines. However, Rep1 protein expression was not detected on Chm^{null} cells, thus confirming the applicability of such cells as a model for Chm/Rep1 KO (Figure 4.11C).

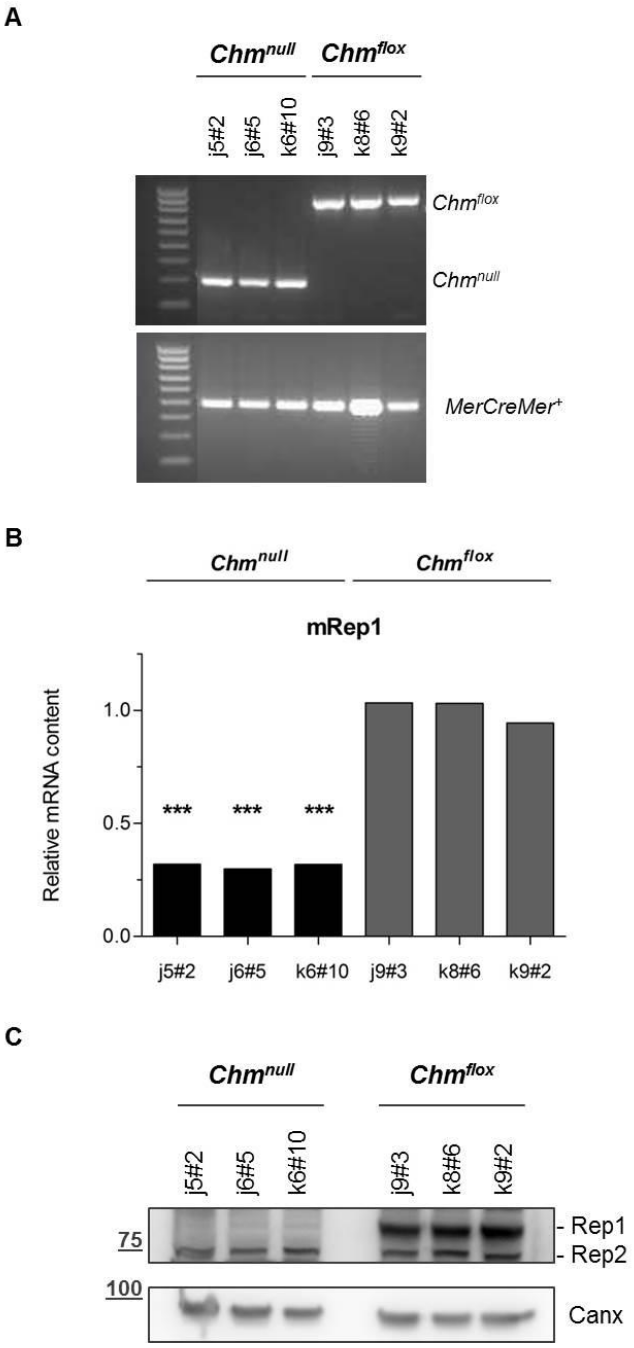

Figure 4.11: Generated *Chm^{null}* iPS cell lines display an efficient KO of *Rep1* gene.

(A) gDNA of *Chm^{null}* (j5#2, j6#5, k6#10) and *Chm^{flox}* (j9#3, k8#6, k9#2) iPS cell clones was isolated and analysed by PCR to confirm the genotype. Primers to distinguish *Chm^{null}* (330 bp) and *Chm^{flox}* (860 bp) alleles (top panel) or to confirm the presence of *MerCreMer* transgene (510 bp) (bottom panel) were used. (B) Total RNA content of same clones was analysed by RT-qPCR to determine *Rep1* levels. *Chm^{null}* iPS cell lines display a reduction of approximately 70% of *Rep1* expression when compared to *Chm^{flox}* iPS cell clones. *Gapdh* was used as endogenous control; mean ± SD, n=3. Statistically significant values relative to control are indicated (one-way ANOVA with Dunnett's multiple comparison test); *** $p<0.001$. (C) Protein lysates from the same clones were subjected to western blot analysis using pan-REP (J906) antibody, which recognizes both Rep1 and Rep2 proteins. Rep1 protein is not detected on *Chm^{null}* iPS cells lysates, contrarily to *Chm^{flox}* iPS cell lines. Rep2 protein is detected on both cell lines. Canx antibody was used as loading control.

REP1 protein, and its ortholog REP2, are responsible for the prenylation of Rab proteins, a post-translational modification essential for their function as key regulators of intracellular trafficking. Mutations in human *CHM/REP1* gene are responsible for X-linked disorder CHM, characterized by progressive degeneration of choroid, RPE and photoreceptor cells. It is assumed that CHM phenotype is restricted to the eye due to the presence of REP2 protein which compensates for the absence of functional REP1 protein in all organs and tissues, except the eye (Seabra, 1996). Nevertheless, CHM pathogenesis remains quite unclear at the molecular level. In *Saccharomyces cerevisiae*, the REP1 homologue, MRS6, is essential for cell growth (Alory and Balch, 2000; Waldherr et al., 1993). Moreover, in a mutagenic screen in zebrafish, REP1 was shown to be essential for survival and development of hair cells in the inner ear and some cell types from the retina (Starr et al., 2004).

Therefore, after establishing *Chm*^{null} and *Chm*^{flox} iPS cell lines, it was pertinent to investigate the potential effect of *Rep1* absence in survival and growth rates of pluripotent cells. For that purpose, an MTT assay was performed. Several plating densities of 3 iPS cells lines (j6#5, k6#10 and j9#3) and ES cells were tested, and MTT assay was performed 24 hours later. At this timepoint, cells are expected to have adhered and recovered from splitting, whereas not yet actively dividing. In the range tested, despite some variability between cell lines, absorbance measures were shown to have a linear relationship with the number of cells, confirming their applicability to infer cell number/viability (Figure 4.12A). Moreover, optimal initial seeding density was also determined to be $1x10^4$ cells.

Subsequently, all 9 extensively characterized iPS cell clones (3 of each genotype, including WT) and ES cells were plated and MTT assay was performed at 24, 48, 72 and 96 h (Figure 4.12B). As expected, absorbance measures increased overtime in a logarithmic way up to 72 hours after plating, for all tested cells. Afterwards, cells reached a plateau due to increased cell density, as confirmed by microscopic observation. Typically, these cell lines are enzymatically splitted every 2-3 days, so consistently, 96 hours after plating, cells were over-confluent and probably cell death was already occurring.

Interestingly, there was no indication supporting the hypothesis that *Rep1* absence could affect cell survival. All cell lines displayed different growth rates but there was no evident reduced value for *Chm*^{null} iPS cell lines when comparing them to *Chm*^{flox} or *WT* ones. It is possible that Rep2 protein, expressed by both cell types, compensates for the lack of functional Rep1, consistently with the restricted phenotype observed in CHM patients.

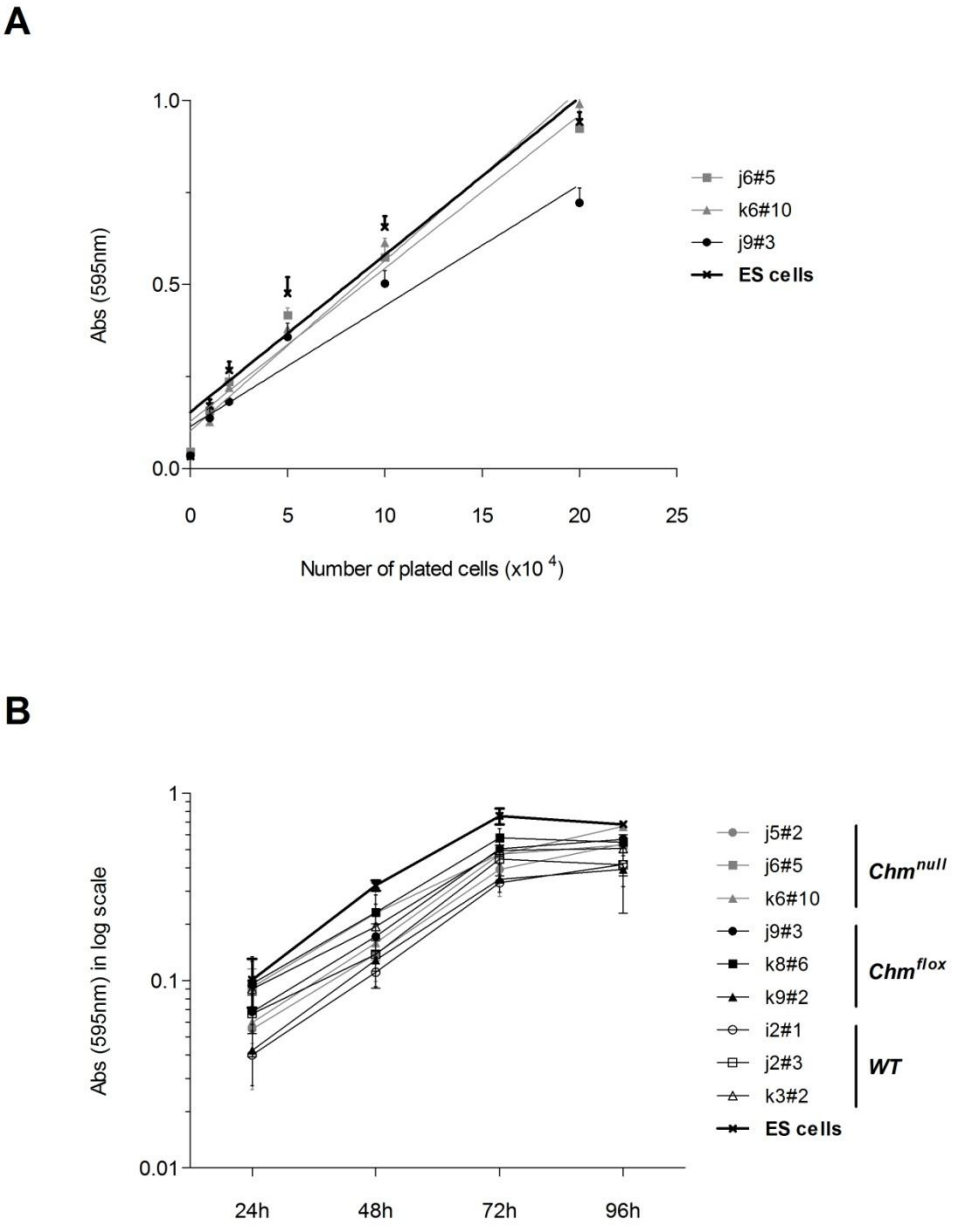

Figure 4.12: All iPS cells have equivalent growth rates, as assessed by MTT assay.

(A) Increasing number of cells (0, 1, 2, 5, 10 and 20x10^4) were plated and subjected to MTT assay after 24 h. ES cells and 3 different iPS clones were tested; n=3. Lines represent linear regressions for the 4 different cells. (B) MTT assay was conducted 24, 48, 72 and 96 hours after plating 1x10^4 cells, in order to obtain growth curves for 9 mentioned iPS clones (3 clones from each genotype) and ES cells. Absorbance represented in Y-axes is in log scale. Mean ± SD, n=3.

Chm iPS cell lines fail to differentiate into a polarized neuroepithelium when subjected to a protocol adapted from Zhu *et al.*

Prior to use in disease modelling or cell therapy, stem cells must be differentiated into functional adult cells. Several protocols have been described for differentiation of ES or iPS cells into RPE, most of them sharing the common feature of first promoting conversion of stem cells into a neuroectodermal-like cell and then differentiation into RPE cells. Mimicry of the patterning and developmental events that occur during embryogenesis is achieved by changing the media composition in terms of small molecules and growth factors. In the mentioned protocols, factors involved in *in vivo* retinal development were used to establish a defined culture method that induces *in vitro* differentiation of stem cells into retinal progenitors and subsequently in retinal cells (Bharti et al., 2011). Moreover, most protocols rely in a non-adherent cell culture system in at least one of the differentiation steps.

Given the panoply of published protocols with variable efficiencies, three different approaches were chosen and undertaken in an attempt to obtain RPE cells by differentiation of obtained Chm iPS cells (as well as WT).

Recently, Zhu and colleagues established a three-dimensional (3D) epithelial cyst culture of human ES cells to promote the induction of a polarized neuroepithelium that could be converted into human RPE cells in a quantitative way (Zhu et al., 2013). The obtained cells could be transplanted into RCS rats without any selection or further expansion.

Chm^{null} (k6#10), *Chm*^{flox} (j9#3) and WT (k3#2) iPS cell lines, as well as ES cells, were submitted to the first step of this protocol, a 3D culture system using basement membrane matrix components (Matrigel) (Figure 4.13A) and their morphology was observed over the first 5 days (Figure 4.13B). Unlike what was described for human ES cells, floating aggregates were observed with different shapes and sizes, but no pseudoestratified neuroepithelial structures (“cysts”) with a single lumen were perceived.

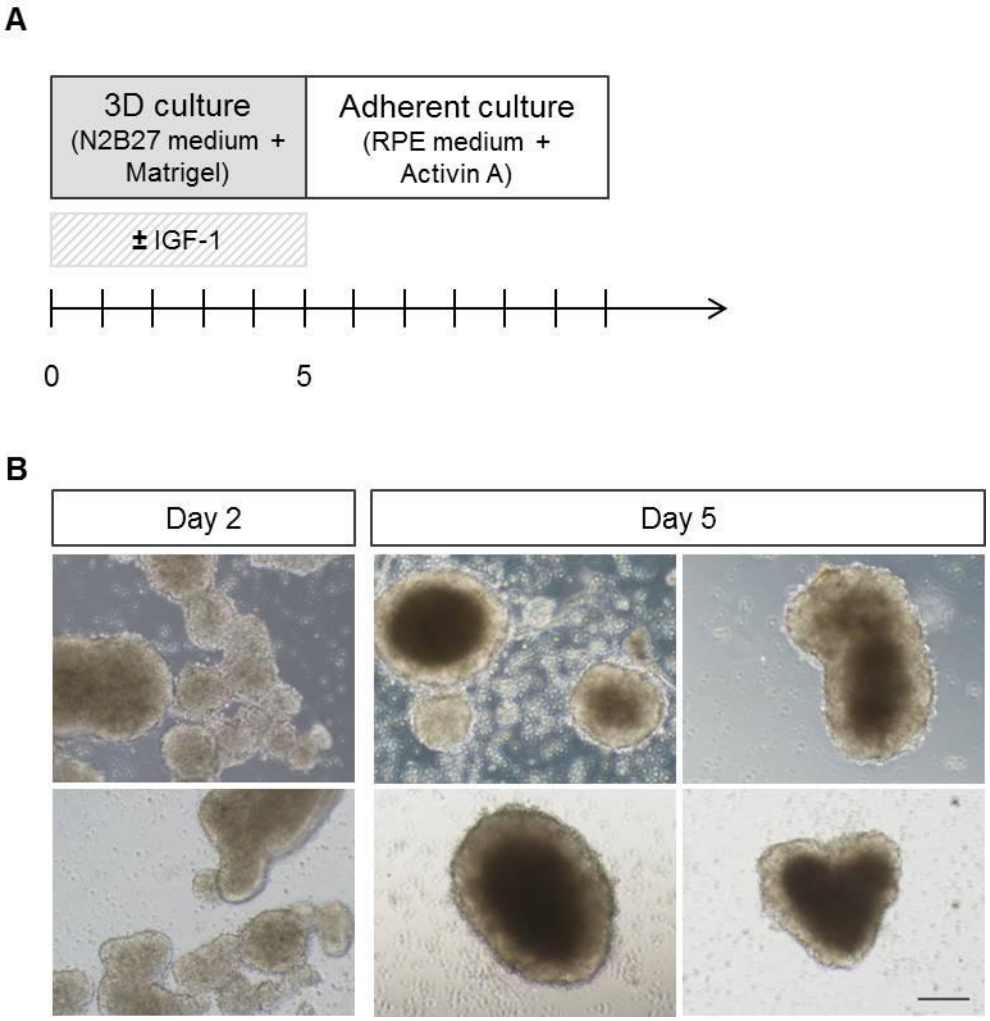

Figure 4.13: iPS cell lines submitted to differentiation protocol adapted from Zhu *et al.* display morphological alterations.

(A) Schematic representation of the protocol composed of 2 subsequent steps. At first, a Matrigel-based 3D culture system is used in conjunction with neuroinduction media N2B27. In some cases IGF-1 recombinant protein was also added (10 ng/mL). After 5 days, cells would be submitted to an adherent culture and RPE specific medium containing Activin A. (B) Representative brightfield images of iPS cells on day 2 and day 5, without IGF-1. iPS cell clusters observed have variable sizes and shapes. No remarkable difference on morphologic alterations was identified in the presence of IGF-1. Scale bar 50 µm.

Total RNA samples were collected at day 5, cDNA was synthetized and conventional RT-PCR analysis was undertaken in order to characterize the occurring differentiation process. Consistent with a differentiation process, expression of pluripotency markers (*Oct4*, *Nanog* and *Fgf4*) at day 5 of the protocol was reduced when compared to undifferentiated (UD) status of pluripotent cells (Figure 4.14). Expression of Eye Field TFs (EFTFs; namely *Pax6*, *Rax*, *Six3* and *Six6*) was also evaluated but, contrarily to what was described by Zhu and co-workers for human cells, no up-regulation was observed.

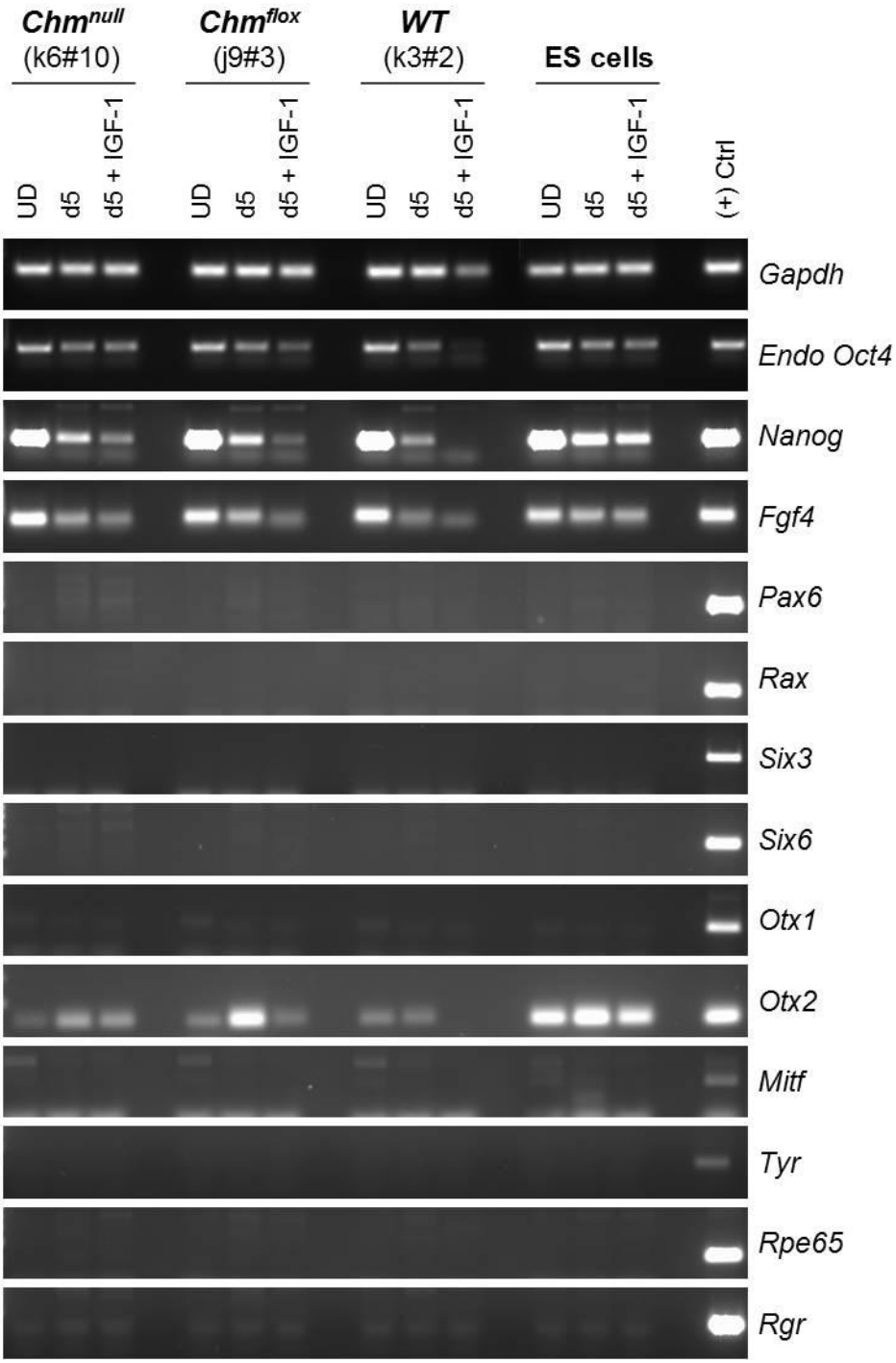

Figure 4.14: iPS cell lines submitted to differentiation protocol adapted from Zhu *et al.* have diminished levels of pluripotency markers expression but no detectable levels of EFTFs (except *Otx2*) and RPE markers at day 5.

RT-PCR analysis of mentioned iPS cell lines and ES cells is shown for the denoted genes. For each cell, samples collected after 5 days of differentiation protocol in the absence (d5) or presence (d5+IGF-1) of IGF-1 10 ng/mL are compared with undifferentiated (UD) samples. Pluripotency markers (*Endo Oct4*, *Nanog* and *Fgf4*) have reduced expression. No substantial expression of EFTFs (namely *Pax6*, *Rax*, *Six3* and *Six6*) is detected, even when IGF-1 protein is added. *Gapdh* is used as endogenous control.

Given that it was also described that IGF-1/insulin signalling was responsible for a significant role in head and eye formation and for directing human iPS cells to a retinal progenitor identity (Lamba et al., 2006; Pera et al., 2001), differentiation protocol was also tested in the presence of IGF-1 recombinant protein. Morphologically, floating aggregates were indistinguishable of the ones obtained without IGF-1. Samples collected at day 5 (d5+IGF-1) were also evaluated but once again no expression of EFTFs was observed (Figure 4.14).

Expression of TFs involved in RPE specification (*Otx1*, *Otx2* and *Mitf*) or mature RPE (*Tyr*, *Rpe65* and *Rgr*) genes was also assessed and, as expected for an initial step in the protocol, no transcripts were detected either in UD status or after differentiation, except for *Otx2*. *Otx2* transcripts were detected in UD samples and after differentiation, in some cases with increased levels. Several studies have indicated the crucial role played by Otx2 in the development of anterior neuroectoderm. Also, in the eye Otx2 plays relevant roles in early EF and subsequent RPE specification (Beby and Lamonerie, 2013). Despite some increased transcriptional levels of *Otx2* upon differentiation, expression of EFTFs was not observed and a retinal identity could not be attributed to the floating aggregates formed with this protocol. Therefore, subsequent steps of the described protocol (such as RPE specification) were not pursued.

Chm iPS cell lines give rise to OV-like protusions when subjected to a differentiation protocol adapted from Eiraku *et al.* and Gonzalez-Cordero *et al.*

Concomitantly, another differentiation protocol was attempted based on the work of Eiraku and colleagues and of Gonzalez-Cordero and co-workers (Eiraku and Sasai, 2012; Eiraku et al., 2011; Gonzalez-Cordero et al., 2013).

A 3D cell culture system has been shown to promote the self-formation of optic-cup structures, when ES cells floating aggregates are cultured under low growth factor conditions (serum-free floating cultures of EB-like aggregates with quick reaggregation or SFEBq) and supplemented with Matrigel. The details of the adapted protocol we used are depicted at Figure 4.15A.

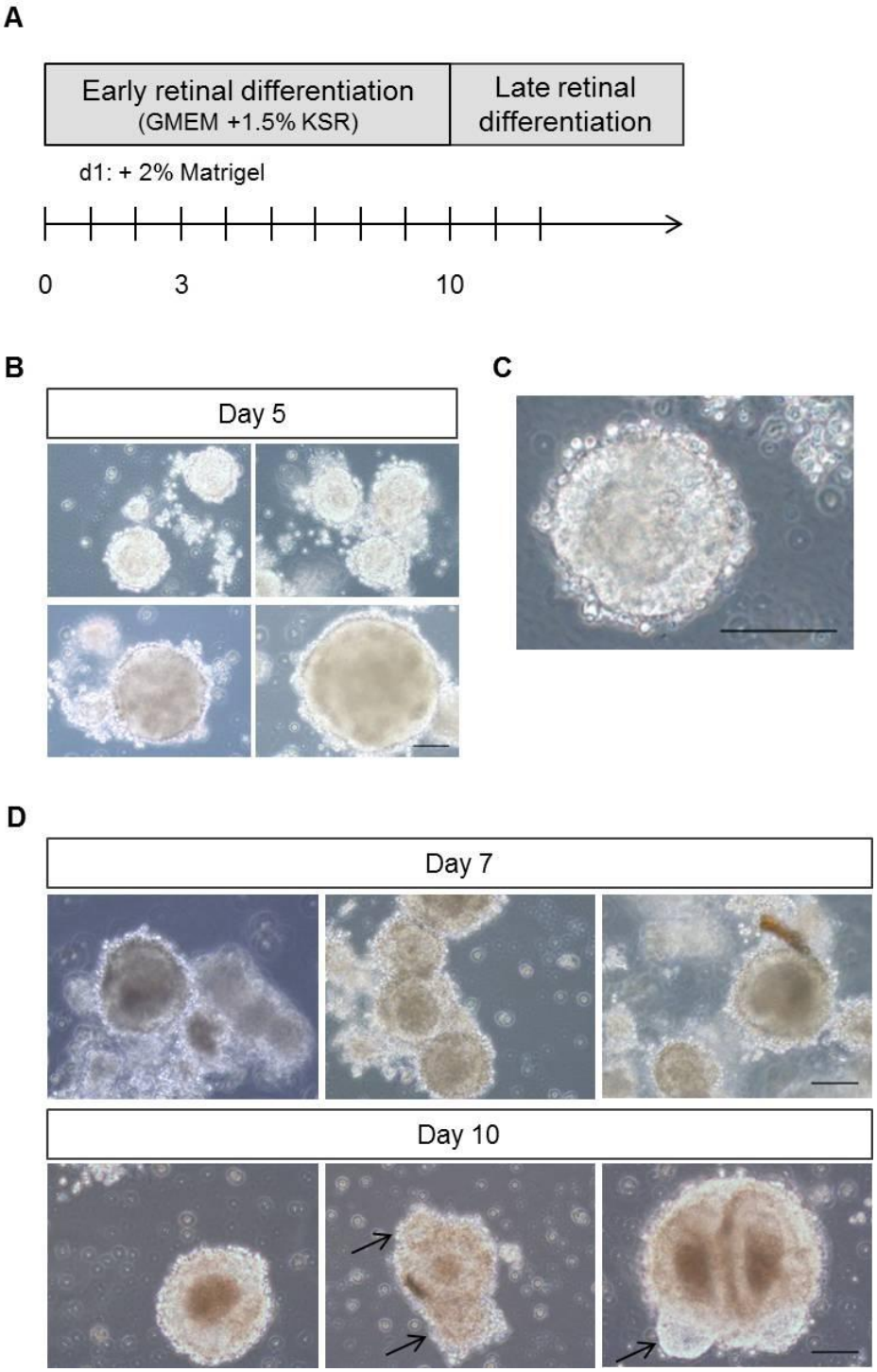

Figure 4.15: iPS cell lines submitted to differentiation protocol adapted from Eiraku *et al.* and Gonzalez-Cordero *et al.* display morphological alterations.

(A) Schematic representation of the protocol composed of 2 subsequent steps. First, cells are cultured in low-adherent and serum-free conditions. Matrigel to final 2% (v/v) is added on day 1. After 10 days, aggregates would be transferred for another low-adherent culture system with culture media to promote late retinal differentiation. (B and C) Representative brightfield images of iPS cells on day 5. Frequently, observed iPS cell aggregates display a continuous neuroepithelium-like around the whole circumference. (C) Higher magnification of iPS cell aggregates on day 5. (D) Representative brightfield images of iPS cells on day 7 and 10. Interestingly, on day 10 some protusions from the aggregates are observed and denoted with the black arrow. Scale bar 25 µm.

Chm^{null} (k6#10) and *Chm*^{flox} (j9#3) iPS cell lines, as well as ES cells, were submitted to the Early Retinal Differentiation step in SFEBq+Matrigel conditions, and morphological alterations were monitored. RNA samples were collected at day 3 and 10 for later analysis. As described by the authors, continuous neuroepithelium-like structures were detected as early as day 5 of differentiation (Figure 4.15B and C). However, it was stated that OV-like structures containing thickened regions of the neuroepithelium that protruded from the iPS/ES cell aggregate were visible around day 7, followed by invagination of these same structures to form OC-like ones around day 9 (Gonzalez-Cordero et al., 2013). OV-like aggregates were only detected latter (day 10) and never with the 50% abundance mentioned by Gonzalez-Cordero and colleagues (Figure 4.15D). Moreover, OC-like structures were not detected. Unfortunately, this differentiation protocol did not follow for longer period due to cell death.

Regarding transcriptional modifications during differentiation protocol, as for the previous protocol, a set of genes was analysed (Figure 4.16).

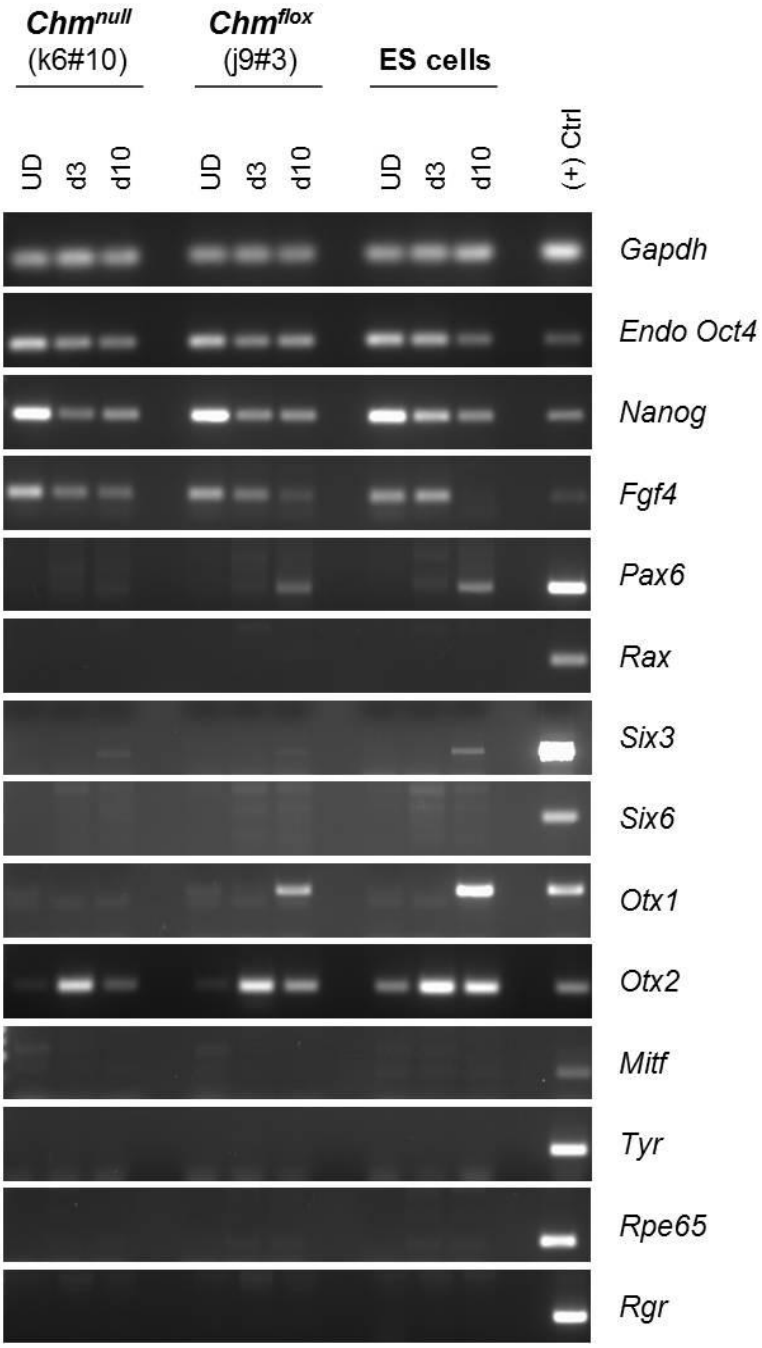

Figure 4.16: iPS cell lines submitted to differentiation protocol adapted from Eiraku *et al.* and Gonzalez-Cordero *et al.* have diminished levels of expression of pluripotency markers and increased expression of EFTFs.

RT-PCR analysis of mentioned iPS cell lines and ES cells is shown for the denoted genes. For each cell, samples collected after 3 or 10 days of differentiation protocol (d3, d10) are compared with undifferentiated (UD) samples. Pluripotency markers (*Endo Oct4*, *Nanog* and *Fgf4*) show reduced expression. *Pax6*, *Six3*, *Otx2* and *Otx1* genes have increased levels of expression. No expression of RPE-specific markers is detected. *Gapdh* is used as endogenous control.

The expression of pluripotency genes gradually diminished during the protocol for all tested cells, as expected for a differentiation process. It was also observed that the expression of EFTFs, like *Pax6* and *Six3*, was up-regulated after 10 days of differentiation, in accordance with the observed OV-like structures. Regarding *Rax* and *Six6* no expression was observed. As already mentioned Otx2 plays a key role in neuroectodermal specification. Furthermore Otx1 cooperates with Otx2, being both expressed simultaneously in the forming OV (Martinez-Morales et al., 2001). Consistently, *Otx2* transcripts increased upon differentiation and *Otx1* was detected at day 10 in at least 2 cells. Expression of RPE specific genes (namely *Mitf*, *Tyr*, *Rpe65* and *Rgr*) was not detected in either cell line, at day 3 or 10 of differentiation.

Importantly, one should stress the fact that this protocol was not performed in low-adherent 96 well-plates but using petri dishes, which can account for heterogeneity in formed aggregates and lack of reproducibility of the process.

Chm iPS cell lines differentiate into retinal progenitor cells when subjected to a protocol from La Torre *et al.* and Osakada *et al.*

Concurrently, taking into consideration growth factors and signalling molecules described as key regulators of the retina's developmental process, a third approach was tackled. Explicitly, it has been described that inhibition of BMP and Wnt pathways are important for anterior neural plate patterning (del Barco Barrantes et al., 2003). Furthermore, IGF-1/insulin signalling plays a significant role in head and eye formation (Pera et al., 2001). Based on work published by La Torre and others, as well as Osakada and colleagues, a protocol with a EB-based step, followed by a RPE specification phase, was implemented (Osakada et al., 2009; Torre et al., 2012).

Initially, iPS cells [Chm^{null} (k6#10), Chm^{flox} (j9#3) and WT (k3#2)] and ES cells were cultured in low-attachment petri dishes in Retinal Induction Media, composed of N2B27 media supplemented with Noggin (BMP antagonist), Dkk1 (Wnt inhibitor) and IGF-1 recombinant proteins (Figure 4.17A). All cells formed EB-like structures at day 1, as described. Cells were kept at these conditions for at least 10 days or, alternatively, floating aggregates were plated in Matrigel-coated cell culture dishes after 3 days (P protocol).

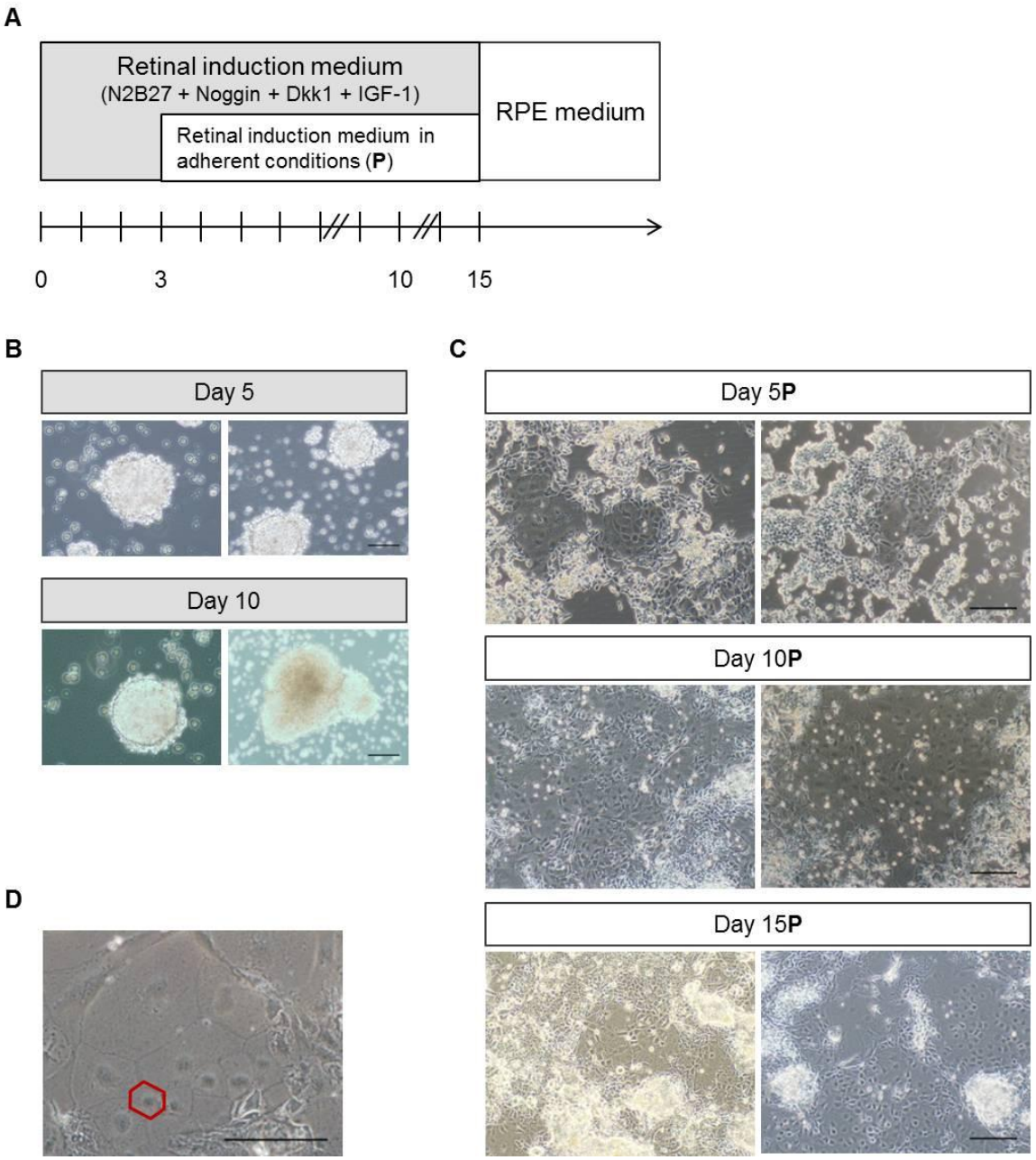

Figure 4.17: iPS cell lines submitted to differentiation protocol adapted from La Torre *et al.* and Osakada *et al.* display morphological alterations.

(A) Schematic representation of the protocol composed of 2 or 3 subsequent steps. First, cells were cultured in low adherent conditions in Retinal induction media (N2B27 supplemented with Noggin, Dkk1 and IGF-1, all 10 ng/mL). Conditions were kept until day 15 or, alternatively, cells were plated (**P**) in Matrigel-coated plates at day 3. A third step to promote RPE specification may occur later on time. (B) Representative brightfield images of iPS cells under floating conditions on day 5 and day 10. EB-like structures are observed. (C) Representative brightfield images of iPS cells on day 5, 10 and 15 after cultured in adherent conditions (**P**). (D) Higher magnification of (C) day 10P displaying epithelial-like organization (red hexagon highlighting the hexagonal cell shape). Scale bar 25 µm.

Regarding morphology, EB-like aggregates kept their characteristics along the differentiation period, with no evident neuroepithelial-like formation as described for previous protocols reported on the previous sections (Figure 4.17B). Conversely, when these structures were plated in Matrigel after 3 days and cultured in Retinal Induction Media, cells acquired a neuroepithelial-like morphology in culture, resembling neural progenitor cells (Figure 4.17C). Cells were actively proliferating and grew into confluency in some areas at day 10 and 15. Moreover, hexagonal-packed epithelial patches of cells were visible at day 10 and 15 (Figure 4.17D).

Gene expression was also analysed for the same set of genes as before (Figure 4.18). Pluripotency genes (*Oct4*, *Nanog* and *Fgf4*) display diminished expression levels after differentiation when comparing with UD status. Interestingly, at day 15P (adherent conditions) expression levels seemed to be augmented relative to day 10P. This fact may be due to proliferation of neural progenitor cells, since it has been described that they might also express these pluripotency markers (Lee et al., 2010). Moreover, for Nanog and Fgf4, a role for proliferation of neural progenitor cells has recently been proposed (Garg et al., 2013; Kosaka et al., 2006).

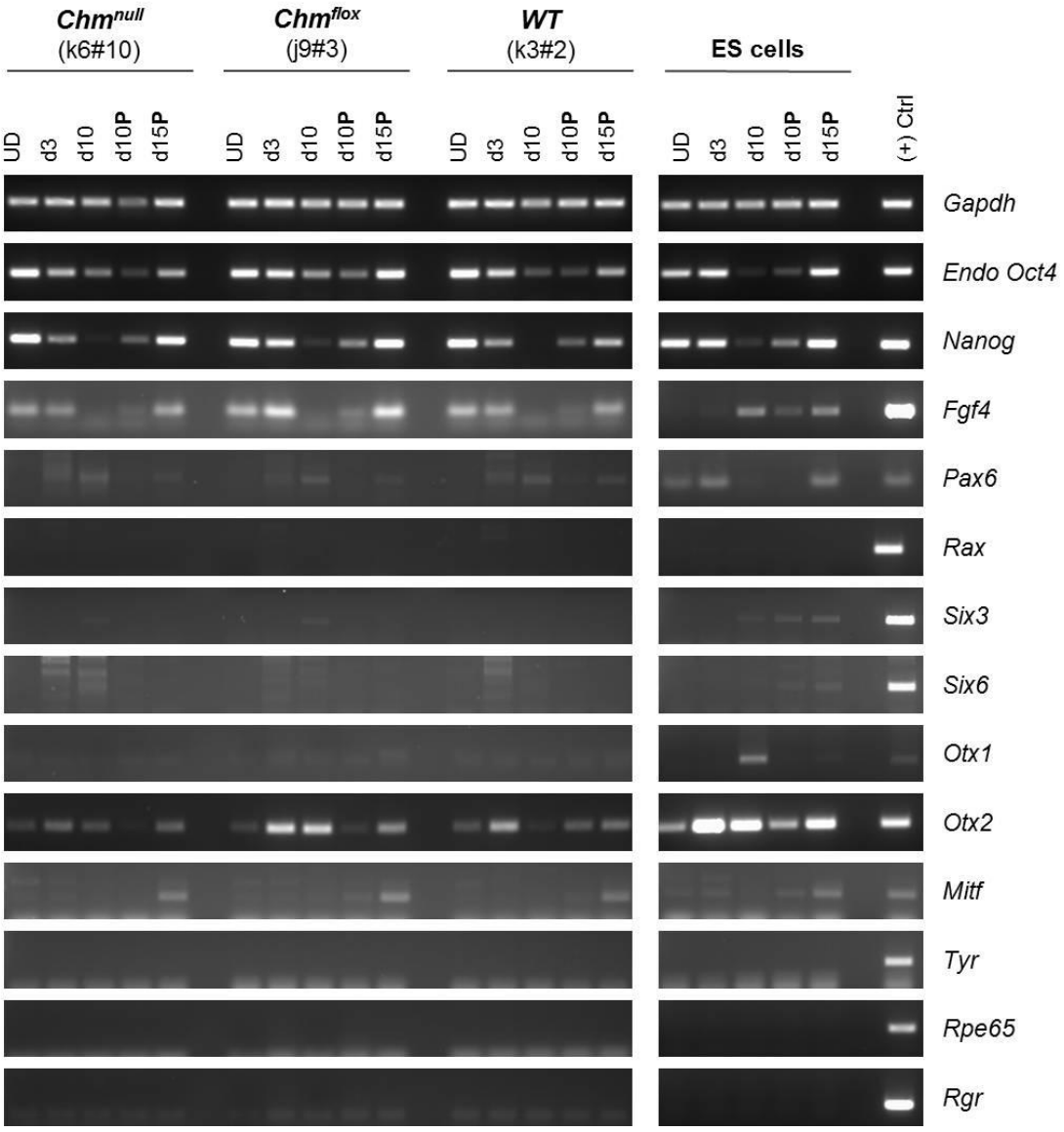

Figure 4.18: iPS cell lines submitted to differentiation protocol adapted from La Torre *et al.* and Osakada *et al.* have diminished levels of pluripotency markers expression and increased expression of EFTFs.

RT-PCR analysis of mentioned iPS cell lines and ES cells is shown for the denoted genes. For each cell, samples collected after 3 or 10 days of differentiation protocol (d3/d10) are compared with undifferentiated (UD) samples. At day 3, a fraction of each cell was plated in adherent conditions and samples were also analysed at day 10 and day 15 (10P and 15P). Pluripotency markers (*Endo Oct4*, *Nanog* and *Fgf4*) have reduced expression that later on increases for adherent conditions. *Pax6*, *Six3*, *Six6*, *Otx2* and *Otx1* genes have increased levels of expression. *Mitf* expression is observed for day 15P although no other RPE marker is detected. *Gapdh* is used as endogenous control.

EFTF expression was also examined and *Pax6* transcripts were detected in all cells at day 3 and/or 10 under floating conditions, as well as at day 15P. Despite the fact that *Rax* transcripts were never detected, discrete levels of *Six3* and *Six6* were observed only for ES cells at day 10P and 15P of differentiation. *Six3* was also detected at day 10 for

ES cells and j9#3. *Otx2* gene was expressed in all cells either in floating or adherent conditions, consistent with its role in neuroectoderm specification. Its ortholog *Otx1* was also detected in ES cells at day 10 of differentiation. Regarding RPE specific genes, *Mitf* transcripts were perceived at day 15 on adherent conditions (day 15P), even though some residual levels may be present earlier. Other RPE markers, like *Tyr*, *Rpe65* and *Rgr* were not detected in these conditions.

To summarize, three different differentiation protocols were tested and, except for the first case, promising results were obtained. Despite no mature RPE cells were properly isolated and characterized yet, significant steps towards that ultimate goal were undertaken, with the generation of OV-like structures in one case and the identification of a population of retinal progenitor cells. Subsequent RPE specification steps will be pursued in order to obtain the desired cell type.

Discussion

CHM is a rare monogenic disorder caused by loss-of-function mutations on *CHM/REP1* gene encoding for REP1 protein, which is responsible for the prenylation of Rab GTPases, key regulators of intracellular vesicular transport and organelle dynamics (van Bokhoven et al., 1994). It is an X-linked disorder characterized by a progressive degeneration of different retinal layers, namely the PRs, the RPE and the choroid. The pathogenesis of CHM still remains unclear, despite recent scientific advances pointing out to a therapeutic improvement when the RPE function is rescued (Tolmachova et al., 2013).

Cellular reprogramming strategies have been applied to several human diseases, including retinal degenerative disorders, demonstrating their potential use as therapeutic tools for the replacement of diseased cells or as experimental instruments to model disease. One can postulate that substitution of diseased RPE cells might be therapeutically advantageous for CHM patients in later phases of the degenerative process. Additionally, disease modelling studies using cells originated by reprogramming experiments will accelerate the characterization of the molecular events underlying CHM retinal degeneration.

Here we report the generation of iPS cell lines derived from a Chm mouse model carrying a conditional KO of *Rep1* gene. This model was previously generated by Tolmachova and colleagues, with heterozygous-null females exhibiting characteristic hallmarks of CHM: progressive degeneration of the PRs, patchy depigmentation of the

RPE, and Rab prenylation defects (Tolmachova et al., 2006). MEFs were isolated from timed matings between *Chm*$^{flox/flox}$ and *Chm*$^{flox/Y}$ mice. Established primary cultures were genotyped in order to select *Chm*^{flox} cells carrying the *MerCreMer* transgene. Treatment of such cells with optimized conditions of TM exposure induced genomic recombination between the 2 *loxP* sites flanking exon 4 of *Rep1* gene, which generates a premature stop codon. Resultant *Chm*^{null} cells displayed reduced levels of *Rep1* gene, confirming the successful Rep1 KO and its utility as a Chm model.

Taking advantage of the conditional nature of the mouse model, *Chm*^{null} and *Chm*^{flox} MEFs were concomitantly subjected to reprogramming protocols in order to feasibly highlight differences derived from the Rep1 KO. Such differences were not observed in our system, contrarily to a few reports on different models, which suggested that correction of a different genetic alteration conferred a selective advantage for iPS cell generation and/or maintenance (Raya et al., 2009). In our study, iPS cells were generated from both *Chm*^{null} (Rep1 KO) and *Chm*^{flox} MEFs, applying the reprogramming protocol optimized using WT MEFs, as described on Chapter 3. The inducible lentiviral system efficiently transduced Chm cells, which expressed the 4 reprogramming factors (OSKM) upon DOX addition. Morphological alterations, previously observed with WT MEFs, were also perceived for transduced *Chm*^{null} and *Chm*^{flox} cells, with arising colonies allowing the establishment of several pluripotent cell lines.

Generated iPS cell lines were then characterized to confirm: 1. their molecular and functional equivalence to ES cells; 2. their Rep1 expression status and potential usage as Chm model. Firstly, *Chm*^{null} and *Chm*^{flox} iPS cell lines exhibited morphologic appearance similar to pluripotent cells. Expression of several key pluripotency markers was detected, such as AP, Oct4, Nanog and SSEA1. Additionally, *Eras*, *Ecat1*, *Esg1*, *Fgf4* and *Zfp42* expression was also detected at a transcriptional level. At this point, viral transcripts were not expressed confirming that the observed molecular profile was due to an endogenous reactivation of the pluripotent cell identity. Naïve pluripotency was attained with culture in 2i conditions, and *in vitro* and *in vivo* functional tests confirmed the ability to give rise to cells derived from the 3 germ layers. The differentiation of *Chm*^{null} and *Chm*^{flox} iPS cell lines, either using EB bodies or after injection on an immunodeficient mice, generated cells and tissues with characteristic molecular and morphological features of ectoderm, mesoderm and endoderm.

Subsequently to the confirmation of pluripotent state, generated iPS cell lines were characterized in terms of Rep1 expression. Genotyping confirmed the maintenance of the original *Chm*^{null} or *Chm*^{flox} alleles. As expected, *Chm*^{null} iPS cell clones exhibited reduced expression of Rep1 when compared with *Chm*^{flox} iPS cell lines, at both a

transcriptional and protein level. Aditionally, Rep1 KO seems not to be affecting cellular proliferation of iPS cell lines, as similar growth rates were observed for both genotypes.

In the context of CHM disease, it was relevant to differentiate the obtained pluripotent cells into RPE, one of the retinal layers affected by this degenerative disorder. Several protocols, including directed differentiation processes, have been described over the years with different efficiencies and purities of obtained RPE-like cells (Bharti et al., 2011; Borooah et al., 2013). Three protocols were tested, sharing a stepwise differentiation process initiated by a serum-free floating culture system promoting the anterior neuroepithelial fate. A subsequent phase of guided RPE-specification would follow. Transcriptional alterations were determined for the tested protocols and are summarized in Table 4.1.

Zhu and colleagues reported a 3D system that allowed quantitative production of RPE cells from human ES cells within 30 days (Zhu et al., 2013). The initial step of the protocol was implemented with mouse iPS cells (*Chm*^{null}, *Chm*^{flox} and WT) and ES cells. However, the aggregates of mouse pluripotent cells did not acquire the reported neural-like tube structures nor the expression of early retinal markers, when cultured in neural induction media. The authors demonstrated a role for IGF1 signalling in the formation of the pseudostratified neuroepithelium, which lead to observed differences on the efficiency of the process as a consequence of variations in IGF1 levels present in the lot of Matrigel used to embed the floating aggregates. As an alternative to test different lots of Matrigel (with possible different levels of IGF1), IGF1 recombinant protein was added to the system to further promote the retinal fate. Nevertheless this strategy was also shown to be unsuccessful. In neither condition (with or without IGF-1), expression of EFTFs was observed. The only observed significant alterations on gene expression were down-regulation of pluripotency markers as well as discrete up-regulation of *Otx2* levels. Besides its role on OV evagination and RPE specification, Otx2 is responsible for specifying the anterior neuroectoderm, with its expression preceding the expression of the early EFTFs (Hever et al., 2006). Thus, one can hypothesize that the early molecular events towards an anterior neuroepithelial fate had begun to take place in our system but failed to progress, probably due to lack of other patterning cues or to species-specific differences.

Table 4.1: Transcriptional alterations observed for tested protocols.

Dark and light grey boxes represent strong and weak expression, respectively. White boxes symbolize undetectable levels of transcripts. Unless mentioned (for example, 2 out of 3 cell lines), expression levels are common in all tested cell lines.

	UD	Zhu *et al.*		Eiraku *et al.* and Gonzalez-Cordero *et al.*		La Torre *et al.* and Osakada *et al.*			
		d5	d5 + IGF-1	d3	d10	d3	d10	d10**P**	d15**P**
Endo Oct4									
Nanog									
Fgf4									
Pax6					2/3				
Rax									
Six3							3/4	1/4	1/4
Six6								1/4	1/4
Otx1					2/3		1/4		
Otx2							3/4	2/4	
Mitf									
Tyr									
Rpe65									
Rgr									

Recently, groundbreaking work described the recapitulation of *in vivo* organogenesis in self-organizing aggregates of ES and iPS cells (Eiraku et al., 2011; Gonzalez-Cordero et al., 2013; Nakano et al., 2012). When aggregates of mouse and human pluripotent cells are cultured in suspension with the appropriate medium for efficient retinal differentiation, ES cell-derived retinal epithelia evaginate to form OV-like structures, which subsequently

undergo an invagination step and give rise to bi-layered OC, without any external cues or forces. In an attempt to reproduce these results, obtained mouse iPS cells were submitted to SFEBq culture supplemented with Matrigel. Cell aggregates were formed in suspension culture and neuroepithelia surrounding the whole circumference of the EB was observed after 5 days.

However, OV-like structures were observed later and less frequently than reported and no bilayered OCs were observed. Self-organization of the OC from pluripotent cells has been reported to be a size-sensitive phenomenon with retinal cell differentiation occurring in small aggregates of 300 mouse ES cells, but OC failing to form unless the number of cells reaches a critical mass of 1000-2000 cells (Eiraku et al., 2011; Nakano et al., 2012). Since the SFEBq culture was not performed in low-cell-adhesion 96-well plates, we could not control for the numbers of dissociated cells forming each cell aggregate. In our experiments, cell aggregates had variable sizes, probably justifying the lack of formation of OV and OC-like structures whilst still recapitulating some neuroepithelial phenotype confirmed by morphology and gene expression evaluations. Regarding gene expression, at day 10 of differentiation, a down-regulation of pluripotency markers was observed concomitantly with up-regulation of some EFTFs and *Otx2*/*Otx1*.

Another differentiation protocol was tested giving promising results. Taking in consideration that forebrain development is dependent of IGF1 signalling and inhibition of both BMP and Wnt signalling, defined molecules that modulate these signalling pathways were employed by other groups to induce the generation of neural retinal progenitors from pluripotent cells (Lamba et al., 2006; Osakada et al., 2009; Torre et al., 2012). In order to apply this protocol to our system, generated iPS cell lines and ES cells were cultured in low-adhesion conditions in retinal induction media containing Noggin, Dkk1 and IGF1. After 3 days in these conditions, expression of pluripotency genes was already diminished and *Pax6* and *Otx2* transcripts were detected. If low-adhesion culture conditions were continued after day 3, *Six3* EFTF was also detected at day 10 as well as Otx2 ortholog, *Otx1*. Alternatively, at day 3 cells were plated in Matrigel-coated wells acquiring a neuroepithelial-like morphology resembling neural progenitor cells. Besides these actively proliferating cells, patches of cells displaying cobblestone morphology were also observed. Expression of EFTFs and *Otx2* was detected, and also *Mitf* in some cases, possibly revealing that some cells are being specified into the RPE cell fate. A quantitative analysis of mRNA content and imaging techniques are needed to confirm the expression differences, to confirm expression at protein level and to distinguish whether there was nuclear or cytoplasmic expression of pluripotency factors *Oct4*,

Nanog and *Fgf4* at day 15P. One possibility is that the proliferative neural progenitor population has a “primitive phenotype” and still share markers with ES cells (Lee et al., 2010). Nevertheless, the observed morphologic and transcriptional alterations pointed out to the generation of a neural progenitor population that in some cases generated RPE-like hexagonal-packed cells. Since NR and RPE arise from a common embryonic progenitor pool, after expansion of the obtained population of cells, defined factors (such as Activin and Nicotinamide) can be added to the culture medium to favour RPE cell fate as previously reported (Buchholz et al., 2013; Idelson et al., 2009). Besides Matrigel, other extracellular matrix components can and should be employed to potentiate RPE differentiation and/or maintenance (Rowland et al., 2013).

In summary, iPS cells were obtained from a mouse model of the retinal degenerative disorder Chm. Differentiation of such pluripotent cells into RPE cell fate was attempted with promising results. Additional systematic experiments are needed to further elucidate the molecular events of the differentiation process of pluripotent cells into RPE cells. A further protocol optimization is needed to allow the more efficient generation of RPE cells. These cells should be isolated from the mixed population of cells and characterized morphological, molecular and functionally to confirm the RPE phenotype (Bharti et al., 2011). Concomitantly further experiments aiming at reproducing the 3D OC self-organization will allow an alternative approach to obtain RPE cells from iPS cells, with the supplementary advantage of also providing NR structures (Eiraku et al., 2011). iPS cell-derived RPE cells are therapeutically interesting for the replacement of degenerated RPE. In fact, the first clinical trials exploiting iPS cell therapeutic potential were established for retinal degenerative disorders given the facilitated surgical accessibility and functional monitoring of the eye. Besides the number of cells needed for transplantation are quite small (Ramsden et al., 2013). Furthermore, iPS cell-derived RPE can be used in disease modelling studies, as already showed for several retinal degenerations, recently including CHM (Cereso et al., 2014; Meyer et al., 2011; Singh et al., 2013; Vasireddy et al., 2013). In our case, the establishment of Chm iPS cell-derived RPE cells will allow us to generate a proper mouse model of Chm RPE cells, complementary to other existing models that can be used in systematic studies to dissect molecular events underlying Chm pathogenesis. Interestingly, the concomitant generation of Chm^{null} and Chm^{flox}-derived cells provides the ideal control for these experiments. Additionally, given the conditional nature of the Rep1 KO, this system allows a timely-control of the recombination event, which can help to highlight phenotypic differences. Moreover, the generation of Chm self-organized OCs will bring into the field an *in vitro* model for the simultaneous characterization of degenerative events on both

the RPE and NR layers and their potential interaction, providing helpful insights into the pathogenesis of CHM.

Chapter 5 Direct Reprogramming of fibroblasts into RPE cells

Chapter 5 : Direct Reprogramming of fibroblasts into RPE cells

Summary

The developmental process in which an initial totipotent cell is progressively committed and differentiated into multiple cells types was for long considered to be an irreversible process. Initial cloning experiments placed these concepts into argue and the possibility to reprogram somatic cells into pluripotent counterparts finally changed the dogma in the field.

Notwithstanding reprogramming into pluripotency experiments, some recent reports also disclosed that somatic cells can be interconverted into alternative differentiated cell types. These direct lineage conversion strategies, mediated by forced expression of TFs, occur without de-differentiation or intermediate non-differentiated states. Besides relevant input into developmental and disease modelling studies, these novelty approaches attracted much interest as an alternative way to obtain cells and tissues for cell replacement therapies without the use of pluripotent stem cells.

The RPE is a polarized monolayer of pigmented cells located at the back of the eye. Together with choroidal vasculature and PRs, it composes the retina, a complex multi-layered tissue responsible for vision. RPE cells are high metabolically active and responsible for multiple functions essential to support and maintain PR' integrity. Primary RPE functions include ion and nutrient transport, light absorption, retinal recycling, phagocytosis of the OS of the PRs and secretion of growth factors (Strauss, 2005). Given its relevant role in maintaining retina functionality, not surprisingly RPE dysfunction is a common feature (if not a direct cause) in several retina disorders, like AMD, the leading cause of blindness worldwide.

Multiple RPE *in vitro* systems have been developed and studied along the years, including immortalized cell lines, primary cultures from different species, and RPE cells differentiated from pluripotent stem cells (either ES or iPS cells) (Bharti et al., 2011). Nevertheless, current *in vitro* RPE cultures still display recurrent loss of key features (pigmentation and expression of some characteristic markers) and phenotypic instability and heterogeneity. Moreover, differentiation processes from pluripotent stem cells depend on inefficient and time-consuming protocols.

Direct conversion of somatic cells into an active RPE will provide an alternate and more straightforward route to obtain RPE cells for functional and therapeutic studies. Here, we report the generation of several molecular tools to force the expression of key TFs

involved in the formation and patterning of the eye (namely *Tbx3*, *Rax*, *Six3*, *Pax6*, *Lhx2*, *Six6* and *Nr2e1*), as well as in subsequent RPE specification steps (*Pax6*, *Mitf*, *Otx1* and *Otx2*). Fibroblasts transduced with this pool of TFs gained some RPE key features, such as pigmentation and expression of RPE-specific markers (*Mitf*, *Tyr*, *Rpe65* and *Rlbp1*). Two lentiviral reporter systems were also generated in order to optimize the TFs' pool, with the purpose of increasing the direct reprogramming efficiency. These studies provide an experimental platform to gain insight in RPE developmental process and transcriptional identity, as well as prospective use for drug screening, disease modelling studies and regenerative medicine approaches.

Results

MEFs have different morphology and expression profiles when compared to RPE cells

Lineage conversion strategies have been based in a deep and extensive knowledge on the developmental process and phenotypic characteristics of the cells aimed to be obtained. First and foremost, one needs to easily distinguish both somatic cell populations, in this case fibroblasts from RPE cells.

MEF primary cultures obtained from WT pregnant mice displayed typical flat and elongated morphology and no pigmented granules were observed (Figure 5.1A). Primary cultures of mouse RPE cells were established from 3 week old WT mice. Besides contamination with a few different cell types (like choroidal melanocytes) inherent to isolation protocol, some RPE sheets of pigmented epithelial cells were obtained, maintaining characteristic features similar to RPE *in situ*. After enzymatic subculture of the RPE primary cultures however, phenotypic heterogeneity was observed, as already described (Burke et al., 1996). As epithelial architecture was lost, a mixed population of epithelioid and fusiform cells was present in RPE primary cultures (Figure 5.1A), in non-polarized culture conditions. The typical pigment content was retained, even after cell passaging.

Gene expression was also assessed for MEF and RPE primary cultures. Interestingly, early EFTFs, *Pax6* and *Rax*, important for eye developmental process, were expressed by RPE cells from 3 week old mice, as well as by Embryonic eye, the positive control . It was also observed that transcripts for these 2 genes were not detected in MEFs (Figure 5.1B).

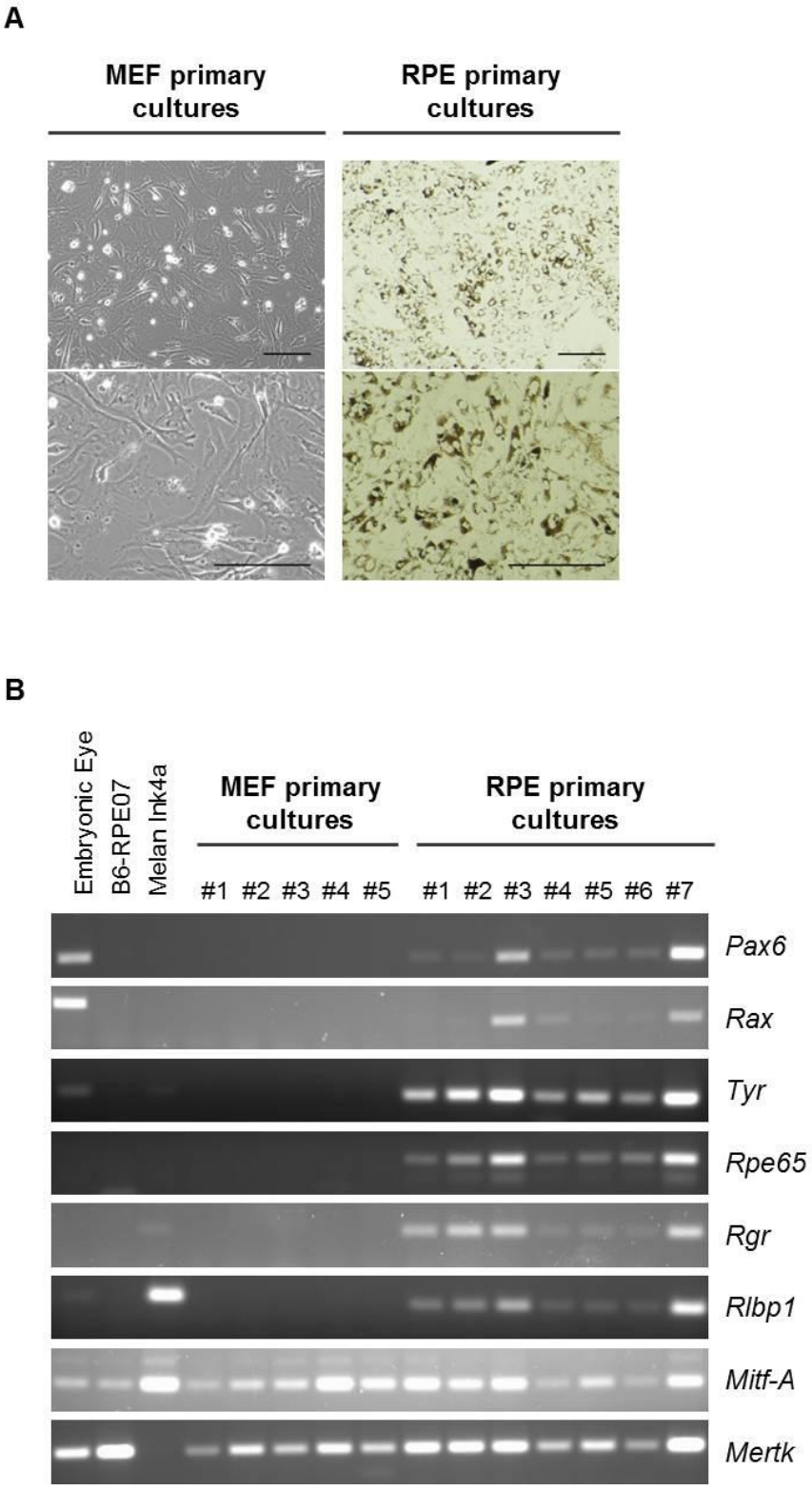

Figure 5.1: MEFs and RPE primary cultures display different morphology and gene expression profiles.

(A) Brighfield images of representative primary cultures of MEFs and RPE. Scale bar 50 µm. (B) RT-PCR analysis of 5 MEF primary cultures and 7 RPE primary cultures is shown for the denoted genes. Samples of Embryonic Eye (isolated at E13.5), a mouse RPE cell line (B6-RPE07 (Chen et al., 2008)) and a mouse melanocyte cell line (Melan Ink4a (Sviderskaya et al., 2002)) were also used as positive controls.

Additionally, genes important for RPE's functional properties were analysed, and *Tyr*, the rate-limiting melanogenic enzyme essential for pigment synthesis, was found to be expressed by RPE cells and not MEFs. Identical expression specificity was also observed for *Rpe65, Rgr* and *Rlbp1* transcripts, genes involved in the RPE's visual cycle responsible for reisomerization of retinal. Contrarily, for other known to be RPE-specific genes, expression was observed for both RPE and MEF cells, namely for *Mitf-A* and *Mertk*.

Primers designed to specifically amplify isoform A of *Mitf* were used in this analysis. The basic helix-loop-helix leucine zipper TF *Mitf* plays an essential role in development and survival of pigmented cells, like melanocytes and RPE cells. At least 9 isoforms with different amino termini have been identified so far, and Mitf-A has been known to regulate RPE development (Šamija et al., 2010; Tachibana, 2000). *Mitf-A* transcripts were observed for all cell lines and primary cultures tested, confirming previous findings reporting that *Mitf-A* mRNA is widely expressed in several cultured cells and tissues (Amae et al., 1998).

Mertk has been known to play a role in POS phagocytosis, by activation of second messenger cascade events that trigger POS internalization by RPE cells. However, this receptor tyrosine kinase transduces signals from extracellular matrix in response to binding of several ligands. Thus it interferes with the regulation of many physiological processes like cell survival, migration, differentiation and phagocytosis, which may explain the observed expression by embryonic fibroblasts (Hafizi and Dahlbäck, 2006).

Lentiviral molecular tools efficiently induce expression of TFs in transduced MEFs

Direct lineage conversion experiments rely on forcing a high expression of TFs responsible for driving and/or maintaining the differentiated state to be obtained. In this case, it was conjectured that the gene regulatory network responsible for determining RPE development and specification could potentially be used to promote direct conversion of fibroblasts into RPE cells. With this purpose several molecular tools were generated.

Inducible lentiviral systems are commonly used for forced expression of TFs in reprogramming experiments, either into pluripotency or for lineage conversion purposes. In order to facilitate extensive cloning procedures, an inducible lentiviral plasmid compatible with Invitrogen's Gateway® Technology was generated (pLenti6/TetO/Dest), containing the tetracycline operator minimal promoter (TetO).

Inducible expression of the lentiviral system was first confirmed with generated control lentivirus, Lenti-TetO-GFP. MEFs were co-transduced with inducible lentiviral particles as well as Lenti-M2rtTA viral particles that drive the expression of the reverse transactivator M2rtTA necessary for the inducible promoter activation. Either by western blot analysis or by fluorescent microscopy, expression of GFP protein was observed in co-transduced MEFs, cultured in the presence of DOX (Figure 5.2).

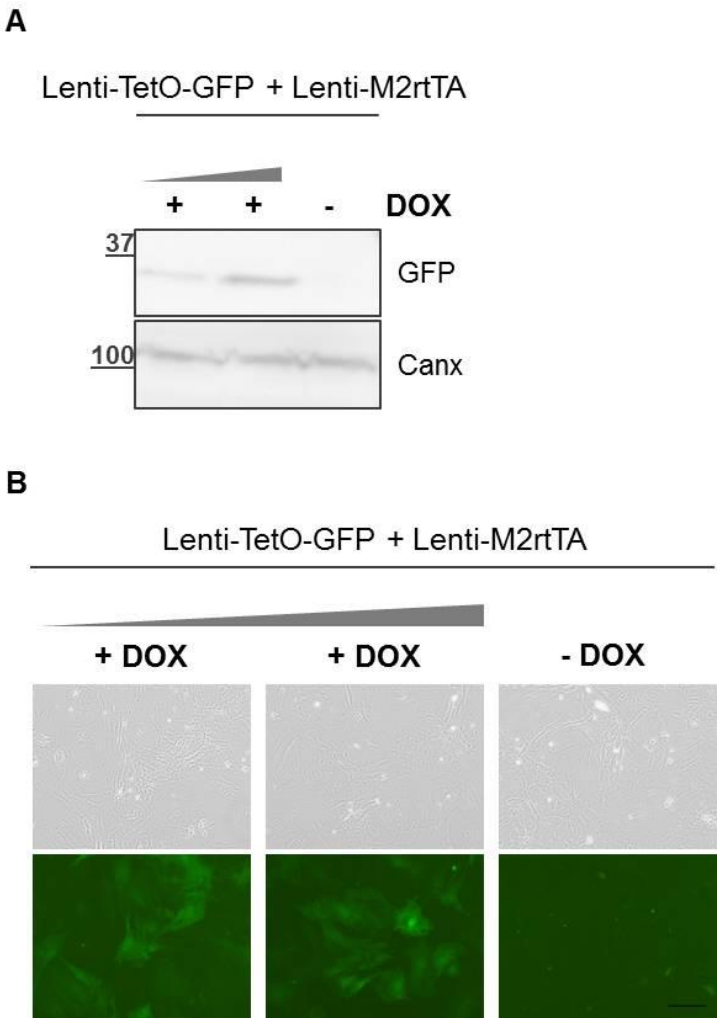

Figure 5.2: Inducible lentiviral vector allows efficient inducible expression of GFP protein.

(A) MEFs were co-transduced with Lenti-TetO-GFP and Lenti-M2rtTA viral particles and cultured in the presence (+) or absence (-) of DOX. Protein lysates were collected 4 dpt and analysed by western blot with the indicated antibodies. GFP protein expression is detected in the presence of DOX and intensified as the volume of lentiviral supernatant increases (as denoted by the grey triangle). Canx was used as loading control. (B) For equivalent experiments, bright-field and fluorescent images are shown. Scale bar 25 µm.

Eye morphogenesis is a multistep complex process that is initiated from a morphologically indistinctive early EF that evaginates to give rise to the OV. The late OV becomes patterned into distinct ocular tissues (NR, RPE and optic stalk) and gives rise to the OC after an invagination event. All these processes are tightly regulated by signalling pathways and a gene regulatory system extensively characterized. Initially, the single early EF, located centrally in the developing forebrain, is characterized molecularly by the expression of a core of TFs. The EFTFs include *Rax* (or *Rx1*), *Pax6*, *Six3*, *Six6*, *Lhx2* and *Nr2e1*, as several genetic studies in mammals and lower vertebrates revealed (Graw, 2010). For the specification of the presumptive RPE in the OV stage, as well as further developmental steps in the OC, key TFs have been described to play a fundamental role: *Mitf*, *Otx2* (and its orthologue *Otx1*) and *Pax6* (Bharti et al., 2006; Martínez-Morales et al., 2004).

Given their role in eye development and RPE patterning events, these 10 TFs (from now on designated as Eye TFs) were selected, as it was hypothesized that they could work as reprogramming factors to mediate the direct conversion of fibroblasts into RPE. cDNAs of the 10 Eye TFs were amplified and cloned into plasmid vectors, as V5-tagged versions to facilitate identification. By western blot analysis, expression of the 10 individual fusion proteins was detected in transfected cells, using an anti-V5 antibody (Figure 5.3A). All vectors were also sequenced to confirm sequence integrity.

All the 10 generated plasmid vectors included features to function as entry vectors in Gateway® system. After two recombination reactions, each V5-Eye TFs' cDNA was shuttled into the pLenti/TetO/Dest, and 10 resulting inducible lentiviral plasmids were obtained (Lenti-TetO-V5 Eye TF) (Figure 5.3B). Inducible expression was confirmed by western blot analysis in MEFs co-transduced with lentiviral particles encoding for each of the 10 Eye TFs and Lenti-M2rtTA viral particles. Protein expression was detected in cells cultured in the presence of DOX, at 4 dpt (Figure 5.3C).

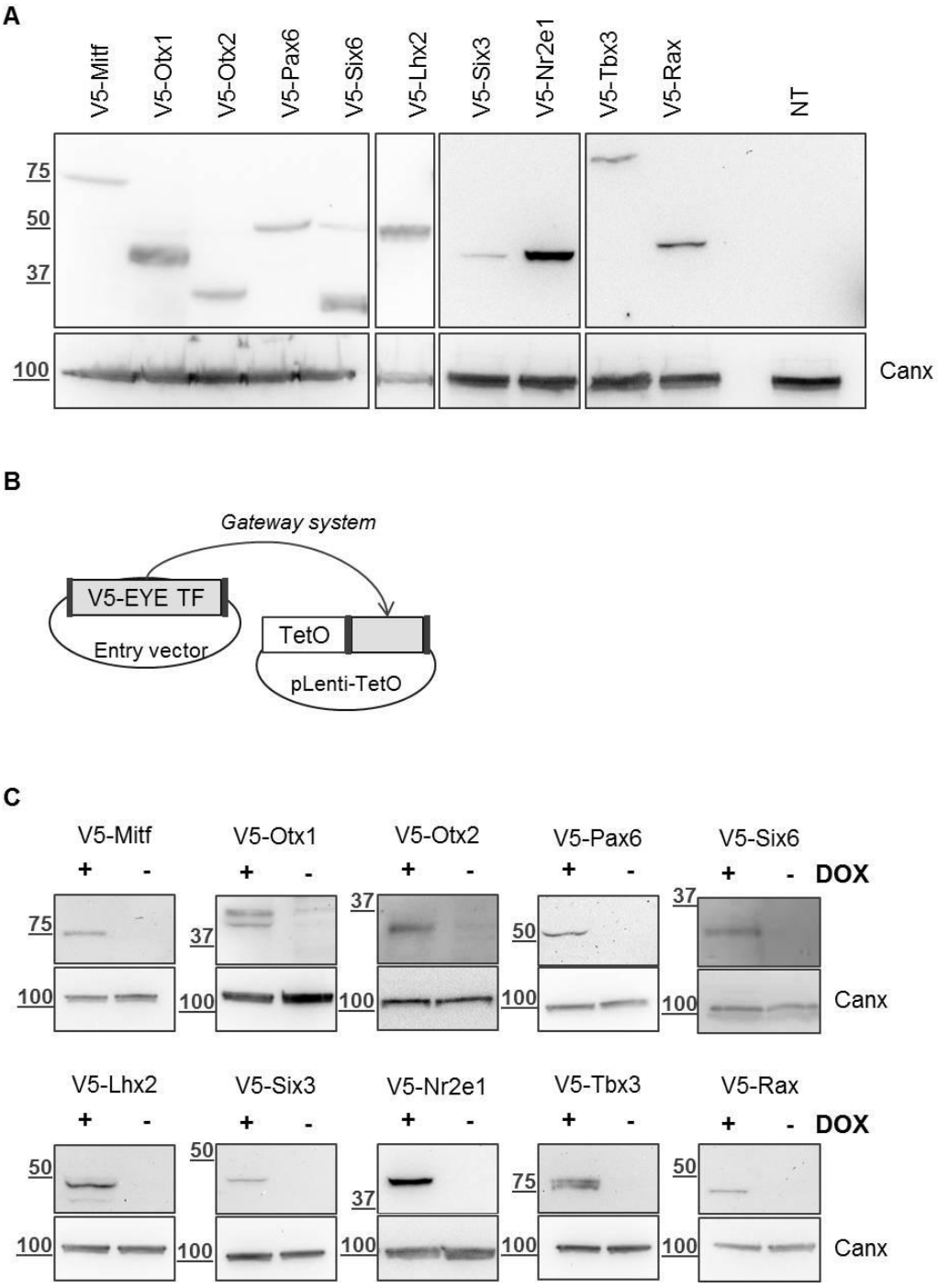

Figure 5.3: V5-tagged versions of 10 TFs involved in eye and RPE developmental processes were successfully cloned into DOX-inducible lentiviral vectors.

(A) HEK293FT cells were transfected with each of the 10 entry vectors expressing V5-tagged versions of the 10 Eye TFs. Protein lysates were collected and analysed by western blot using anti-V5 (top panel) and anti-Calnexin (bottom panel; endogenous control) antibodies. NT (non transfected) cells were assayed as negative control. (B) Schematic representation of cloning strategy. Taking advantage of the Gateway® Technology, V5-Eye TF' cDNAs were recombined from the entry vector into inducible lentiviral vectors (pLenti-TetO). (C) MEFs were co-transduced with each resulting Lenti-TetO-V5-Eye TF and Lenti-M2rtTA, and cultured in the presence (+) or absence (-) of DOX. Protein lysates were collected 4 dpt and analysed by western blot as in (A). Expression of each Eye TF is only observed in the presence of DOX confirming the inducible expression.

Co-transduced MEFs were also subjected to IF techniques to confirm adequate nuclear location of the encoded TFs, as depicted in Figure 5.4.

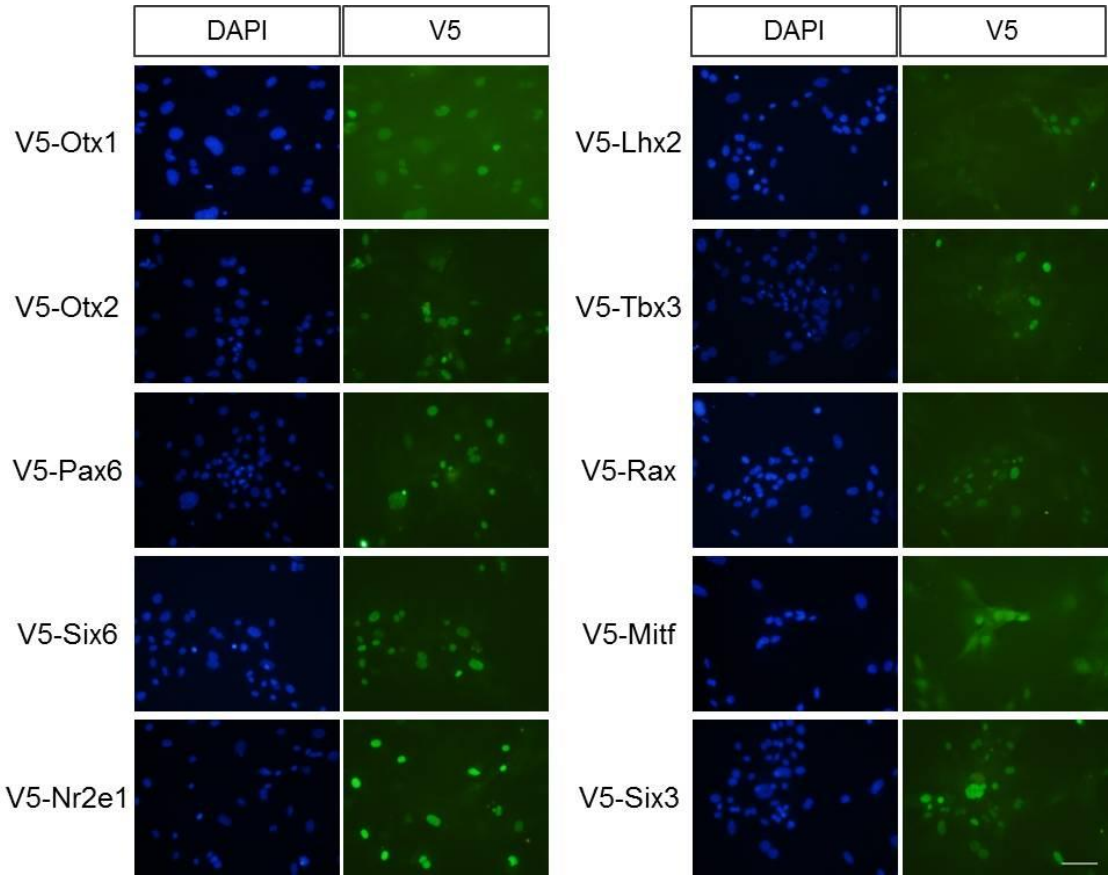

Figure 5.4: Inducible lentiviral particles allow expression of 10 Eye TF in transduced MEFs.

MEFs were co-transduced with each Lenti-TetO-V5-Eye TF and Lenti-M2rtTA, cultured in the presence of DOX and analysed by IF at 4 dpt using an anti-V5 antibody. Nuclei were counterstained with DAPI. Expression of the V5-TF is observed for each of the 10 lentiviral vectors, with nuclear localization.

Transduction with multiple lentiviral particles can be optimized without compromising cell viability

As shown previously, transductions of MEFs with individual TF-encoding lentiviral particles led to an exogenous expression of the Eye TFs. However, in order to implement a direct reprogramming protocol, expression of multiple TFs must be induced. To this end, lentiviral transductions were optimized to maximize the probability of co-transducing fibroblasts with the chosen pool of TFs.

Freshly produced lentiviral particles were always used since repeated freeze-thaw cycles may result in decrease of viral titer. In order to overcome technical restrictions related to

total volume of culture wells and to increase transduction efficiency, multiple transductions with several lentiviral supernatants were performed after supernatant ultracentrifugation.

Control vector Lenti-TetO-GFP was used for these optimization experiments, for simplification purposes, and increasing volumes of fresh concentrated lentiviral particles were used to transduce MEFs. Single transduction experiments were performed using from 50 to 250 µL of lentiviral preparation. Corresponding 10-fold volumes (500 to 2500 µL) were tested in order to mimic multiple transduction of the 10 Eye TF. Lenti-M2rtTA virions were always co-transduced and DOX was added to the system to induce GFP expression.

First, cell viability was assessed by a MTT cytotoxicity assay and results are shown in Figure 5.5A. Within the range of volumes tested, no significant alteration in cell viability was observed.

In addition, transduced cells were also analysed by flow cytometry. Lenti-M2rtTA virions were added in constant amount (50 µL) or in equivalent volume (for example 1000 µL of Lenti-TetO-GFP would correspond to co-transduction with 100 µL of each of the 10 different Lenti-TetO-Eye TF and 100 µL of transactivator lentivirus).

The percentage of GFP-positive (GFP^+) cells increased along the volume range, until the maximum value of approximately 88% (Figure 5.5B). Since it is anticipated that more than one TF will be necessary to reprogram fibroblasts into RPE, transduction of a single cell with multiple virions was desired. Thus, Median Fluorescent Intensities (MFI) were also analysed aiming to dissect the number of viral particles inserted in each GFP^+ cell: the fluorescent intensity of a cell transduced with more than one copy of Lenti-TetO-GFP will be higher than singly transduced cells (Figure 5.5C). As expected, MFI values also increased along with the augment of the volumes tested, from 176 arbitrary units (a.u.) for 50 µL up until 681 a.u. for 2500 µL.

Regarding Lenti-M2rtTA, no significant difference was observed for the 2 conditions tested in parallel, except for 2500 µL of Lenti-TetO-GFP. In this case, co-transducing with equivalent volume (250 µL) of transactivator yielded a higher percentage of GFP^+ cells than using only 50 µL (Figure 5.5B). However, in the actual reprogramming experiments, one cannot exclude the possibility that the use of equivalent volumes of transactivator will increase the probability of having one single cell simultaneously transduced with the 10 different lentivirus and Lenti-M2rtTA.

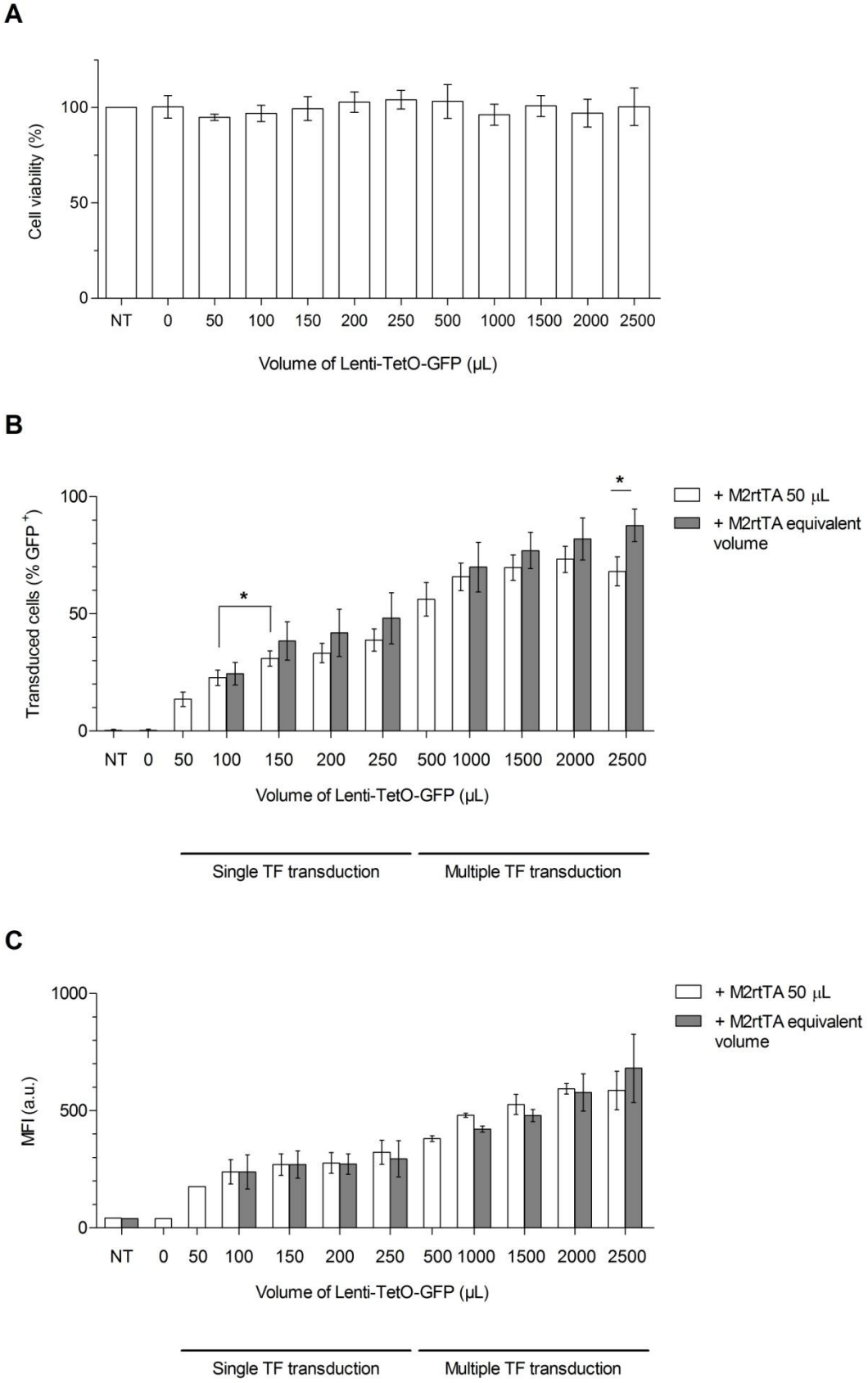

(See caption on the following page)

Figure 5.5: Transduction with multiple lentiviral particles can be optimized without compromising cell viability.

(A) Cell viability of MEFs transduced with increasing volumes (from 0 until 2500 µL) of Lenti-TetO-GFP supernatant and 50 µL of Lenti-M2rtTA was assessed by MTT assay. Absorbance values are normalized to NT cells, used as control. No significant alteration in cell viability is observed. Mean ± SD, n=3; statistical analysis using one-way ANOVA with Dunnett's multiple comparison test. (B) Increasing volumes of Lenti-TetO-GFP supernatant and 50 µL of Lenti-M2rtTA were used to co-transduce MEFs, followed by flow cytometry analysis on 4 dpt. Transduction of 500 up to 2500 µL of Lenti-TetO-GFP was used to mimic simultaneous transduction of 10 different lentiviruses, 50 until 250 µL of each one (multiple TF transduction). Alternatively to constant 50 µL, equivalent volumes of Lenti-M2rtTA were also tested (for instance for 1500 µL of Lenti-TetO-GFP which mimic transduction of 10 different virus 150 µL each, 150 µL of Lenti-M2rtTA were used). Percentage of transduced (GFP+) cells is shown. No significant difference is observed when comparing both Lenti-M2rtTA conditions, except for 2500 µL (two-way ANOVA with Bonferroni post-test; * $p<0.05$). With 150 µL of inducible lentivirus, approximately 31% of cells were GFP^+, which is significantly different from what is achieved with 100 µL (unpaired t-test, * $p<0.05$). Mean ± SD, n=4. (C) For same experiments, Median Fluorescence Intensities (MFI) in arbitrary units (a.u.) are shown.

For a single transduction, it was observed that 150 µL of Lenti-TetO-GFP promoted higher percentage of transduced cells when compared to 100 µL (mean values of 31% versus 23%). However, further increase of Lenti-TetO-GFP volume to 200 or 250 µL did not generate a significant increase on the percentage of GFP^+ cells. When considering multiple transductions with the corresponding 10-fold values, no significance was observed in the total number of transduced cells (Figure 5.5B). Moreover, in terms of MFI, values increased over the range of volumes tested but no significant differences were observed when comparing the abovementioned pairs of values (Figure 5.5C).

Considering all the mentioned aspects and also the limitations due to extensive time- and money-consuming production of lentiviral particles, 150 µL of each individual lentivirus were selected for the subsequent reprogramming experiments. Notwithstanding the oversimplification inherent to the use of only Lenti-TetO-GFP, flow cytometry results showed that multiple transductions with 10-fold volume (1500 µL) increased not only the total number of transduced cells (mean values of 31% versus 70%) but also the fluorescent intensity (MFI of 270 versus 527) (Figure 5.5B and C). The resulting population had a different histogram profile from the corresponding single transduction (Figure 5.6) with higher abundance of cells transduced with multiple copies of the lentivirus. In the subsequent reprogramming experiments, a mixed population of cells transduced with different combinations of the Eye TFs was expected; an event one cannot prevent but can account for.

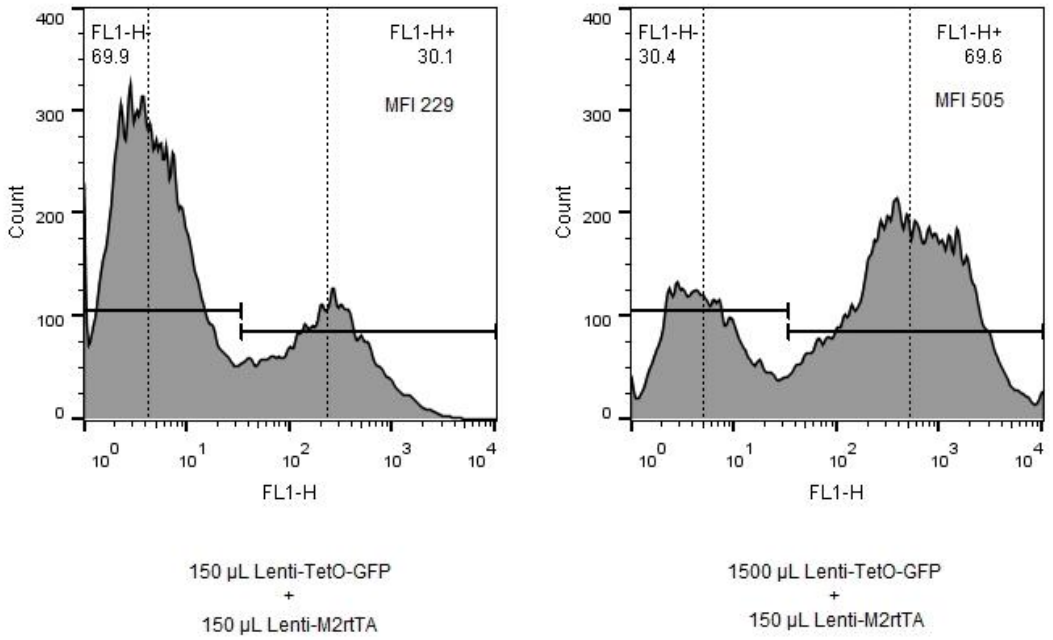

Figure 5.6: Ten-fold increase of lentiviral volumes increases percentage of transduced cells as well as their fluorescent intensity.

Representative flow cytometry histograms of MEFs co-transduced with Lenti-TetO-GFP and Lenti-M2rtTA, in the mentioned quantities. When increasing the volume of inducible lentivirus by 10 fold, the percentage of transduced GFP^+ cells (FL1-H+ population) increases from 30.1 to 69.6%. MFI of this same population also increases from 229 to 505 a.u. (median of the GFP^+ population is represented as the dotted line on the right).

MEFs transduced with lentivirus encoding for 10 Eye TF gain some RPE features

Direct reprogramming of fibroblasts into RPE cells was attempted making use of the generated molecular tools. MEFs were co-transduced with a pool of the 10 lentivirus encoding for the 10 selected Eye TF and Lenti-M2rtTA, 150 µL of each freshly prepared and concentrated lentiviral preparation (Figure 5.7A). DOX was added to the system at 1 dpt to induce expression of the 10 Eye TF (except in control wells, cultured in the absence of DOX) and culture media was changed into DMEM 5% FBS (media used in RPE primary cultures) at 8 dpt. Cells were monitored for 22 days to assess potential morphological and gene expression alterations. In terms of morphology, a significant alteration was observed as soon as 8 dpt: pigmented granules were detected only in cells cultured in the presence of DOX (Figure 5.7B).

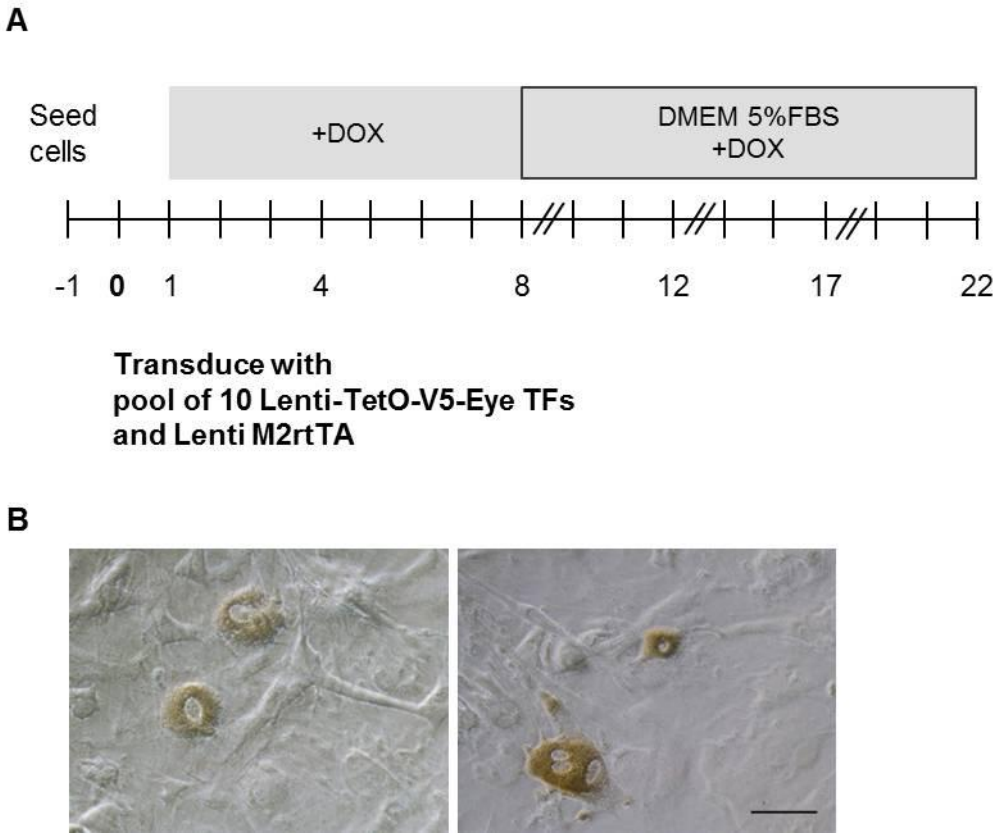

Figure 5.7: MEFs transduced with pool of inducible lentivirus encoding for the 10 Eye TFs display morphological alterations, in terms of pigmentation.

(A) Schematic representation of protocol. Cells were co-transduced with pool of 10 inducible lentivirus and Lenti-M2rtTA. DOX was added to culture media at 1 dpt. Media was changed into 5% FBS at 8 dpt. (B) Pigmented cells were observed as soon as 8 dpt.

Gene expression was assessed by RT-qPCR, using primers to evaluate transcriptional levels of TFs involved in eye and RPE development, as well as RPE-specific markers. Four independent experiments were performed and results showed a consistent increase of transcriptional levels of the analysed genes in transduced cells, when compared with control cells (cells at 4 dpt cultured in the absence of DOX) (Figure 5.8). Variability was observed between experiments, which may be explained by the technical difficulty in controlling co-transduction with multiple lentiviral vectors. Nevertheless, the trend observed over the reprogramming time was consistent between experiments and some conclusions may be drawn from this approach.

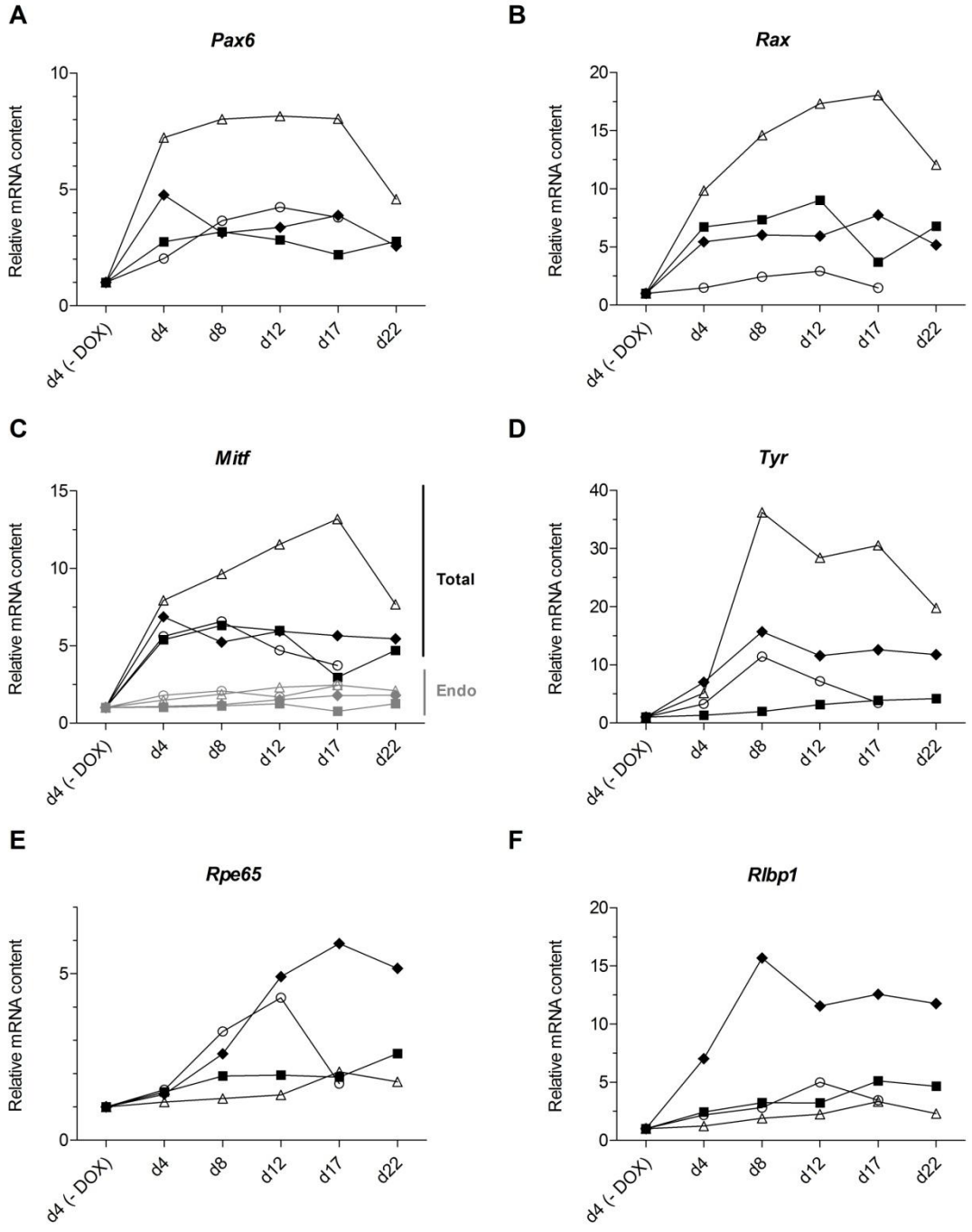

Figure 5.8: MEFs transduced with pool of inducible lentivirus encoding for the 10 Eye TFs display alterations in gene expression.

Quantitative RT-PCR analysis of transduced MEFs revealed expression of RPE-specific TFs (A- *Pax6*, B- *Rax*, C- *Mitf*) and markers (D- *Tyr*, E- *Rpe65* and F- *Rlbp1*) when cultured in the presence of DOX. For *Mitf* (C), 2 sets of primers were used. Top 4 black lines result from amplification with primers that do not distinguish viral from endogenous transcripts (Total). Primers that specifically amplify endogenous transcripts were also used (4 grey lines labelled as Endo). In all cases, *Gapdh* was used as endogenous control; results were normalized to d4 (-DOX). Four independent experiments were performed and displayed (4 lines with different symbols). For all analysed genes, it is observed an increase in mRNA content over time, as compared with control wells (d4 –DOX).

Pax6 and *Rax* mRNA levels increased in all experiments as expected, since these key TFs were included in the pool of transducing lentivirus (Figure 5.8A and B) and primers do not distinguish viral from endogenous expression. To analyse *Mitf* transcriptional levels however, 2 sets of primers were used. *Total Mitf* primers amplify transcripts from both viral and endogenous origin, whilst *Endo Mitf* primers specifically amplify the later (Figure 5.8C). As observed for *Pax6* and *Rax*, *Total Mitf* mRNA levels increase in all experiments since Lenti-TetO-V5-Mitf was included in the reprogramming cocktail. Importantly, endogenous levels of *Mitf* transcripts also increased in cells cultured in the presence of DOX, even though more discrete differences were attained.

Besides TFs involved in eye and RPE specification, mature RPE-specific genes were also analysed, such as *Tyr*, the rate-limiting enzyme responsible for pigment synthesis. *Tyr* transcripts were detected in higher amounts along the reprogramming protocol for all the experiments, despite variations between them (Figure 5.8D). Interestingly, higher values of *Tyr* mRNA levels were observed for the same experiment in which higher values of *Pax6*, *Rax* and *Total Mitf* (triangle-labelled line). Mitf protein has been known to physically interact with *Tyr* gene upstream regulatory sequences and to activate tyrosinase promoter which can explain observed results (Murisier and Beermann, 2006).

Visual cycle is a characteristic RPE function, essential for the recycling of retinal and for the maintenance of PRs' excitability. Relative mRNA levels of genes involved in this process, like *Rpe65* and *Rlbp1*, were also assessed (Figure 5.8E and F). Increased transcriptional levels were observed for both genes, for all the analysed time points.

Another relevant observation was related with the temporal profile of the detected alterations. Expression of TFs included in the transducing pool of lentivirus increased almost until the maximum values within the first 4 to 8 days. Contrarily, expression of RPE-specific markers was almost unaltered at 4 dpt, and increased in subsequent days (8, 12 or even 17 dpt). These genes were not encoded by the lentivirus and alterations at transcriptional levels were most probably due to exogenous TFs driven activation of RPE-specific expression profile. Moreover, for all the genes analysed there was no increase in expression after 17 dpt.

Notably, expression of Rpe65 was also confirmed at protein level by IF (Figure 5.9). At 22 dpt, Rpe65 characteristic cytoplasmic staining was observed specifically in transduced cells cultured in the presence of DOX.

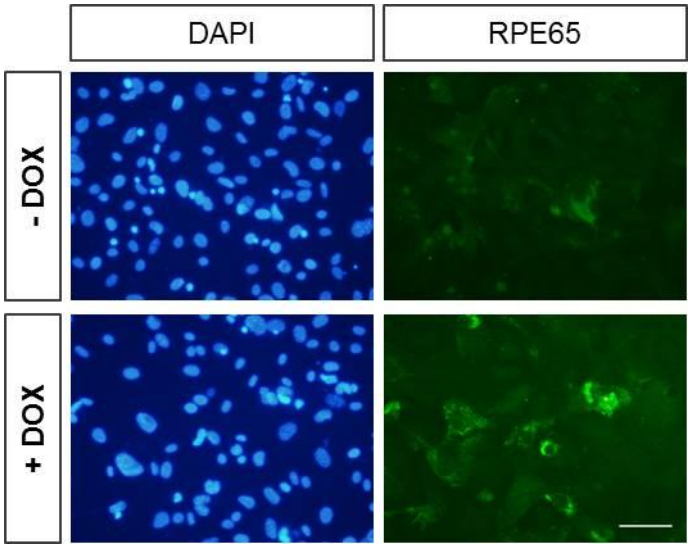

Figure 5.9: MEFs transduced with pool of inducible lentivirus encoding for the 10 Eye TFs express Rpe65 protein at 22 dpt.

IF analysis of transduced MEFs cultured in the presence (+) of DOX reveals a dotted and cytoplasmic staining for Rpe65 protein. Control cells (- DOX) were also analysed to exclude cellular auto-fluorescence due to prolonged time in culture. DAPI was used to counterstain nuclei. Scale bar 25 µm.

Lentiviral reporter systems drive expression of GFP protein in RPE cells

As just demonstrated, the forced expression of 10 Eye TF on fibroblasts induced alterations in terms of morphology and expression of key RPE markers. However, despite the encouraging results, the reprogramming process was quite variable between experiments. In an attempt to overcome this drawback and optimize the process' efficiency, a proper reporter system to better monitor cell fate conversion was desirable.

Two lentiviral reporter systems were generated with this purpose. Upstream regulatory regions of *Tyr* gene have been studied for long and a small fragment of 270 bp has been shown to be sufficient to drive specific expression on pigmented cells, both melanocytes and RPE cells (Klüppel et al., 1991). Besides this "minimal promoter", other regulatory regions were identified as regulators of Tyr expression, named initiator E-box and tyrosinase distal element (Aksan and Goding, 1998). A 2.2 kb promoter fragment of *Tyr* gene including all these regulatory regions was cloned into the upstream of GFP in a lentiviral vector (Lenti-Tyr-GFP). Upstream regions of *Rpe65* gene were also characterized and found to promote RPE-specific expression (Boulanger et al., 2000). A fragment containing bases -655 to +52 of the 5' flanking region of the mouse *Rpe65* gene was cloned into the upstream of GFP in a lentiviral vector, designated as Lenti-Rpe65-GFP (see Chapter 2 for details).

To test the functionality of the generated reporter systems, a human RPE cell line ARPE-19 was transduced with lentiviral particles from both systems (Figure 5.10) (Dunn et al., 1996). As both lentiviral vectors carry a blasticidin-resistance gene, blasticidin was added to the culture medium in order to select for transduced cells. First, exposure time and concentration of blasticidin required to kill untransduced ARPE-19 cells was determined by a MTT assay (Figure 5.10A). Secondly, transduced ARPE-19 cells were analysed by flow cytometry after selection with 16 µg/mL of blasticidin for 120 h. ARPE-19 cells produce pigment after long term and highly confluent cultures. However, even when cultured at normal confluency, GFP expressing cells were observed after transducing with Lenti-Tyr-GFP, as detected by flow cytometry (Figure 5.10B). A smaller percentage of GFP^+ cells was also detected after transduction with Lenti-Rpe65-GFP viral particles. ARPE-19 cells express RPE65 protein so promoter activation was expected in transduced cells. One hypothesis to explain the obtained result is that cloned Rpe65 promoter drives weak expression of GFP, which was hard to specifically detect. Alternatively, Rpe65 expression may also be dependent on the cell confluency, and highly confluent cultures should be tested. Nevertheless, the 2 generated reporter systems were driving expression of GFP protein in the context of a RPE cell line and could be used on the following experiments.

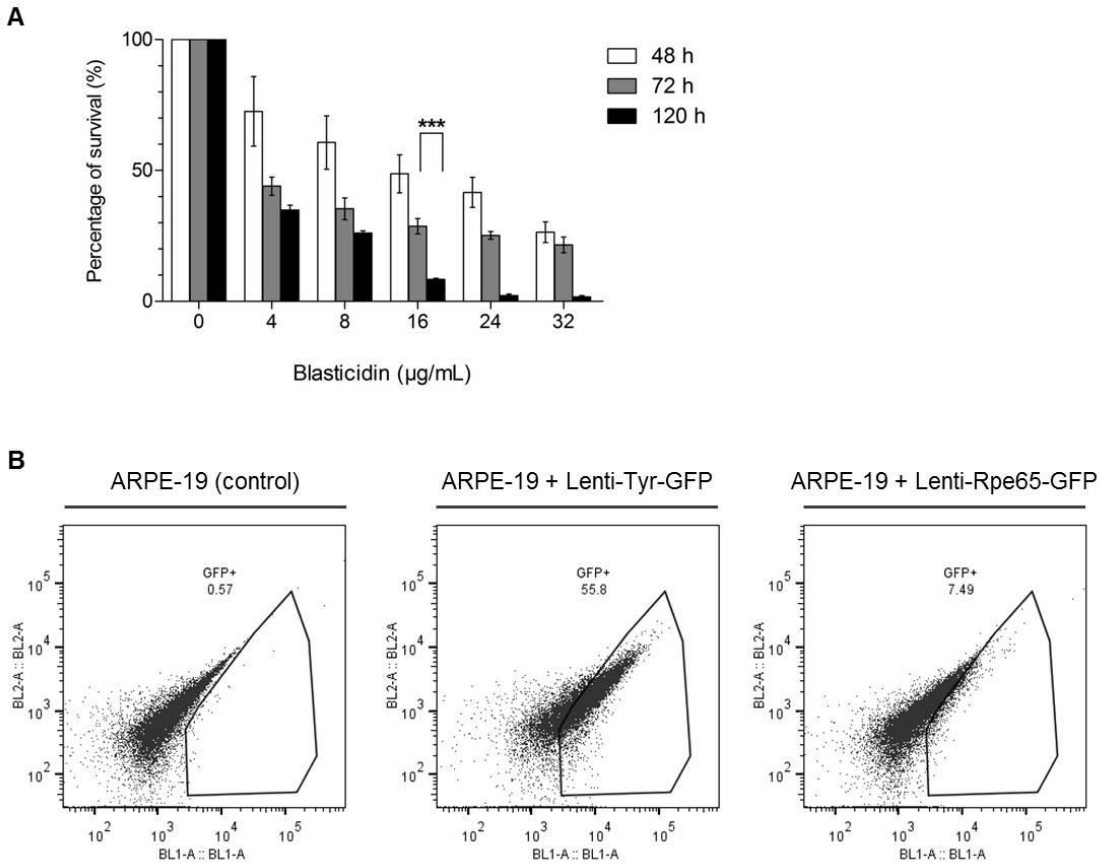

Figure 5.10: Human RPE cell line ARPE-19 transduced with lentiviral reporter systems express GFP protein.

(A) MTT assay was used to asses cell survival of ARPE-19 cells treated with increasing concentrations of blasticidin, for 48 h, 72 h or 96 h. Exposure to 16 µg/mL of blasticidin for 120 h promotes cell death of at least 90% of untransduced ARPE-19 cells. Mean value for these conditions is approximately 8% of cell survival and significantly different from 72 h exposure to the same concentration. Mean ± SD, n=3. Statistically significant values of relevant results from two-way ANOVA with Bonferroni posttest are shown; *** $p<0.001$. (B) ARPE-19 cells were transduced with Lenti-Tyr-GFP and Lenti-Rpe65-GFP lentiviral particles, cultured in the presence of blasticidin (16 µg/mL for 120 h) to select for transduced cells and analysed by flow cytometry to assess GFP protein expression at 7 dpt. Representative plots are shown, including on left panel control (untransduced) cells. GFP^+ cells, included in the defined gate on BL1 versus BL2 plots, are detected for both reporter systems: approximately 56% of GFP^+ cells for Lenti-Tyr-GFP and 8% for Lenti-Rpe65-GFP.

Lentiviral reporter systems can be used to optimize pool of direct reprogramming TFs

Taking advantage of obtained lentiviral reporter systems, a protocol was established with the intent of optimizing direct reprogramming strategy's efficiency.

First, MEFs were transduced with either reporter system (Lenti-Tyr-GFP or Lenti-Rpe65-GFP) and cultured in the presence of blasticidin to select for transduced cells. In order to determine appropriate exposure time and concentration of blasticidin, a MTT-based

cytotoxic assay was used (Figure 5.11). It was observed that treatment with 6 µg/mL of blasticidin for 72 h was sufficient to induce cell death of untransduced MEFs.

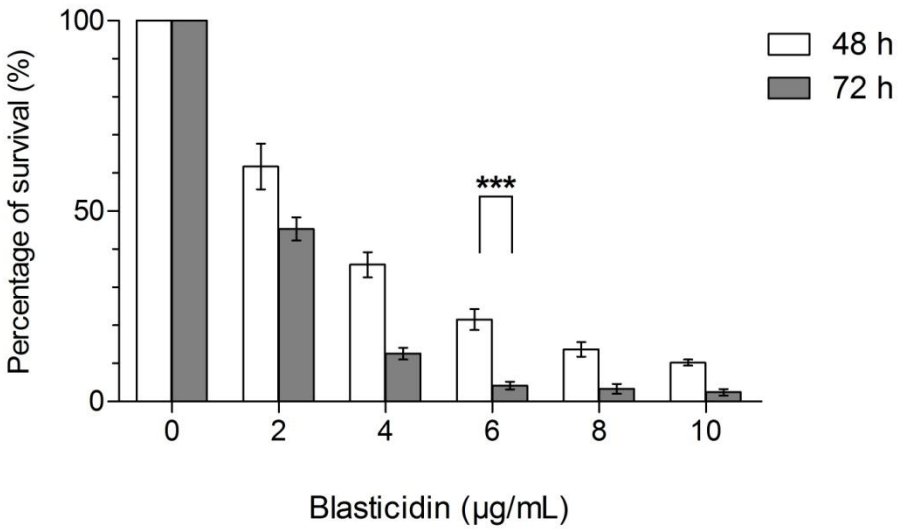

Figure 5.11: Untransduced MEFs' survival is affected by increasing concentrations of blasticidin.

MTT assay was used to asses cell survival of MEFs treated with increasing concentrations of blasticidin, for 48 h or 72 h. Exposure to 6 µg/mL of blasticidin for 72 h promotes cell death of at least 95% of untransduced cells. Mean value for these conditions is approximately 4% of cell survival and significantly different from 48 h exposure to the same concentration. Mean ± SD, n=3. Statistically significant values of relevant results from two-way ANOVA with Bonferroni posttests are shown; *** $p<0.001$.

After treatment with 6 µg/mL of blasticidin for 72 h, the blasticidin-resistant cells (which correspond to reporter system-transduced ones) were then co-transduced with inducible lentiviral particles Lenti-TetO-V5 Eye TF and reverse transactivator Lenti-M2rtTA. For each condition, cells cultured in the absence of DOX were kept in parallel as negative control, as shown in schematic protocol (Figure 5.12A). Different combinations of Eye TFs were tested, including the pool of 10 TFs used before. MEFs untransduced with the Eye TFs were also used as control. Given the relevance of Mitf, Otx2 and Pax6 in RPE specification (Martínez-Morales et al., 2004), these TFs were tested alone or in different combinations. Otx1 or Rax were also added to check if any positive interaction could occur (Figure 5.12B).

A

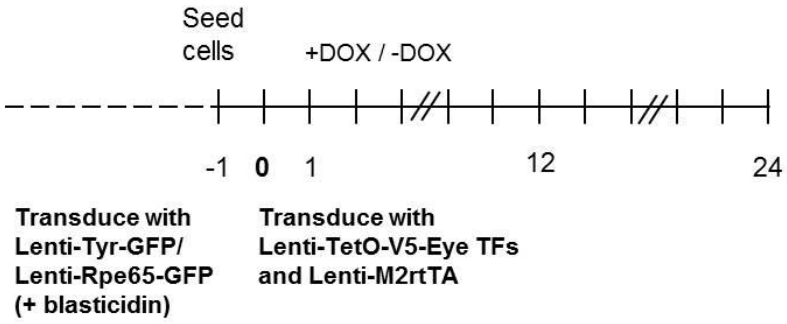

B

Tested conditions:		1	2	3	4	5	6	7	8	9	10
Lenti-TetO-V5-Eye TFs	Mitf	■			■	■		■	■	■	■
	Otx2		■		■		■	■	■	■	■
	Pax6			■		■	■	■	■	■	■
	Otx1								■		■
	Rax									■	■
	Six3										■
	Six6										■
	Lhx2										■
	Nr2e1										■
	Tbx3										■
Lenti-M2rtTA		■	■	■	■	■	■	■	■	■	■
Lenti-Tyr-GFP or Lenti-Rpe65-GFP		■	■	■	■	■	■	■	■	■	■

Figure 5.12: Direct reprogramming protocol using reporter systems to optimize transducing Eye TFs pool.

(A) Schematic representation of protocol. MEFs, previously transduced with lentiviral reporter systems (Lenti-Tyr-GFP or Lenti-Rpe65-GFP) and selected for positively transduced cells using blasticidin, were co-transduced with different combinations of the inducible lentivirus encoding Eye TFs and Lenti-M2rtTA (150 µL each). DOX was added to culture media at 1 dpt, except on control wells (- DOX). At 12 and 24 dpt, GFP levels were assessed by flow cytometry. (B) Summary table with different combinations of transducing Eye TFs tested. Each column of the table represents one combination of Eye TFs tested, with either reporter system. Dark grey boxes indicate lentiviral particles used in each of the 10 conditions tested.

For each reporter system, 10 different combinations of Eye TFs were tested in cells cultured in the presence of DOX, as well as in the absence of DOX (control). GFP expression driven by either reporter system was assessed at 12 and 24 dpt by flow cytometry analysis, using GFP (BL1 axis) versus auto-fluorescence (BL2 axis) to discriminate true GFP expression from auto-fluorescence derived from long culture periods.

Regarding activation of Tyrosinase promoter, cells transduced with tested individual TFs cultured in the presence of DOX did not display GFP levels significantly different from corresponding controls (absence of DOX). However, a discrete population of GFP^+ cells was detected for both Mitf and Otx2 (mean values for 12 dpt were approximately 1%), but not for Pax6 (Figure 5.13A). Additionally, combinations of 2 Eye TFs, revealed that Mitf and Otx2 synergistically activate Tyrosinase promoter with 4% of GFP-expressing cells (mean value for 12 dpt) being detected. These observations are in accordance with described Mitf and Otx2 ability to bind to the promoter regions of genes important for melanogenesis, namely *Tyr*, leading to their transactivation. Moreover, activation by Otx2 has been shown to be enhanced by Mitf, with which Otx2 biochemically interacts (Martínez-Morales et al., 2003a; Reinisalo et al., 2012).

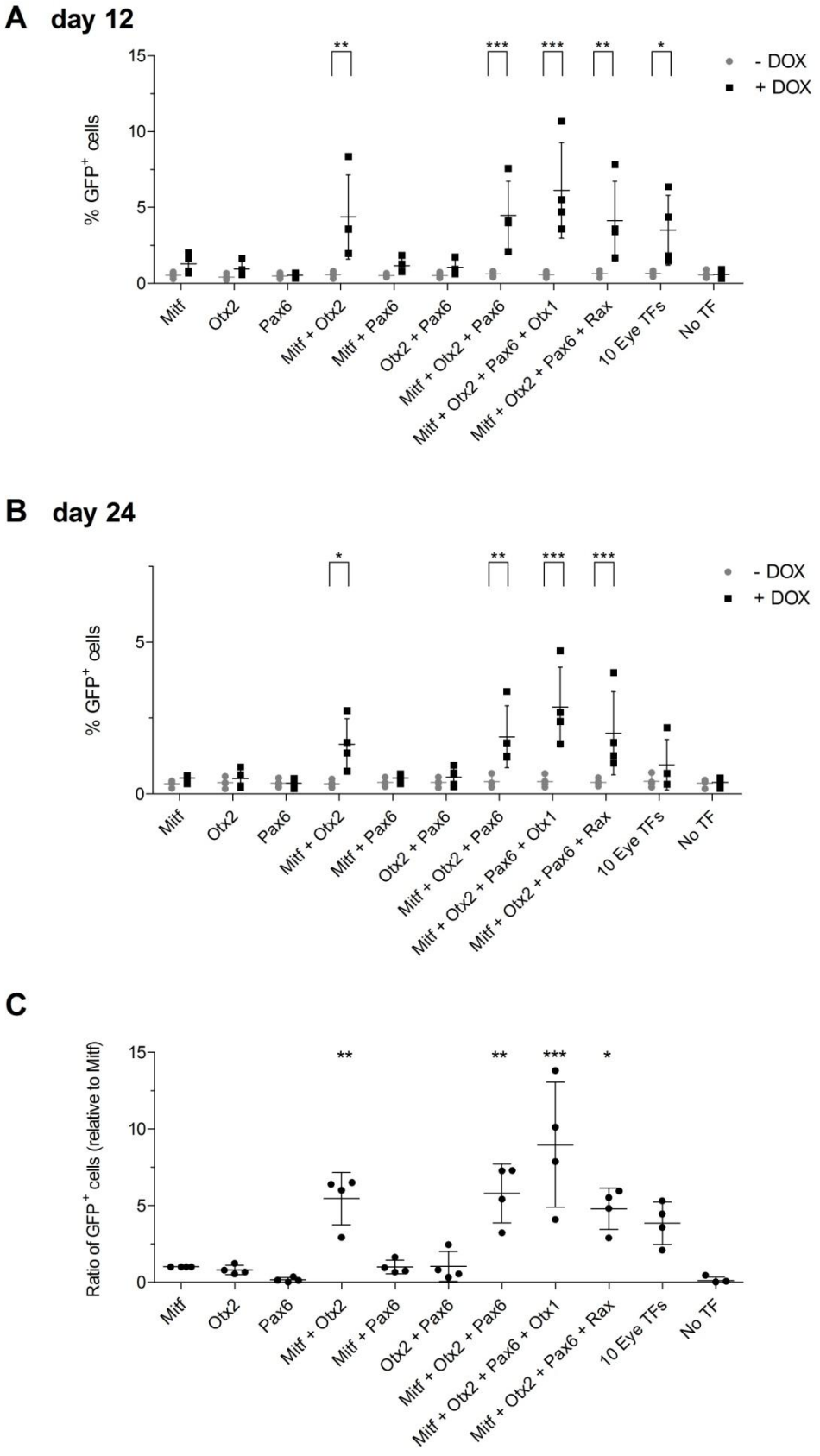

(See caption on the following page)

Figure 5.13: Different pools of transducing Eye TFs promote variable levels of activation of Tyrosinase promoter.

(A) Flow cytometry analysis was used to quantify percentage of GFP^+ cells. Different combinations of Eye TFs were used to transduce MEFs, previously transduced with Lenti-Tyr-GFP reporter system. For each combination, cells were cultured either in the presence (+) or absence (-) of DOX. Results for 12 dpt show that 5 combinations promote GFP levels significantly different from corresponding control condition (- DOX) as denoted. (B) Results for 24 dpt show that 4 combinations promote GFP levels significantly different from corresponding control condition (- DOX) as indicated. Scatter dot plots with mean ± SD, n=4; two-way ANOVA with Bonferroni posttests. (C) For 12 dpt, ratio of GFP+ cells was calculated by first subtracting % of GFP+ cells obtained for control (- DOX) condition and then dividing by the value obtained for Mitf alone as transducing Eye TF in the corresponding experiment. Results point that Mitf+Otx2, Mitf+Otx2+Pax6, Mitf+Otx2+Pax6+Otx1 and Mitf+Otx2+Pax6+Rax combinations yield higher GFP levels when compared to control (Mitf alone). Scatter dot plots with mean ± SD, n=4; one-way ANOVA with Dunnett's multiple comparison test; *** $p<0.001$, ** $p<0.01$, * $p<0.05$.

Combinations of 3, 4 or all 10 TFs were also tested and generated a percentage of GFP^+ cells significantly different from corresponding controls (absence of DOX) (Figure 5.13A). All these combinations included the core Mitf+Otx2 mix and extra TFs. Despite some variability when comparing values between experiments, in all cases the Mitf+Otx2+Pax6+Otx1 pool of transducing lentivirus produced a bigger population of GFP^+ cells than Mitf+Otx2 (or Mit+Otx2+Pax6) pool for the same independent experiment (see representative flow cytometry plots for 12 dpt in Figure 5.14). It is known that the homeodomain-containing TFs Otx1 and Otx2 are expressed in the OV and later in the presumptive RPE. Experiments with *Otx1* and *2* double-deficient mice showed that these genes are required in a dose-dependent manner for the normal development of the eye, and in their absence an improperly patterned RPE differentiates into a NR-like structure (Martinez-Morales et al., 2001).Thus, these cooperative activity of *Otx* genes might explain the slight increase in the percentage of GFP^+ cells observed when Otx1 was added to the pool.

Regarding the 2 experimental timepoint analysed, equivalent results were observed for 12 dpt (Figure 5.13A) and 24 dpt (Figure 5.13B). Nevertheless the population of GFP-expressing cells was smaller for the latter timepoint, suggesting that the observed alterations occur with a fast kinetics and that prolonged culture times have no advantage for the process. Given this observation and the mentioned Mitf key role, the ratio of GFP^+ cells relative to Mitf alone was also determined for 12 dpt (Figure 5.13C). Combination of Mitf+Otx2 and also Mitf+Otx2+Pax6, Mitf+Otx2+Pax6+Otx1 or Mitf+Otx2+Pax6+Rax yielded a higher ratio of GFP^+ cells, when comparing to control (Mitf alone), thus promoting a more efficient activation of Tyrosinase promoter.

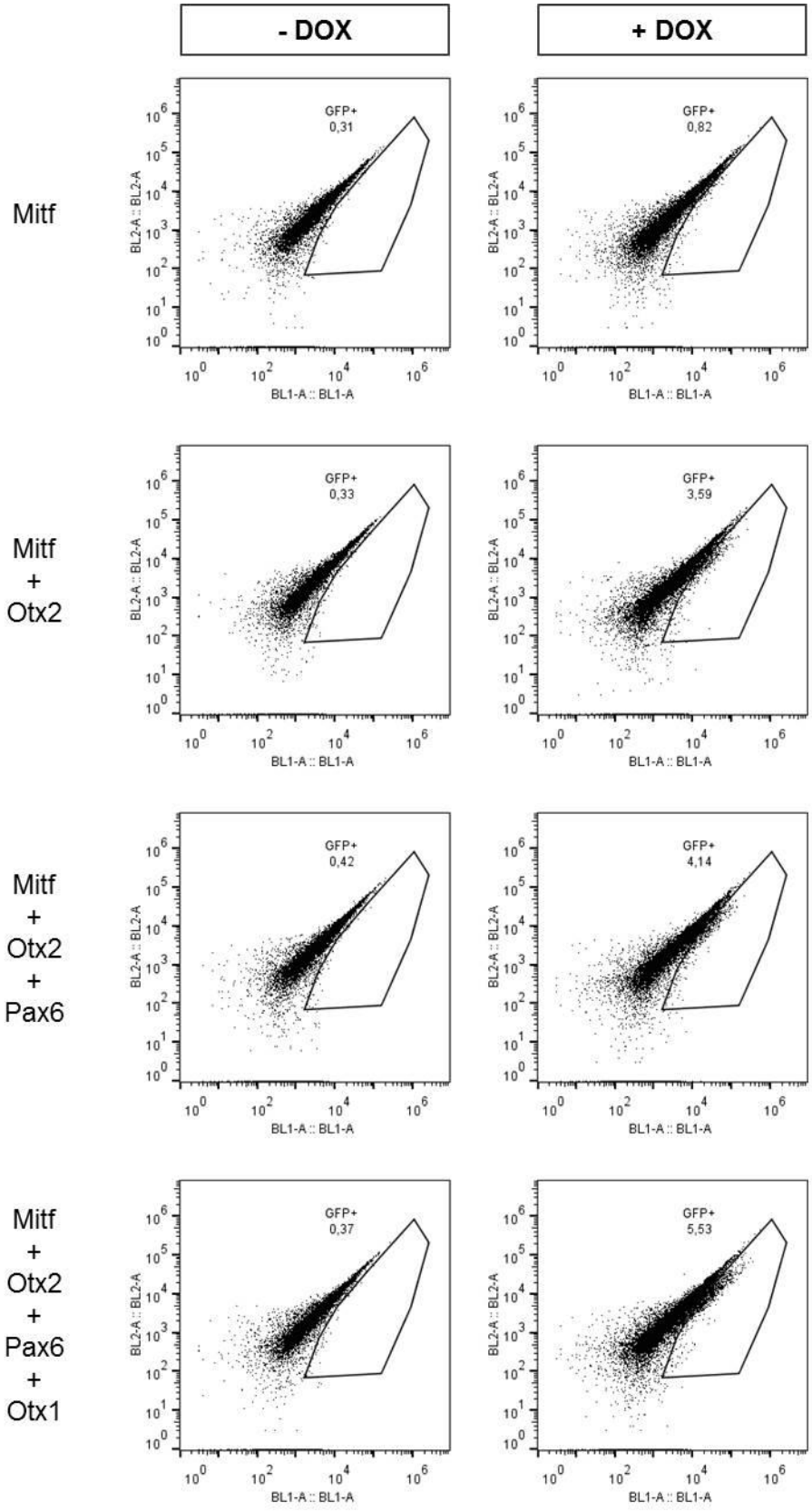

(Figure continues on the following page)

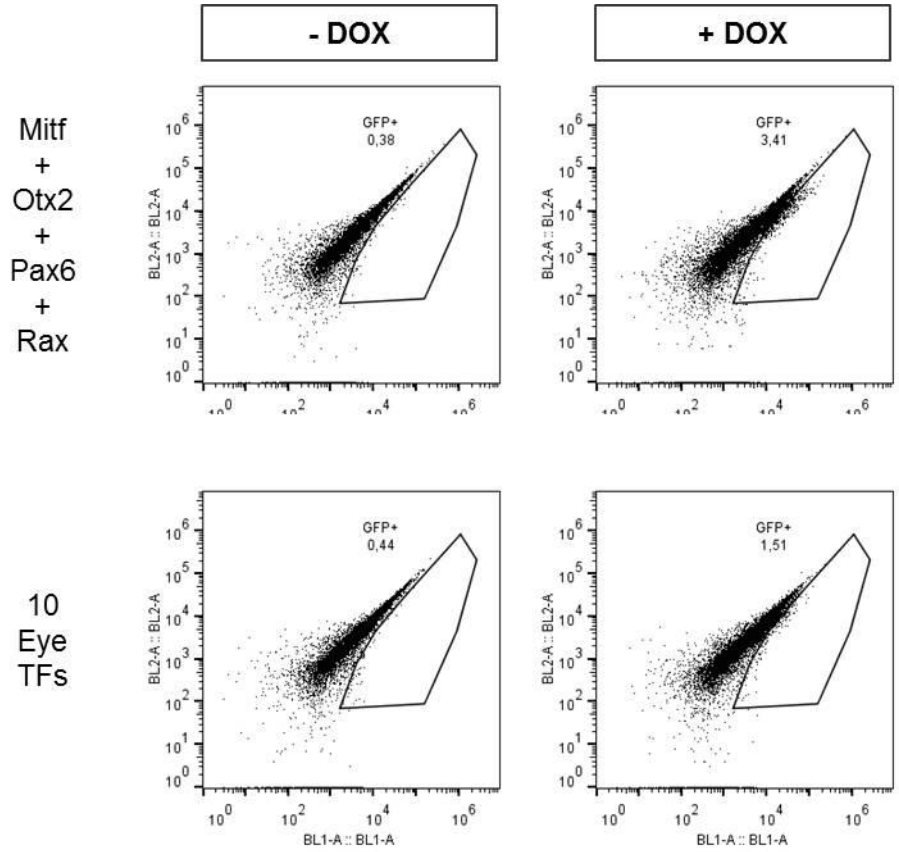

Figure 5.14: Pools of transducing Eye TFs including Mitf promote variable levels of activation of Tyrosinase promoter.

Representative flow cytometry plots of Lenti-Tyr-GFP-transduced MEFs at 12 dpt with different combinations of Lenti-TetO-V5 Eye TFs, as mentioned. Cells were cultured in the presence (+) or absence (-) of DOX and percentage of GFP^+ cells was determined in BL1 versus BL2 plots (notice differences in gated population).

Similar experiments were performed to evaluate activation of Rpe65 promoter by different pools of Eye TFs. However, the percentage of GFP^+ cells was not significantly different when comparing cells cultured in the presence of DOX (in which the Eye TF expression was induced) with control cells (absence of DOX). This was true for either 12 dpt (Figure 5.15A) and 24 dpt analysis (Figure 5.15B). Nevertheless, for the pool of 10 Eye TFs a discrete activation of Rpe65 promoter might occur since a small population of GFP-expressing cells was identified (Figure 5.16). This result was concordant with the previously shown expression of Rpe65, at a transcriptional and protein level, after transduction with the pool of 10 lentivirus (recall Figure 5.8E and Figure 5.9).

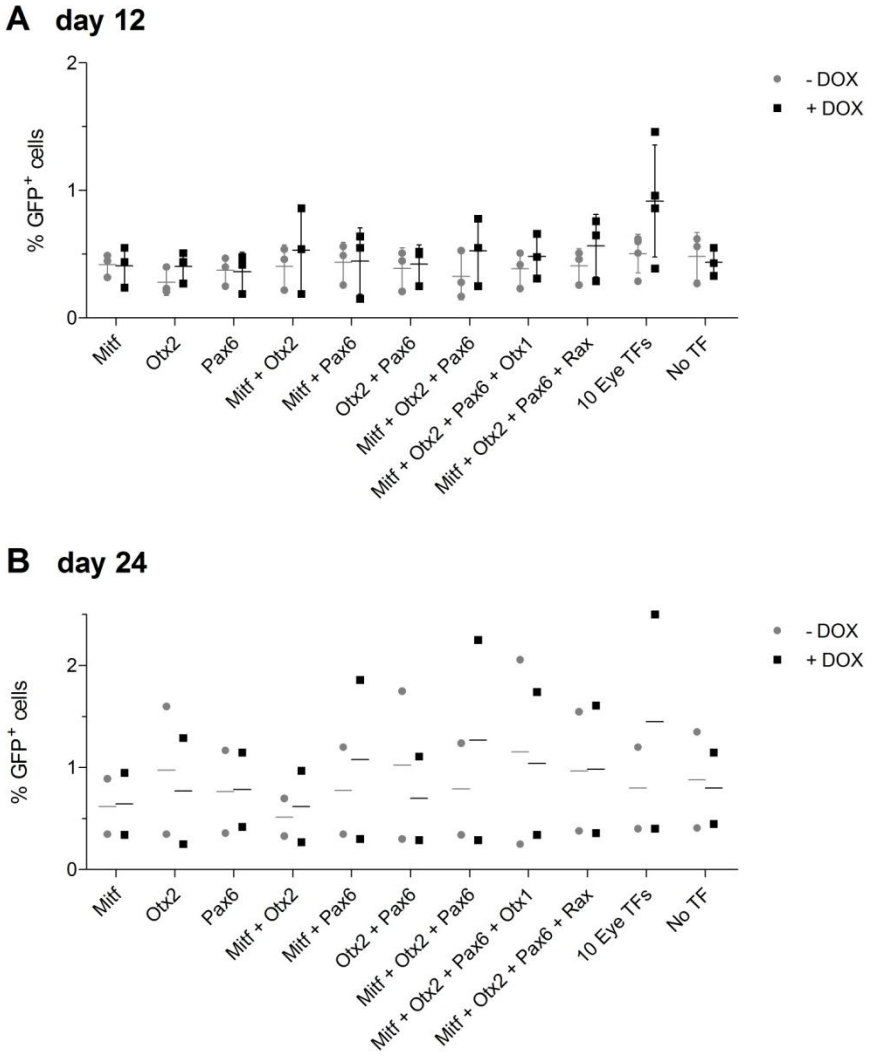

Figure 5.15: Different pools of transducing Eye TFs promote discrete levels of activation of Rpe65 promoter.

(A) Flow cytometry analysis was used to quantify percentage of GFP^+ cells. Different combinations of Eye TFs were used to transduce MEFs, previously transduced with Lenti-Rpe65-GFP reporter system. For each combination, cells were cultured either in the presence (+) or absence (-) of DOX. Results for 12 dpt show that no combination promote GFP levels significantly different from corresponding control condition (- DOX) as denoted. Scatter dot plots with mean ± SD, n=3; two-way ANOVA with Bonferroni posttests. (B) Results for 24 dpt show that no combination promote GFP levels significantly different from corresponding control condition (- DOX) as indicated. Scatter dot plots with mean ± SD, n=2; two-way ANOVA with Bonferroni posttests.

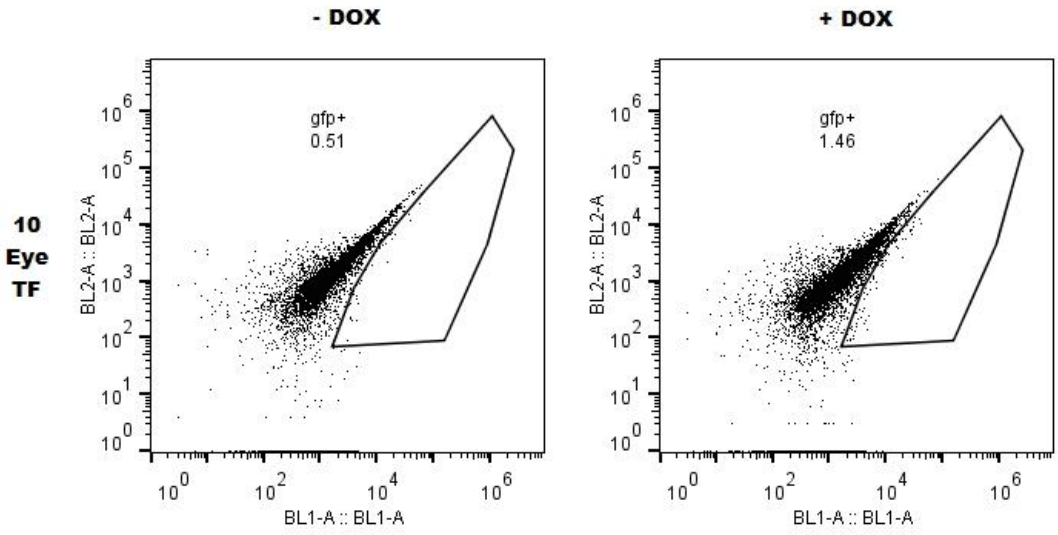

Figure 5.16: Transduction with pool of 10 Eye TFs promotes discrete levels of activation of Rpe65 promoter.

Representative flow cytometry plots of Lenti-Rpe65-GFP-transduced MEFs at 12 dpt with pool of 10 Lenti-TetO-V5 Eye TFs. Cells were cultured in the presence (+) or absence (-) of DOX and percentage of GFP^+ cells was determined in BL1 versus BL2 plots (notice differences in gated population).

Rpe65 promoter was characterized and was shown to drive tissue-specific expression in the RPE, which could be valuable for gene therapy studies (Acland et al., 2005; Boulanger et al., 2000; Nicoletti et al., 1998). Nonetheless, its transcriptional activity was shown to be weak (Zhang et al., 2004). Moreover, only a few studies have addressed the regulatory mechanisms that regulate expression of *Rpe65* gene. For instance, Otx2 and Lhx2 were shown to synergistically activate Rpe65 promoter, along with other factors, which can account for the subtle activation observed for the pool of 10 TFs (the only pool including Lhx2) (Masuda et al., 2014). Therefore, additional combinations of TFs can be tested in order to optimize Rpe65 promoter activation. Positive insight on the regulation of *Rpe65* expression can also be drawn from such experiments.

Discussion

Cellular reprogramming experiments have highlighted the plasticity of adult somatic cells, providing new technologies for the generation of any desired cell types. Through the forced expression of TFs, it was possible to reprogram somatic cells into iPS cells that share pluripotency features with ES cells and can be differentiated into any adult somatic cell (Takahashi and Yamanaka, 2006; Takahashi et al., 2007a). Alternatively, but also

using a TF-mediated approach, a somatic cell can be interconverted into another somatic cell type. In this direct lineage conversion methodology, no pluripotent/multipotent intermediate is formed (Ladewig et al., 2013). Direct lineage conversion has proven successful to reprogram mouse and human fibroblasts into several cell types, using TFs defining or specifying the target-cell identity (Huang et al., 2011; Ieda et al., 2010; Vierbuchen et al., 2010). Here we report a set of experiments performed towards the goal of direct reprogramming mouse fibroblasts into functional RPE cells.

Firstly, morphology and gene expression parameters were analysed using primary mouse RPE cultures in order to establish the criteria for the proper distinction between the initial fibroblastic population and the target cell to be obtained, RPE cells. Secondly, after a thorough literature review (see Chapter 1), a set of TFs was selected based on their described role on the establishment of early EF (*Rax, Pax6*, *Six3*, *Six6*, *Lhx2, Nr2e1* and *Otx2*) as well as in subsequent steps of RPE cell fate specification and maintenance (*Mitf*, *Otx2, Otx1* and *Pax6*). Commonly used in reprogramming experiments due to the high efficiency and possibility to timely control the forced expression, an inducible lentiviral system was elected for the delivery of the 10 chosen TFs. Entry vectors encoding for V5-tagged versions of the 10 Eye TFs and a lentiviral plasmid containing an inducible promoter and recombination sites compatible with Invitrogen's Gateway® Technology were generated. After the recombination reactions, 10 inducible lentiviral vectors encoding for V5-tagged versions of the 10 Eye TFs were generated, as well as a control Lenti-TetO-GFP vector. The obtained molecular tools were shown to efficiently transduce MEFs and to force the expression of V5-Eye TFs upon addition of DOX. Subsequently, the experimental conditions for multiple transductions of MEFs were optimized and defined using the control vector, in order to guarantee no effect on cell viability while maximizing the efficiency. With the adopted protocol, in single transductions one can anticipate approximately 31% of transduced cells, as it was observed for the control Lenti-TetO-GFP vector.

Reprogramming experiments were performed using a pool containing viral particles encoding for the 10 Eye TFs. Transduced MEFs were monitored for alterations in morphology and gene expression, and pigmented cells were detected as soon as 8 dpt. Regarding transcriptional alterations, an expected increase on the expression of transduced TF was observed, concomitantly with an up-regulation of RPE-specifying TF *Mitf* and mature RPE markers (*Tyr*, *Rpe65*, *Rlbp1*). Rpe65 was also detected at a protein level on transduced cells. Interestingly, the pigmentation and gene expression alterations observed between 8-12 dpt revealed that reprogramming events were taking place with

a rapid kinetics. On described direct lineage conversion methodologies, high levels of expression of TFs must be capable of surmounting the genetic and epigenetic landscape of the original cell fate, forcing the establishment of a new program typical of the target cell to be obtained. Mechanistically, the reprogramming events take place in a short period of time after the forced expression of the set of TFs and occur in the absence of cellular proliferation, contrarily to what is observed for iPS cell generation (Sancho-Martinez et al., 2012). Thus, the observed alterations occurring with a rapid kinetics are optimistic indicators that a reprogramming process may be taking place.

In order to facilitate the identification/selection of the obtained RPE-like cells, as well as to optimize the cocktail of reprogramming TFs to provide an increased efficiency of the process, two lentiviral reporter systems were generated. *Tyrosinase* and *Rpe65* upstream regulatory regions were cloned into lentiviral vectors that elicited the expression of GFP protein in a RPE-specific manner, as confirmed after transducing a RPE cell line (Aksan and Goding, 1998; Boulanger et al., 2000). Different combinations of the 10 Eye TFs were used to transduce MEFs previously transduced with either reporter system, and resultant GFP expressing cells were quantified. For the Rpe65 reporter system, only discrete levels of GFP expression were observed for the pool of 10 Eye TFs, which was consistent with *Rpe65* upregulation previously mentioned. Additional combinations of TFs should be tested in an attempt to potentiate Rpe65 promoter activation.

Conversely, GFP expression driven by tyrosinase promoter was specifically detected in transduced cells cultured in the presence of DOX for several tested combinations, namely the pool of 10 Eye TFs, Mitf+Otx2, Mitf+Otx2+Pax6, Mitf+Otx2+Pax6+Otx1 and Mitf+Otx2+Pax6+Rax. These results were in accordance with the pigmented cells observed for the previously tested pool of 10 Eye TFs, given that tyrosinase is the rate-limiting enzyme responsible for melanin synthesis (Murisier and Beermann, 2006). Interestingly to notice, during the preparation for flow cytometry analysis, the cells' pellet from some combinations of TFs were noticed to possess a more brownish appearance when compared with the control sample (absence of DOX), which correlates with pigment synthesis and tyrosinase promoter activation. Another interesting evidence was that *Mitf* and *Otx2* cooperatively activate the tyrosinase promoter, as already described, thus confirming the functionality and applicability of the established system (Martínez-Morales et al., 2003b; Murisier et al., 2007). All the mentioned combinations containing the core Mitf+Otx2 generated higher degree of tyrosinase promoter activation when comparing to single transduction of Mitf. Further experiments will be performed in order to clarify the probable increased activation observed for Mitf+Otx2+Pax6+Otx1 compared

with Mitf+Otx2 (or Mitf+Otx2+Pax6) and to investigate the roles of Pax6 and Otx1. Relevantly, it was reported that Pax6, in cooperation with Mitf, has an anti-retinogenic effect in the presumptive RPE. In a Mitf mutant background, Pax6 was critical for early RPE development, as in heterozygous mice for a *Pax6* functional null allele down-regulation of RPE genes (including *Tyr*) was observed (Bharti et al., 2012). Moreover, more recently it was shown that Pax6 both controls the expression of an RPE isoform of *Mitf* and synergizes with Mitf to activate expression of genes involved in pigment biogenesis (Raviv et al., 2014). Regarding Otx1, it was shown that both *Otx* genes are required in a dose-dependent manner for the normal development of the eye and that once mutated the OV fails to invaginate properly and the expression of *Mitf* and *Tyr* is lost (Martinez-Morales et al., 2001).

With this reporter system, we were able to minimize the pool of reprogramming TFs obtaining either equivalent or even higher levels of tyrosinase activation when compared with 10 Eye TFs pool. Average values of around 4% of GFP^+ cells for Mitf+Otx2 were detected at 12 dpt, consistent with a desired rapid kinetics of reprogramming. A similar system with an antibiotic-resistance gene expression driven by the tyrosinase promoter can be easily employed to allow the selection of this population and further characterization. Moreover, one cannot exclude that other TFs would further potentiate the reprogramming process, which can be tested in future experiments. Explicitly, Sox9 has been implied as a key regulator of the expression of several RPE genes, such as *Best1* and visual cycle genes (*Rpe65*, *Rlbp1* and *Rgr*) (Masuda and Esumi, 2010; Masuda et al., 2014). Also, the Pax-family member Pax2, which is co-expressed with Pax6 in the OV stage, has been shown to perform redundant activities along with Pax6. Together, Pax6 and Pax2 are required and sufficient to direct the early patterning of the RPE, probably by directly controlling the expression of RPE determinants (such as Mitf) (Baumer et al., 2003). Additionally, the genomic organization of *Mitf* gene allows generation of multiple mRNA (and resulting protein) isoforms with specific patterns of expression due to different promoter/exon usage. Besides Mitf-A isoform used in this study, Mitf-H, Mitf-J and Mitf-D are also expressed at OV stage in presumptive RPE and later on mature RPE cells, and the inclusion of such isoforms in the reprogramming cocktail might be advantageous (Bharti et al., 2008).

Nevertheless further experiments to optimize and confirm the generation of RPE-like cells through a direct lineage conversion are in order, relevant steps were undertaken towards this final goal. More straightforwardly our lentiviral reporter system may allow us to investigate the gene regulatory network underlying RPE development and specification. Additionally, lineage conversion-derived RPE cells will provide new

opportunities for cell replacement strategies, much desired for the establishment of a therapeutic alternative for retinal degenerative disorders. RPE cells are also valuable tools for disease modelling and basic developmental studies. Recently, Zhang and colleagues claimed that fibroblasts were directly converted into RPE-like cells using a pool of retrovirus encoding for 8 TFs. This pool of TFs included 6 eye/RPE-related TFs but also Klf4 and c-Myc, and promoted the activation of a Bestrophin reporter system and some morphologic alterations. No alterations in reporter activation or morphology were observed with pools including only the eye/RPE-related TFs. This approach also comprised the addition of small molecules known to promote RPE differentiation: the obtained cells arose after more than 12 dpt, were actively proliferating and did not exhibit a molecular signature compatible with mature RPE cells. Interestingly, *Tyr* expression was not detected in these cells reported as pigmented (Zhang et al., 2013) and thus, the reported results still raise several questions.

In addition to the abovementioned experiments described in this thesis, another promising strategy to obtain RPE cells is also been tackled as an alternative to iPS cell generation followed by differentiation and by direct lineage conversion. Recent reports stated that indirect lineage conversion has successfully generated cardiomyocytes, neural and mesodermal progenitor cells from fibroblasts (Efe et al., 2011; Kim et al., 2011; Kurian et al., 2013). This plastic induction strategy relies on the transient expression of TFs used for iPS cell generation, promoting an “open” epigenetic landscape. The process occurs via de-differentiation with the generation of proliferating multipotent, partially reprogrammed intermediates. These unstable intermediate states can be subsequently committed into a differentiation state by exposure to developmental cues, either extracellular signals or late-identity specification TFs (Ladewig et al., 2013; Sancho-Martinez et al., 2012). Lineage conversion by plastic induction may be a possible complementary strategy to allow us to reach our final goal of efficiently obtaining RPE cells.

To summarize, several molecular tools were generated and used to transduce MEFs. Promising outcomes were observed, such as pigmentation and up-regulation of RPE-specific genes, suggesting that RPE transcriptional and cellular identity was successfully being induced. Furthermore, 2 reporter systems were also developed, allowing the optimization of the cocktail of reprogramming TFs and the identification of reprogrammed cells. Additionally, positive insights on the RPE gene regulatory mechanism were drawn from the described experiments and will be further examined. We are now a step closer to the proposed objective of obtaining RPE cells by direct conversion of fibroblasts. When compared to the differentiation of pluripotent cells into RPE, this direct approach

may be useful as a fast and hopefully more efficient alternative to obtain functional RPE cells for therapeutic and disease modelling purposes.

Chapter 6 Concluding remarks and future perspectives

Chapter 6 : Concluding remarks and future perspectives

Cellular reprogramming strategies have profoundly changed the dogmatic concept that adult somatic cell identity was stably determined along the differentiation process in an irreversible and unidirectional way. In particular, seminal discoveries by Yamanaka and colleagues, demonstrating that forced expression of TFs could trigger the reprogramming of a somatic cell into an ES cell-like pluripotent state, inspired scientists in a global quest for a better mechanistic understanding, improved efficiency and broader applicability of this Nobel awarded finding (Takahashi and Yamanaka, 2006; Takahashi et al., 2007a). In addition to reprogramming into pluripotency, somatic cell can be successfully directly reprogrammed into a different somatic cell type through the forced expression of specific TFs, as was first demonstrated with lineage conversion of fibroblasts into functional neurons (Vierbuchen et al., 2010).

These reprogramming discoveries have particularly contributed to the regenerative medicine field, as cell sources for prospective cell replacement therapies. Ophthalmic applications have been at the forefront of the drive for clinical translation, given the clinical accessibility of the visual system, its ability to be functionally monitored with noninvasive imaging techniques after a therapeutic intervention, and its relative isolation from other body systems and immune privilege (Bharti et al., 2014; Ramsden et al., 2013). Notwithstanding retina's complex structure, many pathological conditions affecting it and causing visual impairment can be attributed to the degeneration of a relatively simple epithelial monolayer: the RPE. RPE cells perform a multitude of support functions essential to maintain visual function, such as retinol recycling, light absorption, ion buffering, secretion of growth factors, nutrient transport and phagocytosis of the OS of PR cells (Sparrrow et al., 2010; Strauss, 2005). Several retinal degenerative disorders, namely AMD, RP and Stargardt's disease, as well as rare disorders such as CHM, are characterized by an RPE degeneration underlying the pathological process and affect millions of people worldwide with no available curative treatment. Cell replacement of RPE, obtained from different sources (such as ES cells) has been shown to at least partially rescue visual function in such conditions (Ramsden et al., 2013).

Despite the first evidence for the generation of disease-specific iPS cells with valuable therapeutic potential was established for sickle-cell anemia, one could envision such proof-of-concept experiments being applied in the context of retinal disorders (Figure 6.1) (Hanna et al., 2007). In fact, in 2011 Meyer and colleagues corrected the mutation in the gene causing gyrate atrophy (a rare retinal degenerative disorder) in iPS cells, which

were subsequently differentiated into RPE cells that no longer displayed the disease phenotype (Meyer et al., 2011).

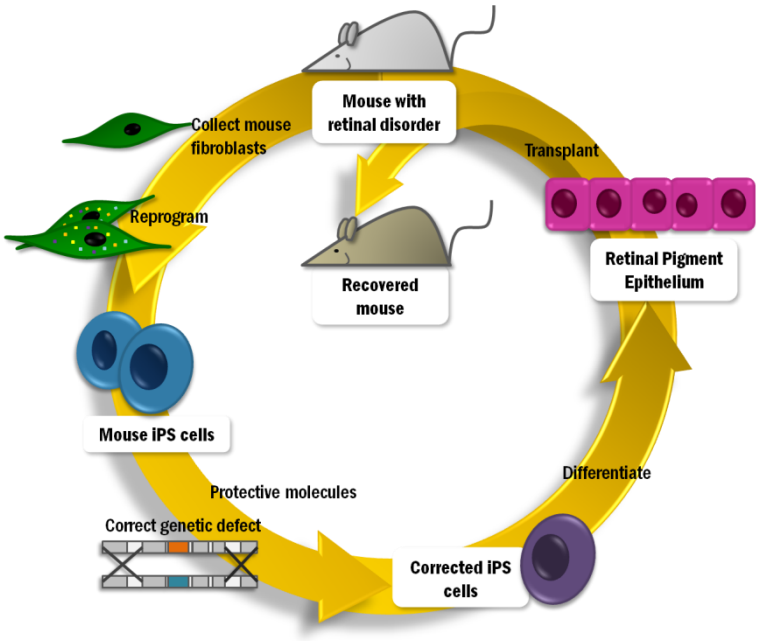

Figure 6.1: Proof-of-concept experiments to confirm the therapeutic potential of iPS cell-based approaches in a mouse model of retinal degenerative disorder.

Mouse fibroblasts can be reprogrammed into pluripotent iPS cells. In the case of genetic disorders, genetic correction is needed to provide disease-free iPS cells. Alternatively, iPS cells could be genetically manipulated to deliver protective molecules with therapeutic advantages. Pluripotent cells can then be differentiated into functional RPE cells, which can be transplanted into the diseased retina and hopefully, contribute to its recovery.

Furthermore, reprogramming strategies also allow the generation of valuable disease models which can be used to comprehensively dissect the molecular events responsible for the pathological condition, still mostly unknown in the case of CHM. Disease modelling studies also permit to investigate the therapeutic potential of new drugs and treatments (Bellin et al., 2012).

In this context, the work presented in this thesis aimed at exploiting cellular reprogramming strategies for cell-based therapies and disease modelling studies focusing on retinal degenerative disorders with underlying RPE dysfunction, particularly in the case of CHM. Two major approaches were undertaken: first, iPS cell generation followed by differentiation into the desired cell type (RPE cells), using both WT and Chm cells; second, direct lineage conversion of fibroblasts into RPE cells.

iPS cell technology was successfully implemented, opening new research possibilities in the case of the present study and also in other studies ongoing in the laboratory. WT

MEFs were subjected to a reprogramming protocol, using an inducible lentiviral system to provide forced expression of the 4 classic reprogramming factors (Oct4, Sox2, Klf4 and c-Myc) (Carey et al., 2009). Morphological and gene expression alterations (up-regulation of *Endo Oct4*, *Nanog* and *Fgf4*) confirmed that the reprogramming events were taking place. Also endogenous protein levels of Nanog and SSEA-1 were detected and AP positively stained arising colonies with ES cell-like morphology were observed. Using LIF+2i culture conditions to allow a full reprogramming process with the attainment of "ground-state" pluripotency (Silva et al., 2008), emerging colonies gave rise to several iPS cell clones, which demonstrated self-renewal properties in a transgene independent way. The obtained iPS cell lines also exhibited typical morphology in culture and gene and protein expression of key pluripotent markers, particularly confirming a naïve pluripotent state. Using both *in vivo* and *in vitro* differentiation assays, functional pluripotency was confirmed by the generation of cells from endoderm, mesoderm and ectoderm lineages. Non-integrative delivery system (adenovirus) of the reprogramming factors was also attempted, although unsuccessfully, in order to implement a strategy with a potential therapeutic advantage. Nevertheless, for other final purposes, such as disease modelling studies, the inducible lentiviral system is still widely used given its high efficiency and reproducibility. Additionally, albeit being an integrative method, genomic integration was minimized by the use of a polycistronic unit encoding for the 4 TFs (Carey et al., 2009). Thus, iPS cell generation was successfully attained, providing a new technological platform that can be explored to answer a panoply of research questions.

The implemented reprogramming protocol was then applied to Chm cells. CHM is an X-linked monogenic disorder caused by loss of function of *CHM/REP1* gene. REP1 protein encoded by this gene is a key regulator of Rab GTPases activity, essential for intracellular trafficking events. CHM is characterized by a progressive degeneration of three retinal cell layers, RPE, PRs and choroid, with a complex and still largely unknown pathology (van Bokhoven et al., 1994; Coussa and Traboulsi, 2012). Evidence points out for a key role of the RPE cells in the degenerative events, with consequent therapeutic advantage of rescuing RPE function, eventually through cell replacement (Tolmachova et al., 2013). A conditional KO mouse model was used in the reprogramming experiments. MEFs were treated with TM to induce recombination events, with obtained Chm^{null} cells demonstrating reduced *Rep1* expression. Control Chm^{flox} cells (untreated with TM) express Rep1 and were used in parallel during the reprogramming events. Both Chm^{null} and Chm^{flox} MEFs were successfully reprogrammed using the inducible lentiviral system encoding for OSKM. Several Chm^{null} and Chm^{flox} iPS cell lines were generated, expanded and characterized morphological, molecular and functionally as mentioned for

WT cells. Besides the confirmation of self-renewal and pluripotency attributes, *Chm*^{null} and *Chm*^{flox} iPS cell lines were analysed in terms of Rep1 expression, at both transcriptional and protein levels. *Chm*^{null} iPS cell lines had reduced Rep1 expression when compared to *Chm*^{flox} iPS cell lines, thus validating a proper Rep1 KO to be potentially used as a Chm model.

Subsequently, *Chm*^{null}, *Chm*^{flox} and WT iPS cell lines were subjected to three differentiation protocols in order to obtain RPE cells, selected from the multitude of protocols for differentiation of pluripotent cells (ES and/or iPS cells) currently available in the literature. The stepwise differentiation process described by Zhu and co-workers, envolving the formation of 3D neuroepithelial cysts subsequently giving rise to RPE cells in a quantitative way, was not properly replicated from human ES cells into our mouse iPS cell lines (Zhu et al., 2013). However, attempts to replicate the self-organizing formation of OC-like structures from mouse pluripotent cells provided more enthusiastic results (Eiraku and Sasai, 2012; Eiraku et al., 2011; Gonzalez-Cordero et al., 2013). iPS cell lines were submitted to Early Retinal Differentiation step in SFEBq+Matrigel conditions, with resultant down-regulation of pluripotency markers and up-regulation of *Otx2* and some EFTFs (*Pax6* and *Six3*). These transcriptional alterations were consistent with the observed appearance of neuroepithelium-like structures followed by OV-like protrusions of the pluripotent cell aggregates. Despite the full differentiation process was not completed, a positive insight was collected to facilitate further optimization of the protocol towards the generation of RPE cells within an OC context. Additionally, a third differentiation approach was tackled, based in the recapitulation of the signaling pathways involved in the RPE embryonic developmental process: a first step of EB formation in Retinal Induction Media containing Noggin, Dkk1 and IGF1 recombinant proteins to favour neuroectodermal lineage, followed by a RPE specification phase (Osakada et al., 2009; Torre et al., 2012). It was observed a population of cells with morphology and gene expression profiles (*Pax6*, *Six3*, *Otx2*, and in some cases also *Six6*) resembling retinal progenitor cells. Interestingly, *Mitf* expression was also observed as well as patches of RPE-like hexagonal-packed cells.

At this point further experiments should be undertaken in order to complete the differentiation protocols and obtain RPE cells, that should be properly molecular and functionally characterized (Bharti et al., 2011). By using the last protocol described, one can anticipate the generating of a proliferative progenitor population that can be expanded, prior to the final specification signal to induce RPE formation. On the other hand, the self-formation of 3D OC will allow the generation of a proper retinal structure with NR and RPE components tightly associated, which permits a more integrative and

functional study. This is particularly relevant in the case of CHM, since both cell layers are affected and there is still no definite conclusion if the degeneration process occurs in a sequential or simultaneous way. With our *in vitro* models, this question could be tackled as well as the still unanswered quest for the molecular events underlying CHM pathogenesis. Several disease-specific iPS cell based models have been generated for retinal degenerative disorders, including CHM, providing helpful insight into the pathophysiology of such conditions (Cereso et al., 2014; Jin et al., 2011; Meyer et al., 2011; Singh et al., 2013). For CHM, the lack of a proper *in vitro* model possible contributes to the still speculative molecular pathogenesis. Thus, we postulate that our *in vitro* system of Chm^{null} and Chm^{flox} iPS cell-derived RPE (either in 3D systems or in single layers) will be an advantageous complementary model for disease modelling studies. Interestingly, the conditional nature of the *Rep1* KO establishes the proper control for such experiments, as well as providing a timely control of the KO event. This model could also be used to investigate age-related changes already observed in the Chm mouse models, with probable correlation with AMD condition (Wavre-Shapton et al., 2013). Finally, these *in vitro* models can be used to investigate the therapeutic effects of experimental drugs or approaches, such as gene therapy (Cereso et al., 2014; Tolmachova et al., 2013).

Alternatively to the mentioned reprogramming into pluripotency experiments, direct lineage conversion was also attempted. It was hypothesized that the TFs involved in RPE developmental process could promote the conversion of fibroblasts into RPE cells. Ten TFs were chosen, based on their described role in establishment of the EF (*Tbx3*, *Rax*, *Six3*, *Pax6*, *Lhx2*, *Six6* and *Nr2e1)* and subsequent RPE specification and maturation process (*Pax6*, *Mitf*, *Otx1* and *Otx2)* (Fuhrmann, 2010; Graw, 2010; Martínez-Morales et al., 2004). Extensive molecular cloning was undertaken with the successful generation of inducible lentivirus encoding for V5-tagged versions of the 10 Eye TFs. MEFs transduced with a pool of the 10 TFs acquired morphology and gene expression attributes characteristic of RPE cells, in a short period of time, which is consistent with a direct lineage conversion. In order to optimize the pool of 10 TFs and to facilitate the identification of reprogrammed cells, two lentiviral reporter systems were also generated. Equivalent or higher tyrosinase promoter activation was observed with combined pools containing less TFs, when comparing with the 10 TFs pool. Explicitly, the known role of *Mitf* and *Otx2* in RPE specification, including their binding and transactivation of promoter regions of genes involved in the terminal differentiation of RPE, such as tyrosinase, was confirmed in our system. The possibility of a positive effect of *Otx1* and *Pax6* in the cooperative effect of *Mitf* with *Otx2* was also raised, and it needs to be

tackled more extensively. Thus, besides contributing to the optimization of the reprogramming cocktail of TFs, we generated a technological system that can be used to investigate the molecular events responsible for RPE specification and activation and maintenance of RPE-specific transcriptional program. Moreover, a similar system although driving the expression of an antibiotic resistance gene is already being implemented to allow selection of the arising pigmented RPE-like cells, followed by an extensive characterization step. Prospectively, RPE cells generated by lineage conversion methodologies are important complementary tools for disease modelling studies and regenerative medicine application. Direct lineage conversions have some advantageous over the iPS cell-based strategy, which implies a longer experimental period, with more cellular manipulations, and a subsequent differentiation process. Moreover, the differentiation protocols frequently generate phenotypically unstable cells in an inefficiently way (Bharti et al., 2011).

Important progress towards the applicability of cellular reprogramming strategies in RPE-related degenerative disorders was described in this work. Nevertheless, additional, yet complementary, experimental approaches could also be undertaken. In the case of a prospective therapeutic application, a non-integrative delivery system to force the expression of the defined factors should be applied. In the case of iPS cells generation, several alternatives have been described, with the more efficient and promising approach being the use of modified RNAs (González et al., 2011; Yakubov et al., 2010). Subsequently, in the case of monogenic diseases such as CHM, the underlying gene defect must be genetically corrected prior to the therapeutic use. Homologous recombination techniques were classically applied in different models (Meyer et al., 2011), but also non-viral plasmids harbouring scaffold/matrix attachment regions (S/MARs) encoding for *REP1/CHM* cDNA have been designed to promote effective and sustained long term gene delivery to the RPE (Argyros et al., 2011; Ostad-Saffari et al., 2010). More recently, the development of zinc finger nucleases, transcription activator-like effector nucleases and clustered regularly interspaced short palindromic repeat/CAS9 RNA-guided nucleases profoundly improved gene editing technologies and can advantageously be used for gene correction of disease-specific iPS cell lines (Li et al., 2014). Gene corrected iPS cells must be differentiated into RPE cells, which can be used in transplantation studies. Transplantation of iPS cells-derived RPE has been shown to improve visual function in animal models of other retinal degenerations, such as AMD (Carr et al., 2009). Pluripotent stem cells-derived RPE can be transplanted as single cell suspension or in a monolayer cultured on top of a thin sheet of polymer (Carr et al., 2013). In the case of CHM, a gene therapy trial has recently started with promising

results. Nevertheless, in patients in whom extensive degenerative process has already occurred, cell replacement strategies based on reprogramming strategies can be therapeutically advantageous (MacLaren et al., 2014). Moreover, CHM and also other retinal degenerative disorders could benefit from the transplantation of not only the RPE but also the NR layer. Protocols for differentiation of pluripotent stem cells into PRs have also been established, with preliminary transplantation studies confirming their prospective therapeutic usage (Lamba et al., 2009, 2010; Tucker et al., 2011).

The identity of cells is defined by a network of specific TFs, which can be overexpressed in order to manipulate the established cell fate into a pluripotent state or another cell lineage. To facilitate the analysis of complex TF networks and the choice for the correct reprogramming cocktail, a correlation matrix of global gene expression profiles have recently been described. It would be interesting to confirm if the TFs predicted to be important for the establishment of a retinal transcriptome could be applied successfully in our reprogramming experiments (Yamamizu et al., 2013). Moreover, in addition to the 2 approaches of cellular reprogramming exploited in this work, a third approach has been recently described to successfully reprogram fibroblasts into other cell lineages. This approach implies a transient overpression of the Yamanaka's TF used to generate iPS cells. An "open" epigenetic state is induced, with the generation of multipotent partially reprogrammed intermediates, which can be forced into different cell lineages by manipulating culture conditions or forcing the expression of specific TFs (Ladewig et al., 2013; Sancho-Martinez et al., 2012). This lineage conversion through plastic induction provides new alternatives to the retinal degenerative field. Relevantly, one can postulate the generation of a retinal progenitor multipotent intermediate that could be triggered into RPE and/or NR lineages, both being therapeutically relevant.

In conclusion, we have exploited cellular reprogramming technologies, applying described protocols and also attempting to generate new approaches, with promising results. We focused in the application of such technologies in the retinal degenerative field, particularly in the case where RPE dysfunction is involved, as observed for CHM. Our results positively shed light into the prospective use of cellular reprogramming methods for therapeutic applications, drug screening, disease modelling and basic developmental process studies, in the context of RPE-related degenerative conditions.

Chapter 7 References

Chapter 7 : References

Aasen, T., Raya, A., Barrero, M.J., Garreta, E., Consiglio, A., Gonzalez, F., Vassena, R., Bilić, J., Pekarik, V., Tiscornia, G., et al. (2008). Efficient and rapid generation of induced pluripotent stem cells from human keratinocytes. Nat. Biotechnol. *26*, 1276–1284.

Acland, G.M., Aguirre, G.D., Bennett, J., Aleman, T.S., Cideciyan, A. V, Bennicelli, J., Dejneka, N.S., Pearce-Kelling, S.E., Maguire, A.M., Palczewski, K., et al. (2005). Long-term restoration of rod and cone vision by single dose rAAV-mediated gene transfer to the retina in a canine model of childhood blindness. Mol. Ther. *12*, 1072–1082.

Adelmann, H.B. (1929). Experimental studies on the development of the eye. II. The eye-forming potencies of the median portions of the urodelan neural plate (Triton teniatus and Amblystoma punctatum). J. Exp. Zool. *54*, 291–317.

Adler, R., and Belecky-Adams, T.L. (2002). The role of bone morphogenetic proteins in the differentiation of the ventral optic cup. Development *129*, 3161–3171.

Agathocleous, M., and Harris, W.A. (2009). From progenitors to differentiated cells in the vertebrate retina. Annu. Rev. Cell Dev. Biol. *25*, 45–69.

Aksan, I., and Goding, C.R. (1998). Targeting the microphthalmia basic helix-loop-helix-leucine zipper transcription factor to a subset of E-box elements in vitro and in vivo. Mol. Cell. Biol. *18*, 6930–6938.

Aldahmesh, M.A., Khan, A.O., Hijazi, H., and Alkuraya, F.S. (2013). Homozygous truncation of SIX6 causes complex microphthalmia in humans. Clin. Genet. *84*, 198–199.

Allikmets, R., Singh, N., Sun, H., Shroyer, N.F., Hutchinson, A., Chidambaram, A., Gerrard, B., Baird, L., Stauffer, D., Peiffer, A., et al. (1997). A photoreceptor cell-specific ATP-binding transporter gene (ABCR) is mutated in recessive Stargardt macular dystrophy. Nat. Genet. *15*, 236–246.

Alory, C., and Balch, W.E. (2000). Molecular basis for Rab prenylation. J. Cell Biol. *150*, 89–103.

Amae, S., Fuse, N., Yasumoto, K., Sato, S., Yajima, I., Yamamoto, H., Udono, T., Durlu, Y.K., Tamai, M., Takahashi, K., et al. (1998). Identification of a novel isoform of microphthalmia-associated transcription factor that is enriched in retinal pigment epithelium. Biochem. Biophys. Res. Commun. *247*, 710–715.

Aoi, T., Yae, K., Nakagawa, M., Ichisaka, T., Okita, K., Takahashi, K., Chiba, T., and Yamanaka, S. (2008). Generation of pluripotent stem cells from adult mouse liver and stomach cells. Science (80-.). *321*, 699–702.

Argyros, O., Wong, S.-P., and Harbottle, R.P. (2011). Non-viral episomal modification of cells using S/MAR elements. Expert Opin. Biol. Ther. *11*, 1177–1191.

Ashery-Padan, R., and Gruss, P. (2001). Pax6 lights-up the way for eye development. Curr. Opin. Cell Biol. *13*, 706–714.

Avilion, A.A., Nicolis, S.K., Pevny, L.H., Perez, L., Vivian, N., and Lovell-Badge, R. (2003). Multipotent cell lineages in early mouse development depend on SOX2 function. Genes Dev. *17*, 126–140.

Bailey, T.J., El-Hodiri, H., Zhang, L., Shah, R., Mathers, P.H., and Jamrich, M. (2004). Regulation of vertebrate eye development by Rx genes. Int. J. Dev. Biol. *48*, 761–770.

Ban, Y., and Rizzolo, L.J. (2000). Regulation of glucose transporters during development of the retinal pigment epithelium. Dev. Brain Res. *121*, 89–95.

Del Barco Barrantes, I., Davidson, G., Gröne, H.-J., Westphal, H., and Niehrs, C. (2003). Dkk1 and noggin cooperate in mammalian head induction. Genes Dev. *17*, 2239–2244.

Barnstable, C.J., and Tombran-Tink, J. (2004). Neuroprotective and antiangiogenic actions of PEDF in the eye: molecular targets and therapeutic potential. Prog. Retin. Eye Res. *23*, 561–577.

Barrilleaux, B., and Knoepfler, P.S. (2011). Inducing iPSCs to escape the dish. Cell Stem Cell *9*, 103–111.

Baumer, N., Marquardt, T., Stoykova, A., Spieler, D., Treichel, D., Ashery-Padan, R., and Gruss, P. (2003). Retinal pigmented epithelium determination requires the redundant activities of Pax2 and Pax6. Development *130*, 2903–2915.

Bayart, E., and Cohen-Haguenauer, O. (2013). Technological overview of iPS induction from human adult somatic cells. Curr. Gene Ther. *13*, 73–92.

Bazan, N.G., Gordon, W.C., and Rodriguez de Turco, E.B. (1992). Docosahexaenoic acid uptake and metabolism in photoreceptors: retinal conservation by an efficient retinal pigment epithelial cell-mediated recycling process. Adv. Exp. Med. Biol. *318*, 295–306.

Beatty, S., Boulton, M., Henson, D., Koh, H.-H., and Murray, I.J. (1999). Macular pigment and age related macular degeneration. Br. J. Ophthalmol. *83*, 867–877.

Beby, F., and Lamonerie, T. (2013). The homeobox gene Otx2 in development and disease. Exp. Eye Res. *111*, 9–16.

Béby, F., Housset, M., Fossat, N., Le Greneur, C., Flamant, F., Godement, P., and Lamonerie, T. (2010). Otx2 gene deletion in adult mouse retina induces rapid RPE dystrophy and slow photoreceptor degeneration. PLoS One *5*, e11673.

Bellin, M., Marchetto, M.C., Gage, F.H., and Mummery, C.L. (2012). Induced pluripotent stem cells: the new patient? Nat. Rev. Mol. Cell Biol. *13*, 713–726.

Bernhardt, M., Galach, M., Novak, D., and Utikal, J. (2012). Mediators of induced pluripotency and their role in cancer cells - current scientific knowledge and future perspectives. Biotechnol. J. *7*, 810–821.

Bernstein, B.E., Mikkelsen, T.S., Xie, X., Kamal, M., Huebert, D.J., Cuff, J., Fry, B., Meissner, A., Wernig, M., Plath, K., et al. (2006). A Bivalent Chromatin Structure Marks Key Developmental Genes in Embryonic Stem Cells. Cell *125*, 315–326.

Bharti, K., Nguyen, M.-T.T., Skuntz, S., Bertuzzi, S., and Arnheiter, H. (2006). The other pigment cell: specification and development of the pigmented epithelium of the vertebrate eye. Pigment Cell Res. *19*, 380–394.

Bharti, K., Liu, W., Csermely, T., Bertuzzi, S., and Arnheiter, H. (2008). Alternative promoter use in eye development: the complex role and regulation of the transcription factor MITF. Development *135*, 1169–1178.

Bharti, K., Miller, S.S., and Arnheiter, H. (2011). The new paradigm: retinal pigment epithelium cells generated from embryonic or induced pluripotent stem cells. Pigment Cell Melanoma Res. *24*, 21–34.

Bharti, K., Gasper, M., Ou, J., Brucato, M., Clore-Gronenborn, K., Pickel, J., and Arnheiter, H. (2012). A regulatory loop involving PAX6, MITF, and WNT signaling controls retinal pigment epithelium development. PLoS Genet. *8*, e1002757.

Bharti, K., Rao, M., Hull, S.C., Stroncek, D., Brooks, B.P., Feigal, E., van Meurs, J.C., Huang, C. a, and Miller, S.S. (2014). Developing cellular therapies for retinal degenerative diseases. Invest. Ophthalmol. Vis. Sci. *55*, 1191–1202.

Bhutani, N., Brady, J.J., Damian, M., Sacco, A., Corbel, S.Y., and Blau, H.M. (2010). Reprogramming towards pluripotency requires AID-dependent DNA demethylation. Nature *463*, 1042–1047.

Bhutto, I., and Lutty, G. (2012). Understanding age-related macular degeneration (AMD): relationships between the photoreceptor/retinal pigment epithelium/Bruch's membrane/choriocapillaris. Mol. Aspects Med. *33*, 295–317.

Blau, H.M., Chiu, C.P., and Webster, C. (1983). Cytoplasmic activation of human nuclear genes in stable heterocaryons. Cell *32*, 1171–1180.

Van Bokhoven, H., van den Hurk, J.A., Bogerd, L., Philippe, C., Gilgenkrantz, S., de Jong, P., Ropers, H.H., and Cremers, F.P. (1994). Cloning and characterization of the human choroideremia gene. Hum. Mol. Genet. *3*, 1041–1046.

Bonilha, V.L., Trzupek, K.M., Li, Y., Francis, P.J., Hollyfield, J.G., Rayborn, M.E., Smaoui, N., and Weleber, R.G. (2008). Choroideremia: analysis of the retina from a female symptomatic carrier. Ophthalmic Genet. *29*, 99–110.

Booij, J.C., Baas, D.C., Beisekeeva, J., Gorgels, T.G.M.F., and Bergen, A.A.B. (2010). The dynamic nature of Bruch's membrane. Prog. Retin. Eye Res. *29*, 1–18.

Borooah, S., Phillips, M.J., Bilican, B., Wright, a F., Wilmut, I., Chandran, S., Gamm, D., and Dhillon, B. (2013). Using human induced pluripotent stem cells to treat retinal disease. Prog. Retin. Eye Res. *37*, 163–181.

Boulanger, A., Liu, S., Henningsgaard, A.A., Yu, S., and Redmond, T.M. (2000). The upstream region of the Rpe65 gene confers retinal pigment epithelium-specific expression in vivo and in vitro and contains critical octamer and E-box binding sites. J. Biol. Chem. *275*, 31274–31282.

Bringmann, A., Pannicke, T., Grosche, J., Francke, M., Wiedemann, P., Skatchkov, S.N., Osborne, N.N., and Reichenbach, A. (2006). Müller cells in the healthy and diseased retina. Prog. Retin. Eye Res. *25*, 397–424.

Buchholz, D., Pennington, B., Croze, R., Hinman, C., Coffey, P., and Clegg, D.O. (2013). Rapid and efficient directed differentiation of human pluripotent stem cells into retinal pigmented epithelium. Stem Cells Transl. Med. *2*, 384–393.

Buchholz, D.E., Hikita, S.T., Rowland, T.J., Friedrich, A.M., Hinman, C.R., Johnson, L. V, and Clegg, D.O. (2009). Derivation of functional retinal pigmented epithelium from induced pluripotent stem cells. Stem Cells *27*, 2427–2434.

Buganim, Y., Faddah, D. a, Cheng, A.W., Itskovich, E., Markoulaki, S., Ganz, K., Klemm, S.L., van Oudenaarden, A., and Jaenisch, R. (2012). Single-cell expression analyses during cellular reprogramming reveal an early stochastic and a late hierarchic phase. Cell *150*, 1209–1222.

Burke, J.M., Skumatz, C.M., Irving, P.E., and McKay, B.S. (1996). Phenotypic heterogeneity of retinal pigment epithelial cells in vitro and in situ. Exp. Eye Res. *62*, 63–73.

Burke, J.M., Kaczara, P., Skumatz, C.M.B., Zareba, M., Raciti, M.W., and Sarna, T. (2011). Dynamic analyses reveal cytoprotection by RPE melanosomes against non-photic stress. Mol. Vis. *17*, 2864–2877.

Caiazzo, M., Dell'Anno, M.T., Dvoretskova, E., Lazarevic, D., Taverna, S., Leo, D., Sotnikova, T.D., Menegon, A., Roncaglia, P., Colciago, G., et al. (2011). Direct generation of functional dopaminergic neurons from mouse and human fibroblasts. Nature *476*, 224–227.

Cameron, J.D., Fine, B.S., and Shapiro, I. (1987). Histopathologic observations in choroideremia with emphasis on vascular changes of the uveal tract. Ophthalmology *94*, 187–196.

Cantone, I., and Fisher, A.G. (2013). Epigenetic programming and reprogramming during development. Nat. Struct. Mol. Biol. *20*, 282–289.

Carey, B.W., Markoulaki, S., Hanna, J., Saha, K., Gao, Q., Mitalipova, M., and Jaenisch, R. (2009). Reprogramming of murine and human somatic cells using a single polycistronic vector. Proc. Natl. Acad. Sci. U. S. A. *106*, 157–162.

Carmichael, J., DeGraff, W.G., Gazdar, A.F., Minna, J.D., and Mitchell, J.B. (1987). Evaluation of a Tetrazolium-based Semiautomated Colorimetric Assay: Assessment of Chemosensitivity Testing. Cancer Res. *47* , 936–942.

Carr, A.-J., Vugler, A. a, Hikita, S.T., Lawrence, J.M., Gias, C., Chen, L.L., Buchholz, D.E., Ahmado, A., Semo, M., Smart, M.J.K., et al. (2009). Protective effects of human iPS-derived retinal pigment epithelium cell transplantation in the retinal dystrophic rat. PLoS One *4*, e8152.

Carr, A.-J.F., Smart, M.J.K., Ramsden, C.M., Powner, M.B., da Cruz, L., and Coffey, P.J. (2013). Development of human embryonic stem cell therapies for age-related macular degeneration. Trends Neurosci. *36*, 385–395.

Cereso, N., Pequignot, M.O., Robert, L., Becker, F., De Luca, V., Nabholz, N., Rigau, V., De Vos, J., Hamel, C.P., and Kalatzis, V. (2014). Proof of concept for AAV2/5-mediated gene therapy in iPSC-derived retinal pigment epithelium of a choroideremia patient. Mol. Ther. — Methods Clin. Dev. *1*.

Chambers, I., Silva, J., Colby, D., Nichols, J., Nijmeijer, B., Robertson, M., Vrana, J., Jones, K., Grotewold, L., and Smith, A. (2007). Nanog safeguards pluripotency and mediates germline development. Nature *450*, 1230–1234.

Chen, M., Muckersie, E., Robertson, M., Fraczek, M., Forrester, J. V, and Xu, H. (2008). Characterization of a spontaneous mouse retinal pigment epithelial cell line B6-RPE07. Invest. Ophthalmol. Vis. Sci. *49*, 3699–3706.

Chen, P., Lee, T.D., and Fong, H.K. (2001). Interaction of 11-cis-retinol dehydrogenase with the chromophore of retinal g protein-coupled receptor opsin. J. Biol. Chem. *276*, 21098–21104.

Chow, R.L., and Lang, R.A. (2001). EARLY EYE DEVELOPMENT IN VERTEBRATES. Annu. Rev. Cell Dev. Biol. 255–296.

Cideciyan, A. V. (2010). Leber congenital amaurosis due to RPE65 mutations and its treatment with gene therapy. Prog. Retin. Eye Res. *29*, 398–427.

Collinson, J.M., Quinn, J.C., Hill, R.E., and West, J.D. (2003). The roles of Pax6 in the cornea, retina, and olfactory epithelium of the developing mouse embryo. Dev. Biol. *255*, 303–312.

Coulombre, J.L., and Coulombre, A.J. (1965). Regeneration of neural retina from the pigmented epithelium in the chick embryo. Dev. Biol. *12*, 79–92.

Coussa, R.G., and Traboulsi, E.I. (2012). Choroideremia: a review of general findings and pathogenesis. Ophthalmic Genet. *33*, 57–65.

Coussa, R.G., Kim, J., and Traboulsi, E.I. (2012). Choroideremia: Effect of age on visual acuity in patients and female carriers. Ophthalmic Genet. *33*, 66–73.

Cremers, F.P., van de Pol, D.J., van Kerkhoff, L.P., Wieringa, B., and Ropers, H.H. (1990). Cloning of a gene that is rearranged in patients with choroideraemia. Nature *347*, 674–677.

Cremers, F.P., Armstrong, S.A., Seabra, M.C., Brown, M.S., and Goldstein, J.L. (1994). REP-2, a Rab escort protein encoded by the choroideremia-like gene. J. Biol. Chem. *269*, 2111–2117.

D'Cruz, P.M., Yasumura, D., Weir, J., Matthes, M.T., Abderrahim, H., LaVail, M.M., and Vollrath, D. (2000). Mutation of the receptor tyrosine kinase gene Mertk in the retinal dystrophic RCS rat. Hum. Mol. Genet. *9*, 645–651.

Davidson, R.L., Ephrussi, B., and Yamamoto, K. (1966). Regulation of pigment synthesis in mammalian cells, as studied by somatic hybridization. Proc. Natl. Acad. Sci. U. S. A. *56*, 1437–1440.

Davis, H.E., Rosinski, M., Morgan, J.R., and Yarmush, M.L. (2004). Charged Polymers Modulate Retrovirus Transduction via Membrane Charge Neutralization and Virus Aggregation. Biophys. J. *86*, 1234–1242.

Davis, R.L., Weintraub, H., and Lassar, A.B. (1987). Expression of a single transfected cDNA converts fibroblasts to myoblasts. Cell *51*, 987–1000.

Davis-Silberman, N., Kalich, T., Oron-Karni, V., Marquardt, T., Kroeber, M., Tamm, E.R., and Ashery-Padan, R. (2005). Genetic dissection of Pax6 dosage requirements in the developing mouse eye. Hum. Mol. Genet. *14*, 2265–2276.

Dunn, K., Aotaki-Keen, A., Putkey, F., and Hjelmeland, L. (1996). ARPE-19, a human retinal pigment epithelial cell line with differentiated properties. Exp. Eye … 155–169.

Ebert, A., Yu, J., Rose, F., and Mattis, V. (2009). Induced pluripotent stem cells from a spinal muscular atrophy patient. Nature *457*, 277–280.

Efe, J.A., Hilcove, S., Kim, J., Zhou, H., Ouyang, K., Wang, G., Chen, J., and Ding, S. (2011). Conversion of mouse fibroblasts into cardiomyocytes using a direct reprogramming strategy. Nat. Cell Biol. *13*, 215–222.

Ehrlich, R., Harris, A., Kheradiya, N.S., Winston, D.M., Ciulla, T. a, and Wirostko, B. (2008). Age-related macular degeneration and the aging eye. Clin. Interv. Aging *3*, 473–482.

Eiraku, M., and Sasai, Y. (2012). Mouse embryonic stem cell culture for generation of three-dimensional retinal and cortical tissues. Nat. Protoc. *7*, 69–79.

Eiraku, M., Takata, N., Ishibashi, H., Kawada, M., Sakakura, E., Okuda, S., Sekiguchi, K., Adachi, T., and Sasai, Y. (2011). Self-organizing optic-cup morphogenesis in three-dimensional culture. Nature *472*, 51–56.

Engle, S.J., and Puppala, D. (2013). Integrating human pluripotent stem cells into drug development. Cell Stem Cell *12*, 669–677.

Engle, S.J., and Vincent, F. (2014). Small molecule screening in human induced pluripotent stem cell-derived terminal cell types. J. Biol. Chem. *289*, 4562–4570.

Esmailpour, T., and Huang, T. (2012). TBX3 promotes human embryonic stem cell proliferation and neuroepithelial differentiation in a differentiation stage-dependent manner. Stem Cells *30*, 2152–2163.

Esposito, G., De Falco, F., Tinto, N., Testa, F., Vitagliano, L., Tandurella, I.C.M., Iannone, L., Rossi, S., Rinaldi, E., Simonelli, F., et al. (2011). Comprehensive mutation analysis (20 families) of the choroideremia gene reveals a missense variant that prevents the binding of REP1 with rab geranylgeranyl transferase. Hum. Mutat. *32*, 1460–1469.

Evans, M.J., and Kaufman, M.H. (1981). Establishment in culture of pluripotential cells from mouse embryos. Nature *292*, 154–156.

Faunes, F., Hayward, P., Descalzo, S.M., Chatterjee, S.S., Balayo, T., Trott, J., Christoforou, A., Ferrer-Vaquer, A., Hadjantonakis, A.-K., Dasgupta, R., et al. (2013). A membrane-associated β-catenin/Oct4 complex correlates with ground-state pluripotency in mouse embryonic stem cells. Development *140*, 1171–1183.

Federation, A.J., Bradner, J.E., and Meissner, A. (2013). The use of small molecules in somatic-cell reprogramming. Trends Cell Biol. 1–9.

Feng, R., Desbordes, S.C., Xie, H., Tillo, E.S., Pixley, F., Stanley, E.R., and Graf, T. (2008). PU.1 and C/EBPalpha/beta convert fibroblasts into macrophage-like cells. Proc. Natl. Acad. Sci. U. S. A. *105*, 6057–6062.

Feng, W., Yasumura, D., Matthes, M.T., LaVail, M.M., and Vollrath, D. (2002). Mertk triggers uptake of photoreceptor outer segments during phagocytosis by cultured retinal pigment epithelial cells. J. Biol. Chem. *277*, 17016–17022.

Fink, K.D., Rossignol, J., Lu, M., Leveque, X., Hulse, T.D., Crane, A.T., Nerriere-Daguin, V., Wyse, R.D., Starski, P. a, Schloop, M.T., et al. (2013). Survival and Differentiation of Adenovirus-Generated Induced Pluripotent Stem Cells Transplanted into the Rat Striatum. Cell Transplant. 1–40.

Finnemann, S.C., and Silverstein, R.L. (2001). Differential roles of CD36 and alphavbeta5 integrin in photoreceptor phagocytosis by the retinal pigment epithelium. J. Exp. Med. *194*, 1289–1298.

Finnemann, S.C., Bonilha, V.L., Marmorstein, a D., and Rodriguez-Boulan, E. (1997). Phagocytosis of rod outer segments by retinal pigment epithelial cells requires alpha(v)beta5 integrin for binding but not for internalization. Proc. Natl. Acad. Sci. U. S. A. *94*, 12932–12937.

Flannery, J.G., Bird, A.C., Farber, D.B., Weleber, R.G., and Bok, D. (1990). A histopathologic study of a choroideremia carrier. Invest. Ophthalmol. Vis. Sci. *31*, 229–236.

Fuhrmann, S. (2010). Eye morphogenesis and patterning of the optic vesicle. Curr. Top. Dev. Biol. *93*, 61–84.

Fuhrmann, S., Levine, E.M., and Reh, T.A. (2000). Extraocular mesenchyme patterns the optic vesicle during early eye development in the embryonic chick. Development *127*, 4599–4609.

Furukawa, T., Kozak, C.A., and Cepko, C.L. (1997). Rax, a novel paired-type homeobox gene, shows expression in the anterior neural fold and developing retina. Proc. Natl. Acad. Sci. *94*, 3088–3093.

Gafni, O., Weinberger, L., Mansour, A.A., Manor, Y.S., Chomsky, E., Ben-Yosef, D., Kalma, Y., Viukov, S., Maza, I., Zviran, A., et al. (2013). Derivation of novel human ground state naive pluripotent stem cells. Nature *504*, 282–286.

Gal, A., Li, Y., Thompson, D.A., Weir, J., Orth, U., Jacobson, S.G., Apfelstedt-Sylla, E., and Vollrath, D. (2000). Mutations in MERTK, the human orthologue of the RCS rat retinal dystrophy gene, cause retinitis pigmentosa. Nat. Genet. *26*, 270–271.

Gallardo, M.E., Lopez-Rios, J., Fernaud-Espinosa, I., Granadino, B., Sanz, R., Ramos, C., Ayuso, C., Seller, M.J., Brunner, H.G., Bovolenta, P., et al. (1999). Genomic cloning and characterization of the human homeobox gene SIX6 reveals a cluster of SIX genes in chromosome 14 and associates SIX6 hemizygosity with bilateral anophthalmia and pituitary anomalies. Genomics *61*, 82–91.

Garg, N., Po, A., Miele, E., Campese, A.F., Begalli, F., Silvano, M., Infante, P., Capalbo, C., De Smaele, E., Canettieri, G., et al. (2013). microRNA-17-92 cluster is a direct Nanog target and controls neural stem cell through Trp53inp1. EMBO J. *32*, 2819–2832.

Ghosh, M., and McCulloch, J.C. (1980). Pathological findings from two cases of choroideremia.

González, F., Boué, S., and Izpisúa Belmonte, J.C. (2011). Methods for making induced pluripotent stem cells: reprogramming à la carte. Nat. Rev. Genet. *12*, 231–242.

Gonzalez-Cordero, A., West, E.L., Pearson, R. a, Duran, Y., Carvalho, L.S., Chu, C.J., Naeem, A., Blackford, S.J.I., Georgiadis, A., Lakowski, J., et al. (2013). Photoreceptor precursors derived from three-dimensional embryonic stem cell cultures integrate and mature within adult degenerate retina. SUP. Nat. Biotechnol. *31*, 741–747.

Gordiyenko, N. V, Fariss, R.N., Zhi, C., and MacDonald, I.M. (2010). Silencing of the CHM gene alters phagocytic and secretory pathways in the retinal pigment epithelium. Invest. Ophthalmol. Vis. Sci. *51*, 1143–1150.

Goverdhana, S., Puntel, M., Xiong, W., Zirger, J.M., Barcia, C., Curtin, J.F., Soffer, E.B., Mondkar, S., King, G.D., Hu, J., et al. (2005). Regulatable gene expression systems for gene therapy applications: progress and future challenges. Mol. Ther. *12*, 189–211.

Graw, J. (2003). The genetic and molecular basis of congenital eye defects. Nat Rev Genet *4*, 876–888.

Graw, J. (2010). Eye development. Curr. Top. Dev. Biol. *90*, 343–386.

Gropp, M., Shilo, V., Vainer, G., Gov, M., Gil, Y., Khaner, H., Matzrafi, L., Idelson, M., Kopolovic, J., Zak, N.B., et al. (2012). Standardization of the teratoma assay for analysis of pluripotency of human ES cells and biosafety of their differentiated progeny. PLoS One *7*, e45532.

Gurdon, J.B. (1962). The developmental capacity of nuclei taken from intestinal epithelium cells of feeding tadpoles. J. Embryol. Exp. Morphol. *10*, 622–640.

Hafizi, S., and Dahlbäck, B. (2006). Signalling and functional diversity within the Axl subfamily of receptor tyrosine kinases. Cytokine Growth Factor Rev. *17*, 295–304.

Halder, G., Callaerts, P., and Gehring, W.J. (1995). Induction of ectopic eyes by targeted expression of the eyeless gene in Drosophila. Science *267*, 1788–1792.

Halilagic, A., Ribes, V., Ghyselinck, N.B., Zile, M.H., Dollé, P., and Studer, M. (2007). Retinoids control anterior and dorsal properties in the developing forebrain. Dev. Biol. *303*, 362–375.

Han, D.W., Tapia, N., Hermann, A., Hemmer, K., Höing, S., Araúzo-Bravo, M.J., Zaehres, H., Wu, G., Frank, S., Moritz, S., et al. (2012). Direct Reprogramming of Fibroblasts into Neural Stem Cells by Defined Factors. Cell Stem Cell 1–8.

Han, J., Yuan, P., Yang, H., Zhang, J., Soh, B.S., Li, P., Lim, S.L., Cao, S., Tay, J., Orlov, Y.L., et al. (2010). Tbx3 improves the germ-line competency of induced pluripotent stem cells. Nature *463*, 1096–1100.

Hanna, J., Wernig, M., Markoulaki, S., Sun, C.-W., Meissner, A., Cassady, J.P., Beard, C., Brambrink, T., Wu, L.-C., Townes, T.M., et al. (2007). Treatment of sickle cell anemia mouse model with iPS cells generated from autologous skin. Science *318*, 1920–1923.

Hanna, J., Carey, B.W., and Jaenisch, R. (2008). Reprogramming of somatic cell identity. Cold Spring Harb. Symp. Quant. Biol. *73*, 147–155.

Harding, J., and Mirochnitchenko, O. (2014). Preclinical studies for induced pluripotent stem cell-based therapeutics. J. Biol. Chem. *289*, 4585–4593.

Hartong, D.T., Berson, E.L., and Dryja, T.P. (2006). Retinitis pigmentosa. Lancet *368*, 1795–1809.

Haruta, M., Sasai, Y., Kawasaki, H., Amemiya, K., Ooto, S., Kitada, M., Suemori, H., Nakatsuji, N., Ide, C., Honda, Y., et al. (2004). In Vitro and In Vivo Characterization of Pigment Epithelial Cells Differentiated from Primate Embryonic Stem Cells. Invest. Ophthalmol. Vis. Sci. *45*, 1020–1025.

Heng, L.Z., Comyn, O., Peto, T., Tadros, C., Ng, E., Sivaprasad, S., and Hykin, P.G. (2013). Diabetic retinopathy: pathogenesis, clinical grading, management and future developments. Diabet. Med. *30*, 640–650.

Hershey, C.L., and Fisher, D.E. (2005). Genomic analysis of the Microphthalmia locus and identification of the MITF-J/Mitf-J isoform. Gene *347*, 73–82.

Hever, A.M., Williamson, K.A., and van Heyningen, V. (2006). Developmental malformations of the eye: the role of PAX6, SOX2 and OTX2. Clin. Genet. *69*, 459–470.

Hewirr, A.T., Nakazawa, K., and Newsome, D.A. (1989). Analysis of Newly Synthesized Bruch's Membrane Proteoglycans. Investig. Ophthalmol. Vis. Sci. *30*, 478–486.

Hill, R.E., Favor, J., Hogan, B.L.M., Ton, C.C.T., Saunders, G.F., Hanson, I.M., Prosser, J., Jordan, T., Hastie, N.D., and Heyningen, V. van (1991). Mouse Small eye results from mutations in a paired-like homeobox-containing gene. Nature *354*, 522–525.

Hirami, Y., Osakada, F., Takahashi, K., Okita, K., Yamanaka, S., Ikeda, H., Yoshimura, N., and Takahashi, M. (2009). Generation of retinal cells from mouse and human induced pluripotent stem cells. Neurosci. Lett. *458*, 126–131.

Hochedlinger, K., and Jaenisch, R. (2002). Monoclonal mice generated by nuclear transfer from mature B and T donor cells. Nature *415*, 1035–1038.

Hodgkinson, C.A., Moore, K.J., Nakayama, A., Steingrimsson, E., Copeland, N.G., Jenkins, N.A., and Arnheiter, H. (1993). Mutations at the mouse microphthalmia locus are associated with defects in a gene encoding a novel basic-helix-loop-helix-zipper protein. Cell *74*, 395–404.

Hong, S.G., Dunbar, C.E., and Winkler, T. (2013). Assessing the risks of genotoxicity in the therapeutic development of induced pluripotent stem cells. Mol. Ther. *21*, 272–281.

Horsford, D.J., Nguyen, M.-T.T., Sellar, G.C., Kothary, R., Arnheiter, H., and McInnes, R.R. (2005). Chx10 repression of Mitf is required for the maintenance of mammalian neuroretinal identity. Development *132*, 177–187.

Hou, P., Li, Y., Zhang, X., Liu, C., Guan, J., Li, H., Zhao, T., Ye, J., Yang, W., Liu, K., et al. (2013). Pluripotent stem cells induced from mouse somatic cells by small-molecule compounds. Science *341*, 651–654.

Housset, M., Samuel, A., Ettaiche, M., Bemelmans, A., Béby, F., Billon, N., and Lamonerie, T. (2013). Loss of Otx2 in the adult retina disrupts retinal pigment epithelium function, causing photoreceptor degeneration. J. Neurosci. *33*, 9890–9904.

Huang, A.S., Kim, L. a, and Fawzi, A. a (2012). Clinical characteristics of a large choroideremia pedigree carrying a novel CHM mutation. Arch. Ophthalmol. *130*, 1184–1189.

Huang, P., He, Z., Ji, S., Sun, H., Xiang, D., Liu, C., Hu, Y., Wang, X., and Hui, L. (2011). Induction of functional hepatocyte-like cells from mouse fibroblasts by defined factors. Nature *475*, 386–389.

Huh, S., Hatini, V., Marcus, R.C., Li, S.C., and Lai, E. (1999). Dorsal-ventral patterning defects in the eye of BF-1-deficient mice associated with a restricted loss of shh expression. Dev. Biol. *211*, 53–63.

Hunter, J.J., Morgan, J.I.W., Merigan, W.H., Sliney, D.H., Sparrow, J.R., and Williams, D.R. (2012). The susceptibility of the retina to photochemical damage from visible light. Prog. Retin. Eye Res. *31*, 28–42.

Van den Hurk, J. a, Schwartz, M., van Bokhoven, H., van de Pol, T.J., Bogerd, L., Pinckers, a J., Bleeker-Wagemakers, E.M., Pawlowitzki, I.H., Rüther, K., Ropers, H.H., et al. (1997a). Molecular basis of choroideremia (CHM): mutations involving the Rab escort protein-1 (REP-1) gene. Hum. Mutat. *9*, 110–117.

Van den Hurk, J. a, Hendriks, W., van de Pol, D.J., Oerlemans, F., Jaissle, G., Rüther, K., Kohler, K., Hartmann, J., Zrenner, E., van Bokhoven, H., et al. (1997b). Mouse choroideremia gene mutation causes photoreceptor cell degeneration and is not transmitted through the female germline. Hum. Mol. Genet. *6*, 851–858.

Idelson, M., Alper, R., Obolensky, A., Ben-Shushan, E., Hemo, I., Yachimovich-Cohen, N., Khaner, H., Smith, Y., Wiser, O., Gropp, M., et al. (2009). Directed differentiation of human embryonic stem cells into functional retinal pigment epithelium cells. Cell Stem Cell *5*, 396–408.

Ieda, M., Fu, J.-D., Delgado-Olguin, P., Vedantham, V., Hayashi, Y., Bruneau, B.G., and Srivastava, D. (2010). Direct reprogramming of fibroblasts into functional cardiomyocytes by defined factors. Cell *142*, 375–386.

Ikeda, H., Osakada, F., Watanabe, K., Mizuseki, K., Haraguchi, T., Miyoshi, H., Kamiya, D., Honda, Y., Sasai, N., Yoshimura, N., et al. (2005). Generation of Rx+/Pax6+ neural retinal precursors from embryonic stem cells. Proc. Natl. Acad. Sci. U. S. A. *102*, 11331–11336.

Jacobson, S.G., Cideciyan, A. V, Sumaroka, A., Aleman, T.S., Schwartz, S.B., Windsor, E. a M., Roman, A.J., Stone, E.M., and MacDonald, I.M. (2006). Remodeling of the human retina in choroideremia: rab escort protein 1 (REP-1) mutations. Invest. Ophthalmol. Vis. Sci. *47*, 4113–4120.

Jaenisch, R., and Young, R. (2008). Stem cells, the molecular circuitry of pluripotency and nuclear reprogramming. Cell *132*, 567–582.

Jayawardena, T.M., Egemnazarov, B., Finch, E.A., Zhang, L., Payne, J.A., Pandya, K., Zhang, Z., Rosenberg, P., Mirotsou, M., and Dzau, V.J. (2012). MicroRNA-Mediated In Vitro and In Vivo Direct Reprogramming of Cardiac Fibroblasts to Cardiomyocytes. Circ. Res. *110*, 1465–1473.

Jean, D., Bernier, G., and Gruss, P. (1999). Six6 (Optx2) is a novel murine Six3-related homeobox gene that demarcates the presumptive pituitary/hypothalamic axis and the ventral optic stalk. Mech. Dev. *84*, 31–40.

Jia, F., Wilson, K.D., Sun, N., Gupta, D.M., Huang, M., Li, Z., Panetta, N.J., Chen, Z.Y., Robbins, R.C., Kay, M. a, et al. (2010). A nonviral minicircle vector for deriving human iPS cells. Nat. Methods *7*, 197–199.

Jin, Z.-B., Okamoto, S., Osakada, F., Homma, K., Assawachananont, J., Hirami, Y., Iwata, T., and Takahashi, M. (2011). Modeling retinal degeneration using patient-specific induced pluripotent stem cells. PLoS One *6*, e17084.

Kaji, K., Norrby, K., Paca, A., Mileikovsky, M., Mohseni, P., and Woltjen, K. (2009). Virus-free induction of pluripotency and subsequent excision of reprogramming factors. Nature *458*, 771–775.

Kang, L., Wang, J., Zhang, Y., Kou, Z., and Gao, S. (2009). iPS cells can support full-term development of tetraploid blastocyst-complemented embryos. Cell Stem Cell *5*, 135–138.

Kawamura, T., Suzuki, J., Wang, Y. V, Menendez, S., Morera, L.B., Raya, A., Wahl, G.M., and Izpisúa Belmonte, J.C. (2009). Linking the p53 tumour suppressor pathway to somatic cell reprogramming. Nature *460*, 1140–1144.

Kay, P., Yang, Y.C., and Paraoan, L. (2013). Directional protein secretion by the retinal pigment epithelium: roles in retinal health and the development of age-related macular degeneration. J. Cell. Mol. Med. *17*, 833–843.

Keiser, N.W., Tang, W., Wei, Z., and Bennett, J. (2005). Spatial and temporal expression patterns of the choroideremia gene in the mouse retina. Mol. Vis. *11*, 1052–1060.

Kevany, B., and Palczewski, K. (2010). Phagocytosis of retinal rod and cone photoreceptors. Physiology *25*, 8–15.

Kim, J., Efe, J.A., Zhu, S., Talantova, M., Yuan, X., Wang, S., Lipton, S.A., Zhang, K., and Ding, S. (2011). Direct reprogramming of mouse fibroblasts to neural progenitors. Proc. Natl. Acad. Sci. U. S. A. *108*, 7838–7843.

Kim, J.B., Greber, B., Araúzo-Bravo, M.J., Meyer, J., Park, K.I., Zaehres, H., and Schöler, H.R. (2009). Direct reprogramming of human neural stem cells by OCT4. Nature *461*, 649–3.

Klimanskaya, I., Hipp, J., Rezai, K.A., West, M., Atala, A., and Lanza, R. (2004). Derivation and Comparative Assessment of Retinal Stem Cells Using Transcriptomics. *6*.

Klüppel, M., Beermann, F., Ruppert, S., Schmid, E., Hummler, E., and Schütz, G. (1991). The mouse tyrosinase promoter is sufficient for expression in melanocytes and in the pigmented epithelium of the retina. Proc. Natl. Acad. Sci. U. S. A. *88*, 3777–3781.

Kobayashi, M., Toyama, R., Takeda, H., Dawid, I.B., and Kawakami, K. (1998). Overexpression of the forebrain-specific homeobox gene six3 induces rostral forebrain enlargement in zebrafish. Development *125*, 2973–2982.

Köhnke, M., Delon, C., Hastie, M.L., Nguyen, U.T.T., Wu, Y.-W., Waldmann, H., Goody, R.S., Gorman, J.J., and Alexandrov, K. (2013). Rab GTPase prenylation hierarchy and its potential role in choroideremia disease. PLoS One *8*, e81758.

Kolaja, K. (2014). Stem cells and stem cell-derived tissues and their use in safety assessment. J. Biol. Chem. *289*, 4555–4561.

Kosaka, N., Kodama, M., Sasaki, H., Yamamoto, Y., Takeshita, F., Takahama, Y., Sakamoto, H., Kato, T., Terada, M., and Ochiya, T. (2006). FGF-4 regulates neural progenitor cell proliferation and neuronal differentiation. FASEB J. *20*, 1484–1485.

Krock, B.L., Bilotta, J., and Perkins, B.D. (2007). Noncell-autonomous photoreceptor degeneration in a zebrafish model of choroideremia. Proc. Natl. Acad. Sci. U. S. A. *104*, 4600–4605.

Kunath, T., Saba-El-Leil, M.K., Almousailleakh, M., Wray, J., Meloche, S., and Smith, A. (2007). FGF stimulation of the Erk1/2 signalling cascade triggers transition of pluripotent embryonic stem cells from self-renewal to lineage commitment. Development *134*, 2895–2902.

Kurian, L., Sancho-Martinez, I., and Nivet, E. (2013). Conversion of human fibroblasts to angioblast-like progenitor cells. Nat. Methods *10*, 77–83.

Kurosawa, H. (2007). Methods for inducing embryoid body formation: in vitro differentiation system of embryonic stem cells. J. Biosci. Bioeng. *103*, 389–398.

Ladewig, J., Koch, P., and Brüstle, O. (2013). Leveling Waddington: the emergence of direct programming and the loss of cell fate hierarchies. Nat. Rev. Mol. Cell Biol. *14*, 225–236.

Lagutin, O., Zhu, C.C., Furuta, Y., Rowitch, D.H., McMahon, A.P., and Oliver, G. (2001). Six3 promotes the formation of ectopic optic vesicle-like structures in mouse embryos. Dev. Dyn. *221*, 342–349.

Lagutin, O. V, Zhu, C.C., Kobayashi, D., Topczewski, J., Shimamura, K., Puelles, L., Russell, H.R.C., McKinnon, P.J., Solnica-Krezel, L., and Oliver, G. (2003). Six3 repression of Wnt signaling in the anterior neuroectoderm is essential for vertebrate forebrain development. Genes Dev. *17*, 368–379.

Lamb, T.D., Collin, S.P., and Pugh, E.N. (2007). Evolution of the vertebrate eye: opsins, photoreceptors, retina and eye cup. Nat. Rev. Neurosci. *8*, 960–976.

Lamba, D., Karl, M., and Reh, T. (2008). Neural regeneration and cell replacement: a view from the eye. Cell Stem Cell *2*, 538–549.

Lamba, D. a, Karl, M.O., Ware, C.B., and Reh, T. a (2006). Efficient generation of retinal progenitor cells from human embryonic stem cells. Proc. Natl. Acad. Sci. U. S. A. *103*, 12769–12774.

Lamba, D. a, Gust, J., and Reh, T. a (2009). Transplantation of human embryonic stem cell-derived photoreceptors restores some visual function in Crx-deficient mice. Cell Stem Cell *4*, 73–79.

Lamba, D. a, McUsic, A., Hirata, R.K., Wang, P.-R., Russell, D., and Reh, T. a (2010). Generation, purification and transplantation of photoreceptors derived from human induced pluripotent stem cells. PLoS One *5*, e8763.

Larijani, B., Hume, A.N., Tarafder, A.K., and Seabra, M.C. (2003). Multiple factors contribute to inefficient prenylation of Rab27a in Rab prenylation diseases. J. Biol. Chem. *278*, 46798–46804.

LaVail, M.M. (1976). Rod outer segment disk shedding in rat retina: relationship to cyclic lighting. Sci. *194* , 1071–1074.

Lee, B., Rizzoti, K., Kwon, D.S., Kim, S.-Y., Oh, S., Epstein, D.J., Son, Y., Yoon, J., Baek, K., and Jeong, Y. (2012). Direct transcriptional regulation of Six6 is controlled by SoxB1 binding to a remote forebrain enhancer. Dev. Biol. *366*, 393–403.

Lee, S.-H., Jeyapalan, J.N., Appleby, V., Mohamed Noor, D.A., Sottile, V., and Scotting, P.J. (2010). Dynamic methylation and expression of Oct4 in early neural stem cells. J. Anat. *217*, 203–213.

Leung, K.F., Baron, R., and Seabra, M.C. (2006). Thematic review series: lipid posttranslational modifications. geranylgeranylation of Rab GTPases. J. Lipid Res. *47*, 467–475.

Li, M., Suzuki, K., Kim, N.Y., Liu, G.-H., and Izpisua Belmonte, J.C. (2014). A cut above the rest: targeted genome editing technologies in human pluripotent stem cells. J. Biol. Chem. *289*, 4594–4599.

Li, R., Liang, J., Ni, S., Zhou, T., Qing, X., Li, H., He, W., Chen, J., Li, F., Zhuang, Q., et al. (2010a). A mesenchymal-to-epithelial transition initiates and is required for the nuclear reprogramming of mouse fibroblasts. Cell Stem Cell *7*, 51–63.

Li, X.-H., Kishore, A.H., Dao, D., Zheng, W., Roman, C.A., and Word, R.A. (2010b). A novel isoform of microphthalmia-associated transcription factor inhibits IL-8 gene expression in human cervical stromal cells. Mol. Endocrinol. *24*, 1512–1528.

Li, Y., Tsai, Y.-T., Hsu, C.-W., Erol, D., Yang, J., Wu, W.-H., Davis, R.J., Egli, D., and Tsang, S.H. (2012). Long-term safety and efficacy of human-induced pluripotent stem cell (iPS) grafts in a preclinical model of retinitis pigmentosa. Mol. Med. *18*, 1312–1319.

Liang, G., and Zhang, Y. (2013). Genetic and epigenetic variations in iPSCs: potential causes and implications for application. Cell Stem Cell *13*, 149–159.

Lim, L.S., Mitchell, P., Seddon, J.M., Holz, F.G., and Wong, T.Y. (2012). Age-related macular degeneration. Lancet *379*, 1728–1738.

Liu, W., Lagutin, O. V, Mende, M., Streit, A., and Oliver, G. (2006). Six3 activation of Pax6 expression is essential for mammalian lens induction and specification. EMBO J. *25*, 5383–5395.

Liu, W., Lagutin, O., Swindell, E., Jamrich, M., and Oliver, G. (2010). Neuroretina specification in mouse embryos requires Six3-mediated suppression of Wnt8b in the anterior neural plate. J. Clin. Invest. *120*, 3568–3577.

Livak, K.J., and Schmittgen, T.D. (2001). Analysis of relative gene expression data using real-time quantitative PCR and the 2(-Delta Delta C(T)) Method. Methods *25*, 402–408.

Loosli, F., Winkler, S., and Wittbrodt, J. (1999). Six3 overexpression initiates the formation of ectopic retina. Genes Dev. *13*, 649–654.

Lorda-Sanchez, I.J., Ibañez, A.J., Sanz, R.J., Trujillo, M.J., Anabitarte, M.E., Querejeta, M.E., Rodriguez de Alba, M., Gimenez, A., Infantes, F., Ramos, C., et al. (2000). Choroideremia, sensorineural deafness, and primary ovarian failure in a woman with a balanced X-4 translocation. Ophthalmic Genet. *21*, 185–189.

Lujan, E., and Wernig, M. (2013). An indirect approach to generating specific human cell types. Nat. Methods *10*, 44–45.

Lujan, E., Chanda, S., Ahlenius, H., Südhof, T.C., and Wernig, M. (2012). Direct conversion of mouse fibroblasts to self-renewing, tripotent neural precursor cells. Proc. Natl. Acad. Sci. U. S. A. *109*, 2527–2532.

MacDonald, I., Smaoui, N., and Seabra, M. (2003). Choroideremia. In GeneReviews® [Internet], E. Pagon RA, Adam MP, Ardinger HH, et al., ed. (Seattle (WA): University of Washington, Seattle;), p. [updated 2010].

MacDonald, I.M., Russell, L., and Chan, C.-C. (2009). Choroideremia: new findings from ocular pathology and review of recent literature. Surv. Ophthalmol. *54*, 401–407.

Machemer, R., and Steinhorst, U.H. (1993). Retinal separation, retinotomy, and macular relocation: II. A surgical approach for age-related macular degeneration? Graefe's Arch. Clin. Exp. Ophthalmol. *231*, 635–641.

MacLaren, R.E., Uppal, G.S., Balaggan, K.S., Tufail, A., Munro, P.M.G., Milliken, A.B., Ali, R.R., Rubin, G.S., Aylward, G.W., and da Cruz, L. (2007). Autologous Transplantation of the Retinal Pigment Epithelium and Choroid in the Treatment of Neovascular Age-Related Macular Degeneration. Ophthalmology *114*.

MacLaren, R.E., Groppe, M., Barnard, A.R., Cottriall, C.L., Tolmachova, T., Seymour, L., Clark, K.R., During, M.J., Cremers, F.P.M., Black, G.C.M., et al. (2014). Retinal gene therapy in patients with choroideremia: initial findings from a phase 1/2 clinical trial. Lancet *383*, 1129–1137.

Maherali, N., and Hochedlinger, K. (2008). Guidelines and techniques for the generation of induced pluripotent stem cells. Cell Stem Cell *3*, 595–605.

Maherali, N., and Hochedlinger, K. (2009). Tgf?? Signal Inhibition Cooperates in the Induction of iPSCs and Replaces Sox2 and cMyc. Curr. Biol. *19*, 1718–1723.

Marks, H., Kalkan, T., Menafra, R., Denissov, S., Jones, K., Hofemeister, H., Nichols, J., Kranz, A., Francis Stewart, A., Smith, A., et al. (2012). The transcriptional and epigenomic foundations of ground state pluripotency. Cell *149*, 590–604.

Marmorstein, A.D., Cross, H.E., and Peachey, N.S. (2009). Functional roles of bestrophins in ocular epithelia. Prog. Retin. Eye Res. *28*, 206–226.

Marquardt, T., Ashery-Padan, R., Andrejewski, N., Scardigli, R., Guillemot, F., and Gruss, P. (2001). Pax6 is required for the multipotent state of retinal progenitor cells. Cell *105*, 43–55.

Martinez-Morales, J.R., and Wittbrodt, J. (2009). Shaping the vertebrate eye. Curr. Opin. Genet. Dev. *19*, 511–517.

Martinez-Morales, J.R., Signore, M., Acampora, D., Simeone, a, and Bovolenta, P. (2001). Otx genes are required for tissue specification in the developing eye. Development *128*, 2019–2030.

Martínez-Morales, J.R., Dolez, V., Rodrigo, I., Zaccarini, R., Leconte, L., Bovolenta, P., and Saule, S. (2003a). OTX2 activates the molecular network underlying retina pigment epithelium differentiation. J. Biol. Chem. *278*, 21721–21731.

Martínez-Morales, J.R., Dolez, V., Rodrigo, I., Zaccarini, R., Leconte, L., Bovolenta, P., and Saule, S. (2003b). OTX2 activates the molecular network underlying retina pigment epithelium differentiation. J. Biol. Chem. *278*, 21721–21731.

Martínez-Morales, J.R., Rodrigo, I., and Bovolenta, P. (2004). Eye development: a view from the retina pigmented epithelium. Bioessays *26*, 766–777.

Masuda, T., and Esumi, N. (2010). SOX9, through interaction with microphthalmia-associated transcription factor (MITF) and OTX2, regulates BEST1 expression in the retinal pigment epithelium. J. Biol. Chem. *285*, 26933–26944.

Masuda, T., Wahlin, K., Wan, J., Hu, J., Maruotti, J., Yang, X., Iacovelli, J., Wolkow, N., Kist, R., Dunaief, J.L., et al. (2014). SOX9 Plays a Key Role in the Regulation of Visual Cycle Gene Expression in the Retinal Pigment Epithelium. J. Biol. Chem. 0–27.

Masui, S., Nakatake, Y., Toyooka, Y., Shimosato, D., Yagi, R., Takahashi, K., Okochi, H., Okuda, A., Matoba, R., Sharov, A.A., et al. (2007). Pluripotency governed by Sox2 via regulation of Oct3/4 expression in mouse embryonic stem cells. Nat. Cell Biol. *9*, 625–635.

Mathers, P.H., Grinberg, a, Mahon, K. a, and Jamrich, M. (1997). The Rx homeobox gene is essential for vertebrate eye development. Nature *387*, 603–607.

Matsuda, T., Nakamura, T., Nakao, K., Arai, T., Katsuki, M., Heike, T., and Yokota, T. (1999). STAT3 activation is sufficient to maintain an undifferentiated state of mouse embryonic stem cells. EMBO J. *18*, 4261–4269.

Merkle, F.T., and Eggan, K. (2013). Modeling human disease with pluripotent stem cells: from genome association to function. Cell Stem Cell *12*, 656–668.

Meyer, J., Howden, S., and Wallace, K. (2011). Optic Vesicle-like Structures Derived from Human Pluripotent Stem Cells Facilitate a Customized Approach to Retinal Disease Treatment. Stem Cells *29*, 1206–1218.

Meyer, J.S., Shearer, R.L., Capowski, E.E., Wright, L.S., Wallace, K. a, McMillan, E.L., Zhang, S.-C., and Gamm, D.M. (2009). Modeling early retinal development with human embryonic and induced pluripotent stem cells. Proc. Natl. Acad. Sci. U. S. A. *106*, 16698–16703.

Miyanari, Y., and Torres-Padilla, M.-E. (2012). Control of ground-state pluripotency by allelic regulation of Nanog. Nature 2–7.

Miyazono, S., Shimauchi-Matsukawa, Y., Tachibanaki, S., and Kawamura, S. (2008). Highly efficient retinal metabolism in cones. Proc. Natl. Acad. Sci. U. S. A. *105*, 16051–16056.

Mochizuki, M., Sugita, S., and Kamoi, K. (2013). Immunological homeostasis of the eye. Prog. Retin. Eye Res. *33*, 10–27.

Moiseyev, G., Takahashi, Y., Chen, Y., Gentleman, S., Redmond, T.M., Crouch, R.K., and Ma, J.-X. (2006). RPE65 is an iron(II)-dependent isomerohydrolase in the retinoid visual cycle. J. Biol. Chem. *281*, 2835–2840.

Molday, R.S., and Zhang, K. (2010). Defective lipid transport and biosynthesis in recessive and dominant Stargardt macular degeneration. Prog. Lipid Res. *49*, 476–492.

Monaghan, a P., Grau, E., Bock, D., and Schütz, G. (1995). The mouse homolog of the orphan nuclear receptor tailless is expressed in the developing forebrain. Development *121*, 839–853.

Montserrat, N., Nivet, E., Sancho-Martinez, I., Hishida, T., Kumar, S., Miquel, L., Cortina, C., Hishida, Y., Xia, Y., Esteban, C.R., et al. (2013). Reprogramming of human fibroblasts to pluripotency with lineage specifiers. Cell Stem Cell *13*, 341–350.

Moosajee, M., Tulloch, M., Baron, R.A., Gregory-Evans, C.Y., Pereira-Leal, J.B., and Seabra, M.C. (2009). Single choroideremia gene in nonmammalian vertebrates explains early embryonic lethality of the zebrafish model of choroideremia. Invest. Ophthalmol. Vis. Sci. *50*, 3009–3016.

Moosajee, M., Ramsden, S.C., Black, G.C.M., Seabra, M.C., and Webster, A.R. (2014). Clinical utility gene card for: choroideremia. Eur. J. Hum. Genet. *22*, 1–4.

Moretti, A., Bellin, M., Welling, A., Jung, C.B., Lam, J.T., Bott-Flügel, L., Dorn, T., Goedel, A., Höhnke, C., Hofmann, F., et al. (2010). Patient-specific induced pluripotent stem-cell models for long-QT syndrome. N. Engl. J. Med. *363*, 1397–1409.

Müller, F., Rohrer, H., and Vogel-Höpker, A. (2007). Bone morphogenetic proteins specify the retinal pigment epithelium in the chick embryo. Development *134*, 3483–3493.

Mukkamala, K., Gentile, R.C., Willner, J., and Tsang, S. (2010). Choroideremia in a woman with ectodermal dysplasia and complex translocations involving chromosomes X, 1, and 3.

Mura, M., Sereda, C., Jablonski, M.M., MacDonald, I.M., and Iannaccone, A. (2007). Clinical and functional findings in choroideremia due to complete deletion of the CHM gene.

Murisier, F., and Beermann, F. (2006). Genetics of pigment cells: lessons from the tyrosinase gene family. Histol. Histopathol. *21*, 567–578.

Murisier, F., Guichard, S., and Beermann, F. (2007). Distinct distal regulatory elements control tyrosinase expression in melanocytes and the retinal pigment epithelium. Dev. Biol. *303*, 838–847.

Nakagawa, M., Koyanagi, M., Tanabe, K., Takahashi, K., Ichisaka, T., Aoi, T., Okita, K., Mochiduki, Y., Takizawa, N., and Yamanaka, S. (2008). Generation of induced pluripotent stem cells without Myc from mouse and human fibroblasts. Nat. Biotechnol. *26*, 101–106.

Nakaizumi, Y. (1964). The ultrastructure of bruch's membrane: I. human, monkey, rabbit, guinea pig, and rat eyes. Arch. Ophthalmol. *72*, 380–387.

Nakano, T., Ando, S., Takata, N., Kawada, M., Muguruma, K., Sekiguchi, K., Saito, K., Yonemura, S., Eiraku, M., and Sasai, Y. (2012). Self-formation of optic cups and storable stratified neural retina from human ESCs. Cell Stem Cell *10*, 771–785.

Nguyen, M., and Arnheiter, H. (2000). Signaling and transcriptional regulation in early mammalian eye development: a link between FGF and MITF. Development *127*, 3581–3591.

Nichols, J., and Smith, A. (2009). Naive and primed pluripotent states. Cell Stem Cell *4*, 487–492.

Nichols, J., Zevnik, B., Anastassiadis, K., Niwa, H., Klewe-Nebenius, D., Chambers, I., Sch??ler, H., and Smith, A. (1998). Formation of pluripotent stem cells in the mammalian embryo depends on the POU transcription factor Oct4. Cell *95*, 379–391.

Nicoletti, a, Kawase, K., and Thompson, D. a (1998). Promoter analysis of RPE65, the gene encoding a 61-kDa retinal pigment epithelium-specific protein. Invest. Ophthalmol. Vis. Sci. *39*, 637–644.

Nishihara, D., Yajima, I., Tabata, H., Nakai, M., Tsukiji, N., Katahira, T., Takeda, K., Shibahara, S., Nakamura, H., and Yamamoto, H. (2012). Otx2 is involved in the regional specification of the developing retinal pigment epithelium by preventing the expression of sox2 and fgf8, factors that induce neural retina differentiation. PLoS One *7*, e48879.

Niwa, H., Burdon, T., Chambers, I., and Smith, A. (1998). Self-renewal of pluripotent embryonic stem cells is mediated via activation of STAT3. Genes Dev. *12*, 2048–2060.

Niwa, H., Miyazaki, J., and Smith, a G. (2000). Quantitative expression of Oct-3/4 defines differentiation, dedifferentiation or self-renewal of ES cells. Nat. Genet. *24*, 372–376.

Okita, K., Ichisaka, T., and Yamanaka, S. (2007). Generation of germline-competent induced pluripotent stem cells. Nature *448*, 313–317.

Okita, K., Nakagawa, M., Hyenjong, H., Ichisaka, T., and Yamanaka, S. (2008). Generation of mouse induced pluripotent stem cells without viral vectors. Science *322*, 949–953.

Oliver, G., Mailhos, a, Wehr, R., Copeland, N.G., Jenkins, N. a, and Gruss, P. (1995). Six3, a murine homologue of the sine oculis gene, demarcates the most anterior border of the developing neural plate and is expressed during eye development. Development *121*, 4045–4055.

Osakada, F., Ikeda, H., Sasai, Y., and Takahashi, M. (2009). Stepwise differentiation of pluripotent stem cells into retinal cells. Nat. Protoc. *4*, 811–824.

Ostad-Saffari, E., Moosajee, M., Wong, S., Tracey-White, D., Tolmachova, T., Harbottle, R., and Seabra., M. (2010). Persistent Expression of Non-Viral S/MAR Vectors in the RPE for Choroideremia Gene Therapy. ARVO Conf. *Abstract #*.

Pan, Y., Martinez-De Luna, R.I., Lou, C.-H., Nekkalapudi, S., Kelly, L.E., Sater, A.K., and El-Hodiri, H.M. (2010). Regulation of photoreceptor gene expression by the retinal homeobox (Rx) gene product. Dev. Biol. *339*, 494–506.

Pang, Z.P., Yang, N., Vierbuchen, T., Ostermeier, A., Fuentes, D.R., Yang, T.Q., Citri, A., Sebastiano, V., Marro, S., Südhof, T.C., et al. (2011). Induction of human neuronal cells by defined transcription factors. Nature *476*, 220–223.

Park, I., Arora, N., Huo, H., Maherali, N., Ahfeldt, T., Shimamura, A., Lensch, M.W., Cowan, C., Hochedlinger, K., and Daley, G.Q. (2008). Disease-specific induced pluripotent stem cells. Cell *134*, 877–886.

Parver, L.M. (1991). Temperature modulating action of choroidal blood flow. Eye (Lond). *5 (Pt 2)*, 181–185.

Patricia Becerra, S., Fariss, R.N., Wu, Y.Q., Montuenga, L.M., Wong, P., and Pfeffer, B.A. (2004). Pigment epithelium-derived factor in the monkey retinal pigment epithelium and interphotoreceptor matrix: apical secretion and distribution. Exp. Eye Res. *78*, 223–234.

Pease, S., Braghetta, P., Gearing, D., Grail, D., and Williams, R.L. (1990). Isolation of embryonic stem (ES) cells in media supplemented with recombinant leukemia inhibitory factor (LIF). Dev. Biol. *141*, 344–352.

Pera, M.F., and Tam, P.P.L. (2010). Extrinsic regulation of pluripotent stem cells. Nature *465*, 713–720.

Pera, E.M., Wessely, O., Li, S.Y., and De Robertis, E.M. (2001). Neural and Head Induction by Insulin-like Growth Factor Signals. Dev. Cell *1*, 655–665.

Pereira, C.F., Terranova, R., Ryan, N.K., Santos, J., Morris, K.J., Cui, W., Merkenschlager, M., and Fisher, A.G. (2008). Heterokaryon-based reprogramming of human B lymphocytes for pluripotency requires Oct4 but not Sox2. PLoS Genet. *4*.

Peterson, S.E., and Loring, J.F. (2014). Genomic instability in pluripotent stem cells: implications for clinical applications. J. Biol. Chem. *289*, 4578–4584.

Pittack, C., Grunwald, G.B., and Reh, T.A. (1997). Fibroblast growth factors are necessary for neural retina but not pigmented epithelium differentiation in chick embryos. Development *124*, 805–816.

Polo, J.M., Anderssen, E., Walsh, R.M., Schwarz, B. a, Nefzger, C.M., Lim, S.M., Borkent, M., Apostolou, E., Alaei, S., Cloutier, J., et al. (2012). A molecular roadmap of reprogramming somatic cells into iPS cells. Cell *151*, 1617–1632.

Ponjavic, V., Abrahamson, M., Andréasson, S., Van Bokhoven, H., Cremers, F.P., Ehinger, B., and Fex, G. (1995). Phenotype variations within a choroideremia family lacking the entire CHM gene. Ophthalmic Genet. *16*, 143–150.

Porter, F.D., Drago, J., Xu, Y., Cheema, S.S., Wassif, C., Huang, S.P., Lee, E., Grinberg, A., Massalas, J.S., Bodine, D., et al. (1997). Lhx2, a LIM homeobox gene, is required for eye, forebrain, and definitive erythrocyte development. Development *124*, 2935–2944.

Preising, M.N., Wegscheider, E., Friedburg, C., Poloschek, C.M., Wabbels, B.K., and Lorenz, B. (2009). Fundus Autofluorescence in Carriers of Choroideremia and Correlation with Electrophysiologic and Psychophysical Data. Ophthalmology *116*.

Del Priore, L. V, Geng, L., Tezel, T.H., and Kaplan, H.J. (2002). Extracellular matrix ligands promote RPE attachment to inner Bruch's membrane. Curr. Eye Res. *25*, 79–89.

Pritchard, D.J. (1981). Transdifferentiation of chicken embryo neural retina into pigment epithelium: indications of its biochemical basis. J. Embryol. Exp. Morphol. *62*, 47–62.

Pylypenko, O., Rak, A., Reents, R., Niculae, A., Sidorovitch, V., Cioaca, M.D., Bessolitsyna, E., Thom??, N.H., Waldmann, H., Schlichting, I., et al. (2003). Structure of Rab escort protein-1 in complex with Rab geranylgeranyltransferase. Mol. Cell *11*, 483–494.

Qian, L., Huang, Y., Spencer, C.I., Foley, A., Vedantham, V., Liu, L., Conway, S.J., Fu, J., and Srivastava, D. (2012). In vivo reprogramming of murine cardiac fibroblasts into induced cardiomyocytes. Nature.

Qiang, L., Fujita, R., Yamashita, T., Angulo, S., Rhinn, H., Rhee, D., Doege, C., Chau, L., Aubry, L., Vanti, W.B., et al. (2011). Directed conversion of Alzheimer's disease patient skin fibroblasts into functional neurons. Cell *146*, 359–371.

Quiring, R., Walldorf, U., Kloter, U., and Gehring, W. (1994). Homology of the eyeless gene of Drosophila to the Small eye gene in mice and Aniridia in humans. Science (80-.). *265*, 785–789.

Radcliffe, P. a, and Mitrophanous, K. a (2004). Multiple gene products from a single vector: "self-cleaving" 2A peptides. Gene Ther. *11*, 1673–1674.

Radzisheuskaya, A., and Silva, J.C.R. (2013). Do all roads lead to Oct4? The emerging concepts of induced pluripotency. Trends Cell Biol. *24*, 275–284.

Radzisheuskaya, A., Chia, G.L. Bin, dos Santos, R.L., Theunissen, T.W., Castro, L.F.C., Nichols, J., and Silva, J.C.R. (2013). A defined Oct4 level governs cell state transitions of pluripotency entry and differentiation into all embryonic lineages. Nat. Cell Biol. *15*, 579–590.

Rahl, P.B., Lin, C.Y., Seila, A.C., Flynn, R.A., McCuine, S., Burge, C.B., Sharp, P.A., and Young, R.A. (2010). C-Myc regulates transcriptional pause release. Cell *141*, 432–445.

Rak, A., Pylypenko, O., Niculae, A., Pyatkov, K., Goody, R.S., and Alexandrov, K. (2004). Structure of the Rab7:REP-1 complex: insights into the mechanism of Rab prenylation and choroideremia disease. Cell *117*, 749–760.

Ramsden, C.M., Powner, M.B., Carr, A.-J.F., Smart, M.J.K., da Cruz, L., and Coffey, P.J. (2013). Stem cells in retinal regeneration: past, present and future. Development *140*, 2576–2585.

Raviv, S., Bharti, K., Rencus-Lazar, S., Cohen-Tayar, Y., Schyr, R., Evantal, N., Meshorer, E., Zilberberg, A., Idelson, M., Reubinoff, B., et al. (2014). PAX6 Regulates Melanogenesis in the Retinal Pigmented Epithelium through Feed-Forward Regulatory Interactions with MITF. PLoS Genet. *10*, e1004360.

Raya, A., Rodríguez-Pizà, I., Guenechea, G., Vassena, R., Navarro, S., Barrero, M.J., Consiglio, A., Castellà, M., Río, P., Sleep, E., et al. (2009). Disease-corrected haematopoietic progenitors from Fanconi anaemia induced pluripotent stem cells. Nature *460*, 53–59.

Reinisalo, M., Putula, J., Mannermaa, E., Urtti, A., and Honkakoski, P. (2012). Regulation of the human tyrosinase gene in retinal pigment epithelium cells: the significance of transcription factor orthodenticle homeobox 2 and its polymorphic binding site. Mol. Vis. *18*, 38–54.

Renner, A.B., Kellner, U., Cropp, E., Preising, M.N., MacDonald, I.M., van den Hurk, J.A.J.M., Cremers, F.P.M., and Foerster, M.H. (2006). Choroideremia: Variability of Clinical and Electrophysiological Characteristics and First Report of a Negative Electroretinogram. Ophthalmology *113*.

Renner, A.B., Fiebig, B.S., Cropp, E., Weber, B.H.F., and Kellner, U. (2009). Progression of retinal pigment epithelial alterations during long-term follow-up in female carriers of choroideremia and report of a novel CHM mutation. Arch. Ophthalmol. *127*, 907–912.

Ring, K.L., Tong, L.M., Balestra, M.E., Javier, R., Andrews-Zwilling, Y., Li, G., Walker, D., Zhang, W.R., Kreitzer, A.C., and Huang, Y. (2012). Direct reprogramming of mouse and human fibroblasts into multipotent neural stem cells with a single factor. Cell Stem Cell *11*, 100–109.

Rizzolo, L.J. (1991). Basement membrane stimulates the polarized distribution of integrins but not the Na,K-ATPase in the retinal pigment epithelium. Cell Regul. *2*, 939–949.

Rizzolo, L., Peng, S., Luo, Y., and Xiao, W. (2011). Integration of tight junctions and claudins with the barrier functions of the retinal pigment epithelium. Prog. Retin. Eye Res. *30*, 296–323.

Roberts, M.F., Fishman, G.A., Roberts, D.K., Heckenlively, J.R., Weleber, R.G., Anderson, R.J., and Grover, S. (2002). Retrospective, longitudinal, and cross sectional study of visual acuity impairment in choroideraemia. Br. J. Ophthalmol. *86*, 658–662.

Rowland, T., Blaschke, A., Buchholz, D., Hikita, S., Johnson, L., and Clegg, D.O. (2013). Differentiation of human pluripotent stem cells to retinal pigmented epithelium in defined conditions using purified extracellular matrix proteins. J. Tissue … *7*, 642–653.

Roy, A., de Melo, J., Chaturvedi, D., Thein, T., Cabrera-Socorro, A., Houart, C., Meyer, G., Blackshaw, S., and Tole, S. (2013). LHX2 is necessary for the maintenance of optic identity and for the progression of optic morphogenesis. J. Neurosci. *33*, 6877–6884.

Rudolph, G., Preising, M., Kalpadakis, P., Haritoglou, C., Lang, G.E., and Lorenz, B. (2003). Phenotypic variability in three carriers from a family with choroideremia and a frameshift mutation 1388delCCinsG in the REP-1 gene.

Salero, E., Blenkinsop, T. a, Corneo, B., Harris, A., Rabin, D., Stern, J.H., and Temple, S. (2012). Adult human RPE can be activated into a multipotent stem cell that produces mesenchymal derivatives. Cell Stem Cell *10*, 88–95.

Šamija, I., Lukač, J., and Kusić, Z. (2010). Microphthalmia-associated transcription factor (MITF) – from Waardenburg syndrome genetics to melanoma therapy. Acta Med. Acad. 175–193.

Sancho-Martinez, I., Baek, S.H., and Izpisua Belmonte, J.C. (2012). Lineage conversion methodologies meet the reprogramming toolbox. Nat. Cell Biol. *14*, 892–899.

Sasai, Y. (2013a). Next-generation regenerative medicine: organogenesis from stem cells in 3D culture. Cell Stem Cell *12*, 520–530.

Sasai, Y. (2013b). Cytosystems dynamics in self-organization of tissue architecture. Nature *493*, 318–326.

Saunders, A., Faiola, F., and Wang, J. (2013). Concise review: pursuing self-renewal and pluripotency with the stem cell factor Nanog. Stem Cells *31*, 1227–1236.

Scheiner, Z.S., Talib, S., and Feigal, E.G. (2014). The potential for immunogenicity of autologous induced pluripotent stem cell-derived therapies. J. Biol. Chem. *289*, 4571–4577.

Schmouth, J.-F., Banks, K.G., Mathelier, A., Gregory-Evans, C.Y., Castellarin, M., Holt, R.A., Gregory-Evans, K., Wasserman, W.W., and Simpson, E.M. (2012). Retina Restored and Brain Abnormalities Ameliorated by Single-Copy Knock-In of Human NR2E1 in Null Mice. Mol. Cell. Biol. *32*, 1296–1311.

Schneuwly, S., Klemenz, R., and Gehring, W.J. (1987). Redesigning the body plan of Drosophila by ectopic expression of the homoeotic gene Antennapedia. Nature *325*, 816–818.

Schraermeyer, U., and Heimann, K. (1999). Current understanding on the role of retinal pigment epithelium and its pigmentation. Pigment Cell Res *12*, 219–236.

Schwartz, S.D., Hubschman, J.-P., Heilwell, G., Franco-Cardenas, V., Pan, C.K., Ostrick, R.M., Mickunas, E., Gay, R., Klimanskaya, I., and Lanza, R. (2012). Embryonic stem cell trials for macular degeneration: a preliminary report. Lancet *379*, 713–720.

Schwarz, M., Cecconi, F., Bernier, G., Andrejewski, N., Kammandel, B., Wagner, M., and Gruss, P. (2000). Spatial specification of mammalian eye territories by reciprocal transcriptional repression of Pax2 and Pax6. Development *127*, 4325–4334.

Seabra, M.C. (1996). New insights into the pathogenesis of choroideremia: a tale of two REPs. Ophthalmic Genet. *17*, 43–46.

Seabra, M.C., and Wasmeier, C. (2004). Controlling the location and activation of Rab GTPases. Curr. Opin. Cell Biol. *16*, 451–457.

Seabra, M., Ho, Y., and Anant, J. (1995). Deficient geranylgeranylation of Ram/Rab27 in choroideremia. J. Biol. Chem. *270*, 24420–24427.

Seabra, M.C., Brown, M.S., Slaughter, C. a, Südhof, T.C., and Goldstein, J.L. (1992). Purification of component A of Rab geranylgeranyl transferase: possible identity with the choroideremia gene product. Cell *70*, 1049–1057.

Seabra, M.C., Mules, E.H., and Hume, A.N. (2002). Rab GTPases, intracellular traffic and disease. Trends Mol. Med. *8*, 23–30.

Seagle, B.-L.L., Rezai, K.A., Kobori, Y., Gasyna, E.M., Rezaei, K.A., and Norris, J.R. (2005). Melanin photoprotection in the human retinal pigment epithelium and its correlation with light-induced cell apoptosis. Proc. Natl. Acad. Sci. U. S. A. *102*, 8978–8983.

Sergeev, Y. V, Smaoui, N., Sui, R., Stiles, D., Gordiyenko, N., Strunnikova, N., and Macdonald, I.M. (2009). The functional effect of pathogenic mutations in Rab escort protein 1. Mutat. Res. *665*, 44–50.

Shen, F., and Seabra, M.C. (1996). Mechanism of digeranylgeranylation of Rab proteins. Formation of a complex between monogeranylgeranyl-Rab and Rab escort protein. J. Biol. Chem. *271*, 3692–3698.

Shi, W., van den Hurk, J. a J.M., Alamo-Bethencourt, V., Mayer, W., Winkens, H.J., Ropers, H.-H., Cremers, F.P.M., and Fundele, R. (2004). Choroideremia gene product affects trophoblast development and vascularization in mouse extra-embryonic tissues. Dev. Biol. *272*, 53–65.

Shibahara, S., Yasumoto, K., Amae, S., Udono, T., Watanabe, K., Saito, H., and Takeda, K. (2000). Regulation of pigment cell-specific gene expression by MITF. Pigment Cell Res. *13 Suppl 8*, 98–102.

Shu, J., Wu, C., Wu, Y., Li, Z., Shao, S., Zhao, W., Tang, X., Yang, H., Shen, L., Zuo, X., et al. (2013). Induction of pluripotency in mouse somatic cells with lineage specifiers. Cell *153*, 963–975.

Silva, J., and Smith, A. (2008). Capturing pluripotency. Cell *132*, 532–536.

Silva, J., Chambers, I., Pollard, S., and Smith, A. (2006). Nanog promotes transfer of pluripotency after cell fusion. Nature *441*, 997–1001.

Silva, J., Barrandon, O., Nichols, J., Kawaguchi, J., Theunissen, T.W., and Smith, A. (2008). Promotion of reprogramming to ground state pluripotency by signal inhibition. PLoS Biol. *6*, e253.

Simó, R., Villarroel, M., Corraliza, L., Hernández, C., and Garcia-Ramírez, M. (2010). The retinal pigment epithelium: Something more than a constituent of the blood-retinal barrier-implications for the pathogenesis of diabetic retinopathy. J. Biomed. Biotechnol. *2010*.

Simonsson, S., and Gurdon, J. (2004). DNA demethylation is necessary for the epigenetic reprogramming of somatic cell nuclei. Nat. Cell Biol. *6*, 984–990.

Singh, R., Shen, W., Kuai, D., Martin, J.M., Guo, X., Smith, M. a, Perez, E.T., Phillips, M.J., Simonett, J.M., Wallace, K. a, et al. (2013). iPS cell modeling of Best disease: insights into the pathophysiology of an inherited macular degeneration. Hum. Mol. Genet. *22*, 593–607.

Sivaprasad, S., Bailey, T.A., and Chong, V.N.H. (2005). Bruch's membrane and the vascular intima: is there a common basis for age-related changes and disease? Clin. Experiment. Ophthalmol. *33*, 518–523.

Sliney, D.H. (2005). Exposure Geometry and Spectral Environment Determine Photobiological Effects on the Human Eye. Photochem. Photobiol. *81*, 483–489.

Son, E.Y., Ichida, J.K., Wainger, B.J., Toma, J.S., Rafuse, V.F., Woolf, C.J., and Eggan, K. (2011). Conversion of mouse and human fibroblasts into functional spinal motor neurons. Cell Stem Cell *9*, 205–218.

Song, K., Nam, Y.-J., Luo, X., Qi, X., Tan, W., Huang, G.N., Acharya, A., Smith, C.L., Tallquist, M.D., Neilson, E.G., et al. (2012). Heart repair by reprogramming non-myocytes with cardiac transcription factors. Nature.

Sonoda, S., Spee, C., Barron, E., Ryan, S.J., Kannan, R., and Hinton, D.R. (2009). A protocol for the culture and differentiation of highly polarized human retinal pigment epithelial cells. Nat. Protoc. *4*, 662–673.

Sonoda, S., Sreekumar, P., and Kase, S. (2010). Attainment of polarity promotes growth factor secretion by retinal pigment epithelial cells: relevance to age-related macular degeneration. Aging (Albany. NY). *2*, 28–42.

Soufi, A., Donahue, G., and Zaret, K.S. (2012). Facilitators and impediments of the pluripotency reprogramming factors' initial engagement with the genome. Cell *151*, 994–1004.

Sparrrow, J., Hicks, D., and Hamel, C. (2010). The Retinal Pigment Epithelium in Health and Disease. Curr. Mol. Med. *10*, 802–823.

Spraul, C.W., Lang, G.E., Grossniklaus, H.E., and Lang, G.K. (1999). Histologic and Morphometric Analysis of the Choroid, BrM and RPE in Postmortem Eyes With AMD and Histologic Examination of Surgically Excised CNV Membranes. Surv. Ophthalmol. *44, Supple*, 10–32.

Stadtfeld, M., Nagaya, M., Utikal, J., Weir, G., and Hochedlinger, K. (2008). Induced pluripotent stem cells generated without viral integration. Science *322*, 945–949.

Starr, C.J., Kappler, J. a, Chan, D.K., Kollmar, R., and Hudspeth, a J. (2004). Mutation of the zebrafish choroideremia gene encoding Rab escort protein 1 devastates hair cells. Proc. Natl. Acad. Sci. U. S. A. *101*, 2572–2577.

Steinberg, R.H., Linsenmeier, R.A., and Griff, E.R. (1983). Three light-evoked responses of the retinal pigment epithelium. Vision Res. *23*, 1315–1323.

Steinfeld, J., Steinfeld, I., Coronato, N., Hampel, M.-L., Layer, P.G., Araki, M., and Vogel-Höpker, A. (2013). RPE specification in the chick is mediated by surface ectoderm-derived BMP and Wnt signalling. Development *140*, 4959–4969.

Stenmark, H. (2009). Rab GTPases as coordinators of vesicle traffic. Nat. Rev. Mol. Cell Biol. *10*, 513–525.

Stern, J.H., and Temple, S. (2011). Stem cells for retinal replacement therapy. Neurotherapeutics *8*, 736–743.

Strauss, O. (2005). The retinal pigment epithelium in visual function. Physiol. Rev. *85*, 845–881.

Strunnikova, N., Zein, W.M., Silvin, C., and Macdonald, I.M. (2012). Serum Biomarkers and Trafficking Defects in Peripheral Tissues Reflect the Severity of Retinopathy in Three Brothers Affected by Choroideremia. Retin. Degener. Dis. Adv. Exp. Med. Biol. *723*, 381–387.

Strunnikova, N. V, Barb, J., Sergeev, Y. V, Thiagarajasubramanian, A., Silvin, C., Munson, P.J., and Macdonald, I.M. (2009). Loss-of-function mutations in Rab escort protein 1 (REP-1) affect intracellular transport in fibroblasts and monocytes of choroideremia patients. PLoS One *4*, e8402.

Suda, Y., Nakabayashi, J., Matsuo, I., and Aizawa, S. (1999). Functional equivalency between Otx2 and Otx1 in development of the rostral head. Development *126*, 743–757.

Sung, C.-H., and Chuang, J.-Z. (2010). The cell biology of vision. J. Cell Biol. *190*, 953–963.

Sviderskaya, E. V, Hill, S.P., Evans-Whipp, T.J., Chin, L., Orlow, S.J., Easty, D.J., Cheong, S.C., Beach, D., DePinho, R. a, and Bennett, D.C. (2002). p16(Ink4a) in melanocyte senescence and differentiation. J. Natl. Cancer Inst. *94*, 446–454.

Syed, N., Smith, J.E., John, S.K., Seabra, M.C., Aguirre, G.D., and Milam, A.H. (2001). Evaluation of retinal photoreceptors and pigment epithelium in a female carrier of choroideremia. Ophthalmology *108*, 711–720.

Syed, R., Sundquist, S.M., Ratnam, K., Zayit-Soudry, S., Zhang, Y., Crawford, J.B., MacDonald, I.M., Godara, P., Rha, J., Carroll, J., et al. (2013). High-resolution images of retinal structure in patients with choroideremia. Invest. Ophthalmol. Vis. Sci. *54*, 950–961.

Taberlay, P.C., Kelly, T.K., Liu, C.C., You, J.S., De Carvalho, D.D., Miranda, T.B., Zhou, X.J., Liang, G., and Jones, P.A. (2011). Polycomb-repressed genes have permissive enhancers that initiate reprogramming. Cell *147*, 1283–1294.

Tachibana, M. (2000). MITF : A Stream Flowing for Pigment Cells. Pigment Cell Res. 230–240.

Tachibana, M., Amato, P., Sparman, M., Gutierrez, N.M., Tippner-Hedges, R., Ma, H., Kang, E., Fulati, A., Lee, H.-S., Sritanaudomchai, H., et al. (2013). Human embryonic stem cells derived by somatic cell nuclear transfer. Cell *153*, 1228–1238.

Tada, M., Takahama, Y., Abe, K., Nakatsuji, N., and Tada, T. (2001). Nuclear reprogramming of somatic cells by in vitro hybridization with ES cells. Curr. Biol. *11*, 1553–1558.

Takahashi, K., and Yamanaka, S. (2006). Induction of pluripotent stem cells from mouse embryonic and adult fibroblast cultures by defined factors. Cell *126*, 663–676.

Takahashi, K., and Yamanaka, S. (2013). Induced pluripotent stem cells in medicine and biology. Development *140*, 2457–2461.

Takahashi, K., Tanabe, K., Ohnuki, M., Narita, M., Ichisaka, T., Tomoda, K., and Yamanaka, S. (2007a). Induction of pluripotent stem cells from adult human fibroblasts by defined factors. Cell *131*, 861–872.

Takahashi, K., Okita, K., Nakagawa, M., and Yamanaka, S. (2007b). Induction of pluripotent stem cells from fibroblast cultures. Nat. Protoc. *2*, 3081–3089.

Tassabehji, M., Newton, V.E., and Read, A.P. (1994). Waardenburg syndrome type 2 caused by mutations in the human microphthalmia (MITF) gene. Nat. Genet. *8*, 251–255.

Tesar, P.J., Chenoweth, J.G., Brook, F.A., Davies, T.J., Evans, E.P., Mack, D.L., Gardner, R.L., and McKay, R.D.G. (2007). New cell lines from mouse epiblast share defining features with human embryonic stem cells. Nature *448*, 196–199.

Tétreault, N., Champagne, M.-P., and Bernier, G. (2009). The LIM homeobox transcription factor Lhx2 is required to specify the retina field and synergistically cooperates with Pax6 for Six6 trans-activation. Dev. Biol. *327*, 541–550.

Thier, M., Wörsdörfer, P., Lakes, Y.B., Gorris, R., Herms, S., Opitz, T., Seiferling, D., Quandel, T., Hoffmann, P., Nöthen, M.M., et al. (2012). Direct Conversion of Fibroblasts into Stably Expandable Neural Stem Cells. Cell Stem Cell 473–479.

Thomson, J.A., Itskovitz-Eldor, J., Shapiro, S.S., Waknitz, M.A., Swiergiel, J.J., Marshall, V.S., and Jones, J.M. (1998). Embryonic stem cell lines derived from human blastocysts. Science (80-.). *282*, 1145–1147.

Tolmachova, T., Anders, R., Abrink, M., Bugeon, L., Dallman, M.J., Futter, C.E., Ramalho, J.S., Tonagel, F., Tanimoto, N., Seeliger, M.W., et al. (2006). Independent degeneration of photoreceptors and retinal pigment epithelium in conditional knockout mouse models of choroideremia. J. Clin. Invest. *116*, 386–394.

Tolmachova, T., Wavre-Shapton, S.T., Barnard, A.R., MacLaren, R.E., Futter, C.E., and Seabra, M.C. (2010). Retinal pigment epithelium defects accelerate photoreceptor degeneration in cell

type-specific knockout mouse models of choroideremia. Invest. Ophthalmol. Vis. Sci. *51*, 4913–4920.

Tolmachova, T., Tolmachov, O.E., Wavre-Shapton, S.T., Tracey-White, D., Futter, C.E., and Seabra, M.C. (2012). CHM/REP1 cDNA delivery by lentiviral vectors provides functional expression of the transgene in the retinal pigment epithelium of choroideremia mice. J. Gene Med. *14*, 158–168.

Tolmachova, T., Tolmachov, O.E., Barnard, A.R., de Silva, S.R., Lipinski, D.M., Walker, N.J., Maclaren, R.E., and Seabra, M.C. (2013). Functional expression of Rab escort protein 1 following AAV2-mediated gene delivery in the retina of choroideremia mice and human cells ex vivo. J. Mol. Med. (Berl). *91*, 825–837.

Ton, C.C.T., Hirvonen, H., Miwa, H., Weil, M.M., Monaghan, P., Jordan, T., van Heyningen, V., Hastie, N.D., Meijers-Heijboer, H., Drechsler, M., et al. (2014). Positional cloning and characterization of a paired box- and homeobox-containing gene from the aniridia region. Cell *67*, 1059–1074.

Torre, A. La, Lamba, D.A., Jayabalu, A., and Reh, T.A. (2012). Production and transplantation of retinal cells from human and mouse embryonic stem cells. In Retinal Development: Methods and Protocols, S.-Z. Wang, ed. (Totowa, NJ: Humana Press), pp. 229–246.

Tucker, B. a, Park, I.-H., Qi, S.D., Klassen, H.J., Jiang, C., Yao, J., Redenti, S., Daley, G.Q., and Young, M.J. (2011). Transplantation of adult mouse iPS cell-derived photoreceptor precursors restores retinal structure and function in degenerative mice. PLoS One *6*, e18992.

Turner, M., Leslie, S., Martin, N.G., Peschanski, M., Rao, M., Taylor, C.J., Trounson, A., Turner, D., Yamanaka, S., and Wilmut, I. (2013). Toward the development of a global induced pluripotent stem cell library. Cell Stem Cell *13*, 382–384.

Vajaranant, T.S., Fishman, G.A., Szlyk, J.P., Grant-Jordan, P., Lindeman, M., and Seiple, W. (2008). Detection of Mosaic Retinal Dysfunction in Choroideremia Carriers Electroretinographic and Psychophysical Testing. Ophthalmology *115*, 723–729.

Vasireddy, V., Mills, J. a, Gaddameedi, R., Basner-Tschakarjan, E., Kohnke, M., Black, A.D., Alexandrov, K., Zhou, S., Maguire, A.M., Chung, D.C., et al. (2013). AAV-mediated gene therapy for choroideremia: preclinical studies in personalized models. PLoS One *8*, e61396.

Vierbuchen, T., and Wernig, M. (2012). Molecular roadblocks for cellular reprogramming. Mol. Cell *47*, 827–838.

Vierbuchen, T., Ostermeier, A., Pang, Z.P., Kokubu, Y., Südhof, T.C., and Wernig, M. (2010). Direct conversion of fibroblasts to functional neurons by defined factors. Nature *463*, 1035–1041.

Voronina, V. a, Kozhemyakina, E. a, O'Kernick, C.M., Kahn, N.D., Wenger, S.L., Linberg, J. V, Schneider, A.S., and Mathers, P.H. (2004). Mutations in the human RAX homeobox gene in a patient with anophthalmia and sclerocornea. Hum. Mol. Genet. *13*, 315–322.

Vugler, A., Carr, A.-J., Lawrence, J., Chen, L.L., Burrell, K., Wright, A., Lundh, P., Semo, M., Ahmado, A., Gias, C., et al. (2008). Elucidating the phenomenon of HESC-derived RPE: anatomy of cell genesis, expansion and retinal transplantation. Exp. Neurol. *214*, 347–361.

Waddington, C. (1957). The Strategy of the Genes: A Discussion of Some Aspects of Theoretical Biology (London: Ruskin House).

Wakayama, T., Perry, A.C., Zuccotti, M., Johnson, K.R., and Yanagimachi, R. (1998). Full-term development of mice from enucleated oocytes injected with cumulus cell nuclei. Nature *394*, 369–374.

Waldherr, M., Ragnini, A., Schweyen, R.J., and Boguski, M.S. (1993). MRS6 - yeast homologue of the choroideraemia gene. Nat Genet *3*, 193–194.

Wallis, D.E., Roessler, E., Hehr, U., Nanni, L., Wiltshire, T., Richieri-Costa, A., Gillessen-Kaesbach, G., Zackai, E.H., Rommens, J., and Muenke, M. (1999). Mutations in the homeodomain of the human SIX3 gene cause holoprosencephaly. Nat. Genet. *22*, 196–198.

Warren, L., Manos, P.D., Ahfeldt, T., Loh, Y.-H., Li, H., Lau, F., Ebina, W., Mandal, P.K., Smith, Z.D., Meissner, A., et al. (2010). Highly efficient reprogramming to pluripotency and directed differentiation of human cells with synthetic modified mRNA. Cell Stem Cell *7*, 618–630.

Wavre-Shapton, S.T., Tolmachova, T., Lopes da Silva, M., da Silva, M.L., Futter, C.E., and Seabra, M.C. (2013). Conditional ablation of the choroideremia gene causes age-related changes in mouse retinal pigment epithelium. PLoS One *8*, e57769.

Wawersik, S., and Maas, R.L. (2000). Vertebrate eye development as modeled in Drosophila. Hum. Mol. Genet. *9*, 917–925.

Wenkel, H., and Streilein, J. (2000). Evidence that Retinal Pigment Epithelium Functions as an Immune-Privileged Tissue. Invest. Ophthalmol. Vis. Sci. *41*, 3467–3473.

Westenskow, P., Piccolo, S., and Fuhrmann, S. (2009). Beta-catenin controls differentiation of the retinal pigment epithelium in the mouse optic cup by regulating Mitf and Otx2 expression. Development *136*, 2505–2510.

Westenskow, P.D., McKean, J.B., Kubo, F., Nakagawa, S., and Fuhrmann, S. (2010). Ectopic Mitf in the embryonic chick retina by co-transfection of β-catenin and Otx2. Invest. Ophthalmol. Vis. Sci. *51*, 5328–5335.

Williams, R.L., Hilton, D.J., Pease, S., Willson, T.A., Stewart, C.L., Gearing, D.P., Wagner, E.F., Metcalf, D., Nicola, N.A., and Gough, N.M. (1988a). Myeloid leukaemia inhibitory factor maintains the developmental potential of embryonic stem cells. Nature *336*, 684–687.

Williams, R.L., Hilton, D.J., Pease, S., Willson, T.A., Stewart, C.L., Gearing, D.P., Wagner, E.F., Metcalf, D., Nicola, N.A., and Gough, N.M. (1988b). Myeloid leukaemia inhibitory factor maintains the developmental potential of embryonic stem cells. Nature *336*, 684–687.

Wilmut, I., Schnieke, A.E., McWhir, J., Kind, A.J., and Campbell, K.H. (1997). Viable offspring derived from fetal and adult mammalian cells. Nature *385*, 810–813.

Wimmers, S., Karl, M.O., and Strauss, O. (2007). Ion channels in the RPE. Prog. Retin. Eye Res. *26*, 263–301.

Winkler, B.S., Boulton, M.E., Gottsch, J.D., and Sternberg, P. (1999). Oxidative damage and age-related macular degeneration. Mol. Vis. *5*, 32.

Witmer, A. (2003). Vascular endothelial growth factors and angiogenesis in eye disease. Prog. Retin. Eye Res. *22*, 1–29.

Wolff, G. (1895). Entwicklungsphhhysiologische Studien: I. Die Regeneration der Urodelenlise. Arch. Entwicklungsmech. Org *1*, 380–390.

Woltjen, K., Michael, I.P., Mohseni, P., Desai, R., Mileikovsky, M., Hämäläinen, R., Cowling, R., Wang, W., Liu, P., Gertsenstein, M., et al. (2009). piggyBac transposition reprograms fibroblasts to induced pluripotent stem cells. Nature *458*, 766–770.

Wray, J., Kalkan, T., and Smith, A.G. (2010). The ground state of pluripotency. Biochem. Soc. Trans. *38*, 1027–1032.

Wray, J., Kalkan, T., Gomez-Lopez, S., Eckardt, D., Cook, A., Kemler, R., and Smith, A. (2011). Inhibition of glycogen synthase kinase-3 alleviates Tcf3 repression of the pluripotency network and increases embryonic stem cell resistance to differentiation. Nat. Cell Biol. *13*, 838–845.

Wu, J., Peachey, N.S., and Marmorstein, A.D. (2004). Light-evoked responses of the mouse retinal pigment epithelium. J. Neurophysiol. *91*, 1134–1142.

Xie, H., Ye, M., Feng, R., and Graf, T. (2004). Stepwise reprogramming of B cells into macrophages. Cell *117*, 663–676.

Yakubov, E., Rechavi, G., Rozenblatt, S., and Givol, D. (2010). Reprogramming of human fibroblasts to pluripotent stem cells using mRNA of four transcription factors. Biochem. Biophys. Res. Commun. *394*, 189–193.

Yamamizu, K., Piao, Y., Sharov, A.A., Zsiros, V., Yu, H., Nakazawa, K., Schlessinger, D., and Ko, M.S.H. (2013). Identification of Transcription Factors for Lineage-Specific ESC Differentiation. Stem Cell Reports *1*, 545–559.

Yamanaka, S., and Blau, H.M. (2010). Nuclear reprogramming to a pluripotent state by three approaches. Nature *465*, 704–712.

Yau, K., and Hardie, R. (2009). Phototransduction motifs and variations. Cell *139*, 246–264.

Yeo, J.-C., and Ng, H.-H. (2013). The transcriptional regulation of pluripotency. Cell Res. *23*, 20–32.

Ying, Q.L., Nichols, J., Chambers, I., and Smith, A. (2003). BMP induction of Id proteins suppresses differentiation and sustains embryonic stem cell self-renewal in collaboration with STAT3. Cell *115*, 281–292.

Ying, Q.-L., Wray, J., Nichols, J., Batlle-Morera, L., Doble, B., Woodgett, J., Cohen, P., and Smith, A. (2008). The ground state of embryonic stem cell self-renewal. Nature *453*, 519–523.

Yokoyama, T., Silversides, D.W., Waymire, K.G., Kwon, B.S., Takeuchi, T., and Overbeek, P. a (1990). Conserved cysteine to serine mutation in tyrosinase is responsible for the classical albino mutation in laboratory mice. Nucleic Acids Res. *18*, 7293–7298.

Yoo, A.S., Sun, A.X., Li, L., Shcheglovitov, A., Portmann, T., Li, Y., Lee-Messer, C., Dolmetsch, R.E., Tsien, R.W., and Crabtree, G.R. (2011). MicroRNA-mediated conversion of human fibroblasts to neurons. Nature *476*, 228–231.

Young, R. a (2011). Control of the embryonic stem cell state. Cell *144*, 940–954.

Young, R.W., and Bok, D. (1969). PARTICIPATION OF THE RETINAL PIGMENT EPITHELIUM IN THE ROD OUTER SEGMENT RENEWAL PROCESS. J. Cell Biol. *42* , 392–403.

Young, K.A., Berry, M.L., Mahaffey, C.L., Saionz, J.R., Hawes, N.L., Chang, B., Zheng, Q.Y., Smith, R.S., Bronson, R.T., Nelson, R.J., et al. (2002). Fierce: A new mouse deletion of Nr2e1; violent behaviour and ocular abnormalities are background-dependent. Behav. Brain Res. *132*, 145–158.

Yu, J., Vodyanik, M. a, Smuga-Otto, K., Antosiewicz-Bourget, J., Frane, J.L., Tian, S., Nie, J., Jonsdottir, G. a, Ruotti, V., Stewart, R., et al. (2007). Induced pluripotent stem cell lines derived from human somatic cells. Science *318*, 1917–1920.

Yu, J., Hu, K., Smuga-Otto, K., Tian, S., Stewart, R., Slukvin, I.I., and Thomson, J. a (2009). Human induced pluripotent stem cells free of vector and transgene sequences. Science *324*, 797–801.

Yun, S., Saijoh, Y., Hirokawa, K.E., Kopinke, D., Murtaugh, L.C., Monuki, E.S., and Levine, E.M. (2009). Lhx2 links the intrinsic and extrinsic factors that control optic cup formation. Development *136*, 3895–3906.

Zhang, X.M., and Yang, X.J. (2001). Temporal and spatial effects of Sonic hedgehog signaling in chick eye morphogenesis. Dev. Biol. *233*, 271–290.

Zhang, D., Sutanto, E., and Rakoczy, P. (2004). Concurrent enhancement of transcriptional activity and specificity of a retinal pigment epithelial cell-preferential promoter. Mol. Vis 208–214.

Zhang, K., Liu, G.-H., Yi, F., Montserrat, N., Hishida, T., Rodriguez Esteban, C., and Izpisua Belmonte, J.C. (2013). Direct conversion of human fibroblasts into retinal pigment epithelium-like cells by defined factors. Protein Cell *4*, 259–265.

Zhang, W.Y., de Almeida, P.E., and Wu, J.C. (2012). Teratoma formation: A tool for monitoring pluripotency in stem cell research. In StemBook, (The Stem Cell Research Community), pp. 1–14.

Zhao, L., Saitsu, H., Sun, X., Shiota, K., and Ishibashi, M. (2010). Sonic hedgehog is involved in formation of the ventral optic cup by limiting Bmp4 expression to the dorsal domain. Mech. Dev. *127*, 62–72.

Zhao, S., Hung, F.C., Colvin, J.S., White, A., Dai, W., Lovicu, F.J., Ornitz, D.M., and Overbeek, P.A. (2001). Patterning the optic neuroepithelium by FGF signaling and Ras activation. Development *128*, 5051–5060.

Zhou, H., Wu, S., Joo, J.Y., Zhu, S., Han, D.W., Lin, T., Trauger, S., Bien, G., Yao, S., Zhu, Y., et al. (2009). Generation of induced pluripotent stem cells using recombinant proteins. Cell Stem Cell *4*, 381–384.

Zhou, Q., Brown, J., Kanarek, A., Rajagopal, J., and Melton, D. a (2008). In vivo reprogramming of adult pancreatic exocrine cells to beta-cells. Nature *455*, 627–632.

Zhou, Q., Liu, L., Xu, F., Li, H., Sergeev, Y., Dong, F., Jiang, R., MacDonald, I., and Sui, R. (2012). Genetic and phenotypic characteristics of three Mainland Chinese families with choroideremia. Mol. Vis. *18*, 309–316.

Zhu, Y., Carido, M., Meinhardt, A., Kurth, T., Karl, M.O., Ader, M., and Tanaka, E.M. (2013). Three-dimensional neuroepithelial culture from human embryonic stem cells and its use for quantitative conversion to retinal pigment epithelium. PLoS One *8*, e54552.

Zuber, M.E. (2010). Eye field specification in Xenopus laevis. Curr. Top. Dev. Biol. *93*, 29–60.

Zuber, M.E., Perron, M., Philpott, A., Bang, A., and Harris, W.A. (1999). Giant eyes in Xenopus laevis by overexpression of XOptx2. Cell *98*, 341–352.

Zuber, M.E., Gestri, G., Viczian, A.S., Barsacchi, G., and Harris, W. a (2003). Specification of the vertebrate eye by a network of eye field transcription factors. Development *130*, 5155–5167.

Chapter 8 Supplementary material

Chapter 8 : Supplementary material

Resumo alargado

Os organismos multicelulares são formados por um conjunto de diferentes células e tecidos, todos derivados duma única célula inicial através dum processo de diferenciação. Durante muito tempo este processo de especificação progressiva dos diversos tipos de células foi considerado unidireccional e irreversível. Contudo, este conceito foi posto em causa pelas experiências inovadoras de transferência nuclear de células somáticas (ou clonagem) realizadas por Gurdon nos anos 60, em que o núcleo de uma célula do epitélio intestinal dum girino foi transferido para um oócito enucleado dando origem a um organismo adulto completo. Esta evidência experimental de que a identidade celular é plástica deu origem a um novo conceito em que as especificidades epigenéticas e transcricionais de uma célula somática podem ser reprogramadas de modo a originar outro tipo celular diferente, num processo designado de reprogramação celular.

Para além da clonagem, outras tecnologias de reprogramação nuclear foram desenvolvidas ao longo dos anos, como a fusão celular e a reprogramação mediada por factores de transcrição (FT). Este último caso foi reportado pela primeira vez por Yamanaka e a sua equipa em 2006, causando uma verdadeira revolução na área científica de investigação em células estaminais. Recorrendo à expressão forçada de 4 FT com funções conhecidas no estabelecimento e manutenção de um estado pluripotente, os fibroblastos foram convertidos em células com propriedades de auto-renovação e pluripotência semelhantes às células estaminais embrionárias (CEE). Deste modo, Yamanaka obteve aquilo que designou por células estaminais pluripotentes induzidas (CEPi). Dada a relevância destas descobertas, Yamanaka e Gurdon receberam o Prémio Nobel da Medicina em 2012 pela “descoberta de que células maduras podem ser reprogramadas para um estado pluripotente”.

A reprogramação celular de células somáticas para um estado pluripotente foi conseguida usando FT, técnica também utilizada na conversão directa de uma célula somática noutro tipo de célula (da mesma ou de diferentes linhagens). Estas inovações tecnológicas suscitam muito interesse em termos de aplicações em medicina regenerativa. Uma célula pluripotente, por definição, é capaz de dar origem aos vários tipos de células das 3 linhagens celulares, endoderme, mesoderme e ectoderme. Deste modo, e como as CEPi podem ser obtidas dos próprios doentes e diferenciadas nas respectivas células em falta, esta tecnologia permite obter células autólogas e sem

necessidade de recorrer a embriões, contornando por isso os problemas éticos levantados pelas CEE. Para além disso, a possibilidade de gerar células de indivíduos com determinadas patologias permite obter modelos *in vitro* de várias doenças que podem ser usados para compreender melhor os mecanismos patogénicos. Ensaios para confirmar a eficiência e toxicidade de novos fármacos também podem ser realizados usando as células obtidas por reprogramação celular. Adicionalmente, estas células podem ser utilizadas para investigar os mecanismos reguladores da pluripotência, da identidade celular e dos processos de diferenciação.

As técnicas de reprogramação celular têm sido aplicadas com sucesso a várias áreas da medicina regenerativa, nomeadamente em situações de degeneração da retina. A retina é o tecido que se encontra na zona posterior do olho, responsável pela captação da informação visual. Várias doenças hereditárias ou adquiridas são caracterizadas pela degenerescência das várias camadas celulares que constituem a retina: a neuroretina, o epitélio pigmentar da retina (EPR) e a coróide. Em diversas situações, o processo degenerativo está relacionado com a disfunção do EPR, um tecido de suporte que desempenha funções vitais para a manutenção da capacidade de captura e transmissão da informação visual dos foto-receptores da neuroretina. Nesse caso, há uma progressiva perda visual que pode conduzir à cegueira. A Coroideremia (CHM) é um dos casos em que isto acontece. Esta é uma doença hereditária ligada ao cromossoma X e causada por mutações que causam perda de função da proteína REP1, essencial para a regulação do tráfico intracelular. Esta doença é caracterizada por uma degenerescência progressiva da neuroretina, EPR e coróide, e leva à perda parcial de visão nos jovens adultos, evoluindo para cegueira total com o tempo. Apesar de os mecanismos moleculares subjacentes à patologia da CHM ainda serem parcialmente desconhecidos, existem dados que sugerem um envolvimento crucial do EPR. Terapias génicas com o objectivo de corrigir o defeito genético no EPR de doentes estão neste momento em ensaios clínicos de fase I, com resultados promissores. No entanto, em doentes em que a progressão dos eventos degenerativos já se encontra em fase avançada, apenas estratégias de substituição celular podem ser vantajosas para os doentes com CHM. Para além disso, existe uma lacuna nos modelos *in vitro* existentes, o que, uma vez colmatada, poderia implicar um avanço significativo na caracterização dos eventos degenerativos.

Deste modo, o trabalho apresentado nesta tese foi desenhado com o objectivo principal de explorar as potenciais aplicações das técnicas de reprogramação celular no contexto das doenças degenerativas da retina com disfunção do EPR, em particular no caso da CHM. O primeiro objectivo consistiu em implementar a técnica de reprogramação celular

para a pluripotência no laboratório, de modo a ser usada no âmbito deste trabalho e abrindo novas portas para trabalhos subsequentes. Diversos protocolos para a obtenção de CEPi foram entretanto descritos, com diferentes células de origem, sistemas de transdução e conjunto de FT usados na reprogramação. Devido à sua alta eficiência, fidelidade e reprodutibilidades, foi escolhido um sistema lentiviral induzido, em que uma só unidade policistrónica codifica os 4 FT descritos por Yamanaka: Oct4, Sox2, Klf4 e c-Myc. Fibroblastos de embrião de murganho (FEM) de estirpe selvagem foram transduzidos com as partículas lentivirais e submetidos a condições de cultura favoráveis às células pluripotentes. A citocina Factor Inibidor da Leucemia (LIF) e dois inibidores de determinadas vias de sinalização celular (2i, "dual inhibition) fazem parte integrante do meio de cultura, de modo a favorecer o estabelecimento dum estado de pluripotência *naïve*. Durante o processo de reprogramação, foi detectada a expressão de genes e proteínas características de células pluripotentes (*Oct4* endógeno, Nanog, *Fgf4*, e SSEA-1). Observou-se também o aparecimento de colónias com morfologia semelhante às CEE e positivas para a fosfatase alcalina (AP). Estas colónias deram origem a diversas linhas celulares de CEPi, que demonstraram ter propriedades de auto-renovação mesmo quando o sistema lentiviral deixou de ser induzido, indicando que a activação da identidade celular pluripotente endógena foi conseguida. Para além disso, a morfologia e expressão de genes e proteínas característicos (Oct4, Nanog, SSEA-1 e AP) das células pluripotentes foi também avaliada e confirmada. Em termos funcionais, a pluripotência das células obtidas foi posteriormente avaliada *in vitro* e *in vivo*, tendo sido observado que após diferenciação as CEPi deram origem a células das 3 linhagens germinativas em ambos os casos. Como alternativa a este protocolo, e de modo a obter células mais adequadas a possíveis aplicações terapêuticas, foi também testado um sistema de transdução adenoviral, que tem a vantagem de não integrar o genoma, evitando eventos de mutagénese por inserção. No entanto, não foi possível estabelecer linhas celulares de CEPi usando este método. Outros métodos não integrativos foram entretanto descritos; contudo, o sistema lentiviral continua a ser o mais usado e robusto no estabelecimento de modelos celulares de doença.

Seguidamente ao estabelecimento e otimização do protocolo lentiviral de obtenção de CEPi, em células de estirpe selvagem, este foi aplicado a células obtidas de um modelo animal de Chm, em que o *knockout* do gene *Rep1* ocorre de maneira condicional, após tratamento com tamoxifeno. As experiências envolveram o uso de FEM tratados e não tratados com a droga indutora da recombinação homóloga. Os primeiros, FEM Chm^{null}, possuem expressão reduzida de *Rep1*, quando comparadas com os segundos, FEM Chm^{flox} em que o knockout não foi induzido. Obtiveram-se diversas linhas celulares de

CEPi *Chm*^{null} e *Chm*^{flox} que foram caracterizadas como referido anteriormente para as células de estirpe selvagem. Para além de demonstrarem propriedades de auto-renovação e pluripotência, estas CEPi foram caracterizadas em termos de expressão de Rep1, tendo-se observado que as CEPi *Chm*^{null} possuem expressão reduzida quando comparadas com as CEPi *Chm*^{flox}, confirmando a aplicabilidade das primeiras como modelo de Chm.

O facto de serem pluripotentes torna as CEPi capazes de serem diferenciadas nas células de interesse, neste caso células do EPR. Vários protocolos estão descritos na literatura, e três foram testados simultaneamente em CEPi de estirpe selvagem, CEPi *Chm*^{null} e CEPi *Chm*^{flox}. O primeiro protocolo estabelecido usando CEE humanas não foi reproduzido com sucesso no nosso sistema, uma vez que não se observou a formação das estruturas neuroepiteliais descritas, nem alterações de expressão genética concordantes. Pelo contrário, com o segundo protocolo, adaptado dos trabalhos pioneiros do grupo de Sasai, obtiveram-se resultados promissores. Em condições de cultura em suspensão na ausência de soro e com adição de Matrigel, a auto-formação de cálices ópticos tridimensionais foi reportada previamente. No nosso caso, observou-se a formação de estruturas neuroepiteliais com protusões correspondentes a vesículas ópticas que, no entanto, não evoluíram para a formação dos cálices ópticos. Concomitantemente observou-se a expressão de FT que estabelecem primariamente e especificam o “eye field” (nomeadamente *Otx2*, *Pax6* e *Six3*). Apesar de o processo de diferenciação não ter sido finalizado, obtiveram-se resultados promissores que facilitarão a prossecução do objectivo final de obter células do EPR, no contexto 3D dos cálices ópticos. Por último, foi testado um terceiro protocolo de diferenciação baseado nas vias de transdução de sinal que se sabem estarem implicadas no desenvolvimento embrionário do olho. Numa primeira fase, as células foram sujeitas a cultura em suspensão em meio de cultura contendo Noggin, Dkk1 e IGF-1 para favorecer a linhagem neuroepitelióide. Seguidamente, e já em cultura aderente, observou-se o aparecimento duma população celular proliferativa com morfologia e padrão de expressão génico (*Pax6*, *Six3*, *Otx2*, e em alguns caso também *Six6*) caracteristicamente observados em células retinianas progenitoras.

Simultaneamente observou-se a expressão de *Mitf* e zonas com células hexagonais compactadas semelhantes ao EPR. Em suma, apesar de não se ter conseguido obter ainda uma população de EPR maduro, estas experiências abriram o caminho para a obtenção do mesmo, integrado numa estrutura tridimensional. Deste modo, será possível estudar as interações estruturais e funcionais do EPR e neuroretina, o que será muito vantajoso para compreender melhor a patogénese da CHM. Por outro lado, as

células retinianas progenitoras podem ser expandidas antes da aplicação do estímulo final de especificação do EPR, que será assim obtido de maneira mais quantitativa, facilitando os estudos de modelação da CHM.

Outro objectivo explorado na presente tese, para além de implementar técnicas de reprogramação para a pluripotência que requerem a subsequente diferenciação em EPR, foi a conversão directa de fibroblastos em células do EPR. Segundo a hipótese de que os FT envolvidos nos processos de desenvolvimento embrionário do olho primitivo (*Tbx3*, *Rax*, *Six3*, *Pax6*, *Lhx2*, *Six6* e *Nr2e1)* e subsequente especificação do EPR (*Pax6*, *Mitf*, *Otx1* e *Otx2)* poderiam ser usados nesta conversão directa, foram criadas diversas ferramentas moleculares. Foram produzidos vectores lentivirais indutíveis que codificam para os 10 FT selecionados com base na literatura. A transdução de FEM com uma mistura dos 10 FT revelou o aparecimento de células pigmentadas, assim como o aumento da expressão de genes característicos do EPR. Para facilitar a identificação/isolamento das células reprogramadas e a otimização da mistura dos FT a usar, foram também produzidos sistemas lentivirais repórteres usando as regiões promotoras dos genes *tirosinase* e *Rpe65*. Nestas experiências, observou-se que a combinação de apenas 2 FT, *Mitf* e *Otx2*, induzia activação do promotor da tirosinase de maneira equivalente ao observado para o cocktail de 10 FT. Este resultado confirma também o funcionamento do sistema, uma vez que estes FT são conhecidos reguladores da expressão da tirosinase. Foi proposto também um papel para uma possível interacção positiva destes FT com *Otx1* e/ou *Pax6*, contudo são necessários mais estudos para se poderem tirar conclusões definitivas. Pelo acima mencionado, estas experiências promissoras para além de permitiram optimizar uma mistura de FT que origina uma conversão directa mais eficiente, podem também ajudar a descobrir novos mecanismos moleculares que contribuem para a identidade transcricional do EPR. Mais ainda, está a ser implementado um sistema repórter semelhante ao já estabelecido, mas que permite a selecção positiva das células reprogramadas, de modo a futuramente se prosseguir com a caracterização molecular e funcional das mesmas e a confirmação da identidade de EPR. Uma vez optimizado o protocolo, este pode ser utilizado em células modelo de CHM para permitir estudos funcionais.

Globalmente, os trabalhos apresentados nesta tese evidenciam as amplas aplicabilidades das tecnologias de reprogramação celular. Aplicando as técnicas descritas de reprogramação para a pluripotência, obtiveram-se CEPi de estirpes selvagens e Chm que, uma vez diferenciadas em EPR, constituem ferramentas importantes para futuros trabalhos na área da retina. No âmbito desta tese foram também desenvolvidos métodos inovadores para permitir a conversão directa de

fibroblastos em EPR. No seu conjunto e a longo prazo, as células do EPR obtidas por reprogramação celular abrem novas possibilidades para o desenvolvimento de terapias de substituição celular. Por outro lado, a curto prazo, contribuem para o estabelecimento de modelos *in vitro* para estudos funcionais de doenças degenerativas da retina no geral, e de CHM em particular.

To the Infinity...

And beyond!

Buzz Lightyear